



**André Miguel da  
Costa Lopes**

**Pré-tratamento de biomassa lignocelulósica com  
líquidos iónicos**

**Pre-treatment of lignocellulosic biomass with ionic  
liquids**



**André Miguel da  
Costa Lopes**

**Pré-tratamento de biomassa lignocelulósica com  
líquidos iónicos**

**Pre-treatment of lignocellulosic biomass with ionic  
liquids**

Dissertação apresentada à Universidade de Aveiro para cumprimento dos requisitos necessários à obtenção do grau de Mestre em Biotecnologia, realizada sob a orientação científica do Doutor Rafal Marcin Bogel-Lukasik, Investigador Auxiliar da Unidade de Bioenergia do Laboratório Nacional de Energia e Geologia de Lisboa e da Professora Doutora Luísa Alexandre Seuanes Serafim Leal, Professora Auxiliar Convidada do Departamento de Química da Universidade de Aveiro

## **o júri**

presidente

**Prof. Doutor João Manuel da Costa e Araújo Pereira Coutinho**  
Professor Associado com Agregação do departamento de Química da Universidade de Aveiro

**Doutor Rafal Marcin Bogel-Lukasik**  
Investigador Auxiliar da Unidade de Bioenergia do Laboratório Nacional de Energia e Geologia

**Prof. Doutora Luísa Alexandra Seuanes Serafim Leal**  
Professora Auxiliar Convidada do departamento de Química da Universidade de Aveiro

**Doutora Mara Guadalupe Freire Martins**  
Investigadora de Pós-Doutoramento no Instituto de Tecnologia Química e Biológica, ITQB II,  
Universidade Nova de Lisboa

## agradecimentos

Com muita sinceridade agradeço ao meu orientador de mestrado Doutor Rafal Lukasik pela disponibilidade, conhecimentos, esforço e colaboração que foram prestados e essenciais para o sucesso deste trabalho, pela amizade e interajuda e também pelo forte incentivo que sempre me foi dado. Sem dúvida um muito obrigado... Agradeço também à minha orientadora Professora Doutora Luísa Serafim pela disponibilidade, ajuda e acompanhamento do meu trabalho ao longo deste último ano letivo. Agradeço ao Dr. Luís Duarte pelo conhecimento que me transmitiu e pela sua amizade, um verdadeiro professor que qualquer aluno gosta de ter e que o LNEG tem o privilégio de ter assim uma pessoa tão profissional. Obrigado Doutora Florbela Carvalheiro pela simpatia e amizade que sempre mostrou a todos nós no edifício K2.

Um grande muito obrigado à minha colega e amiga Karen João pelo trabalho, dedicação e interajuda. Obrigado Karen por partilhares as minhas frustrações no trabalho. Aprendi contigo a importância de saber tirar partido do otimismo que deve estar sempre presente connosco em situações mais adversas. Obrigado por ouvires muitos dos meus desabafos e de seres uma verdadeira amiga. Agradeço às minhas colegas e amigas Rita Morais, Filipa Bandeira, Ivone Torrado e Patrícia Moniz, Mafalda Viegas e Sofia Graça pela amizade, simpatia e pela força que sempre me proporcionaram ao longo deste ano.

Agradeço também a todos os que me fizeram sentir um ambiente amigo e familiar no edifício K2: Céu Penedo, Belina Ribeiro, Diana Oliveira, Pedro Branco, António Lopes, Gabriela Augusto, Doutor Roseiro, Doutora Luísa e Doutor Duarte.

Agora um eterno obrigado às pessoas mais importantes da minha vida, os meus pais, à minha namorada e à minha irmã, sem vocês não era o homem que sou hoje. Agradeço aos meus pais e à minha irmã que sempre torceram por mim, que sempre me deram a confiança e ajuda para ultrapassar os momentos mais difíceis, vocês serão sempre únicos e serão sempre o meu suporte. Obrigado mãe por me ouvires e me aconselhares, nunca conseguirei retribuir a força e carinho que sempre me deste. Obrigado pai pela tua força e a ti irmã minha segunda conselheira de casa. Muito obrigado minha querida Rita tens sido meu braço direito em tudo, muitas saudades, muitas opiniões, muitos desabafos, muitos momentos que partilhamos juntos que fazem de ti uma namorada com que sempre sonhei ter. Obrigado por acreditares em mim, pela tua enorme força e obrigado pelo teu amor, do qual ser-te-ei sempre grato.

A todos os meus restantes familiares e queridos amigos um muito obrigado pois sempre estiveram quando mais precisava.

Por fim, agradeço a oportunidade de ter efetuado este trabalho no âmbito do projeto europeu PROETHANOL2G (FP7-ENERGY-2009-BRAZIL; Grant agreement: 251151) e agradeço ao Departamento de Química da Faculdade de Ciências e Tecnologias da Universidade Nova de Lisboa por disponibilizar o acesso ao equipamento de FT-IR e análises de RMN.

## palavras-chave

Líquidos iônicos, pré-tratamento, biomassa lignocelulósica, palha de trigo e hidrólise enzimática.

## resumo

O objetivo deste trabalho foi estudar o pré-tratamento de biomassa lignocelulósica, como a palha de trigo, usando líquidos iônicos (LIs) de modo a obter a separação dos principais componentes, nomeadamente, celulose, hemicelulose e lignina.

O processo de pré-tratamento foi otimizado com base em duas metodologias descritas na literatura utilizando o líquido iônico acetato de 1-etil-3-metilimidazólio ([emim][CH<sub>3</sub>COO]). A metodologia otimizada permitiu separar as frações ricas em hidratos de carbono das frações de lignina, ambas com elevada pureza, e com uma recuperação de LIs até um máximo de 97% da sua massa inicial. Desta forma, o LI pode ser reusado confirmando a flexibilidade do processo desenvolvido. A versatilidade do método foi testada com a investigação de três líquidos iônicos diferentes, nomeadamente hidrogenossulfato de 1-butil-3-metilimidazólio ([bmim][HSO<sub>4</sub>]), tiocianato de 1-butil-3-metilimidazólio ([bmim][SCN]) e dicianamida de 1-butil-3-metilimidazólio ([bmim][N(CN)<sub>2</sub>]). No processo de dissolução de palha de trigo observou-se uma dissolução completa a nível macroscópico apenas para os líquidos iônicos [emim][CH<sub>3</sub>COO] e [bmim][HSO<sub>4</sub>]. O [emim][CH<sub>3</sub>COO] apresentou maior eficiência no processo de dissolução e regeneração da biomassa. Contrariamente, o [bmim][SCN] demonstrou ser o menos eficiente em todo o processo de pré-tratamento. Um comportamento diferente foi observado para o [bmim][HSO<sub>4</sub>], cujo pré-tratamento apresentou similaridades a uma hidrólise ácida. Os pré-tratamentos com [bmim][HSO<sub>4</sub>] e [bmim][N(CN)<sub>2</sub>] permitiram a obtenção de frações ricas em celulose com um conteúdo em hidratos de carbono de 87 a 90%.

Para as frações ricas em celulose provenientes do pré-tratamento com [emim][CH<sub>3</sub>COO] foram efetuados ensaios de hidrólise enzimática para verificar a potencial aplicação destas frações, bem como, avaliar a eficiência das metodologias de pré-tratamento estudadas. Os resultados obtidos demonstraram elevado índice de digestibilidade da celulose e confirmou o elevado teor de glucose presente na fração celulósica obtida pela metodologia otimizada.

A técnica de Espectroscopia de Infravermelho com Transformadas de Fourier (FT-IR) permitiu efetuar análises qualitativas e quantitativas de todas as amostras obtidas nos pré-tratamentos realizados. Para avaliar a pureza dos LIs após os pré-tratamentos utilizou-se a técnica espectroscópica de ressonância magnética nuclear (RMN). Os resultados provenientes dos ensaios de hidrólise enzimática foram obtidos através da técnica cromatográfica de HPLC.

**keywords**

Ionic liquids, pre-treatment, lignocellulosic biomass, wheat straw and enzymatic hydrolysis.

**abstract**

This work is devoted to the pre-treatment of lignocellulosic biomass using ionic liquids (ILs) to separate cellulose, hemicellulose and lignin fractions. Particularly, research was focused on studying the influence of various ILs on the pre-treatment of wheat straw.

The pre-treatment procedure was optimised basing on two methodologies presented in the literature. In the optimised method 1-ethyl-3-methylimidazolium acetate ([emim][CH<sub>3</sub>COO]) IL was used. The developed method is beneficial as allows a separation of highly-purified carbohydrate and lignin-rich samples and permits to recover ILs with a yield of 97wt%. Therefore, the IL could be reused confirming a great flexibility of the developed method. Furthermore, versatility of the method was confirmed by examination of different ILs such as 1-butyl-3-methylimidazolium hydrogensulfate ([bmim][HSO<sub>4</sub>]), 1-butyl-3-methylimidazolium thiocyanate ([bmim][SCN]) and 1-butyl-3-methylimidazolium dicyanamide ([bmim][N(CN)<sub>2</sub>]). Only [emim][CH<sub>3</sub>COO] and [bmim][HSO<sub>4</sub>] ILs were found to be capable to achieve a macroscopic complete dissolution of wheat straw. Considering dissolution and regeneration process, [emim][CH<sub>3</sub>COO] was the most efficient among investigated ILs. On the contrary, [bmim][SCN] demonstrated the lowest efficiency either in dissolution and regeneration or fractionation processes. The [bmim][HSO<sub>4</sub>] showed different behaviour from other ILs exhibiting similarities to acid hydrolysis pre-treatment. Pre-treatments with [bmim][HSO<sub>4</sub>] and [bmim][N(CN)<sub>2</sub>] allowed to recover cellulose rich-samples with a carbohydrate content between 87 to 90wt%.

In order to verify the potential further applicability of obtained carbohydrate-rich fractions as well as to evaluate the pre-treatment efficiency, the cellulose-rich fraction obtained from treatment with [emim][CH<sub>3</sub>COO] was applied for the enzymatic hydrolysis. Achieved results showed a high digestibility of cellulose-rich samples and confirmed a high glucose yield for the optimised methodology.

Qualitative and quantitative analyses of the pre-treatment with ILs were made using the Fourier-Transform Infrared Spectroscopy (FT-IR). The NMR analysis was used to evaluate the purity of ILs after pre-treatments. Results of enzymatic hydrolysis analysis were controlled by the HPLC.

# Contents

Contents.....	I
List of Figures.....	III
List of Tables.....	V
1 Introduction.....	1
1.1 BIOREFINERY CONCEPT .....	1
1.2 LIGNOCELLULOSIC FEEDSTOCK.....	2
1.3 IONIC LIQUIDS .....	8
1.4 BIOMASS PRE-TREATMENT.....	10
1.4.1 Conventional pre-treatment methods .....	10
1.4.2 Pre-treatment with ionic liquids.....	11
1.4.2.1 Lignocellulosic biomass dissolution .....	11
1.4.2.2 Selection of ionic liquids for the pre-treatment .....	13
1.4.2.3 The biomass pre-treatment with ionic liquids.....	14
1.4.2.4 Fractionation of lignocellulosic material.....	16
1.5 ENZYMATIC HYDROLYSIS .....	18
2 Experimental Procedure.....	20
2.1 MATERIALS.....	20
2.2 WHEAT STRAW PRE-TREATMENT WITH IONIC LIQUIDS .....	21
2.2.1 Wheat straw pre-treatment using [emim][CH <sub>3</sub> COO].....	21
2.2.1.1 Method A .....	21
2.2.1.2 Method B .....	22
2.2.1.3 Method C .....	24
2.2.2 Recycling of ionic liquid for the wheat straw pre-treatment.....	26
2.2.3 Wheat straw pre-treatment using different ILS.....	26
2.3 FT-IR SPECTROSCOPY CHARACTERIZATION .....	26
2.3.1 Sample preparation.....	26
2.3.2 FT-IR Spectra Acquisition .....	26
2.3.3 Lignocellulosic material quantification.....	27
2.4 NMR ANALYSES OF ILS.....	27
2.5 ENZYMATIC HYDROLYSIS.....	28
2.6 EXPERIMENTAL ERROR ANALYSIS .....	28
3 Results .....	29

3.1	FEEDSTOCK COMPOSITION ANALYSIS .....	29
3.2	PRELIMINARY EVALUATION OF WHEAT STRAW PRE-TREATMENT USING [EMIM][CH <sub>3</sub> COO].	29
3.3	WHEAT STRAW PRE-TREATMENT USING [EMIM][CH <sub>3</sub> COO] .....	30
3.4	WHEAT STRAW PRE-TREATMENT USING DIFFERENT ILS .....	34
3.5	FT-IR QUALITATIVE AND QUANTITATIVE ANALYSIS.....	35
3.5.1	<i>Characterisation of wheat straw</i> .....	35
3.5.2	<i>Characterisation of pre-treatment samples using [emim][CH<sub>3</sub>COO]</i> .....	36
3.5.3	<i>Quantification of pre-treatment samples using [emim][CH<sub>3</sub>COO]</i> .....	42
3.5.4	<i>Characterisation of pre-treatment samples using different ILS</i> .....	44
3.5.5	<i>Quantification of pre-treatment samples using different ILS</i> .....	48
3.6	WHEAT STRAW PRE-TREATMENT REUSING [EMIM][CH <sub>3</sub> COO] .....	51
3.7	ENZYMATIC HYDROLYSIS .....	51
3.8	NMR ANALYSIS .....	52
4	Discussion.....	54
4.1	PRELIMINARY EVALUATION OF WHEAT STRAW PRE-TREATMENT USING [EMIM][CH <sub>3</sub> COO].	54
4.2	OPTIMISATION OF WHEAT STRAW PRE-TREATMENT USING [EMIM][CH <sub>3</sub> COO] .....	54
4.3	QUANTIFICATION OF PRE-TREATMENT SAMPLES USING [EMIM][CH <sub>3</sub> COO].....	60
4.4	IL EFFECT ON WHEAT STRAW PRE-TREATMENT .....	63
4.5	QUANTIFICATION OF PRE-TREATMENT SAMPLES USING DIFFERENT ILS .....	67
4.6	IL ABILITY TO BIOMASS PRE-TREATMENT .....	70
4.7	WHEAT STRAW PRE-TREATMENT REUSING [EMIM][CH <sub>3</sub> COO] .....	71
4.8	ENZYMATIC HYDROLYSIS .....	71
5	Conclusions.....	74
6	Future Prospects.....	75
7	Bibliography .....	76
	Appendix .....	81

## List of Figures

Figure 1. The biorefinery concept.....	1
Figure 2. Representation of the lignocellulose complex structure. ....	3
Figure 3. Representation of the cellulose hydrogen bonding network. It is visible intra and intermolecular hydrogen bonds. ....	4
Figure 4. Structures of hemicellulose building block units.....	6
Figure 5. Chemical structure of the three monolignol precursors that compose lignin. ....	7
Figure 6. Lignin structure.....	8
Figure 7. Structures of some IL cations and anions. ....	9
Figure 8. Method A process. ....	22
Figure 9. Method B process.....	23
Figure 10. Method C process.....	25
Figure 11. The FT-IR spectrum of wheat straw. ....	36
Figure 12. The FT-IR spectrum of the regenerated material using the method A. ....	37
Figure 13. The FT-IR spectrum of cellulose-rich material using the method B. ....	38
Figure 14. The FT-IR spectrum of hemicellulose-rich material using the method C.....	39
Figure 15. The FT-IR spectrum of lignin-rich material using the method C. ....	40
Figure 16. The FT-IR spectrum of acetone soluble lignin-rich material using the method B.....	41
Figure 17. The FT-IR spectrum of the residual lignin-rich material using the method C. ...	42
Figure 18. The FT-IR spectrum of the regenerated material from the pre-treatment with [bmim][HSO <sub>4</sub> ]. ....	45
Figure 19. The FT-IR spectrum of the cellulose-rich material from the pre-treatment with [bmim][HSO <sub>4</sub> ]. ....	46
Figure 20. The FT-IR spectrum of the residual lignin-rich material from the pre-treatment with [bmim][HSO <sub>4</sub> ]. ....	47

Figure 21. The FT-IR spectrum of the residual lignin-rich material from the pre-treatment with [bmim][N(CN) <sub>2</sub> ]. .....	48
Figure 22. FT-IR spectra of lignin rich-materials from A2 (black) and A3 (red) pre-treatment experiments. ....	55
Figure 23. FT-IR spectra of standard cellulose (black) and original wheat straw (green) comparing with the fractionated samples of cellulose (red) and hemicellulose (blue).....	58
Figure 24. FT-IR spectra of acetone soluble lignin rich-material from method B (blue), lignin rich-material from method C (red) residual-lignin rich from method C (black) pre-treatment experiments. ....	59
Figure 25. Fractionation of wheat straw by method C using [emim][CH <sub>3</sub> COO].....	62
Figure 26. FT-IR spectrum of standard cellulose (black) comparing with spectra of regenerated material (blue) and cellulose-rich material (red) obtained in the pre-treatment with [bmim][HSO <sub>4</sub> ]. ....	66
Figure 27. Fractionation of wheat straw using [bmim][SCN].....	67
Figure 28. Fractionation of wheat straw by method C using [bmim][N(CN) <sub>2</sub> ]. ....	68
Figure 29. Fractionation of wheat straw by method C using [bmim][HSO <sub>4</sub> ]. ....	69

## List of Tables

Table 1. Contents of cellulose, hemicellulose and lignin in different lignocellulose raw materials. ....	4
Table 2. Macromolecular composition of wheat straw in % (w/w).....	29
Table 3. The wheat straw regeneration after 1, 6 and 16h of pre-treatment with [emim][CH <sub>3</sub> COO].....	30
Table 4. Results of the wheat straw pre-treatment with [emim][CH <sub>3</sub> COO] using method A.....	31
Table 5. Results of the wheat straw pre-treatment with [emim][CH <sub>3</sub> COO] using method B.....	31
Table 6. The fractionation of the regenerated material and material losses using method B.....	32
Table 7. Results of the wheat straw pre-treatment with [emim][CH <sub>3</sub> COO] using method C.....	32
Table 8. The fractionation of the regenerated material and material losses using method C.....	33
Table 9. Results of the wheat straw pre-treatment with [bmim][SCN], [bmim][N(CN) <sub>2</sub> ] and [bmim][HSO <sub>4</sub> ] using method C.....	34
Table 10. The fractionation of the regenerated material and material losses in pre-treatments with [bmim][SCN], [bmim][N(CN) <sub>2</sub> ] and [bmim][HSO <sub>4</sub> ] ILs using method C.....	35
Table 11. The FT-IR quantification of fractionated samples by the method A. ....	43
Table 12. The FT-IR quantification of fractionated samples by the method B.....	43
Table 13. The FT-IR quantification of fractionated samples by the method C.....	44
Table 14. FT-IR quantification of fractionated samples by the method C using [bmim][SCN].....	49

Table 15. The FT-IR quantification of fractionated samples by the method C using [bmim][N(CN) <sub>2</sub> ]. .....	49
Table 16. The FT-IR quantification of fractionated samples by the method C using [bmim][HSO <sub>4</sub> ]. .....	50
Table 17. Results of the wheat straw pre-treatment with the reused [emim][CH <sub>3</sub> COO].....	51
Table 18. Glucose yields (% w/w <sub>biomass</sub> ) and total sugar yields (% w/w) of enzymatic hydrolysis of cellulose-rich samples from methods A and B, regenerated material from method A, standard cellulose and native wheat straw. ....	52
Table 19. The FT-IR quantification of regenerated materials obtained from wheat straw pre-treatment by [emim][CH <sub>3</sub> COO], [bmim][SCN], [bmim][N(CN) <sub>2</sub> ] and [bmim][HSO <sub>4</sub> ]....	70

# 1 Introduction

## 1.1 Biorefinery concept

The biorefinery is a concept aiming at a maximal exploitation of the carbohydrate-rich raw material to produce energy (fuel, heat, power) and high value added products (e.g. chemicals).<sup>1</sup> The biorefinery concept is presented in Figure 1. In general, biorefinery is divided into the two platforms to promote different product routes. The biochemical platform is currently based on biochemical conversion processes and focuses on fermentation of sugars extracted from biomass feedstocks. The thermochemical platform is based on thermochemical conversion processes and focuses on gasification of biomass feedstocks resulted in by-products. Such operations are based on production of high-value and low-volume co-products compared with low-value and bulky biofuels, which creates an economic competitiveness, especially when different biomass feedstocks as primary sources are used.<sup>2-4</sup>

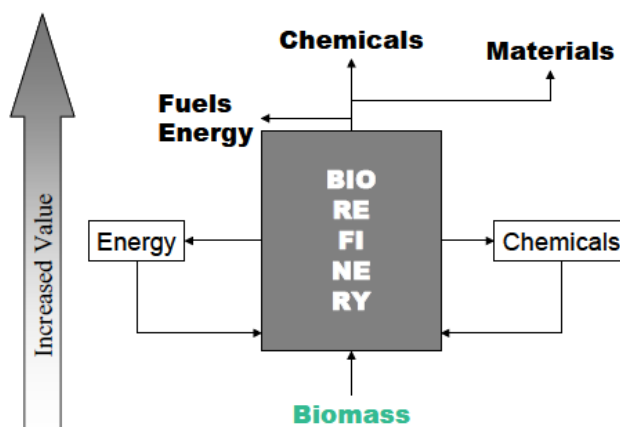


Figure 1. The biorefinery concept.

The implementation of the biorefinery concept is challenging due to technological limitations of the process, and thus, the economic feasibility of processes is questionable. Even so, in the last decade, the significant trend and on-going development of the biorefinery is observed. In Europe the biorefinery's progress is mostly driven by general concerns related to the oil shortage and green-house gas emission, thus significant efforts are taken to develop new, more sustainable processes based on renewable feedstock. One of most common and well known processes is production of biofuels. Global production of

biofuels has increased very fast as a consequence of the investment rising.<sup>2</sup> Independently of the generation of biofuels, each type of biofuels has its own limitation, mostly dependent upon the feedstock chosen and production process adopted which lead to different prices of commercialization.<sup>2</sup> The European Union has a leading role in the World in the implementation of the renewable energy in house-hold and industrial consumption. The EU directive established a 20% share of energy from renewable resources to be achieved, and a level of 10% for biofuels to be accomplished in Portugal by 2020.<sup>5</sup> However, to satisfy social and environmental aspects of biofuel production, a complex biorefinery concept must be explored leading to a maximal valorisation of non-food and non-feed competitive feedstocks.

## **1.2 Lignocellulosic feedstock**

Major types of feedstocks for biorefinery processes are lignocellulosic biomass such as hardwood (willow, poplar, and eucalyptus), softwood (pine, fir and spruce), grasses (miscanthus, switchgrass). Apart of them, agricultural residues (wheat straw, sugarcane bagasse, and corn stover), forest residues (sawdust, thinning rests), domestic and municipal solid wastes, and food industry residues are considered as feedstocks as well.<sup>6-8</sup> Lignocellulosic materials have a worldwide annual production of 10<sup>11</sup> million tonnes,<sup>9</sup> which represent a potential source of a clean, uniform and a low-cost raw material for large-scale and environmentally sustainable biorefineries.<sup>10</sup> Generally, main components of lignocelluloses are separated by thermochemical and/or physical methods as pre-treatment exposing carbohydrate fractions. Next carbohydrates are hydrolysed to sugar monomers and subsequently converted to bioalcohols (ethanol, butanol), biohydrogen or methane by fermentation processes, in biochemical platforms.<sup>11, 12</sup> Not only fuels can be produced from lignocellulose but also many other value-added products, such as: enzymes, furfural and its derivatives, proteins, aminoacids, lipids, organic acids, biopolymers and other miscellaneous compounds.<sup>13</sup>

This great variety of products can be possible to obtain due to the continuous investment in the research and development of new knowledge about integrated biofuel and high value added compounds' production. However, independently of the final product, the major bottleneck of each process with the lignocellulosic material is a deconstruction. There is a lot of research devoted to the deconstruction of biomass that allows to perform sufficient

separation of lignocellulosic biomass fractionation.<sup>14</sup> The major challenge in the biomass deconstruction is related to the physical and chemical composition of the lignocellulosic material. Basically, lignocellulose is located in the cell wall matrix of plant cells and is comprised by three major components: cellulose, hemicellulose and lignin. Cellulose and hemicellulose constitute the carbohydrate fraction, where cellulose is a semi-crystalline fibrous polysaccharide and hemicellulose is an amorphous polysaccharide. Lignin is a very complex and amorphous phenylpropanoid polymer.<sup>15</sup> Inside the lignocellulose compact structure, cellulose appears to be a core of the complex and hemicellulose is situated between both micro- and macro-fibrils of cellulose. Lignin provides a structural role of the matrix in which cellulose and hemicellulose are embedded.<sup>16</sup> A design outline of the lignocellulose complex structure is presented in Figure 2.

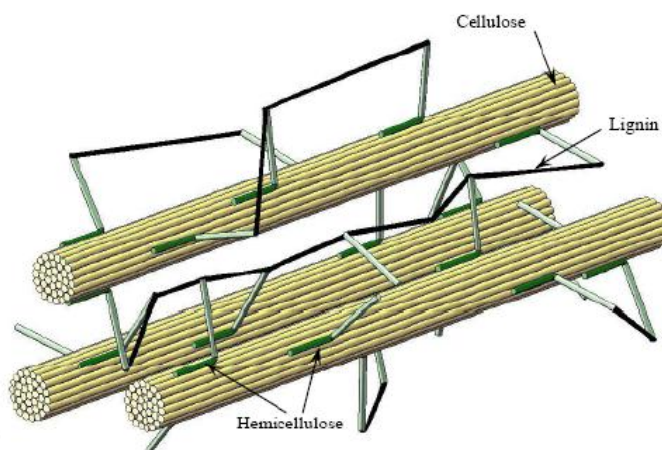


Figure 2. Representation of the lignocellulose complex structure.<sup>17</sup>

The composition of lignocellulosic materials depends mainly on the species, origin and age of biomass. The composition of several most popular types of lignocellulosic biomass is shown in Table 1.

Cellulose ( $C_6H_{10}O_5$ )<sub>n</sub> is a linear homopolysaccharide structurally composed by cellobiose (4-O-β-D-glucopyranosyl-D-glucose) repeating units. However, cellulose is more commonly associated to glucose (D-glucopyranose) units linked together by β-(1→4) glycosidic bond, whereas the hemiacetal group from the glucose unit reacts with the hydroxyl group from other glucose unit.<sup>16, 18</sup> This reaction generates cellobiose units that constitute repeating extended polymer.

Table 1. Contents of cellulose, hemicellulose and lignin in different lignocellulose raw materials.<sup>19</sup>

Lignocellulosic materials	Cellulose/%	Hemicellulose/%	Lignin/%
Hardwoods stems	40–55	24–40	18–25
Softwood stems	45–50	25–35	25–35
Nut shells	25–30	25–30	30–40
Corn cobs	45	35	15
Grasses	25–40	35–50	10–30
Wheat straw	30	50	15
Leaves	15–20	80–85	0
Cotton seed hairs	80–95	5–20	0
Coastal Bermuda grass	25	35.7	6.4
Switchgrass	45	31.4	12.0

One particularity of the cellulose polymer is a highly ordered structure and spatial conformation due to its chemical constitution. Each glucose unit has three hydroxyl groups that are evenly distributed on both sides, allowing the interaction leading to the formation of intra and intermolecular hydrogen bonds.<sup>20</sup> This strong hydrogen bonding network creates several parallel chains attached to each other, as exemplified in Figure 3.

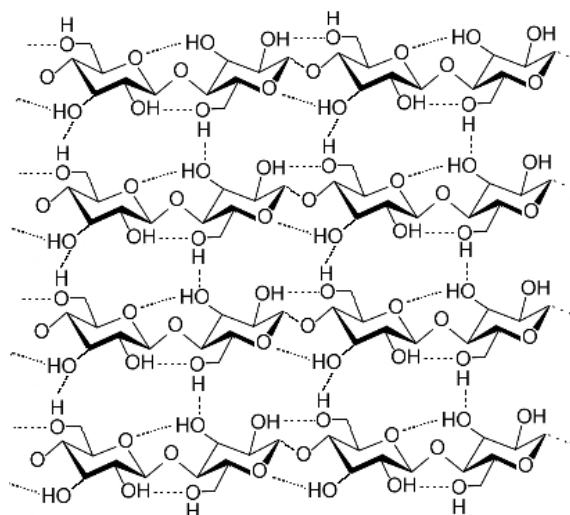


Figure 3. Representation of the cellulose hydrogen bonding network. It is visible intra and intermolecular hydrogen bonds.<sup>21</sup>

The number of glucose units that make up one single chain of cellulose is designated as degree of polymerization (DP). This number depends on the cellulose origin. The DP can achieve 800-10000 glucose units per cellulose chain resulting in a variable molecular weight.<sup>22</sup>

Cellulose is a relatively hygroscopic material absorbing 8-14% water under normal atmospheric conditions. However, it is insoluble in water and other common solvents, where it swells, due to its fibril structure and presence of intra- and intermolecular hydrogen bonds. Thus, solubility of cellulose is strongly related to the degree of polymerization, which could be a drawback for industrial applications.<sup>16, 23</sup> In order to fulfil various demands for its industrial use, cellulose is often modified by physical, chemical, enzymatic, or genetic procedures improving solubility, properties and behaviour of the polymer.<sup>24, 25</sup>

Hemicellulose, unlike cellulose, is a non-crystalline heteropolysaccharide and classically defined as an alkali-soluble material. The term hemicellulose is used to represent a complex family of polysaccharides such as arabinan, xylan, arabinoxylan, glucomannan, galactan, and others, which have different composition and structure depending on their source and extraction method.<sup>16, 26</sup> These polysaccharides have a lower molecular weight than cellulose and they are formed by a wide variety of building blocks including pentose units (mainly xylose, rhamnose and arabinose), hexose units (mostly glucose, mannose and galactose) and uronic acids (e.g., 4-*O*-methyl-glucuronic and galacturonic acids).<sup>18, 27</sup> Examples of sugar unit structures are shown in Figure 4.

The high complexity of hemicellulose, namely type, ratio contents of sugar units and structural conformation, is associated to the different building blocks that constitute this polysaccharide. Hemicellulose structure can be helical, unbranched or branched.<sup>18</sup> Specifically, the hemicellulose polysaccharides form rod-shaped structure with branches and side chains folded back to the main chain by the creation of hydrogen bonding interaction. This rod-like structure facilitates interaction of hemicellulose polysaccharides with cellulose, resulting in a tight association that gives great stability to aggregate.<sup>18</sup>

Main hemicellulose polymers are xylans that exhibit different structures depending on the type of branching, mostly by a backbone chain of  $\beta$ -(1 $\rightarrow$ 4)-linked xylopyranose units (xyloses).<sup>28-30</sup>

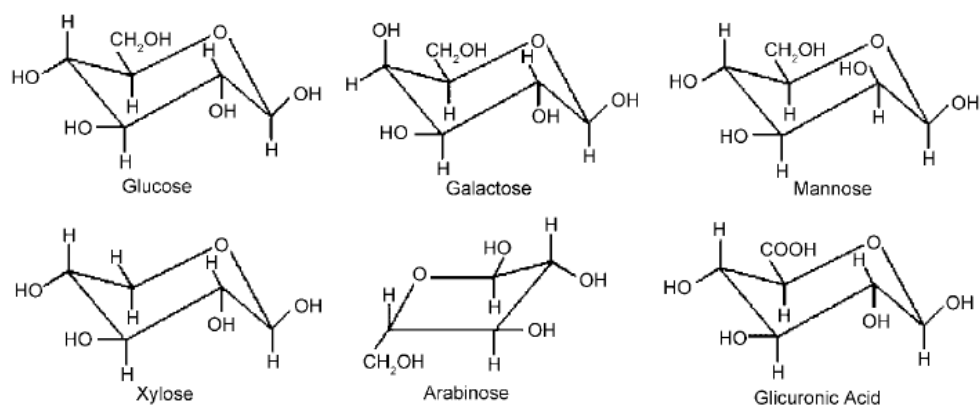


Figure 4. Structures of hemicellulose building block units. Adapted from<sup>12</sup>

Hemicellulose is a branched polymer of a low molecular weight with a DP of 80 to 200, lower than the DP of cellulose.<sup>31, 32</sup> Generally, hemicellulose possesses a high degree of polydispersity, polydiversity and polymolecularity (a broad range of size, shape and mass characteristics), which is dependent upon extraction treatments and the origin material.<sup>16</sup> The highly branched structure and the presence of acetyl groups connected to the polymer chain in hemicellulose lead to lack of crystalline structure.<sup>22</sup>

Even an amorphous hemicellulose is insoluble in water at a low temperature. Nevertheless, hydrolysis of hemicellulose starts at lower temperatures in comparison with cellulose, which renders better solubility at higher temperatures. This is caused by the lack of crystalline structure that establishes a lesser and weaker hydrogen bonding network than that observed in cellulose.<sup>33</sup>

Hemicellulose has particularity of being used either as fermentation sugars to produce biofuels or as raw material for high-value products, namely high-performance polymers as replacements for polymers prepared from petrochemicals.<sup>32</sup> Recently, a growing interest has emerged in hemicellulose as raw material for various technological applications, i.e. in synthesis of cationic polymers,<sup>34</sup> hydrogels,<sup>35</sup> long-chain ester derivatives,<sup>35, 36</sup> and thermoplastic xylan derivatives.<sup>36, 37</sup>

Lignin is a statistically amorphous branched heteropolymer with phenylpropane units as predominant building blocks.<sup>38</sup> This phenolic macromolecule is formed by three monolignol precursors with different degrees of methoxylation (-OCH<sub>3</sub> groups), designated coniferyl alcohol, sinapyl alcohol, and *p*-coumaryl alcohol which are shown in Figure 5. In lignification, lignols can react between each other and can be incorporated into lignin

forming phenylpropanoids guaiacyl (G), syringyl (S) and *p*-hydroxyphenyl (H), respectively.<sup>16, 39</sup>

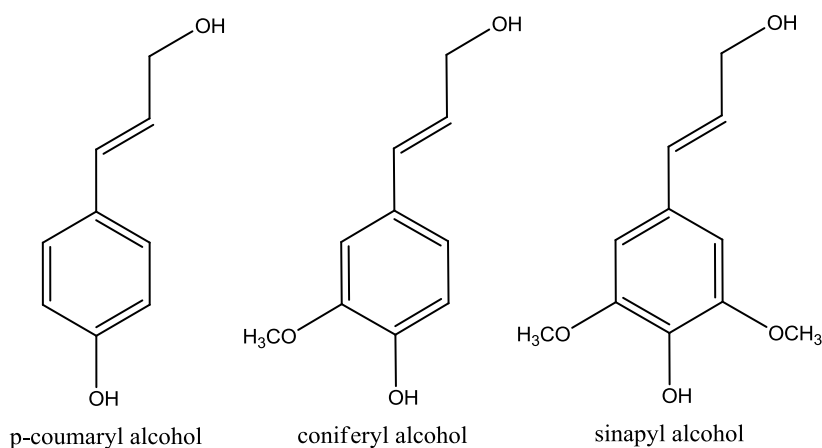


Figure 5. Chemical structure of the three monolignol precursors that compose lignin.

The combination of the three monolignol units form a complex macromolecule with different linkages and various functional groups.<sup>39</sup> Lignin forms two types of linkages between monolignol units: C-C and C-O-C (ether) bonds. Interactions between diverse monolignol free radicals give a high complexity of lignin and by variety of functional groups present in the structure, lignin exhibits great reactivity. The nature of the lignin polymerization reactions results in the formation of a three-dimensional, highly-branched, interlocking network of essentially infinite molecular weight,<sup>39</sup> as shown in Figure 6.

As a by-product of biorefining, lignin has been utilised as a low-value heating fuel, binder, dispersant, emulsifier and sequestrant.<sup>40, 41</sup> Nowadays, isolated lignin is required as a source of high-value molecules, such as aromatic chemicals, that can be obtained by delignification.<sup>40</sup> More recently, research studies have identified polyurethane and polyesters derived from lignin as a valuable renewable bioplastic resource.<sup>42-44</sup> The alkylated lignin derivatives exhibit tensile strength properties similar to polystyrene and were employed to prepare promising thermoplastic blends with aliphatic polyesters.<sup>43, 45</sup> The growing interest in developing new lignin-based products is also driven by the fact that lignin is a renewable, low-cost and environmentally benign bioresource.<sup>46</sup>

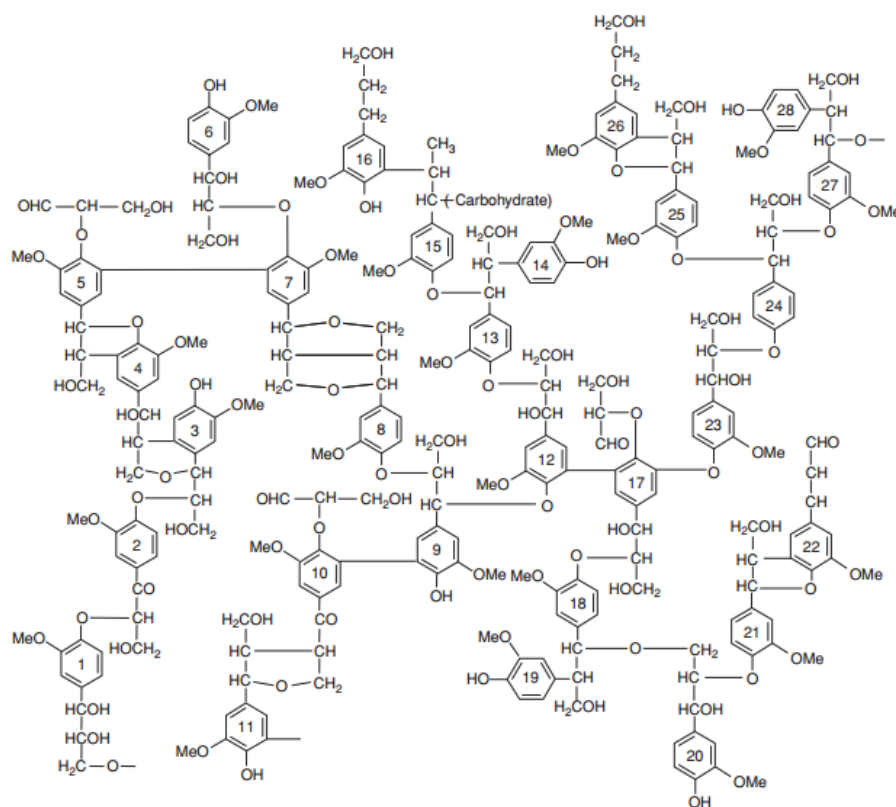


Figure 6. Lignin structure.<sup>47</sup>

### 1.3 Ionic liquids

Ionic liquids are salts with a low melting point (below 100°C). ILs are constituted by a large asymmetric organic cation and a polyatomic organic or inorganic counterion.<sup>48</sup> The example of some cations and anions of ILs are presented in Figure 7.

ILs demonstrate great variety of physico-chemical properties among which the most characteristic are: high polarity,<sup>49</sup> great thermal stability (even above 300°C);<sup>50</sup> high conductivity, large electrochemical window,<sup>51</sup> great solvent power,<sup>52-58</sup> negligible volatility,<sup>59, 60</sup> non-flammability. The great solvent power and practical non-volatility are extremely important for industrial applications as they allow to substitute volatile organic compounds (VOCs). ILs demonstrate excellent solvent capacities for both polar and nonpolar compounds making them remarkable as solvents for chemical reactions and separations. The solubility of ILs is largely determined by the ability of the salt to act as a hydrogen-bond donor and/or an acceptor as well as by the charge delocalisation in IL anions.

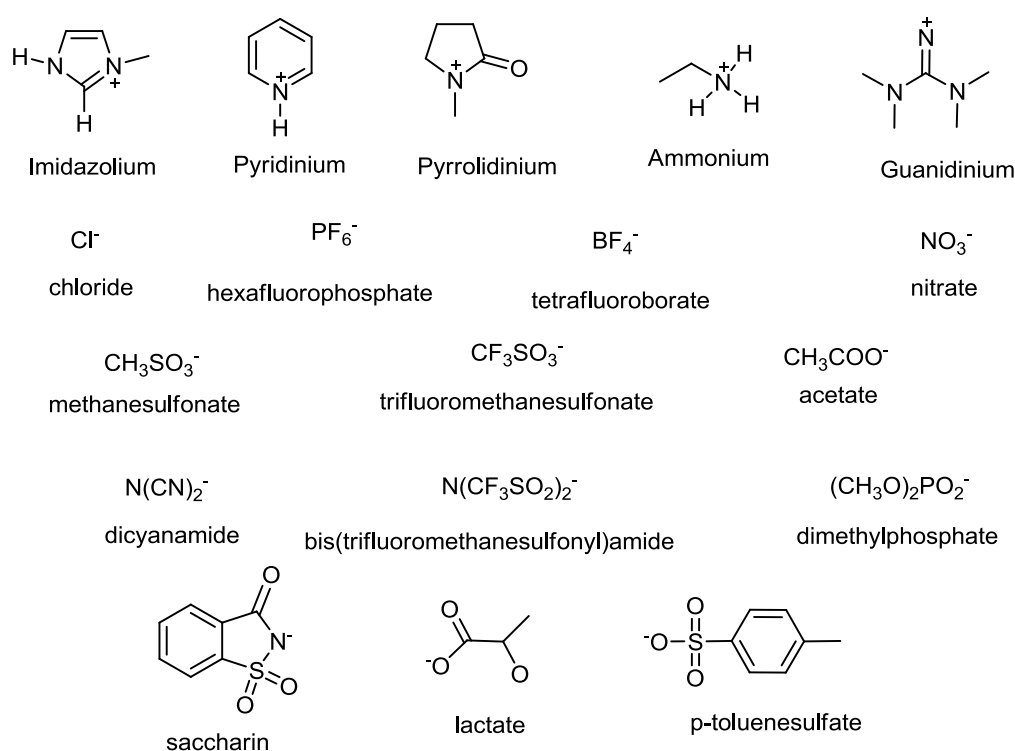


Figure 7. Structures of some IL cations and anions. Adapted from<sup>61</sup>

The current state of the art allows to obtain almost unlimited number of ILs possessing a wide range of chemical and physical properties. For example, density and viscosity can be easily tailored by changing the IL structure. Usually ILs are denser than water ( $1 - 1.6 \text{ g}\cdot\text{cm}^{-3}$ ), although several phosphonium-based ILs possess density lower than  $1 \text{ g}\cdot\text{cm}^{-3}$ .<sup>62</sup> The viscosity is very often one of obstacles in chemical processes as it determines the mass transfer. The viscosity values for ILs are generally up to 3 times higher than conventional organic solvents.<sup>62, 63</sup>

The purity of ILs is a very important issue concerning their applications as solvents. One of the common impurities of ILs is water and the behaviour of ILs towards water is an individual characteristic of each salt. One of examples is the dissolution of cellulose, in which water acts as an antisolvent decreasing solubility.<sup>64</sup>

The toxicity and biodegradability of ILs are currently being extensively studied.<sup>65, 66</sup> Biodegradable and non-toxic ILs are considered as a green alternative for traditional VOCs,<sup>67</sup> such as acetone, toluene, benzene, hexane. This is of an extreme importance to sustainable chemistry in lignocellulosic treatments and in other chemical processes.

## 1.4 Biomass pre-treatment

Lignocellulosic biomass is a complex matrix constituted by cellulose, hemicellulose and lignin. The practical use of this rich composition requires pre-treatment that allows for fractionation of this feedstock into cellulose, hemicellulose and lignin fractions. Among various classifications of biomass pre-treatment the most common is classification determined by the historical development. Pre-treatments can be divided between conventional and novel pre-treatments. This thesis demonstrates results obtained via a novel pre-treatment, namely with ILs; therefore, only a brief introduction to conventional pre-treatments is presented below.

### 1.4.1 Conventional pre-treatment methods

The principal goal of the lignocellulosic pre-treatment is the removal of lignin and hemicellulose content, increase the material porosity (accessible surface area) and reduce cellulose fibre crystallinity.<sup>68, 69</sup> These factors allow to obtain better cellulose hydrolysis rates, but there is still a necessity: (1) to improve the sugars yield; (2) to avoid degradation or loss of carbohydrates; (3) to avoid formation of inhibitory by-products to the subsequent hydrolysis and fermentation processes; and (4) to be cost competitive.<sup>19</sup> These requirements make the pre-treatment a crucial step for the biochemical conversion of lignocellulosic biomass into valuable products.

Pre-treatment technologies are usually classified as physical, chemical, physicochemical, and biological. Physical pre-treatments, such as chipping, milling and gridding, are used to decrease the biomass particle size and the degree of polymerization, making material handling easier for subsequent processing steps.<sup>69</sup> Chemical pre-treatments are associated to chemical reactions that disrupt interactions of lignocellulosic components. The chemical reactions are initiated by a ranging of chemicals as for example, alkali (NaOH, Ca(OH)<sub>2</sub>, NaOH-urea, Na<sub>2</sub>CO<sub>3</sub>), oxidizing agents (H<sub>2</sub>O<sub>2</sub> and ozone), acids (H<sub>2</sub>SO<sub>4</sub>, HCl, HNO<sub>3</sub>), salts (inorganic salts with acidic properties, ammonium salts) and even organic solvents (organic acids, ethanol, acetone, phenols).<sup>13</sup> Generally, chemical pre-treatments tend to dissolve hemicellulose and lignin in order to expose cellulose to acid and/or enzymatic hydrolysis.<sup>16</sup> Steam explosion, ammonia fibre explosion and liquid hot water (autohydrolysis) are main examples of physicochemical pre-treatments. This type of pre-

treatment is generally efficient but uses severe conditions, such as high temperature and pressure rise costs of the pre-treatment process.

Pre-treatment techniques characterised by different physical and chemical conditions applied, give diverse results in the final treated biomass. Because of that, depending on specific requirements of the lignocellulosic processing, pre-treatment needs to be chosen and an evaluation of advantages and disadvantages of each one should be taken in account considering an individual requirement of the process. However, it is important to point out that none of the currently known processes is a highly selective and efficient for the satisfactory and versatile use, thus, new methodologies are still studied broadly. One of them is the IL application that demonstrated promising perspectives for a near future. It was found that pre-treatments with ILs offer advantages over conventional methods, and thus, can serve as a good alternative for the lignocellulosic biomass deconstruction.

## **1.4.2 Pre-treatment with ionic liquids**

### **1.4.2.1 Lignocellulosic biomass dissolution**

The ability of ILs to dissolve carbohydrates and lignin is considered as an effective disrupting of the intricate network of non-covalent interactions between these polymers. A high chloride concentration originated from 1-butyl-3-methylimidazolium chloride ([bmim][Cl]) was found to be responsible for breaking the extensive and well organized hydrogen-bonding network of cellulose.<sup>64</sup> During dissolution of carbohydrates in [bmim][Cl] hydrogen bonds between chloride ions of the IL and hydroxyl protons of sugar units from carbohydrates are formed in a 1:1 stoichiometry.<sup>70</sup> The IL cation affects the dissolution mainly interacting with cellulose hydroxyl oxygen groups but also indirectly by tuning the concentration of the counterion. However, the interaction between the carbohydrate and the anion of an IL was found to be predominant compared with interactions of carbohydrate with the cation.<sup>70, 71</sup>

A partial solubility of wood chips is possible when solvents such as [bmim][Cl]/DMSO-*d*<sub>6</sub> (84/16wt%) are used. Swelling and the size reduction of wood particles during dissolution was noticed. The increasing of colour deep and viscosity of the solution mixture was observed, indicating that dissolution occurred.<sup>72-74</sup> A complete dissolution in the temperature range from 80 to 130°C after 8 hours was achieved (8wt% of dried wood sawdust samples of Norway spruce and Southern pine) with both [bmim][Cl] and 1-allyl-3-

methylimidazolium chloride ([amim][Cl]) ILs. For complete or partial dissolution of wood in these ILs the water content and the particle size of wood samples are responsible.<sup>75</sup> Water was found to significantly reduce solubility of wood in ILs<sup>64, 76</sup> and smaller particles are easier dissolved.<sup>75</sup>

Softwood (southern yellow pine) and hardwood (red oak) can be dissolved in 1-ethyl-3-methylimidazolium acetate ([emim][CH<sub>3</sub>COO]). More than 90% (w/w) of the added wood was dissolved after mild grinding, at 110°C within 16 hours. [Emim][CH<sub>3</sub>COO] was found to be more effective in dissolving biomass than [bmim][Cl] and [amim][Cl] ILs. A reduced time of dissolution was attained when microwave or ultrasound irradiation were used instead of simply heating in an oil bath.<sup>72, 77</sup> Enhancement in the dissolution by irradiation is attributed to the ionic structure of ILs. Therefore, the frequency of collisions between anions and cations of ILs and wood macromolecules increased leading to fast and effective dissolutions. The microwave irradiation depolymerizes the cross-linked phenylpropanoid units of lignin, and hydrogen bonding interactions between the wood matrix and the IL anion are intensified.<sup>72</sup> The improvement in the dissolution can be accomplished when a prior ball-milling treatment of biomass is applied.<sup>78, 79</sup> By breaking the native structure with ball-milling, a reduction of molecular weights of lignin and carbohydrate polymers is observed. An effective reduction of polymers leads to a subsequent dissolution enhancement in ILs.<sup>78</sup>

A high-throughput screening in the dissolution of cellulose and wood chips in ILs with 5% (w/w) at 90°C for 12h allowed to find that only 1-ethyl-3-methylimidazolium chloride [emim][Cl], [bmim][Cl] and 1,3-dimethylimidazolium-dimethylphosphate ([dmim][(OCH<sub>3</sub>)<sub>2</sub>PO<sub>2</sub>]) were able to partially dissolve different wood chips (spruce, silver fir, common beech and chestnut). [Emim][CH<sub>3</sub>COO] was the most efficient IL in dissolving cellulose and [amim][Cl] was the most suitable IL used in dissolving all tested wood. Only Silver fir was not completely dissolved by [emim][CH<sub>3</sub>COO].<sup>80</sup> In a 24h heating (100°C) wheat straw and pine wood, [emim][CH<sub>3</sub>COO] demonstrated to be a poor solvent. At the same conditions, [bmim][Cl] was the most efficient IL in the dissolution of straw and results with [emim][Cl] were more promising considering dissolving both types of biomass. For the best results, transparent solutions were visualized but biomass fibres could still be found after filtration, indicating that complete dissolution was not achieved.<sup>81</sup> A low solubility of wood flour (<5g/kg) and a high solubility of microcrystalline cellulose

(>100g/kg) in [emim][CH<sub>3</sub>COO] was explained by presence of lignin.<sup>73</sup> Microscopic observations indicate that [emim][CH<sub>3</sub>COO] is capable to completely dissolve all major components found in the plant cells of switchgrass after 3h at 120°C.<sup>82</sup> 1-Butyl-3-methylimidazolium acetate ([bmim][CH<sub>3</sub>COO]) dissolved poplar wood in 96wt% of the loaded wood at 130°C during 12h, while [bmim][Cl] only achieved 23wt% of poplar dissolution.<sup>83</sup> This indicates that [CH<sub>3</sub>COO] anion has a great affinity for the dissolution of lignocellulose.

Presented results are affected by the biomass type and size, IL/biomass ratio, temperature and time of dissolution, water content in the solution mixture and others. However, [bmim][Cl], [amim][Cl], [emim][Cl] and [emim][CH<sub>3</sub>COO] demonstrated to be the most efficient ILs in dissolving lignocellulosic biomass. Moreover, a recent study on new ILs show that there is still a room for improvement in dissolution of carbohydrates.<sup>84</sup>

#### **1.4.2.2 Selection of ionic liquids for the pre-treatment**

The selection of ILs for lignocellulosic biomass dissolution is a very challenging issue due to large variety of factors needed to be considered. Basing on the comprehensive review on dissolution of carbohydrates in ILs,<sup>55</sup> it can be stated that ILs constructed by bulky cation and chloride type anion may decrease the concentration of active chloride ion, thus reduce its solvating capacity for both cellulose and lignin.<sup>64</sup> A smaller anion is preferable to be able to diffuse faster within the lignocellulosic matrix as in case of chloride anion. Nevertheless, improvements in lignocellulose dissolution are related with the hydrogen bond basicity of the IL anion. Strong hydrogen bond basicity is effective in weakening the hydrogen-bonding network of polymer chains.<sup>85</sup> The increased basicity of [CH<sub>3</sub>COO]<sup>-</sup> makes it more efficient in disrupting the inter- and intramolecular hydrogen bonding in biopolymers than chloride ion. A lower viscosity and melting point of [emim][CH<sub>3</sub>COO] facilitate the dissolution and handling of the mixture, which makes this IL to be a better solvent than chloride-based ILs.<sup>77</sup> 1-Ethyl-3-methylimidazolium glycinate ([emim][Gly]) was also found to be efficient in processing of biomass.<sup>86</sup>

The viscosity of ILs impacts mixing and mass transfer of lignocellulose and IL itself. As an example, less viscous ILs extracted more amounts of carbohydrates from the bran.<sup>85</sup> ILs with adequate polarity demonstrated good ability to extract polysaccharides in short times. 1-Ethyl-3-methylimidazolium phosphinate ([emim][PO(O)H<sub>2</sub>]), a low viscous and highly

polar IL, allows for rapid extraction of cellulose and other carbohydrates from bran under mild conditions.<sup>85</sup> In dissolution of wood in [benzylmim][Cl], the benzyl ring from the IL cation could interact with phenyl aromatic rings of lignin by  $\pi$ - $\pi$  interactions and a viscous transparent solution appeared indicating good solubility at process conditions. Difficulties in handling with 1-benzyl-3-methylimidazolium chloride ([bzmim][Cl]) due to its high viscosity seem to be a major drawback of its use.<sup>75</sup>

### 1.4.2.3 The biomass pre-treatment with ionic liquids

General procedure assumes the processing of the biphasic mixture (lignocellulosic material and IL at the certain solid/liquid ratio) at a determined temperature for a determined period of time with rigorous stirring. The literature review shows that dissolution can be partial or complete, although complete biomass dissolution improves the efficiency of the treatment. Usually after this step the regeneration of biomass with an addition of a precipitating solvent, such as water, acetone, dichloromethane, and acetonitrile is performed.<sup>74</sup> In the dissolution of wood chips in [bmim][Cl] (100°C, 16h) with an addition of referred precipitating solvents, the regenerated biomass fraction composed essentially by cellulose was obtained. The regenerated carbohydrate-rich material was found to have purities, physical properties, and processing characteristics comparable to those of cellulose standard. The reconstitution yield of biomass ranged from 30 to 60wt%.<sup>74</sup> After biomass filtration a clear and dark brown solution was obtained and by washing with several times with water/DMSO, and the regenerated biomass became white indicating the presence of mainly carbohydrates.<sup>72</sup>

After regeneration, the crystallinity of cellulose is abruptly reduced in comparison with that of cellulose from the original lignocellulosic material. Microscopic studies indicated that after an addition of water, the precipitation of fibrous structures of cellulose (300–500nm long) occurs. By fluorescence techniques, it was observed that lignin appears to be removed from the regenerated product. Therefore, it was concluded that disruption of the lignin–carbohydrate complex occurred simultaneously with cellulose crystallinity reduction.<sup>82</sup> In the pre-treatment using [emim][CH<sub>3</sub>COO] and a dilute acid pre-treatment of switchgrass, little or no change in cellulose crystallinity was noticed for untreated and dilute acid pre-treated switchgrass, in contrary to the pre-treatment with IL that caused a structural transformation from cellulose I to cellulose II.<sup>87</sup> The regeneration method also

influences this occurrence where a vigorous stirring was required. It may partially inhibit the induction of crystalline ordering within the regenerated sample forming an amorphous material.<sup>75</sup>

In the regeneration process<sup>80, 88</sup> water molecules form hydrodynamic shells around ions of the IL disrupting the direct interactions of IL ions to the cellulose. Thus, intra- and intermolecular hydrogen bonds are rebuilt and cellulose precipitates.<sup>80</sup> However, not only cellulose can be dissolved but also other compounds of lignocellulose interact with the IL ions, such as hemicellulose and lignin. Addition of water to pre-treated biomass results in the precipitation of carbohydrates for downstream processing and lignin appears to be partially extracted in the IL/water mixture. The extent of delignification and interaction of lignin with the precipitating solvent, IL, or carbohydrates dictate the purity of the regenerated carbohydrate for further saccharification and sugar yield.<sup>82</sup> It was stated that lignin was first removed in the pre-treatment of rice straw with [emim][CH<sub>3</sub>COO]. The opposite was verified by evaluating the precipitation and composition of regenerated samples from wood sawdust treatment with [amim][Cl]. In the obtained regenerated material the lignin content increased due to the inexistence of delignification and simultaneous dissolution of some polysaccharide component. This may indicate differences in the mode of dissolution between [amim][Cl] and [emim][CH<sub>3</sub>COO] or it may result from differences of used biomass. Precipitation is dependent upon molecular weight, and dissolved a higher molecular weight and partially dissolved wood components precipitate first.<sup>78</sup>

The choice of the antisolvent is needed to be carefully considered because it affects the yield of the regenerated wood. A yield of regenerated wood was found to be higher in water than in methanol due to the easiness and strength of the hydrogen bond formation between anti-solvent and biomass fraction.<sup>89</sup> Mixtures of precipitating solvents can also be used in order to obtain improved lignin extraction yields with simultaneous high regeneration yields of carbohydrate fractions. A mixture of acetone and water in 7:3 ratio allowed to achieve nearly 100wt% of lignin (Indulin AT from Sigma Aldrich) solubility.<sup>86</sup> The pre-treatment process with ILs increases the cellulose surface accessible to cellulase and then enhances the catalytic efficiency of such enzyme.<sup>90</sup> In addition to the ability of IL to reduce cellulose crystallinity and lignin content, other factors such as the capability to

promote inter-crystalline swelling and reduction in fibre size may play an important role in determining efficiency of an IL as a pre-treatment solvent for lignocellulosic biomass.<sup>91</sup>

#### **1.4.2.4 Fractionation of lignocellulosic material**

The subject of the lignocellulosic biomass pre-treatment by ILs is very recent. With this treatment it is possible to separate main components of lignocellulose applying different fractionation after dissolution of biomass in ILs. Different approaches in the fractionation were accomplished depending on IL, lignocellulosic biomass (type, moisture, size and load), temperature, time of the pre-treatment and antisolvent used.

Until now, [emim][CH<sub>3</sub>COO] seems to be the most suitable IL for the pre-treatment of lignocellulosic biomass, once it presents good solubility properties for these materials and by this is commonly studied. In a 5% (w/w) dissolution of southern yellow pine in [emim][CH<sub>3</sub>COO] (110°C, 16h) approximately 59% of original carbohydrates was recovered in the regenerated material. Additionally, around 31% of the original lignin was obtained in free form and 38% linked to carbohydrates as a part of the reconstituted wood, leading to a lignin reduction of 26.1%. The same treatment used for red oak allowed achieving a 34.9% of lignin reduction. Hence, regenerated materials contain less lignin than the original wood, which means a fairly good delignification at a low temperature. However, significant losses of carbohydrates and lignin were observed during the fractionation process. In the case of pine pre-treatment, a total loss of 41% and 31% of original carbohydrates and lignin was reported.<sup>77</sup> In the treatment of the wood flour with [emim][CH<sub>3</sub>COO] approximately 63% of the initial lignin after 90min at 130°C was extracted with a 16% of cellulose and 26% of xylans. Therefore, the process showed a significant delignification with small losses of carbohydrates after the pre-treatment.<sup>73</sup> The decrease in temperature to 90°C and increase in time of the pre-treatment to 24 hours for the same biomass loading allowed to extract nearly 50% of lignin from the initial wood flour sample.<sup>91</sup> This indicated a great influence of applied conditions (temperature and time) in the pre-treatment of lignocellulosic biomass.

A 3h pre-treatment of switchgrass at 160°C with [emim][CH<sub>3</sub>COO] resulted in a delignification of 73.5%. The regenerated solid comprised 31% of glucan (80% of the original glucan from switchgrass) and 8% of glucan composed the liquid fraction (20.5% of original glucan concentration in switchgrass). In contrast, the majority of xylans (19%)

end up in the liquid stream, which was 73% of the original concentration in switchgrass. This means that a depolymerisation of xylans occurred. Therefore, a higher temperature favours hemicellulose hydrolysis using [emim][CH<sub>3</sub>COO]. Using HPAEC only 5% of lignin in the regenerated solid was detected.<sup>92</sup>

In the pre-treatment of triticale straw using 5% (w/w) of biomass treated at 90°C for 24 hours under N<sub>2</sub>, lignin extraction was performed more efficiently with [emim][CH<sub>3</sub>COO] and [bmim][Cl]. Other ILs, such as N,N-dimethylethanolammonium formate (DMEAF), N,N-dimethylethanolammonium acetate (DMEAA), N,N-dimethylethanolammonium glycolate (DMEAG) and N,N-dimethylethanolammonium succinate (DMEAS) have poorly extraction performances. The extraction of lignin with [emim][CH<sub>3</sub>COO] was 30.3% of the original lignin from the triticale straw. This result was 2 and 10 times higher than for [bmim][Cl] and DMEAF lignin extractions, respectively. [Bmim][Cl] is less efficient than [emim][CH<sub>3</sub>COO] for delignification of straw and DMEAF, DMEAA, DMEAG, and DMEAS are not suitable for this purpose. Wheat straw and flax shives were also pre-treated with [emim][CH<sub>3</sub>COO] under same conditions and a 29.6% and 14.0% of lignin extraction from both biomasses was identified, respectively.<sup>93</sup> Therefore it can be concluded that the type of biomass affects the extraction of lignin strongly mostly due to differences in composition and structural interactions occurred in various biomass.

The extraction of lignin is a goal in some pre-treatment studies using ILs. Lignin can be extracted from sugarcane bagasse with high yields performing the treatment at atmospheric pressure and a high temperature (170–190°C). Lignin was recovered from the IL composed of [emim]<sup>+</sup> and alkylbenzenesulfonates and xylenesulfonate anions/NaOH mixture solution with a 93% yield from the original lignin. The NaOH aqueous precipitating solution allowed to obtain a high extraction yield of lignin. The cellulose-rich pulp obtained (with hemicellulose content) corresponded to 45-55% from the original sugarcane bagasse. However, during the heating dissolution process there was possible a formation of lignin carbonium ions able to react with highly available xylenesulfonate anions, producing lignin with xylenesulfonate adducts. Additionally, during delignification some amount of hemicellulose was also removed.<sup>94</sup>

In the isolation of lignin from rubber wood using 1,3-dimethylimidazolium methyl sulfate ([mmim][MeSO<sub>4</sub>]), different concentrations of the IL, varied time and temperature of the treatment were tested.<sup>95</sup> The best concentration for the highest lignin yield was found at 0.5

moles at 100°C for 120 minutes with lignin solubility value of 0.224g. At these conditions only 13.03wt% lignin of the rubber wood was isolated demonstrating that [mmim][MeSO<sub>4</sub>] is not efficient in lignin extraction from rubber wood. However, the isolated lignin was demonstrated to be nearly pure by FT-IR study.<sup>95</sup>

Other studies related to the biomass processing deals with the extraction of carbohydrate fractions using ILs. Extraction of carbohydrates from bran using phosphonate or phosphinate-derived ILs was performed in a short dissolution time and a low temperature. Cellulose, hemicellulose, and residual starch were major components dissolved by these ILs. The insoluble portion was expected to contain lignin and its complexes. The best results were obtained with a highly polar and less viscous [emim][PO(O)H<sub>2</sub>]. Using this IL, the extraction of carbohydrates was 42% of the total amount of carbohydrates present in bran, under mild conditions (50°C for 2h).<sup>85</sup> Pre-treatment with [emim][Cl] (150°C , 60min) allowed to extract 46-48% of carbohydrates from total carbohydrates present in wheat and corn residues. Pre-treatment of eucalyptus at the same conditions resulted in a 33% yield of total sugars. However, a long pre-treatment at temperature of 150°C with an incubation time of 30min yielded a 40% of the original carbohydrates. At 170°C, carbohydrate degradation proceeded that is disadvantageous when the aim is to preserve carbohydrates for subsequent enzymatic hydrolysis.<sup>96</sup>

In a recent fractionation approach cellulose, hemicellulose and lignin were obtained separately as solid fractions.<sup>97</sup> A sugarcane bagasse pre-treatment was performed with 2% (w/w) of sugarcane bagasse, at 110°C for 4h. The complete dissolution of biomass in [bmim][Cl] was achieved followed for a regeneration by adding acetone/water (9:1, v/v) as an anti-solvent. Acetone soluble lignin was extracted to the liquid stream whereas cellulose, hemicellulose and alkaline lignin were fractionated from the solid fraction using 3% NaOH solution and ethanol. The biomass was fractionated to 36.78% cellulose, 26.04% hemicellulose, and 10.51% lignin, giving 47.17% and 33.85% of original polysaccharides and 54.62% of the original lignin.<sup>97</sup> [Bmim][Cl] was easily recycled after concentration and treatment with acetonitrile.

### **1.5 Enzymatic hydrolysis**

Generally, enzymatic hydrolysis is performed using carbohydrate-rich materials to evaluate the efficiency of pre-treatment process. Several enzymatic hydrolysis after the pre-

treatments with ILs demonstrated high glucose yields after cellulose conversion by cellulase enzymes.

Nearly 60% of the theoretical amount of glucose was enzymatic released after pre-treating wood with [amim][Cl] contrasted with only 12% of glucose units obtained in the enzymatic hydrolysis of untreated wood.<sup>75</sup> In a wheat straw pre-treatment with [emim][CH<sub>3</sub>COO] at different temperatures (70-150°C) and time (0.5-24h), regenerated samples of each pre-treatment were enzymatic hydrolysed and an optimum digestibility for sample pre-treated at 150°C after 90min was observed, yielding >95% of cellulose digestibility.<sup>93</sup> However, using 1-ethyl-3-methylimidazolium diethylphosphate ([emim][(CH<sub>3</sub>CH<sub>2</sub>O)<sub>2</sub>PO<sub>2</sub>]) in wheat straw pre-treatment lower yields of reducing sugars was obtained after 30min at 130°C of treatment (only 54.8% reducing sugars after 12h of hydrolysis).<sup>98</sup> These studies show different behaviour in enzyme digestibility when using different ILs in the pre-treatment. In the pre-treatment of sugarcane bagasse with various ILs, [emim][CH<sub>3</sub>COO] was found to be the most efficient IL resulting in glucose yield of 98.2% after a 48h saccharification time. The yield of glucose reached more than 90% in only 15min.<sup>99</sup>

In comparison with other types of pre-treatments, reducing sugars were released faster and to a greater extent in [emim][CH<sub>3</sub>COO] pre-treated switchgrass than in the dilute acid pre-treated switchgrass after enzymatic hydrolysis. For IL pre-treated sample a 12h saccharification time was sufficient for switchgrass to obtain more than 90% hydrolysis yield, whereas the use of dilute sulphuric acid for pre-treatment required a 72h saccharification time to reach 80% yield.<sup>87</sup> Better results were achieved by pre-treating rice straw with combined ammonia and [emim][CH<sub>3</sub>COO]. In this combined pre-treatment, the glucose conversion from enzymatic hydrolysis was measurably higher than in [emim][CH<sub>3</sub>COO] alone method and reached to 97% after 24h of dissolution in the IL.<sup>90</sup>

The enhancement of reducing sugar yields obtained by enzymatic hydrolysis is essentially attributed to lignin removal and reduction in cellulose crystallinity after the pre-treatment with ILs.<sup>73, 100</sup> When 40% of the lignin was removed of wood flour, the cellulose crystallinity index dropped, resulting in >90% of the cellulose to be hydrolysed by cellulase.<sup>73</sup> The increase of the specific surface area in IL-treated samples improves the saccharification yield.<sup>99</sup> These factors allow the better accessibility of cellulase enzyme to perform the enzymatic hydrolysis.

## 2 Experimental Procedure

### 2.1 Materials

Wheat straw was supplied by Estação Nacional de Melhoramento de Plantas (Elvas, Portugal). The feedstock material was ground with a knife mill to particles smaller than 0.5mm, homogenized in a defined lot, and stored in plastic containers at room temperature. The dry matter content was determined to be 92% (w/w).

The ILs selected for this work were [emim][CH<sub>3</sub>COO] with stated purity >95% (2800ppm of water content); [bmim][SCN] with >98% purity (2100ppm of water content); [bmim][N(CN)<sub>2</sub>] with >98% purity (1500ppm of water content) and [bmim][HSO<sub>4</sub>] with 99% purity (5500ppm of water content). Only [bmim][SCN] was supplied by Solchemar Lda. (Lisbon, Portugal) and the other ILs were purchased from Iolitec GmbH (Heilbronn, Germany). ILs were prior dried under a vacuum (0.1Pa) at room temperature for at least 24h before using in pre-treatments. The water content of each IL was determined by a volumetric Karl–Fischer titration.

In pre-treatment experiments, following reagents were used: 0.1M and 3% (w/w) NaOH aqueous solutions prepared from NaOH pellets (99% purity) supplied by Eka Chemicals/Akzonobel - Bohus, Sweden, 1M and 4M HCl aqueous solutions prepared from HCl fuming 37% (w/w) with the purity grade for analysis bought from Merck - Darmstadt, Germany. Ethanol 96% (v/v) and acetonitrile of HPLC-gradient purity for analysis were supplied by Carlo Erba Group - Arese, Italy and acetone (98% purity) was supplied by Valente & Ribeiro, Lda – Belas, Portugal. For NaOH and HCl solutions distilled water - 17MΩcm<sup>-1</sup> and ultrapure water - 18.2MΩcm<sup>-1</sup> both produced by the PURELAB Classic of Elga system were used. For filtration, paper and glass microfibre filters (Whatman GE Healthcare Bio-Sciences Corp. - Piscataway, NJ, USA) and nylon filters, 0.45µm HNPW (Merck Millipore, - Billerica, MA, USA) were used.

Acid hydrolysed wheat straw (130°C, 150min and 1.5% H<sub>2</sub>SO<sub>4</sub>), with known composition (62.6% glucan, 29.9% lignin, 7.5% ash and others content) was used for the construction of FT-IR calibration curves. All FT-IR samples were prepared with KBr (≥99% trace metals basis) purchased from Sigma-Aldrich Co. (St. Louis, MO, USA).

For enzymatic hydrolysis it was used 0.1M sodium citrate buffer at pH 4.8 prepared from citric acid monohydrate (99.7% purity) and tris-sodium citrate (>99% purity) bought from

VWR International Ltd. - Leicester, England. A 2% (w/w) sodium azide solution was prepared from sodium azide reagent (99% purity) delivered by Merck - Darmstadt, Germany. Celluclast® 1.5L (60FPU/g; activity 100.57FPU/mL) and b-glucosidase Novozym 188 (64NPGU/g; activity 436.64pNPGU/mL) enzymes were purchased from Novozymes -Bagsvaerd, Denmark) and were used to perform enzymatic hydrolysis.

## **2.2 Wheat straw pre-treatment with ionic liquids**

### **2.2.1 Wheat straw pre-treatment using [emim][CH<sub>3</sub>COO]**

The pre-treatment procedure was optimised basing on two methodologies presented in literature.<sup>77, 94, 97</sup> For the simplicity these two methods are called in this work as method A and method B. The method A allows only for lignin extraction from the regenerated material (carbohydrate-rich fraction) through the addition of 0.1M NaOH aqueous solution after biomass dissolution in IL. In the method B acetone was used instead of NaOH aqueous solution in the regeneration step. In this method the regenerated material was fractionated into cellulose, hemicellulose and alkaline lignin fractions. The optimised methodology called method C was developed by the combination of the two previous methodologies. Studied methods are described below in detail. In all experiments biomass/IL ratio was 5% (w/w) but in method B was 2% (w/w). All pre-treatment experiments were at least duplicated.

#### **2.2.1.1 Method A**

In a 15mL vial, [emim][CH<sub>3</sub>COO] was mixed with wheat straw (<0.5mm) in a solid/liquid ratio of 5% (w/w) and heated at 120°C for 6h under agitation. After dissolution, 0.1M NaOH was added to the vial until the vial was filled up and the rigorous agitation was performed to precipitate the carbohydrate-rich material. The mixture was then transferred to a 100mL Erlenmeyer. A 40mL total volume of 0.1M NaOH was added with a continuous agitation. The carbohydrate-rich material was collected by filtration, washed with ultrapure water, until the pH of last drops of filtration was neutral (tested with pH paper). The filtrate was acidified to pH = 2.0 with 1M HCl to precipitate lignin-rich material. This solution was next heated at 70°C for 30min to further precipitate lignin and filtered without cooling. The filtered lignin was washed with 10mL of ultrapure water.

Carbohydrate- and lignin-rich materials were placed in the oven at 60°C for 24h. For [emim][CH<sub>3</sub>COO] recovery, the remaining filtrate was neutralised with NaOH pellets. Then water was removed and solid containing NaCl and IL were precipitated. Subsequently, 130mL of acetonitrile was added to dissolve the IL leaving sodium chloride as an insoluble residue, which was removed by filtration. Acetonitrile was evaporated under reduced pressure (Rotavapor Buchi R-210/215 - Switzerland) and the recovered IL was dried under vacuum at least for 24h. In Figure 8 a simplified schematic process of method A is presented. This method was performed basing on procedures described elsewhere.<sup>77, 94</sup>

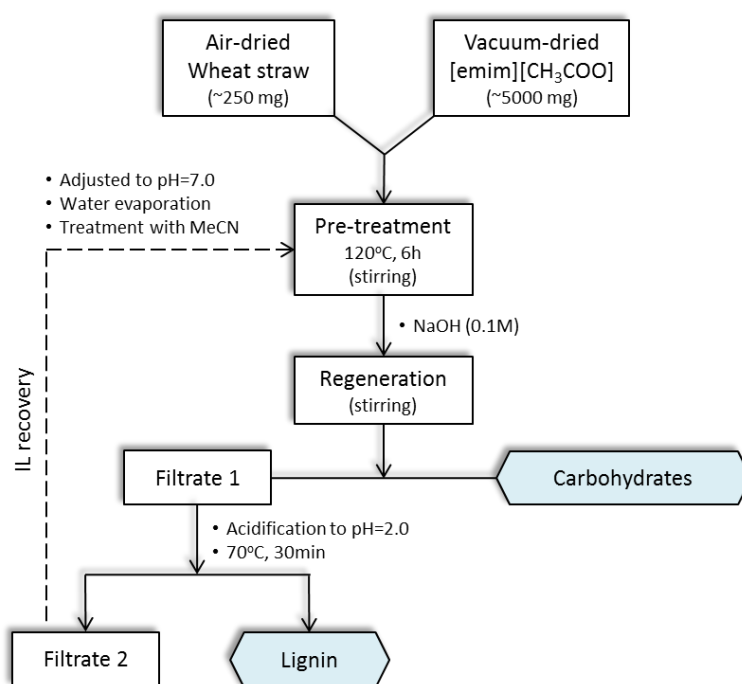


Figure 8. Method A process.

### 2.2.1.2 Method B

To a 15mL vial 5.00g of [emim][CH<sub>3</sub>COO] was added to 0.10g of wheat straw. The dissolution was performed at 110°C for 4h with agitation. Acetone/water mixture (9:1, v/v) was next placed to vial until the vial was filled up with the continuous stirring of the mixture. This solution was then transferred to a 50mL centrifuge tube. The total volume of 40mL of acetone/water (9:1, v/v) was used. After centrifugation (Sigma 2-16K Sartorius, SciQuip - Shropshire, UK) at 4000rpm, 22°C for 15min the carbohydrate-rich material (pellet) was washed with 35mL of acetone/water (1:1, v/v) and then centrifuged at

9000rpm, 4°C for 30min. The resulting solid residue was washed with 35mL of ultrapure water and centrifuged again at 9000rpm, 4°C for 30min. Supernatants were collected to a new flask and were filtered to remove any traces of the solid residue. Next, 5mL of ultrapure water was used to remove the pellet from the centrifuge tube and then filtered to the same filtering flask recovering the carbohydrate-rich material. This material was dried in the oven at 60°C for at least 18h, for later use. The filtrate was concentrated under reduced pressure to remove acetone and the pH was adjusted to 2.0 with 1M HCl, to precipitate lignin-rich material (acetone soluble lignin). Subsequently, lignin was filtered and washed with 10mL of acidified water.

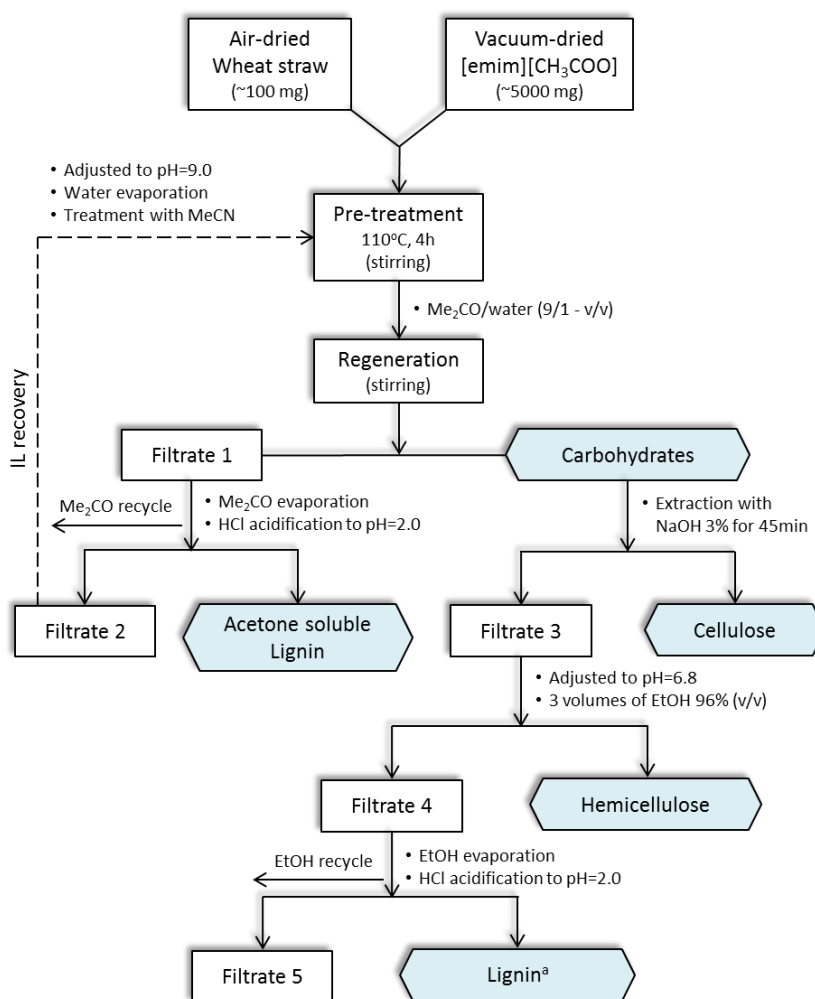


Figure 9. Method B process.

The dried carbohydrate rich-material was treated by 3% (w/w) NaOH aqueous solution with a solid/liquid ratio of 1/25 (g·mL<sup>-1</sup>), at 50°C for 45min with stirring. The insoluble residue (cellulose-rich) was collected by filtration and washed with 12mL of ultrapure

water. The acidity of filtrate was adjusted to pH = 6.8 with 4M HCl and then precipitated with 3 volumes of 96% (v/v) ethanol under continuous agitation. The resulting solid (hemicellulose-rich) was filtered and repeatedly rinsed with 96% (v/v) ethanol. The resulting filtrate was concentrated under reduced pressure to remove ethanol. The concentrated solution was adjusted to pH=2.0 with acidified water to precipitate the residual lignin. The solution was filtered and the residual lignin was washed with 10mL acidified water. All recovered solid samples were placed in the oven at 60°C for 24h. The IL recovery was performed as described in method A, but a pH of the liquid stream containing the IL was adjusted to 9.0. This method was based in the procedure described by Lan et al.<sup>97</sup> with optimisations performed. The schematic representation of method B is shown in Figure 9.

### 2.2.1.3 Method C

To a 15ml vial, 5.00g of [emim][CH<sub>3</sub>COO] was added to 0.250g of wheat straw (<0.5mm). The mixture was heated at 120°C for 6h under agitation. To regenerate the carbohydrate-rich material, 0.1M NaOH was added to the vial until it was filled up. The mixture was then transferred to a 100mL Erlenmeyer. The total volume of 40mL of 0.1M NaOH was used, which was added with a continuous stirring. The carbohydrate-rich material was collected by filtration and washed with distilled water, until the pH of the final drops of filtration was neutral. The solid material was dried in the oven at 60°C for at least 18h, for later use.

The remaining filtrate volume was reduced removing water by evaporation (final solution around 15mL). Then, the pH of the solution was adjusted to 6.8 with 4M and 1M HCl solutions and precipitated in 3 volumes of 96% (v/v) ethanol, under continuous agitation. The resulting solid (residual hemicellulose) was filtered and repeatedly rinsed with distilled water. The ethanol of the filtrate was evaporated under reduced pressure and the pH was adjusted to 2.0 with 4M and 1M HCl solution, to precipitate lignin-rich material. Subsequently, this solution was heated at 70°C for 30min to precipitate further lignin and filtered without cooling. The filtered lignin was washed with 10mL of acidified water. The dried carbohydrate rich-material 3% (w/w) NaOH aqueous solution was added with a solid/liquid ratio of 1:25 (g·mL<sup>-1</sup>), and was kept at 50°C for 1h with a continuous agitation. After 30min of extraction, the vial was removed from the bath to grind some solid particles

that were still insoluble and next it was replaced again in the bath to complete 1h process. The insoluble residue (cellulose-rich) was collected by vacuum filtration and washed with distilled water. The filtrate was adjusted to pH=6.8 with 4M and 1M HCl solutions and then precipitated in 3 volumes of 96% (w/w) ethanol.

The recovery of hemicellulose-rich and residual lignin-rich materials from the filtrate was carried out using the same procedure as described in method B. The IL recovery was performed as described in method A, but the adjustment of pH in the liquid stream containing the IL was alternated between pH=7.0 and 9.0. The schematic presentation of the method C is demonstrated in Figure 10.

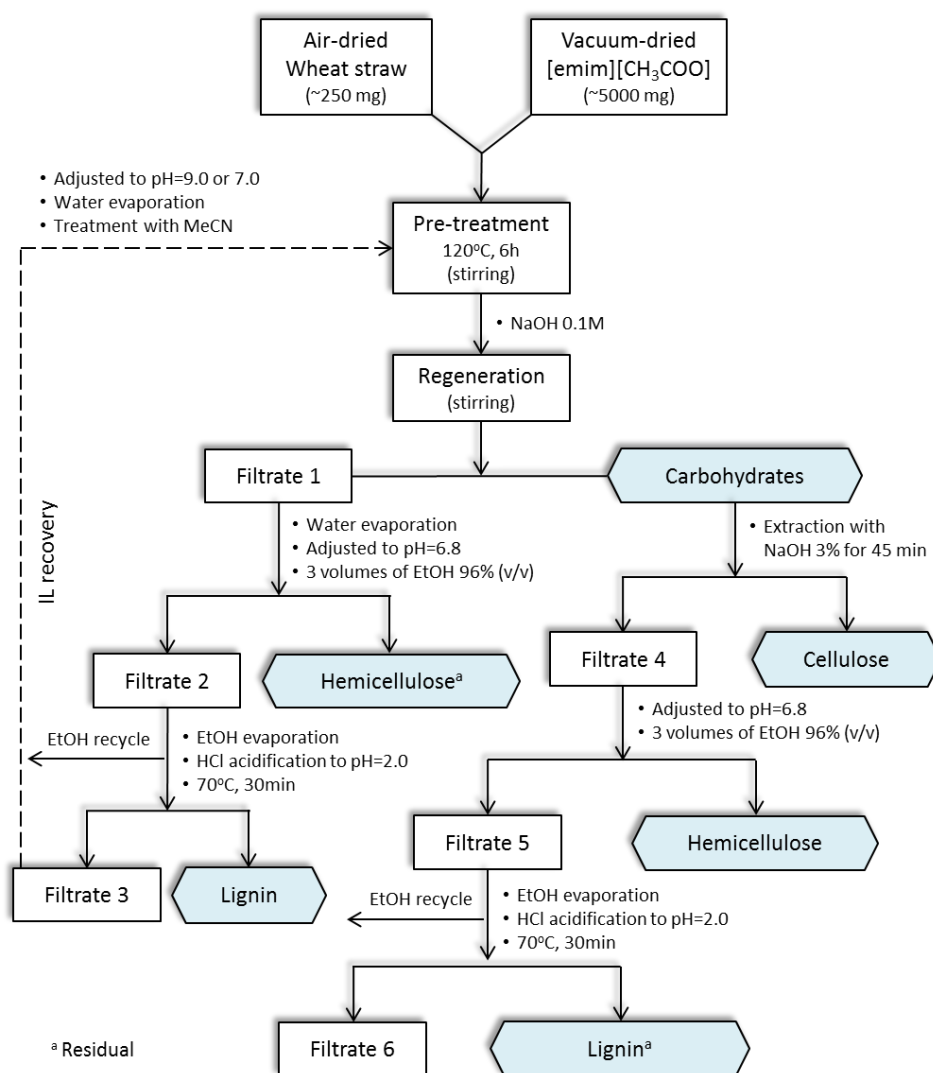


Figure 10. Method C process.

### **2.2.2 Recycling of ionic liquid for the wheat straw pre-treatment**

The procedure used to study the reuse of the IL was performed by method A. At the beginning 5.00g of pure [emim][CH<sub>3</sub>COO] was added to 0.250mg of wheat straw. After pre-treatment the IL was recovered as described in method A and then a new pre-treatment was performed with the recycled IL. All pre-treatments were performed with a solid/liquid ratio of 5% (w/w) being the mass input of wheat straw dependent upon the mass of recovered IL. The IL was reused six times after the first pre-treatment. All fractionated samples were recovered and placed in the oven at 60°C for 24h.

### **2.2.3 Wheat straw pre-treatment using different ILs**

The optimised method (method C) was used to the evaluation of [bmim][SCN], [bmim][N(CN)<sub>2</sub>] and [bmim][HSO<sub>4</sub>] in the pre-treatment of wheat straw. The procedure was performed in duplicate for each IL.

## **2.3 FT-IR spectroscopy characterization**

### **2.3.1 Sample preparation**

For the quantitative analysis, 1 mg of carbohydrate-rich materials (regenerated material, hemicellulose-rich and cellulose-rich samples) was added to 50mg of KBr and grinded in a mortar, until the mixture became homogeneous. The quantitative analysis of lignin-rich materials was performed using the same procedure, but the quantity of lignin used was 0.5mg. The milling time was 10min and samples were placed in the press with 8.5 tonnes for 5min. This sample preparation methodology was performed for all samples equally to avoid errors at this step.

### **2.3.2 FT-IR Spectra Acquisition**

All spectra were scanned using FT-IR spectrometer Spectrum BX, Perkin Elmer, Inc. (San Jose, CA, USA). This instrument was equipped with a DTGS detector and KBr beam splitter. The operating system used was Spectrum software (Version 5.3.1, Perkin Elmer, Inc., San Jose, CA, USA). FT-IR spectra were acquired at region 4000-400cm<sup>-1</sup>, with a total of 64 scans and a resolution of 4cm<sup>-1</sup> with strong apodization. These spectra were subtracted against the background of air spectrum and were recorded as absorbance values.

### 2.3.3 Lignocellulosic material quantification

The quantitative FT-IR analysis was performed by the construction of two separate calibration curves, one for carbohydrates and one for lignin. As standard with the known composition for the curve preparation, the acid hydrolysed pre-treated wheat straw was used changing the amount for each pellet. To minimise the error, the pellet samples were scanned from one to three times and an average value were considered for the calibration curve. After acquiring spectra, it was verified the linearity of the absorptions in characteristic regions of carbohydrates and lignin. Therefore, the spectrum regions with a maximum linearity were selected for quantification, namely the band at  $898\text{cm}^{-1}$  and the range at  $1503\text{-}1537\text{cm}^{-1}$  corresponding to carbohydrates and lignin, respectively. The quantification was made by measuring the total area ( $\text{abs}\cdot\text{cm}^{-1}$ ) in the selected regions. The calibration curve for carbohydrates described by the equation  $y = 0.0221x + 0.0085$ , where  $y$  is the integral of peak at  $898\text{cm}^{-1}$  ( $\text{abs}\cdot\text{cm}^{-1}$ ) and  $x$  is the carbohydrate content (wt%), was obtained. The  $R^2$  was 0.9959. The calibration curve for lignin described by the equation  $y = 0.0599x + 0.3171$ , where  $y$  is the integral of range  $1503\text{-}1537\text{cm}^{-1}$  ( $\text{abs}\cdot\text{cm}^{-1}$ ) and  $x$  corresponds to the lignin content (wt%), was obtained. The  $R^2$  was determined to be 0.9718. The validity of calibration curves was checked regularly before each series of analysis. Examples of calibration curves are illustrated in Appendix A.

The quantification of the experimental samples was performed in the same procedure as described above using constructed calibration curves to determine the composition of samples. The predicted composition was determined as carbohydrate (cellulose + hemicellulose) and lignin content as well as the percentage of others calculated by difference.

### 2.4 NMR analyses of ILs

$^1\text{H}$  NMR and  $^{13}\text{C}$  NMR spectra in  $\text{CDCl}_3$  solution were recorded on a Bruker Avance III 400 spectrometer at REQUIMTE, Associate Laboratory, Universidade Nova de Lisboa, Faculdade de Ciências e Tecnologia, Departamento de Química, Caparica.

## 2.5 Enzymatic Hydrolysis

Cellulose digestibility of carbohydrate-rich materials was evaluated by enzymatic hydrolysis and subsequent HPLC sugars analysis, based on the standard NREL procedure.<sup>101</sup> Samples were prepared in 30mL vials by adding 5.0mL of 0.1M sodium citrate buffer (pH 4.8) and 100 $\mu$ l of a 2% (w/w) sodium azide solution to prevent the growth of organisms during the digestion. Then distilled water was added taking in account the volume of enzyme and sample needed to bring the total volume in each vial to 10.0mL. Celluclast® 1.5L and Novozym 188 enzyme solutions were added at last. Rapidly, vials were sealed and enzymatic hydrolysis reactions were performed on a shaking incubator at 150rpm and 50°C for 72h. After reaction vials were placed in an oil bath and boiled for 5min. Samples were filtrated to remove insoluble solids and filtrates were used to measure reducing sugar concentrations by HPLC analysis. Filtrate aliquots were transferred into HPLC vials and analysed on Agilent 1100 series HPLC system (Santa Clara, CA, USA) equipped with an Bio-Rad Aminex HPX-87H column (Hercules, CA, USA) using a 5mM sulfuric acid mobile phase. The column temperature was 50°C, the flow rate 0.6mL·min<sup>-1</sup>, the injection volume 5 $\mu$ L and the acquisition time 15min for standards and 30min for samples. Glucose and xylose standards were prepared in distilled water to concentrations of 0.25, 0.5, 1.0, 2.5, 5.0 and 10mg·ml<sup>-1</sup> to construct the calibration curve. The cellulose and xylan contents were calculated from glucose and xylose contents multiplied by conversion factors of 0.90 and 0.88, respectively.<sup>101, 102</sup>

## 2.6 Experimental error analysis

For all obtained results standard deviation errors (u) were determined. The applied temperature in pre-treatment experiments demonstrated an  $u(T)=1^{\circ}\text{C}$ . All mass determinations were performed in the balance (Mettler Toledo, XS205 dual range – Germany) with a given  $u(m)=0.1\text{mg}$ . The pre-treatment errors were given as total loss materials for each experiment. For FT-IR quantitative analysis, an arbitrary error 5% of the experimental value was established.

### 3 Results

#### 3.1 Feedstock composition analysis

Wheat straw was chosen as a lignocellulosic biomass to be pre-treated by ILs. The wheat straw moisture was found to be 8% (w/w). The composition analysis of oven-dried biomass was performed<sup>103</sup> and results are shown in Table 2. The same material was used in this work and the carbohydrate content is 57% (w/w) of the total dried biomass being principally represented by cellulose. The total hemicellulose was measured as the sum of xylose, arabinose and acetyl groups content revealing 23.5% (w/w). Lignin was determined to be 18% (w/w) of the total dried biomass. Examples of the chemical composition of wheat straw presented in the literature are shown for comparison.

Table 2. Macromolecular composition of wheat straw in % (w/w).

Component	Carvalho et al. <sup>103</sup>	Pezoa et al. <sup>96</sup>	Fu et al. <sup>104</sup>
Cellulose <sup>a</sup>	38.9	35.7	37.43±0.222
Hemicellulose	23.5	40.2	25.48±0.899
Xylan	18.1±0.3	-	18.97±0.238
Arabinan	3.0±0.2	-	1.50±0.122
Acetyl groups	2.5±0.1	-	2.01±0.347
Mannan	-	-	0.82±0.024
Galactan	-	-	0.77±0.121
Uronic acids	-	-	1.41±0.047
Lignin	18.0±0.5	14.7	18.38±0.164
Ash	9.7±0.03	7.2	1.21±0.104
Protein	4.5±0.5	-	3.57±0.09
Others	5.5	15.7 <sup>b</sup>	11.18±1.44 <sup>c</sup>

<sup>a</sup> Measured as glucan; <sup>b</sup> Extractives; <sup>c</sup> Water-ethanol extractives

#### 3.2 Preliminary evaluation of wheat straw pre-treatment using [emim][CH<sub>3</sub>COO]

Initially, air-dried wheat straw was pre-treated with [emim][CH<sub>3</sub>COO] following a methodology based on experimental protocols presented in the literature.<sup>77, 94</sup> The pre-treatment time optimisation was performed testing three different processing times, namely 1, 6 and 16h. After 16h a complete macroscopic dissolution was obtained and a highly viscous solution was formed. However, by adding 0.1M NaOH aqueous solution a jelly

clot regenerated material was formed, which impedes separate of lignin, carbohydrates and IL. After 6h of treatment the solution mixture showed approximate physical features as those observed at 16h, but in this case with less viscosity. Therefore, after regeneration with 0.1M NaOH no gum formation was obtained and the pre-treatment process could be carried out. Only 1h process resulted in partially dissolution that could decrease the pre-treatment efficiency. Results of these experiments are shown in Table 3.

Table 3. The wheat straw regeneration after 1, 6 and 16h of pre-treatment with [emim][CH<sub>3</sub>COO].

Entry	Time /h	WS /mg	Dried WS /mg	SF	
				RM /mg	RY /% <sub>w/w</sub>
1	1	103.2	94.9	63.0	66.4
2	6	250.5	230.5	120.8	52.4
3	16	251.9	231.7	128.1	55.3

WS - wheat straw; SF- solid fraction; RM - regenerated material; RY- regeneration yield

For the next experiments 6h treatment was selected as it allowed to dissolve material completely without forming difficulties described above for longer time processing.

### 3.3 Wheat straw pre-treatment using [emim][CH<sub>3</sub>COO]

The pre-treatment of wheat straw using method A provides a regenerated carbohydrate-rich material after an addition of alkaline solution (40mL of 0.1M NaOH) as well as a recovery of lignin-rich material extracted in the liquid phase. The used literature based method A was optimised and in the A1 experiment 125mg of wheat straw was used although a very small quantity of the lignin-rich material was obtained. It resulted in difficulties in the qualitative analysis of the fraction. Therefore, the double mass of biomass was used in experiment A2 and considerably larger quantity of lignin was recovered that was later analysed by FT-IR. In A3 experiment 80mL of 0.1M NaOH aqueous solution was added instead of 40mL to evaluate lignin extraction capacity by 0.1M NaOH aqueous solution. The recovered mass of lignin-rich and carbohydrate-rich materials as well as regeneration yields, total losses and IL recovery values of each pre-treatment are presented in Table 4.

Table 4. Results of the wheat straw pre-treatment with [emim][CH<sub>3</sub>COO] using method A.

Entry	WS /mg	Dried WS /mg	SF		LF	ML /% <sub>w/w</sub>	IL recovery	
			RM /mg	RY /% <sub>w/w</sub>	Lignin-rich /mg		/% <sub>w/w</sub>	pH
A1	125.5	115.5	63.9	55.3	9.3	36.7	76.0	
A2	250.3	230.2	156.0	67.8	22.1	22.7	71.2	7.0
A3	250.6	230.5	127.7	55.4	37.3	28.4	76.4	

WS - wheat straw; SF- solid fraction; RM - regenerated material; RY- regeneration yield; LF – liquid fraction; ML –material lost

Higher regeneration yields were observed for A2 than for A1 experiment. The A3 experiment showed a similar regeneration yield of carbohydrates comparing with A1 pre-treatment. The highest lignin recovery was obtained in A3 experiment with 37.3mg. The A1 experiment showed higher material losses in the process. The recovery of IL after pre-treatment varies from 71.2% to 76.4% of the initial mass of the IL used.

In method B an acetone/water mixture was used to regenerate the carbohydrate-rich material. Additionally, a 2% (w/w) solid/liquid ratio and 4h of pre-treatment was used instead of a biomass loading of 5% (w/w) for 6h pre-treatment as it was used in method A. The method B allowed to obtain the regenerated material that was fractionated into cellulose-rich, hemicellulose-rich and residual lignin-rich fractions. From the liquid stream, acetone soluble lignin was extracted and recovered. Two different experiments were performed. In B1 experiment an acetone/water mixture in a 9/1 (v/v) ratio was used in the regeneration step, while in B2 after 9/1 (v/v), additionally 1/1 (v/v) acetone/water mixture and later water were used to wash the precipitated solid. These changes in procedure allowed to boost significantly IL recovery to 92.7% comparing with 53.3% in case of B1 experiment as presented in Table 5. Additionally, a high lignin-rich fraction and regenerated biomass recovery was observed that effected in lower losses of the biomass.

Table 5. Results of the wheat straw pre-treatment with [emim][CH<sub>3</sub>COO] using method B.

Entry	WS /mg	Dried WS /mg	S/L /% <sub>w/w</sub>	SF		LF	ML /% <sub>w/w</sub>	IL recovery	
				RM /mg	RY /% <sub>w/w</sub>	Lignin-rich /mg		/% <sub>w/w</sub>	pH
B1	99.8	91.8	2	55.7	60.7	7.8	30.9	53.3	9.0
B2	100.5	92.5		66.7	72.2	10.1	17.0	92.7	

WS - wheat straw; S/L – solid/liquid ratio; SF - solid fraction; RM - regenerated material; RY - regeneration yield; LF – liquid fraction; ML – material lost

Table 6. The fractionation of the regenerated material and material losses using method B.

Entry	RM Load /mg	RM fractionation			ML /% <sub>w/w</sub>
		Cellulose-rich /mg	Hemicellulose-rich /mg	Lignin-rich <sup>a</sup> /mg	
B1	50.8	31.9	12.9	3.2	5.6
B2	51.7	31.8	15.3	2.5	4.4

RM - regenerated material; ML – material lost; <sup>a</sup>residual

The fractionation of both solid samples (B1 and B2) did not reveal significant differences between them. In general it can be stated that approximately 60% of the regenerated material was the cellulose-rich fraction with a slightly higher hemicellulose-rich recovery obtained in B2 experiment with 15.3mg comparing to 12.9mg for B1 experiment.

From both methods (A and B) an optimised pre-treatment was accomplished creating method C. This methodology focused on the pre-treatment of wheat straw to obtain fractionated samples with a higher purity. A biomass loading of 5% (w/w) and a pre-treatment time of 6h was selected to be optimal for method C. Analogously to the method A, 0.1M NaOH aqueous solution was used to regenerate the carbohydrate-rich material, which was later fractionated by the same procedure as in the method B. Moreover, from the obtained liquid stream in the regeneration step not only lignin-rich material was recovered but also a residual hemicellulose material was produced, simultaneously extracted by the NaOH alkaline solution. Results obtained for the pre-treatment of biomass according to the method C are given in Table 7.

Table 7. Results of the wheat straw pre-treatment with [emim][CH<sub>3</sub>COO] using method C.

Entry	WS /mg	Dried WS /mg	SF		LF		ML /% <sub>w/w</sub>	IL recovery	
			RM /mg	RY /% <sub>w/w</sub>	Hemicellulose-rich <sup>a</sup> /mg	Lignin-rich /mg		/% <sub>w/w</sub>	pH
C1	249.7	229.7	133.2	58.0	128.7	18.5	-22.0	78.2	7.0
C2	250.4	230.4	-	-	38.9	15.3	-	89.1	9.0
C3	250.6	230.5	131.1	56.9	38.3	15.1	20.0	86.2	7.0

WS - wheat straw; S/L – solid/liquid ratio; SF - solid fraction; RM - regenerated material; RY - regeneration yield; LF – liquid fraction; ML – material lost; <sup>a</sup>residual

In C1 experiment lignin-rich and residual hemicellulose-rich materials were obtained from liquid stream fractionation. The procedure was performed as in the fractionation of regenerated material by method B. However, in the course of the process, NaCl was

precipitated together with the residual hemicellulose-rich fraction when ethanol was used as antisolvent for this fraction. Therefore, an extraordinary amount of the residual hemicellulose was recovered, and thus, more material was obtained giving a negative value for material lost yield, as shown in the Table 7. For this reason a modified procedure was used in C2 experiment. Water was used to wash the hemicellulose-rich sample and to dissolve the formed salt. Furthermore, a fractionation of wet regenerated material was used in C2 experiment in order to avoid 18h of drying and to save operational time. Unfortunately, the use of wet regenerated material requires larger volumes of solvents, such as ethanol, therefore is not very convenient from the application point of view. As a consequence, in the C3 experiment the regenerated material dried for 18h was used and the precipitated salt was dissolved adding water to hemicellulose-rich samples. Nevertheless, C2 and C3 experiments presented very similar results in obtained masses of residual hemicellulose-rich and lignin-rich materials. The IL recovery was lower for C1 experiment (78.2%) than for C2 and C3 experiments where 89.1% and 86.2% of IL mass was recovered, respectively.

Table 8 presents data on cellulose-rich, hemicellulose-rich and residual lignin-rich fraction obtained from the fractionation of the regenerated material using method C.

Table 8. The fractionation of the regenerated material and material losses using method C.

Entry	RM Load /mg	RM fractionation			ML /% <sub>w/w</sub>
		Cellulose-rich /mg	Hemicellulose-rich /mg	Lignin-rich <sup>a</sup> /mg	
C1	123.1	94.0	22.2	3.6	2.8
C2	-	83.5	30.2	1.2	-
C3	119.7	87.3	18.4	3.0	9.2

RM - regenerated material; ML – material lost; <sup>a</sup>residual

All methods produced similar quantities of cellulose-rich fractions and more significant differences were observed for hemicellulose-rich material. In C2 experiment 30.2mg of hemicellulose-rich material was achieved with simultaneously less residual lignin. The lowest losses of material are observed for C1 that can be interfered by NaCl residues present in hemicellulose-rich fraction. The C2 experiment does not contain data about the regenerated material due to the use of wet biomass for fractionation. Therefore, material lost cannot be compared with other entries.

### 3.4 Wheat straw pre-treatment using different ILs

The optimised pre-treatment methodology was used to study the influence of ILs on the biomass pre-treatment. The procedure of pre-treatment was strictly followed as in C3 experiment. For this study the following ILs were used: [bmim][SCN], [bmim][N(CN)<sub>2</sub>] and [bmim][HSO<sub>4</sub>]. A complete macroscopic dissolution was observed for pre-treatment with [bmim][HSO<sub>4</sub>], while [bmim][SCN] and [bmim][N(CN)<sub>2</sub>] experiments demonstrate only partial dissolution.

Results obtained from the regeneration process and from the fractionation of liquid stream are provided in Table 9. All reactions were carried out with a solid/liquid ratio 5% (w/w). The pre-treatments using [bmim][SCN] (entry D) and [bmim][N(CN)<sub>2</sub>] (entry E) resulted in high regeneration yields between 77.2%-81.0%. For [bmim][HSO<sub>4</sub>] experiment (entry F) worse regeneration yield and a higher percentage of lost material were observed.

Table 9. Results of the wheat straw pre-treatment with [bmim][SCN], [bmim][N(CN)<sub>2</sub>] and [bmim][HSO<sub>4</sub>] using method C.

Entry	WS /mg	Dried WS /mg	SF		LF		ML /% <sub>w/w</sub>	IL recovery /% <sub>w/w</sub>
			RM /mg	RY /% <sub>w/w</sub>	Hemicellulose-rich <sup>a</sup> /mg	Lignin-rich /mg		
D	250.3	230.3	183.1	79.5	8.0	13.0	11.4	93.5
E	250.7	230.6	179.3	77.7	15.2	10.1	11.3	97.0
F	250.3	230.3	137.1	59.6	4.1	7.1	35.7	94.1

WS - wheat straw; SF - solid fraction; RM - regenerated material; RY - regeneration yield; LF – liquid fraction; ML – material lost; <sup>a</sup> residual

The maximum recovery of the solid fraction was achieved for thiocyanate IL while two others showed lower recovery of the solid fraction. Among studied ILs the highest lignin-rich material was achieved in an experiment with [bmim][SCN] (13.9mg) and this trend decreases in the following order [bmim][SCN]>[bmim][N(CN)<sub>2</sub>]>[bmim][HSO<sub>4</sub>]. The highest concentration of the residual hemicellulose was obtained in a process with dicyanamide IL that is almost 100% more than in case of two others ILs.

All studied ILs were recovered with a high yield exceeding significantly 90% of the initial mass used.

Results of the fractionation of solid containing cellulose-rich, hemicellulose-rich and residual lignin-rich materials obtained with 3 different ionic liquids are presented in Table 10.

Table 10. The fractionation of the regenerated material and material losses in pre-treatments with [bmim][SCN], [bmim][N(CN)<sub>2</sub>] and [bmim][HSO<sub>4</sub>] ILs using method C.

Entry	RM Load /mg	RM fractionation			ML /% <sub>w/w</sub>
		Cellulose-rich /mg	Hemicellulose-rich /mg	Lignin-rich <sup>a</sup> /mg	
D	166.1	138.5	19.4	4.7	2.2
E	155.3	117.7	8.5	11.8	11.2
F	125.6	74.0	1.5	30.8	16.0

RM - regenerated material; ML – material lost; <sup>a</sup> residual

Obtained results show that for pre-treatments with [bmim][N(CN)<sub>2</sub>] and [bmim][HSO<sub>4</sub>] losses of material are significantly higher than in case of [bmim][SCN]. Consequently the amount of hemicellulose recovered from the process with this IL is double than for [bmim][N(CN)<sub>2</sub>] and one order of magnitude higher than for hydrogen sulphate containing the IL. The similar trend although is observed in case of cellulose-rich carbohydrate fraction, where the highest amount was noticed for entry D and decreased for E and F.

### 3.5 FT-IR qualitative and quantitative analysis

Fourier Transform Infrared (FT-IR) was chosen to characterise all the solid samples recovered in the wheat straw pre-treatment process with ILs. The main chemical bond vibrations of lignocellulosic materials are detected in the region of 1800-800cm<sup>-1</sup>. Therefore, this region was selected for the analysis of all samples in this work.

#### 3.5.1 Characterisation of wheat straw

The FT-IR spectrum of untreated wheat straw is presented in Figure 11. Bands at 1376, 1161, 1107, 1049 and 898cm<sup>-1</sup> are attributed to carbohydrates. The band 1376cm<sup>-1</sup> corresponds to O-H bending from hydroxyl groups. The C-O asymmetric bending was observed as the signal at 1161cm<sup>-1</sup>. The band at 898cm<sup>-1</sup> corresponds to the vibration of β-glycosidic C-H deformation with a ring vibration contribution (hexoses/pentoses) characteristic of glycosidic bonds in carbohydrates.<sup>105-107</sup> The characteristic bands of lignin

visible in wheat straw spectrum are at 1508, 1458 and 1420 $\text{cm}^{-1}$  and they are associated to aromatic skeletal vibrations. Bands at 1508 and 1458 $\text{cm}^{-1}$  are assigned to C=C stretching vibration and C-H deformations (CH and CH<sub>2</sub>) in phenol rings, respectively. The symmetric bending vibrations of C-H bonds in methoxyl groups of syringil and guaiacyl units correspond to 1420 $\text{cm}^{-1}$  band.<sup>108</sup> The broad absorption at 1251 $\text{cm}^{-1}$  is originated by the C-O stretching of acetyl groups present in hemicellulose molecular chains.<sup>109</sup> The vibration band at 1734 $\text{cm}^{-1}$  was assigned to ester-linked acetyl, feruloyl and p-coumaroyl groups between hemicellulose and lignin<sup>110</sup> and the band at 1637 $\text{cm}^{-1}$  was associated with water present in the sample.<sup>25</sup> Out of this region, the bands 2852 and 2920 $\text{cm}^{-1}$  are attributed to asymmetric and symmetric C-H stretching of CH, CH<sub>2</sub> and CH<sub>3</sub> groups.<sup>111</sup> The complete spectrum is presented in Appendix B.

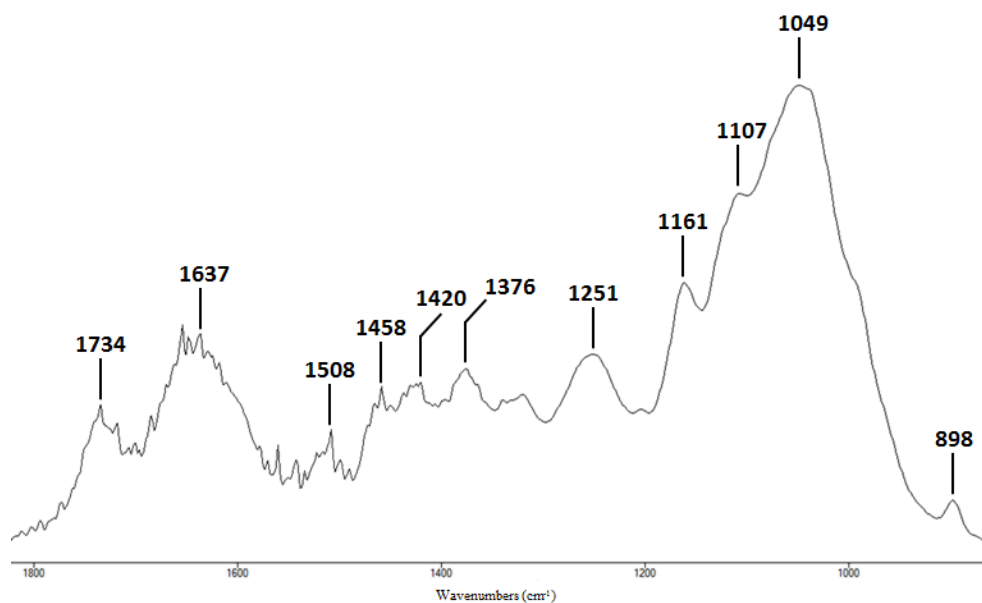


Figure 11. The FT-IR spectrum of wheat straw.

### 3.5.2 Characterisation of pre-treatment samples using [emim][CH<sub>3</sub>COO]

The Figure 12 presents the FT-IR spectrum of regenerated solid material obtained using method A. The regenerated material is essentially composed by carbohydrates due to the lignin extraction in the regeneration process. The already described bands at 1376 and 1161 $\text{cm}^{-1}$  can be observed and the appearance of new bands identified, such as 1066, 1046 and 996 $\text{cm}^{-1}$  characteristic of carbohydrates, was detected. The absorption peak at 1066 $\text{cm}^{-1}$  is an effect of the ether linkage C-O-C skeletal vibration of both pentose and hexose unit contribution.<sup>97</sup> The peak at 1046 $\text{cm}^{-1}$  is regarded to hemicellulose absorptions explicitly to

C-O stretching in C-O-C linkages. Arabinosyl side chains are represented by the absorption peak at  $996\text{cm}^{-1}$ .<sup>112</sup> In fact, the major absorptions of vibrations by carbohydrate chemical bond are presented in a region  $1250\text{-}850\text{cm}^{-1}$ , however, some bands are undefined and less pronounced since sample consists of a mixture of cellulose and hemicellulose. In this spectrum the characteristic band of glycosidic bond vibration was observed at  $896\text{cm}^{-1}$  and simultaneously the absorption increased in comparison with untreated wheat straw spectrum. On the contrary, the absorbance of lignin bands  $1508$ ,  $1458$  and  $1420\text{cm}^{-1}$  showed a slight decrease demonstrating a lower lignin content. The band at  $1734\text{cm}^{-1}$  was not observed also.

The analysis of regenerated material obtained from method C showed in Appendix B demonstrates an identical FT-IR spectrum as for the method A because the same regeneration process was performed. In general the method B gave products with a similar spectrum presented in Appendix B.

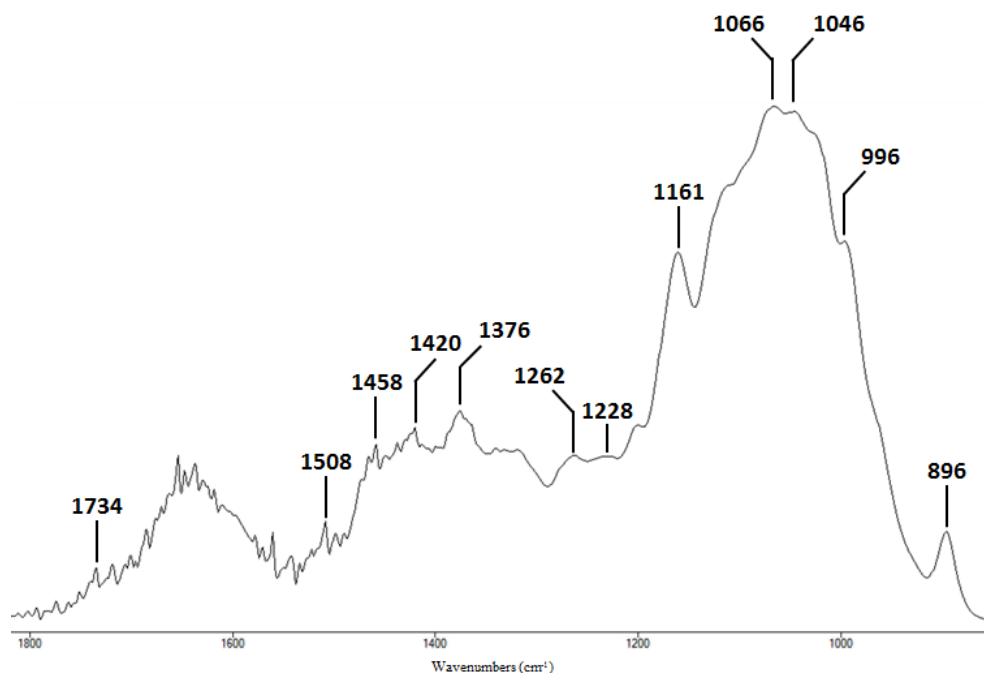


Figure 12. The FT-IR spectrum of the regenerated material using the method A.

The method used for the pre-treatment of biomass allowed to fractionate the solid regenerated material and cellulose and hemicellulose-rich fractions were produced. Figure 13 depicts the FT-IR spectrum of cellulose-rich material obtained from method B. It can be seen that more characteristic bands in a region  $1250\text{-}850\text{cm}^{-1}$  associated to cellulose such as  $1161$ ,  $1112$ ,  $1061$  and  $1035\text{cm}^{-1}$  were identified. All vibrations are related to pyranosyl

rings and the band  $1112\text{cm}^{-1}$  corresponds to C-OH skeletal vibration, while  $1061\text{cm}^{-1}$  is associated to the ether linkage C-O-C skeletal vibration and  $1035\text{cm}^{-1}$  is attributed to C-O stretching vibration characteristic for cellulose. The band at  $1376\text{cm}^{-1}$  representing O-H bending from hydroxyl groups in cellulose was very pronounced and the glycosidic bond vibration occurred at  $897\text{cm}^{-1}$ . The band at  $1320\text{cm}^{-1}$  was produced by C-C and C-O skeletal vibrations.<sup>113</sup> The lignin content can be observed by small bands  $1508$ ,  $1458$  and  $1420\text{cm}^{-1}$ . In this spectrum negligible although visible absorption bands of lignin at  $1235$  and at  $1262\text{cm}^{-1}$  associated to C-O stretching vibrations of syringil and guaiacyl methoxyl groups, respectively is also noticed. Additionally, at  $998\text{cm}^{-1}$  band that represents an existence of arabinose (arabinosyl side chains) is observed as well. Moreover, the absence of band  $1734\text{cm}^{-1}$  is confirmed in the cellulose-rich sample.

The FT-IR spectrum of cellulose-rich material fractionated by the method C is presented in Appendix B and presents small differences in comparison with the presented here obtained for the method B (Figure 13).

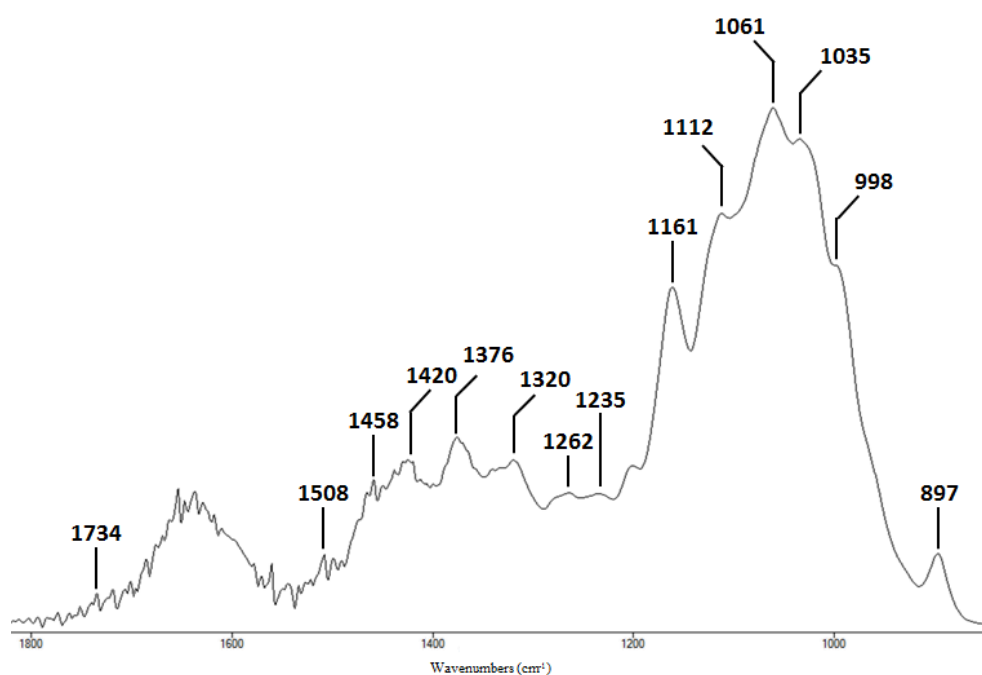


Figure 13. The FT-IR spectrum of cellulose-rich material using the method B.

Analysing the FT-IR spectrum of hemicellulose-rich material (Figure 14) it could be observed significant differences comparing with the spectra of cellulose-rich samples. New absorption bands at  $993$ ,  $1043$ ,  $1080$ ,  $1253$  and  $1388\text{cm}^{-1}$ , characteristic to hemicellulose compound, were determined. Bands at  $993$  and  $1163\text{cm}^{-1}$  indicate the presence of

arabinosyl side chains.<sup>112</sup> The strong absorption band at  $1043\text{cm}^{-1}$  is associated to glycosidic linkage C-O-C contribution in xylans.<sup>114</sup> The small band at  $1080\text{cm}^{-1}$  is associated to galactan side chains.<sup>115</sup> The appearance of band at  $1253\text{cm}^{-1}$  indicates the presence of acetyl groups present in hemicellulose structure.<sup>107</sup> The C-O stretching is attributed to band  $1388\text{cm}^{-1}$ .<sup>116</sup> The Figure 14 displays also that lignin (bands  $1420$  and  $1508\text{cm}^{-1}$ ) is present although bands are even smaller than in others showed above. Two other bands at  $1466$  and  $1508\text{cm}^{-1}$  are also the characteristic for lignin as it was already stated.

Spectra of hemicellulose-rich material from the method B and residual hemicellulose-rich fractions from the methods B and C shows exactly the same shape as demonstrated in Figure 14 (Appendix B).

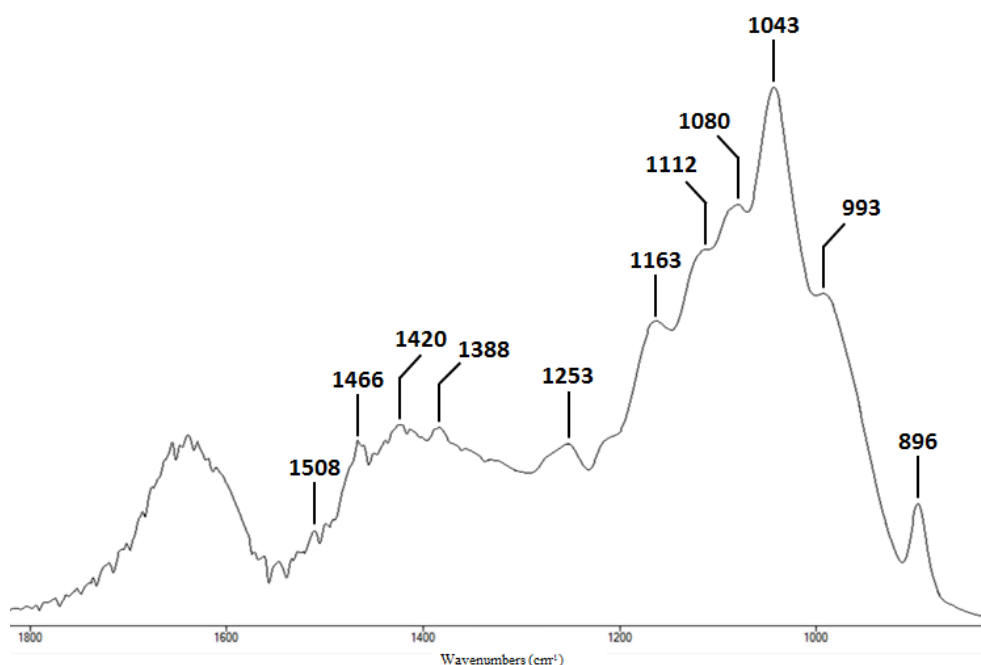


Figure 14. The FT-IR spectrum of hemicellulose-rich material using the method C.

Lignin as a complex structure compound provides many chemical bond vibrations in FT-IR spectra. Spectra of lignin-rich samples are completely different than carbohydrate spectra with well distinguished bands. Figure 15 depicts the spectrum of isolated lignin from the method C. Analysing this spectrum, it can be stated that bands at  $1508$ ,  $1458$  and  $1420\text{cm}^{-1}$  have strong absorptions. In addition other aromatic skeletal vibrations at  $1034\text{cm}^{-1}$  represent aromatic C-H in-plane deformation for guaiacyl units<sup>117</sup> and at  $1597\text{cm}^{-1}$  a contribution of the aromatic skeletal and C=O vibrations.<sup>105</sup> Small bands of

lignin at  $1235$  and  $1265\text{cm}^{-1}$  were also observed in cellulose-rich spectrum (Figure 13) although in the lignin-rich sample their absorption increased and band at  $1235\text{cm}^{-1}$  shifted towards higher value ( $1228\text{cm}^{-1}$ ). Moreover, an absorption vibration is observed at  $840\text{cm}^{-1}$  that corresponds to out-of-plane deformation vibrations of C-H of predominantly syringyl units.<sup>105</sup> An absorption contribution of C-O deformations of secondary alcohols and aliphatic ether linkages present in lignin can be associated to the band present at  $1091\text{cm}^{-1}$ .<sup>105, 117</sup> The strong vibration at  $1127\text{cm}^{-1}$  is characterised to be a contribution of three types of vibrational absorptions, namely C-H in a plane deformation and C=O stretching of syringyl units as well as secondary alcohols present in lignin.<sup>105, 118</sup> The small band at  $1158\text{cm}^{-1}$  is attributed to C-O asymmetric bridge stretching in ester linkages. The strongest band can be noticed at  $1654\text{cm}^{-1}$  and it is associated to C=O stretching in conjugated para-substituted aryl ketones present in the lignin structure.<sup>119</sup> At last, C=O stretching associated to  $1708\text{cm}^{-1}$  band indicates the presence of hydroxycinnamates, such as p-coumarate and ferulate.<sup>97</sup>

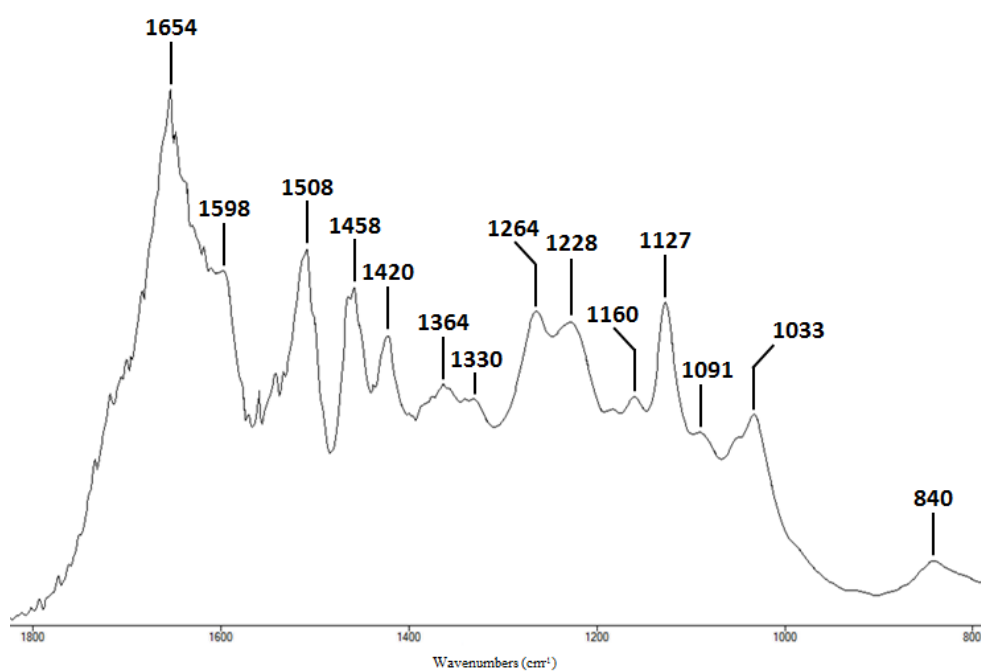


Figure 15. The FT-IR spectrum of lignin-rich material using the method C.

The lignin obtained from the method A and residual lignin-rich material from the method B demonstrates analogous characteristic as the aforementioned spectrum shown in Figure 15. The only difference is that a spectrum of lignin-rich material obtained by the method A shows the carbohydrate band  $896\text{cm}^{-1}$ , while produced by the method B is much pure. The

spectra of lignin obtained from the method A and residual lignin-rich material from the method B are included in Appendix B.

Figure 16 shows a spectrum of acetone soluble lignin-rich material obtained by the method B. The most of bands were already described above and are present in this spectrum as well, although their intensities varied. Moreover, it can be observed the presence of carbohydrates that is associated to bands at 896, 1046, 1080 and 1122 $\text{cm}^{-1}$ .

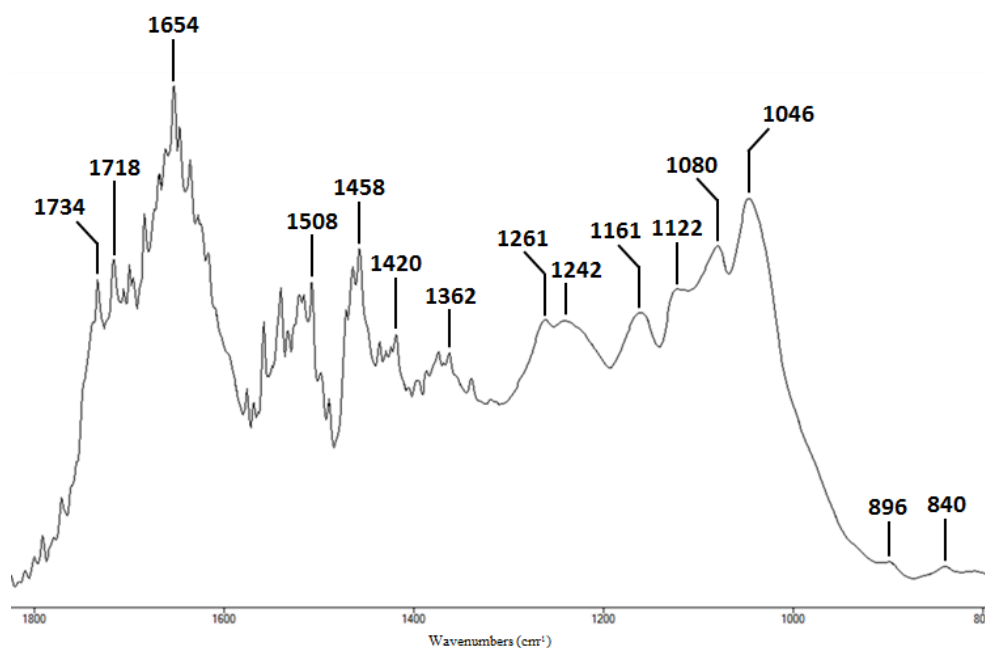


Figure 16. The FT-IR spectrum of acetone soluble lignin-rich material using the method B.

Bands associated to C-O stretching vibrations of syringil and guaiacyl methoxyl groups are shifted to 1261 and 1242 $\text{cm}^{-1}$ , respectively. In addition, absorption bands at 1508, 1458 and 1420 $\text{cm}^{-1}$  decreased and bands are not well defined. The band at 1718 $\text{cm}^{-1}$  is attributed to C=O stretching in unconjugated ketone, carbonyl and ester groups while the absorption band at 1734 $\text{cm}^{-1}$  indicates the existence of ester linkages between lignin and hemicellulose. Additionally, out of the presented spectrum range, it is important to observe the fact that additional two high intensity peaks at 2919 and 2850 $\text{cm}^{-1}$  were detected that are attributed to asymmetric and symmetric C-H stretching in the carbohydrate structure. The complete spectrum is shown in Appendix B.

The FT-IR spectrum of residual lignin-rich material from the method C is presented in Figure 17. This spectrum shows similarities with the spectrum of lignin-rich obtained from the same method (Figure 15). Principle differences are: an increased intensity of the

absorption band at  $1127\text{cm}^{-1}$ , an absence of band at  $1091\text{cm}^{-1}$  and a decrease of intensity of the absorption band at  $1654\text{cm}^{-1}$ . New bands, such as  $1330\text{cm}^{-1}$  associated to C-O vibration of syringyl ring and guaiacyl ring units in a condensed form and  $1702\text{cm}^{-1}$  attributed to unconjugated C=O stretching (ketones and carbonyl groups) were found.<sup>119, 120</sup>

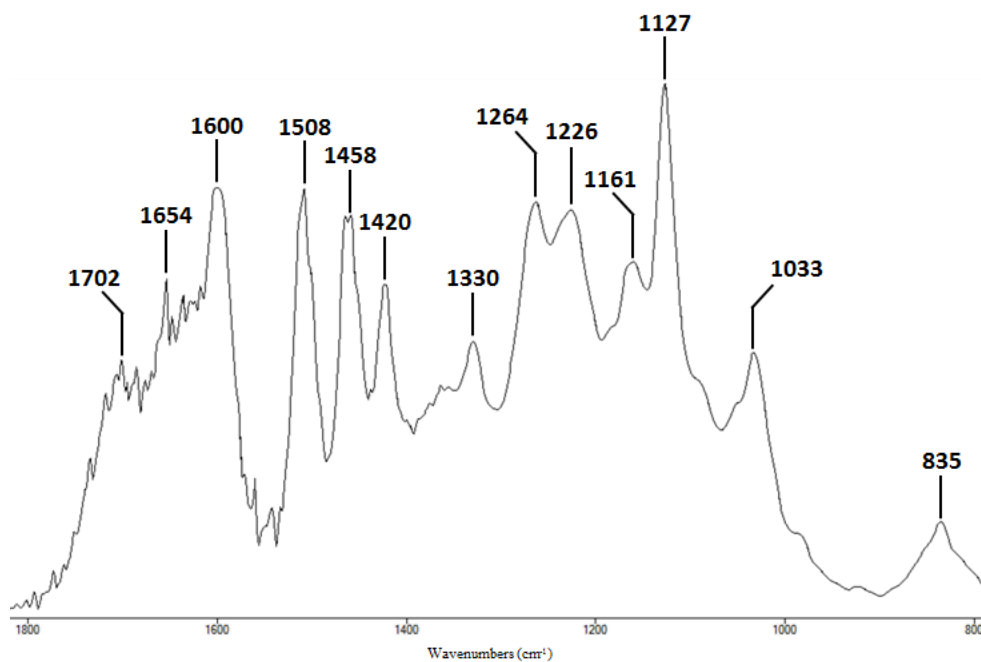


Figure 17. The FT-IR spectrum of the residual lignin-rich material using the method C.

### 3.5.3 Quantification of pre-treatment samples using [emim][CH<sub>3</sub>COO]

A quantitative analysis based on FT-IR measurements was performed for a selected pre-treatment experiment from each method. Therefore, A2, B2 and C3 samples were chosen to evaluate the composition and to verify the selectivity of used methods. The predicted composition was determined as carbohydrate (cellulose + hemicellulose) and lignin content as well as the percentage of other non-identified material calculated by difference. The composition results of samples obtained by methods A, B and C are presented in

Table 11-13.

The quantitative analysis shows that method A revealed an enrichment of almost 20% in the carbohydrate content of the regenerated material as well as a decrease of 10% in the lignin content. The lignin-rich sample was constituted by 70% of lignin and by only 6% of

the carbohydrate content. It is worth to notice that a considerable part of other compounds is present in the lignin-rich sample (24%), similarly to the dry wheat straw and significantly more than in the regenerated solid material (12%).

Table 11. The FT-IR quantification of fractionated samples by the method A.

Entry	Composition						Total /mg
	Carbohydrates		Lignin		Others		
	/mg	/wt%	/mg	/wt%	/mg	/wt%	
Dried WS	142.7	62	41.4	18	46.1	20	230.2
RM	123.2	79	14.0	9	18.8	12	156.0
Lignin	1.3	6	15.9	70	5.5	24	22.7

WS – wheat straw; RM - regenerated material

Table 12. The FT-IR quantification of fractionated samples by the method B.

Entry		Composition						Total /mg
		Carbohydrates		Lignin		Others		
		/mg	/wt%	/mg	/wt%	/mg	/wt%	
Dried WS		57.4	62	16.7	18	18.4	20	92.5
	RM	42.7	64	9.3	14	14.7	22	66.7
Solid fraction	Cellulose	26.1	82	3.2	10	2.5	7	31.8
	Hemicellulose	12.2	80	1.4	9	1.7	11	15.3
	Lignin <sup>a</sup>	0.0	0	2.5	98	0.0	2	2.5
Liquid fraction	Lignin <sup>b</sup>	0.8	8	5.8	57	3.5	35	10.1

WS – wheat straw; RM - regenerated material; <sup>a</sup>residual; <sup>b</sup>acetone soluble

The method B allowed to obtain the regenerated material constituted by the similar fractions as the dry wheat straw. The fractionation of the regenerated material allowed to separate a cellulose-rich fraction with 82% of the carbohydrate content and a hemicellulose-rich material with 80%. The lignin present in these fractions decreased to 10 and 9% in content, respectively. Acetone soluble lignin has a low purity (57%) demonstrating to possess many other compounds that were extracted by acetone and still contains carbohydrates. In contrary, the residual lignin-rich material was obtained with a high purity (98%), free of carbohydrates, regardless of a low quantity recovered.

In the method C the composition of regenerated material was similar to that observed in the method A as expected, because the process is equal at the regeneration step. Following

the process of the fractionation, obtained carbohydrate-rich fractions (cellulose and hemicellulose) demonstrated to have a higher carbohydrate content than that observed in the method B.

Table 13. The FT-IR quantification of fractionated samples by the method C.

Entry		Composition						Total /mg
		Carbohydrates		Lignin		Others		
		/mg	/wt%	/mg	/wt%	/mg	/wt%	
Dried WS		143.9	62	41.5	18	45.4	20	230.5
	RM	106.2	81	7.9	6	17.0	13	131.1
Solid fraction	Cellulose	75.1	86	5.2	6	7.0	8	87.3
	Hemicellulose	15.6	85	0.9	5	1.9	10	18.4
	Lignin <sup>a</sup>	NQ	NQ	NQ	NQ	NQ	NQ	3.0
Liquid fraction	Lignin	0.0	0	13.1	87	1.9	13	15.1
	Hemicellulose <sup>a</sup>	27.2	71	1.1	3	10.0	26	38.3

WS – wheat straw; RM - regenerated material; NQ - not quantified; <sup>a</sup>residual

The carbohydrate content was determined to be 86 and 85% for cellulose-rich and hemicellulose-rich materials, respectively. The lignin content in these samples was very low (5%-6%). The same trend was not observed for residual hemicellulose-rich sample with 71% carbohydrate content and it was composed by 26% of other compounds. The lignin-rich fraction was recovered free of carbohydrates with 87% purity. The residual lignin-rich material was not quantified because it was not possible to recover a sample due to its low quantity (3.0mg).

#### 3.5.4 Characterisation of pre-treatment samples using different ILs

The FT-IR spectra of obtained samples from pre-treatment with [bmim][SCN], [bmim][N(CN)<sub>2</sub>] and [bmim][HSO<sub>4</sub>] were evaluated comparing with data acquired from [emim][CH<sub>3</sub>COO] experiments. The spectra of regenerated material from pre-treatments with [bmim][SCN] and [bmim][N(CN)<sub>2</sub>] are illustrated in Appendix B and in general they are very similar to spectra demonstrated in Figure 12. Some slight differences can be observed in the region 1112-896cm<sup>-1</sup> due to a different ratio of carbohydrates (cellulose/hemicellulose) in each sample. For both spectra the absence of the band at 1228cm<sup>-1</sup> is observed, which in turn is present in spectra of the regenerated material from

[emim][CH<sub>3</sub>COO] experiment. For regenerated material spectrum of [bmim][SCN] experiment the band at 1734cm<sup>-1</sup> is still observed although with a low absorption. Furthermore, the additional band at 2146cm<sup>-1</sup> was observed that corresponds to the C-N stretching vibration of [bmim][N(CN)<sub>2</sub>].

The regenerated material obtained from the pre-treatment using [bmim][HSO<sub>4</sub>] shows different characteristic. The spectrum is presented in Figure 18.

From spectrum analysis a well-defined carbohydrate region can be assumed that possibly indicates the presence of one major type of carbohydrate. The carbohydrate characteristic bands in this spectrum are 897, 1035, 1061, 1108 and 1163cm<sup>-1</sup>. The shape of bands and the presence of bands at 1376 and 1429cm<sup>-1</sup> suggest a significant presence of cellulose. Lignin bands are also observed (1224, 1458, 1508, 1702 and 1718cm<sup>-1</sup>) with a relatively high absorption which are unexpected for the carbohydrate rich-material.

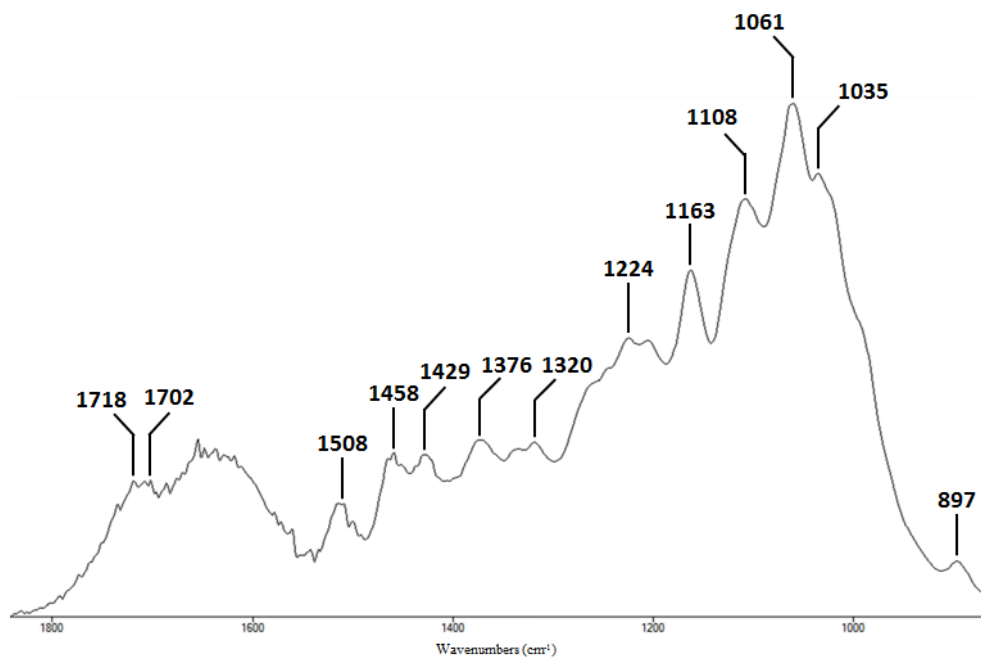


Figure 18. The FT-IR spectrum of the regenerated material from the pre-treatment with [bmim][HSO<sub>4</sub>].

The spectra of fractionated cellulose-rich materials from [bmim][SCN] and [bmim][N(CN)<sub>2</sub>] experiments are shown in Appendix B. The spectra are nearly the same as cellulose-rich material spectra from [emim][CH<sub>3</sub>COO] method, with only significant difference which is a practical disappearance of both bands at 998 and 1235cm<sup>-1</sup>. The spectrum of the cellulose-rich material from [bmim][HSO<sub>4</sub>] experiment demonstrates

almost complete absence of the lignin component in this sample as shown in Figure 19. The band at  $1420\text{cm}^{-1}$  disappears, whereas bands at  $1458$  and  $1508\text{cm}^{-1}$  are almost extinguished. However, comparing with the cellulose-rich material obtained from [emim][CH<sub>3</sub>COO] experiments suggested lignin absorption bands at  $1235$  and  $1260\text{cm}^{-1}$  had a higher absorbance. The presence of  $1718$  and  $1734\text{cm}^{-1}$  absorptions not only indicates the presence of lignin, but also hemicellulose as small characteristic bands.

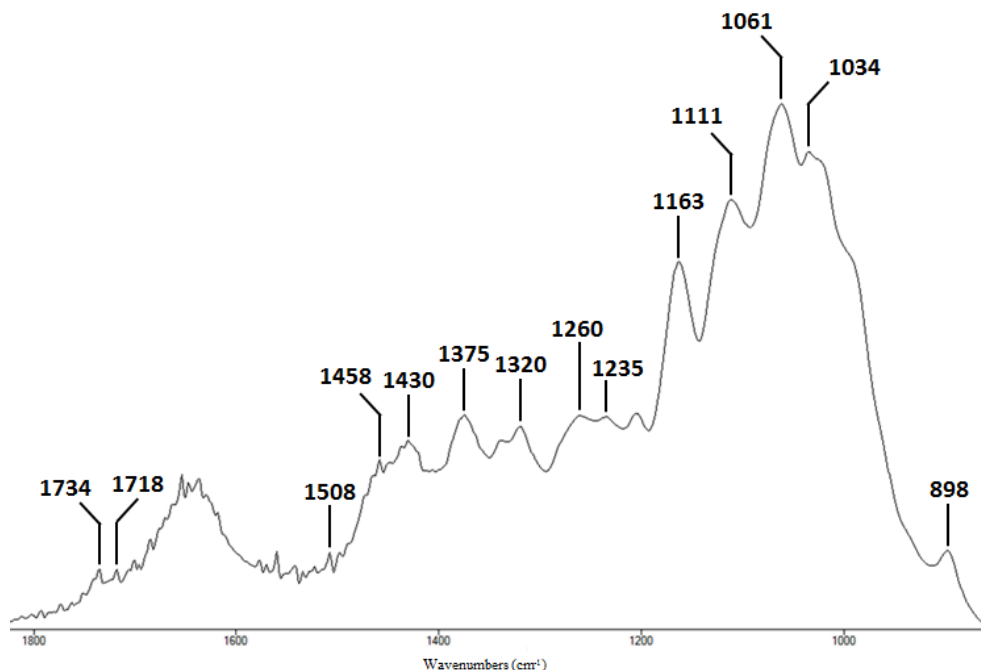


Figure 19. The FT-IR spectrum of the cellulose-rich material from the pre-treatment with [bmim][HSO<sub>4</sub>].

The FT-IR spectra of hemicellulose-rich materials obtained for studied ILs are very similar to that obtained in the pre-treatment with [emim][CH<sub>3</sub>COO]. All spectra of hemicellulose-rich materials obtained with different IL processes are shown in Appendix B. The only difference is the shift that was observed for some bands in the region  $1112$ - $896\text{cm}^{-1}$  as it was also stated for cellulose-rich materials. The residual hemicellulose-rich samples recovered from [bmim][SCN] and [bmim][N(CN)<sub>2</sub>] experiments were contaminated that is indicated by high absorption bands at  $1654$  and  $1327\text{cm}^{-1}$  that are abnormal for these kinds of compounds. In respect to hemicellulose materials obtained in experiment with [bmim][HSO<sub>4</sub>], a low quantity of the recovered sample did not allowed to perform FT-IR analysis.

The FT-IR analysis of obtained lignin samples from pre-treatments with [bmim] based ILs was generally impossible due to technical difficulties in handling, namely a sample recovery from nylon filters that caused a significant contamination of FT-IR spectra (Appendix B).

Samples of the residual-lignin material from E and F experiments demonstrated considerable differences in spectra when comparing with the residual-lignin obtained by the pre-treatment with [emim][CH<sub>3</sub>COO] (Figure 17). The spectra of residual lignin-rich materials from [bmim][N(CN)<sub>2</sub>] and [bmim][HSO<sub>4</sub>] experiments are illustrated in Figure 20 and Figure 21, respectively.

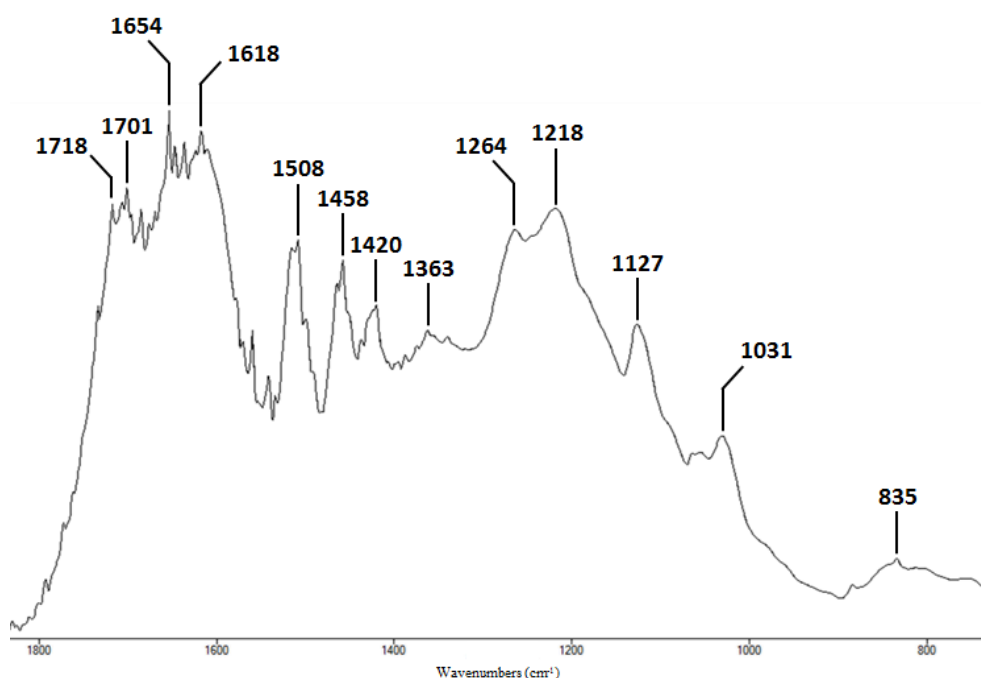


Figure 20. The FT-IR spectrum of the residual lignin-rich material from the pre-treatment with [bmim][HSO<sub>4</sub>].

Figure 20 shows lignin absorptions bands at 835, 1127, 1031, 1420, 1458cm<sup>-1</sup>. Among all the band at 1420cm<sup>-1</sup> dramatically decreased in comparison with the spectrum of residual-lignin (Figure 17) recovered from [emim][CH<sub>3</sub>COO] experiment. On the contrary, the absorption of bands at 1654, 1701 and 1718cm<sup>-1</sup> is significantly more intense. The absence of band at 1330cm<sup>-1</sup> and a shift of 1600 to 1618cm<sup>-1</sup> were also observed.

The spectrum obtained for the pre-treatment with [bmim][N(CN)<sub>2</sub>] shows clearly that the residual lignin-rich material was recovered with a high carbohydrate content (carbohydrate bands at 897, 1041 and 1079cm<sup>-1</sup>). The appearance of absorption band at 1734cm<sup>-1</sup>

indicates also the presence of hemicellulose that remained linked to lignin as well. Additionally a series of bands characteristic for lignin is also found here (1265, 1564, 1701 and  $1718\text{cm}^{-1}$ ).

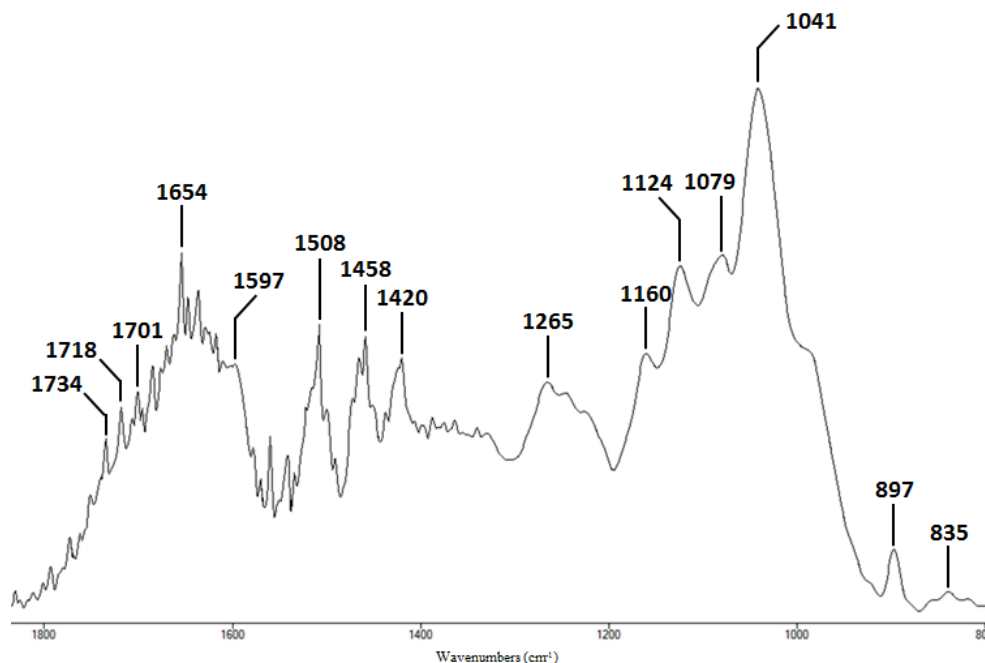


Figure 21. The FT-IR spectrum of the residual lignin-rich material from the pre-treatment with [bmim][N(CN)<sub>2</sub>].

### 3.5.5 Quantification of pre-treatment samples using different ILs

The same FT-IR based quantitative analysis was also performed for pre-treatment experiments using different ILs. Results are shown in Table 14-16 regarded [bmim][SCN], [bmim][N(CN)<sub>2</sub>] and [bmim][HSO<sub>4</sub>], respectively.

The pre-treatment with [bmim][SCN] gave the regenerated material with the carbohydrates content similar to the raw material (57% and 62%, respectively) and with a three times lower concentration of lignin. After the fractionation, cellulose and hemicellulose fractions were enriched in carbohydrates and contained much less lignin than the origin biomass or even regenerated solid fraction. Obtained lignins did not contain carbohydrates and the lignin content was from 72% to 89% depending on the fraction.

Table 14. FT-IR quantification of fractionated samples by the method C using [bmim][SCN].

Entry		Composition						Total /mg
		Carbohydrates		Lignin		Others		
		/mg	/wt%	/mg	/wt%	/mg	/wt%	
Dried WS		142.8	62	41.5	18	46.0	20	230.3
	RM	104.4	57	11.0	6	67.7	37	183.1
Solid fraction	Cellulose	94.2	68	8.3	6	36.0	26	138.5
	Hemicellulose	13.6	70	1.2	6	4.6	24	19.4
	Lignin <sup>a</sup>	0.0	0	3.4	72	1.3	28	4.7
Liquid fraction	Lignin	0.0	0	11.6	89	1.4	11	13.0
	Hemicellulose <sup>a</sup>	5.8	73	0.4	5	1.8	22	8.0

WS – wheat straw; RM - regenerated material; <sup>a</sup> residual

The pre-treatment with [bmim][N(CN)<sub>2</sub>] provided a regenerated material with 68% of the carbohydrate content and 11% of the lignin composition. The percentage of other present compounds changed insignificantly compared to the original dried biomass. The cellulose-rich material was enriched by carbohydrates achieving 87%. An 85% of carbohydrate content was also quantified for the hemicellulose-rich sample.

Table 15. The FT-IR quantification of fractionated samples by the method C using [bmim][N(CN)<sub>2</sub>].

Entry		Composition						Total /mg
		Carbohydrates		Lignin		Others		
		/mg	/wt%	/mg	/wt%	/mg	/wt%	
Dried WS		143.0	62	41.5	18	46.1	20	230.6
	RM	121.9	68	19.7	11	37.7	21	179.3
Solid fraction	Cellulose	102.4	87	9.4	8	5.9	5	117.7
	Hemicellulose	7.2	85	0.8	9	0.5	6	8.5
	Lignin <sup>a</sup>	4.5	38	4.5	38	2.8	24	11.8
Liquid fraction	Lignin	NQ	NQ	NQ	NQ	NQ	NQ	10.1
	Hemicellulose <sup>a</sup>	8.4	55	0.2	1	6.6	44	15.2

WS - wheat straw; RM - regenerated material; NQ - not quantified; <sup>a</sup> residual

For the residual hemicellulose-rich sample a low carbohydrate content was detected due to a large impact of other compounds. The same result was obtained for the residual lignin-rich material which in fact was equally constituted by carbohydrates and lignin with still large impact of other compounds (25%). The lignin-rich fraction was unfortunately not quantified due to technical difficulties caused by recovered quantities and the nylon filter used.

The analysis of the data obtained from [bmim][HSO<sub>4</sub>] showed that the regenerated material is generally equally composed as a pure wheat straw. The following fractionation allowed for a detailed enrichment of the cellulose fraction to 90% of carbohydrates diminishing drastically the lignin content (only 3%). The hemicellulose-rich fraction supposed to be obtained according to the method C, however no sample was produced. Additionally, the liquid fraction did not produce residual hemicellulose-rich fraction and lignin fraction was not quantified due to a large impurity of FT-IR spectra caused by nylon filters. The only quantified lignin fraction was the residual one, mostly composed by lignin and 38% of other compounds.

Table 16. The FT-IR quantification of fractionated samples by the method C using [bmim][HSO<sub>4</sub>].

Entry		Composition						Total /mg
		Carbohydrates		Lignin		Others		
		/mg	/wt%	/mg	/wt%	/mg	/wt%	
Dried WS		142.8	62	41.5	18	46.0	20	230.3
	RM	87.7	64	27.4	20	22.0	16	137.1
Solid fraction	Cellulose	66.6	90	2.2	3	5.2	7	74.0
	Hemicellulose	NQ	NQ	NQ	NQ	NQ	NQ	1.5
	Lignin <sup>a</sup>	0.0	0	19.1	62	11.7	38	30.8
Liquid fraction	Lignin	NQ	NQ	NQ	NQ	NQ	NQ	7.1
	Hemicellulose <sup>a</sup>	NQ	NQ	NQ	NQ	NQ	NQ	4.1

WS - wheat straw; RM - regenerated material; NQ - not quantified; <sup>a</sup>residual

### 3.6 Wheat straw pre-treatment reusing [emim][CH<sub>3</sub>COO]

The potential of the IL reuse in the consecutive pre-treatment of biomass was studied using [emim][CH<sub>3</sub>COO] following the method A. Seven successive processes were carried out providing results compiled in Table 17.

Table 17. Results of the wheat straw pre-treatment with the reused [emim][CH<sub>3</sub>COO].

Entry	WS /mg	Dried WS /mg	SF		LF	ML /% <sub>w/w</sub>	IL recovery /% <sub>w/w</sub>
			RM /mg	RY /% <sub>w/w</sub>	Lignin-rich /mg		
1	250.1	230.1	133.6	58.1	6.0	39.3	85.2
2	203.8	187.5	107.8	57.5	13.0	35.6	79.5
3	159.7	146.9	92.4	62.9	6.0	33.0	94.9
4	143.7	132.2	80.9	61.2	8.9	32.1	92.8
5	127.6	117.4	70.8	60.3	8.2	32.7	90.8
6	103.0	94.8	61.0	59.2	6.0	29.4	86.9
7	77.3	71.1	44.8	58.0	4.2	31.1	83.7

WS - wheat straw;; SF- solid fraction; RM - regenerated material; RY- regeneration yield; LF – liquid fraction; ML – material lost.

This study was started with an initial wheat straw loading of 250.1mg in [emim][CH<sub>3</sub>COO] and following the IL recovery the mass of feedstock was reduced maintaining the solid/liquid ratio constant. Regeneration yields of the pre-treated biomass varied from 57.5 to 62.9% and for lignin the recovery was from 29.4% to 35.6% of the theoretical amount present in a dry feedstock. The IL recovery was always higher than 80% reaching in a maximum 95% of the recovery.

### 3.7 Enzymatic hydrolysis

The enzymatic hydrolysis of carbohydrate-rich fractions from pre-treatments with [emim][CH<sub>3</sub>COO] (methods B and C) were applied. The regenerated material from the method A was also used in this study. In addition a standard pure cellulose and native wheat straw were used for comparison purposes. Results are given in Table 18 where enzymatic hydrolysis was measured as glucose yield (% w/w<sub>biomass</sub>) and total sugar yield (% w/w). The cellulose-rich material from the method C demonstrated a glucose yield of 76.5% (w/w<sub>biomass</sub>), higher than that observed for the method B (68.6%). Only 49.3%

(w/w<sub>biomass</sub>) was achieved for the regenerated material hydrolysis. Almost 100% (w/w<sub>biomass</sub>) of glucose was released after pure cellulose hydrolysis as well as a very low glucose yield for the native wheat straw was observed (19.7%). Complete carbohydrate (cellulose plus hemicellulose) hydrolysis were achieved for cellulose-samples B and C as well as for standard, with total sugar release nearly 100% (w/w). For the regenerated material 91.0% (w/w) of carbohydrates were hydrolysed and only 45.9% (w/w) was observed for native wheat straw. The total sugar yield was calculated basing on the FT-IR quantitated carbohydrate content.

Table 18. Glucose yields (% w/w<sub>biomass</sub>) and total sugar yields (% w/w) of enzymatic hydrolysis of cellulose-rich samples from methods A and B, regenerated material from method A, standard cellulose and native wheat straw.

Entry	Biomass /mg	Total sugar /mg	Glucose mg/mL	Cellulose /mg	Xylose mg/mL	Xylans /mg	Glucose %w/w <sub>biomass</sub>	Total sugar %w/w
Wheat straw	150.0	85.5	3.28	29.5	1.10	9.7	19.7	45.9
Cellulose STD	29.7	29.7	3.25	29.2	0.17	1.5	98.3	103.3
RM A	29.6	23.4	1.62	14.6	0.76	6.7	49.3	91.0
Cellulose B	30.3	24.9	2.31	20.8	0.44	3.8	68.6	99.1
Cellulose C	30.1	25.9	2.56	23.0	0.40	3.5	76.5	102.4

STD – standard; RM A – regenerated material using method A

### 3.8 NMR analysis

The purity of ILs after pre-treatments was verified using <sup>1</sup>H- and <sup>13</sup>C-NMR techniques. The determined chemical shifts are the following:

[Emim][CH<sub>3</sub>COO] <sup>1</sup>HNMR (400 MHz; CDCl<sub>3</sub>) δ(ppm): 1.54 (t, 3H, NCH<sub>2</sub>CH<sub>3</sub>); 1.92 (s, 3H, CH<sub>3</sub>COO); 4.05 (s, 3H, NCH<sub>3</sub>); 4.36 (q, 2H, NCH<sub>2</sub>CH<sub>3</sub>); 7.29 (d, 2H, NCHCHN); 10.63 (s, 1H, CH<sub>3</sub>COOH). <sup>13</sup>CNMR (CDCl<sub>3</sub>) δ(ppm): 15.58 (NCH<sub>2</sub>CH<sub>3</sub>); 24.92 (CH<sub>3</sub>COO); 36.39 (NCH<sub>3</sub>); 45.07 (NCH<sub>2</sub>CH<sub>3</sub>); 121.50 (NCHCHN); 123.36 (NCHCHN); 138.26 (NCHN) and 177.57 (CH<sub>3</sub>COO).

[Bmim][SCN] <sup>1</sup>HNMR (400 MHz; CDCl<sub>3</sub>) δ(ppm): 0.94 (t, 3H, CH<sub>3</sub>CH<sub>2</sub>); 1.38 (m, 2H, CH<sub>3</sub>CH<sub>2</sub>CH<sub>2</sub>); 1.90 (m, 2H, CH<sub>2</sub>CH<sub>2</sub>CH<sub>2</sub>); 4.07 (s, 3H, NCH<sub>3</sub>); 4.30 (t, 2H, NCH<sub>2</sub>); 7.52 (d, 2H, NCHCHN); 9.27 (s, 1H, NCHN). <sup>13</sup>CNMR (CDCl<sub>3</sub>) δ(ppm): 13.44 (CH<sub>3</sub>CH<sub>2</sub>); 19.47 (CH<sub>3</sub>CH<sub>2</sub>CH<sub>2</sub>); 32.06 (CH<sub>2</sub>CH<sub>2</sub>CH<sub>2</sub>); 35.72 (NCH<sub>3</sub>); 50.09 (NCH<sub>2</sub>); 122.40 (NCHCHN); 123.84 (NCHCHN); 136.56 (NCHN).

[Bmim][N(CN)<sub>2</sub>] <sup>1</sup>HNMR (400 MHz; CDCl<sub>3</sub>) δ(ppm): 0.95 (t, 3H, CH<sub>3</sub>CH<sub>2</sub>); 1.36 (m, 2H, CH<sub>3</sub>CH<sub>2</sub>CH<sub>2</sub>); 4.00 (s, 3H, NCH<sub>3</sub>); 4.22 (t, 2H, NCH<sub>2</sub>); 7.41 (d, 2H, NCHCHN); 9.17 (s, 1H, NCHN). <sup>13</sup>CNMR (CDCl<sub>3</sub>) δ(ppm): 13.28 (CH<sub>3</sub>CH<sub>2</sub>); 19.35 (CH<sub>3</sub>CH<sub>2</sub>CH<sub>2</sub>); 31.85 (CH<sub>2</sub>CH<sub>2</sub>CH<sub>2</sub>); 36.47 (NCH<sub>3</sub>); 49.94 (NCH<sub>2</sub>); 122.28 (NCHCHN); 123.68 (NCHCHN); 136.33 (NCHN).

The NMR spectra of ILs are demonstrated in Appendix C.

## 4 Discussion

### 4.1 Preliminary evaluation of wheat straw pre-treatment using [emim][CH<sub>3</sub>COO]

In the pre-treatment preliminary experiments a complete macroscopic dissolution of wheat straw was observed for 6 and 16h of processing. Both pre-treatments produced a dark brown solution, however the addition of antisolvent (NaOH 0.1M) in case of 16h process caused formation of a jelly regenerated material. In literature, similar results were observed for sugarcane bagasse treatment at prolonged times.<sup>121</sup> Furthermore, degradation of biomass compounds and also of ILs was verified by using high pre-treatment times.<sup>72, 77</sup>

In fact, by microscopic observations Singh et al. clearly demonstrated that [emim][CH<sub>3</sub>COO] was capable to completely dissolve switchgrass after 3h at 120°C.<sup>82</sup> Therefore, reducing the time of dissolution should be suitable to pre-treat wheat straw. The complete macroscopic dissolution of wheat straw was achieved in 6h trial experiment and less viscous solution was produced resulted in a clear brownish biomass flocculation after addition of NaOH as an antisolvent. The 1h experiment caused only a partial dissolution noticed by visual observation that could decrease the pre-treatment efficiency as a regenerated material was very similar in structure to the native wheat straw. This is on contradiction to results obtained by Li et al. who stated that 1h pre-treatment of wheat straw with the same IL was sufficient to achieve macroscopic complete dissolution.<sup>98</sup>

Summarising 6h process is the most optimal among tested as complete macroscopic dissolution of biomass is guaranteed and efficient recovery of carbohydrate-rich fraction is produced.

### 4.2 Optimisation of wheat straw pre-treatment using [emim][CH<sub>3</sub>COO]

Considering method A pre-treatment experiments, higher regeneration yield was observed for A2 (67.8%) than for A1 experiment (55.3%). The A3 experiment showed similar regeneration yield of carbohydrate-rich material (55.4%) comparing to A1 experiment. This result could be explained by the ratio wheat straw/antisolvent added (0.1M NaOH) in A2 was two-fold higher than that of A1 or A3. Or other words a higher amount of NaOH maintains a higher concentration of the dissolved compounds from the solution giving lower regeneration yields. The literature reports present similar results in case of 0.1M NaOH used as an antisolvent. Tan et al. obtained 46-55% of regenerated material for 0.1M

NaOH/IL ratio analogous to A3 experiment<sup>94</sup>, while the pre-treatment of wheat straw at 130°C for 1.5h with ratio of 0.1M NaOH/IL as A2 experiment resulted in 62.0% regeneration yield that was lower than A2.<sup>93</sup>

The different amount of 0.1M NaOH has also consequences in the quantity of lignin recovered and by this in purity. For example lignin from the sample A3 regenerated with 80mL of NaOH gave almost 70% mass more than in A2 experiment with only 40mL of NaOH. However as observed in Figure 22 lignin rich-material obtained by A3 was more contaminated by hemicellulose than lignin rich-material obtained by A2 experiment. This difference is especially visible by hemicellulose characteristic bands such as 897, 1042, 1079 and 1158cm<sup>-1</sup>. In A2 samples the same bands exhibited significantly lower intensity therefore 40mL 0.1M NaOH for 250mg/5mL of biomass/IL seemed to be more adequate amount giving high recovery yield of carbohydrate-rich fraction and high purity lignin.

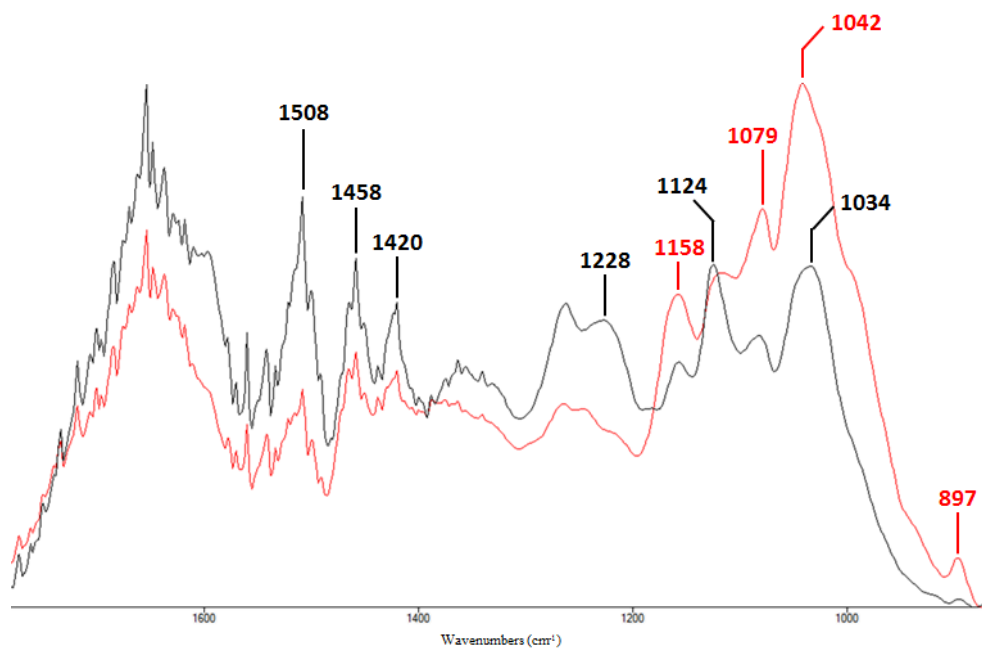


Figure 22. FT-IR spectra of lignin rich-materials from A2 (black) and A3 (red) pre-treatment experiments.

In addition it is important to point out that the IL recovery in A2 experiment was lower than A1 and A3. This small difference might be caused by the fact that lower amount of NaOH as antisolvent was used in A2 experiment. Therefore the more viscous and concentrated IL solution made the inclusion and loss of IL easier, thus the recovery of IL

in A2 was insignificantly lower although noticeable (76.2% vs 71.2%) as presented in Table 4.

Method B served to verify the potential of further fractionation of regenerated material. For this purpose as antisolvent acetone/water mixture in 9/1 (v/v) ratio was used to regenerate the dissolved wheat straw after 4h dissolution in [emim][CH<sub>3</sub>COO]. In B1 experiment, a biphasic solution was formed after antisolvent addition showing that [emim][CH<sub>3</sub>COO] was immiscible with acetone. This phenomenon led to a very low recovery of IL estimated to be 53.3% of the initial mass. To overcome this result the addition of acetone/water mixture in 9/1 (v/v) in the regeneration step of B2 was followed by the addition of acetone/water mixture in 1/1 (v/v) and later water. The solid precipitate was washed and simultaneously [emim][CH<sub>3</sub>COO] was extracted in the liquid stream. A 92.7% yield of IL recovery was achieved for B2 experiment. Indeed, better results were observed for B2 experiment giving higher regeneration yield (72.2%), higher lignin-rich mass (10.1 mg - 10% (w/w) of biomass loaded) and less material lost (17.0%). Therefore, the gradual increase of water content in the mixture solution used to regenerate the dissolved biomass improved the precipitation of carbohydrate-rich material, the extraction and recovery of lignin-rich material and IL as well as less material was lost. The obtained results showed a significant difference comparing to the data presented by Lan et al.<sup>97</sup> It is important to point out that the presented method B was originated from this work, although Lan and co-workers used [bmim][Cl] for sugarcane bagasse fractions. They obtained a regeneration yield of 84.34%, acetone soluble lignin of only 6.54% of biomass loaded.<sup>97</sup> It can be concluded that the depicted differences are principally caused by biomass used because the sugarcane bagasse contained almost 80% of carbohydrates compared with only 62% in case of the studied wheat straw.

The fractionation of regenerated material used in this work was successfully performed into cellulose, hemicellulose and residual lignin in both B1 and B2 experiments with identical mass fractions. In the case of B2 experiment cellulose-rich, hemicellulose-rich and residual lignin-rich materials were recovered with 61.5%, 29.6% and 4.8% of the fractionated regenerated material (72.2% of initial dried biomass). This means that wheat straw (100.5mg) was fractionated into 44.2% cellulose-rich material, 21.4% hemicellulose-rich material and 13.5% total lignin rich-materials (acetone soluble lignin plus residual

lignin) and 20.9% was lost. Comparing to the Lan<sup>97</sup> data the fractionation presented in this work gave generally better results with lower losses of initial biomass.

The main goal of method C was to obtain fractionated samples with a higher purity. For this purpose 5% (w/w) biomass/IL ratio and 40mL of 0.1M NaOH were used to regenerate the dissolved biomass. The type of antisolvent for biomass was selected based on the quantitative analysis of the regenerated material performed by FT-IR quantitative analysis. Carbohydrate contents of 79% and 64% were determined for 0.1M NaOH and acetone/water mixture regeneration, respectively. The third decisive parameter was an additional step leading to removal of the residual hemicellulose from the extracted lignin that gave a higher purity of the extracted lignin. For this purpose ethanol was used, however due to NaCl low solubility in ethanol the simultaneous precipitation of this salt occurred together with residual hemicellulose.<sup>122</sup> To avoid this problem hemicellulose samples were washed with water to wash out NaCl (C2 and C3). Additional test with wet regenerated material was performed to verify the need of drying of the regenerated material, however in the case of wet material after IL processing larger volumes of ethanol were required.

Analysing the IL recover it can be stated that in case of C1 experiment (78.2%) the IL inclusion in the non-washed salt could appear, since in C2 and C3 experiments the quantity of IL was significantly higher (89.1 and 86.2%).

The fractionation of the regenerated material using method C followed results of the method B, since this part of the process was analogous to the mentioned method.

The overall fractionation of wheat straw by the C3 experiment gave the following mass balance: 41.8% cellulose-rich material, 25.4% total hemicellulose-rich material (hemicellulose plus residual hemicellulose), 8.0% total lignin-rich sample (lignin residual plus lignin) and 24.8% material lost. The successful fractionation attained in this work regarding methods B and C is presented in Figure 23. It depicts FT-IR spectra of standard cellulose (black) and original wheat straw (green) comparing with the fractionated samples of cellulose (red) and hemicellulose (blue).

The spectrum of hemicellulose is presented in literature.<sup>97, 112, 114</sup> The spectra of standard and fractionated sample of cellulose demonstrated great similarities especially for the characteristic region 1035-1061cm<sup>-1</sup>. For hemicellulose spectrum there were clearly visible differences in the carbohydrate characteristic region presenting a very strong absorption

band at  $1043\text{cm}^{-1}$  that indicates the presence of xylans contrary to cellulose with the characteristic band at  $1061\text{cm}^{-1}$ . Furthermore, the hemicellulose spectrum demonstrated the absence of the band at  $1734\text{cm}^{-1}$ , indicating successful cleavage of ester linkages between hemicellulose and lignin. Similarly the nearly lack of lignin in both cellulose and hemicellulose-rich fractions can be confirmed by the negligible band at  $1508\text{cm}^{-1}$ .

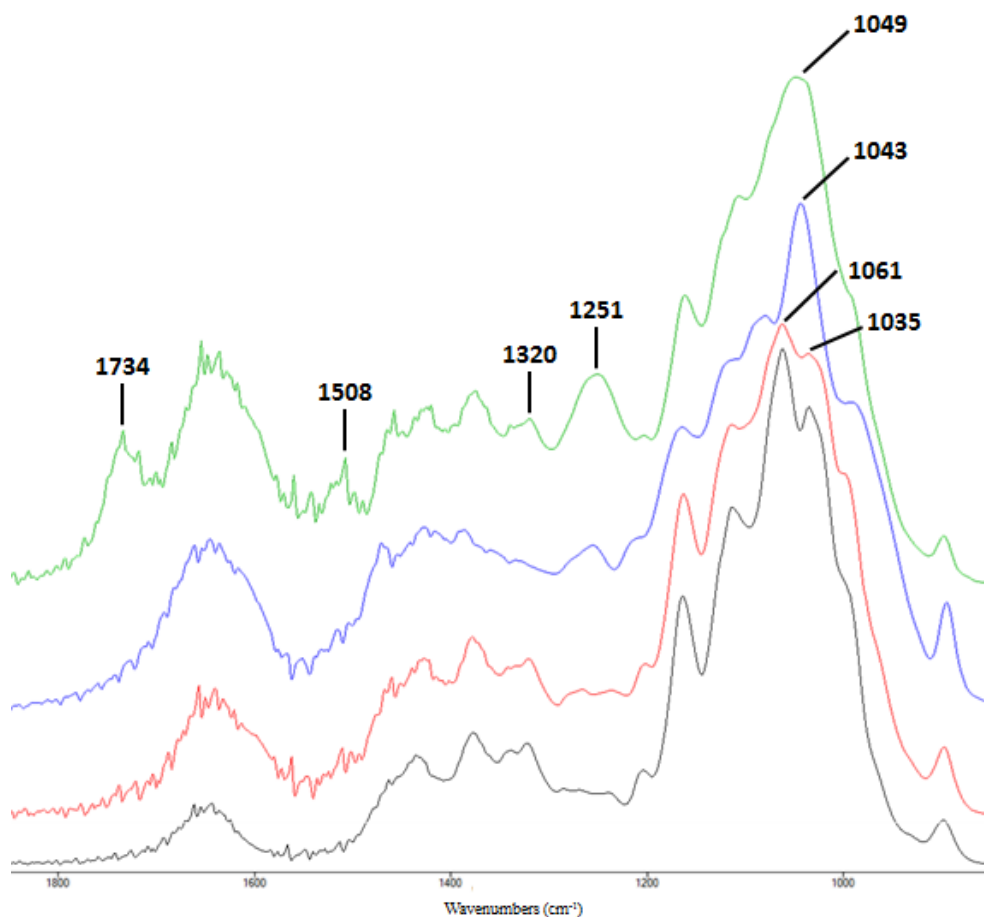


Figure 23. FT-IR spectra of standard cellulose (black) and original wheat straw (green) comparing with the fractionated samples of cellulose (red) and hemicellulose (blue).

The purity of hemicellulose fraction, regarding cellulose content, can be confirmed by the absence of the band at  $1320\text{cm}^{-1}$ . Similar cellulose fraction was of a high purity too as it did not contain the acetyl groups characteristic for hemicellulose ( $1251\text{cm}^{-1}$ ). Additionally it is important to emphasise that the acetyl group band at  $1251\text{cm}^{-1}$  in the hemicellulose fraction was significantly less intense. It may indicate that in the pre-treatment, acetyl groups from hemicellulose molecular chains were partial hydrolysed.

Lignin as a more complex compound can give different composition depending on a pre-treatment process. The obtained lignin samples also demonstrated successful fractionation.<sup>117, 119, 120</sup> The spectra comparison of the lignin-rich material from acetone (blue) and NaOH (red) extraction, as well as residual lignin-rich material (black) are illustrated in Figure 24.

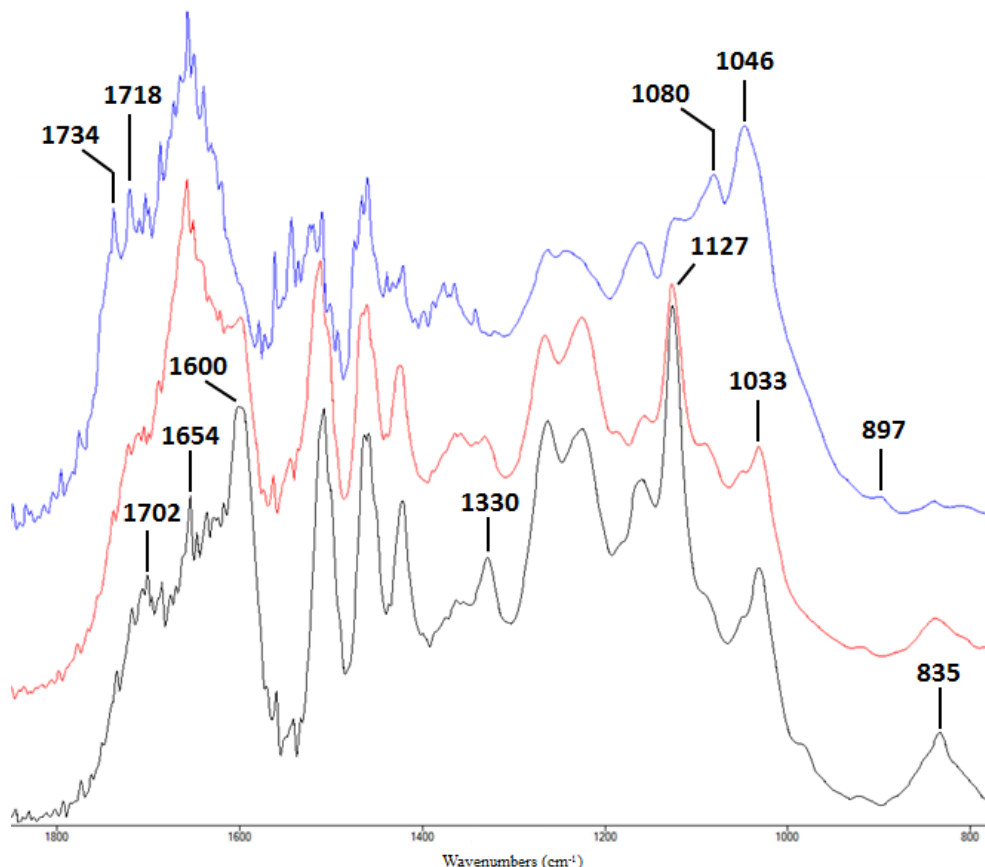


Figure 24. FT-IR spectra of acetone soluble lignin rich-material from method B (blue), lignin rich-material from method C (red) residual-lignin rich from method C (black) pre-treatment experiments.

Significant differences between the three lignins presented here were noticed. First, a less purified lignin was obtained by acetone/water (method B) extraction that can be determined by the carbohydrate presence and confirmed by vibrational absorptions at 897, 1046 and 1080 $\text{cm}^{-1}$ . Furthermore, the multiple small absorptions in region 1200-1600 $\text{cm}^{-1}$  indicated the presence of other compounds. In fact, acetone as a hydrophobic organic solvent is able to dissolve long chain hydrocarbons<sup>123</sup> that can lead to significant increase of absorption intensities at 2852 and 2920 $\text{cm}^{-1}$  observed in the complete spectrum of

acetone soluble lignin (Appendix B). These absorptions are attributed to C-H stretching vibrations that are characteristic of CH, CH<sub>2</sub> and CH<sub>3</sub> groups present in hydrocarbon molecules.

The two other lignins (red and black) can be considered as carbohydrate-free lignin as characteristic bands such 897, 1046 and 1080cm<sup>-1</sup> were not observed.

One of main differences between these three lignin spectra corresponds to the band at 1127cm<sup>-1</sup> that was not observed for acetone soluble lignin spectrum and appeared as strong absorption bands in two other spectra. As it is presented in literature this band corresponds to C=O stretching of syringyl units as well as secondary alcohols present in lignin.<sup>105, 118</sup> Therefore, in acetone soluble lignin lack of syringyl unit was observed. Furthermore, in the presented figures it can be noticed the reduction of the intensity of the band at 1654cm<sup>-1</sup> that is characteristic for conjugated para-substituted aryl ketones and it is observed in the residual lignin-rich spectrum. This occurs due to a higher deformation of the carbonyl existing in the side chains of lignin structural units and modification of functional groups in the side chains.<sup>124</sup> Additionally, the band at 1330cm<sup>-1</sup> indicates the condensation in lignin structure (syringyl and guaiacyl). The lignin condensation phenomenon is usually generated by high heating temperatures during the pre-treatment.<sup>125</sup> These structural changes can be explained by the fact that increased concentration of NaOH solution (3% w/w) used in the fractionation of the regenerated material extracts residual lignin can lead to this structural reconstitution. Apparently it did not happen in the extraction of lignin-rich material with acetone and it was less evidenced with 0.1M NaOH.

### **4.3 Quantification of pre-treatment samples using [emim][CH<sub>3</sub>COO]**

The FT-IR quantitative analysis permits to have a better perspective of sample purities and allowed to compare efficiencies of tested methodologies. Method A only followed the fractionation into carbohydrate-rich sample in a solid state and lignin-rich material that was recovered from the liquid stream by precipitation. A carbohydrate content of 79% was obtained in the regenerated material, although the extracted lignin with 70% purity was not free of carbohydrates (6%). Regarding to the biorefinery concept this methodology has a limited exploitation of potential materials that could be fractionated from the original biomass. Improvements to overcome this limitation were achieved by method B where carbohydrate-rich material was fractionated into cellulose and hemicellulose fractions.

Furthermore, residual lignin retained in carbohydrate-rich material after the regeneration process was recovered ensuring a more efficient process. In fact, cellulose and hemicellulose-rich materials were recovered with a high carbohydrate content reaching 82% and 80%, respectively. Simultaneously, the reduction of lignin content was observed from 18% of dried wheat straw to 14% in the regenerated material, followed by cellulose and hemicellulose fractionation containing 10% and 9% lignin content, respectively. An extremely high pure residual lignin (98% purity) was obtained at the end of the fractionation process. However, it can be pointed out that in the fractionation by method B the lignin coming from the liquid fraction was strongly contaminated, thus lignin-rich material was recovered showing only 57% purity. Secondly, the obtained regenerated material had a similar composition to the original biomass that affected the followed fractionation.

The optimised method C proven to be the most efficient pre-treatment process among studied as it produced samples with the highest purity. A representative scheme of quantitative fractionation results using method C is illustrated in Figure 25. Method C fractionation provided a reduction from 18% lignin content in the initial biomass to 6% for the regenerated material just in one step extraction. The regenerated material was then fractionated and lignin content maintained in the cellulose-rich sample decreasing to 5% in the hemicellulose-rich material. Herein the lignin-rich material extracted by 0.1M NaOH antisolvent demonstrated to be carbohydrate-free. The residual lignin rich-material was not quantified because of a low quantity recovered. The only drawback was the lowest purity of residual hemicellulose-rich samples (71% carbohydrate content) as this sample was still contaminated by NaCl (not detectable by FT-IR measurements), even after washing with water. The very low lignin content (3%) and high amount of other fractions present in this residual hemicellulose confirms this divagation.

Obtained results demonstrated to have a potential impact in this research field. Higher purity samples were processed by performed methods, especially for method C that can be compared with literature results. Treatment of southern yellow pine (68.2% carbohydrates and 31.8% lignin) with [emim][CH<sub>3</sub>COO] (16h, 110°C)<sup>77</sup> demonstrated a fractionation of nearly 100% purity of lignin sample and regenerated material with 76.5% carbohydrate and 23.5% lignin contents. Basing on FT-IR analysis a carbohydrate-free lignin was confirmed; however, presence of other components expected to be in sample was not

studied. It is important to underline that the lignin-rich fraction obtained in this work using method C is also carbohydrate-free; however, nearly 13% of other compounds were present in the sample. Therefore perception results presented in this work are equally good as presented elsewhere.<sup>77</sup> Other literature example corresponds to the pre-treatment of switchgrass (64.5% carbohydrate and 21.8% lignin contents) with [emim][CH<sub>3</sub>COO] (3h, 160°C) that permitted to obtain carbohydrate-rich material with 79.5% carbohydrate content, 13.6% total lignin content and the remaining content as ash and other compounds.<sup>87</sup> As it is depicted in Figure 25 the regenerated material from the method C shows a higher carbohydrate content than that for switchgrass with only 6% lignin content. Furthermore, it can also be emphasised that better delignification occurred in the method C is associated to the NaOH potential lignin extraction that seems to be superior than deionised water usually used in the literature report.<sup>87, 121</sup>

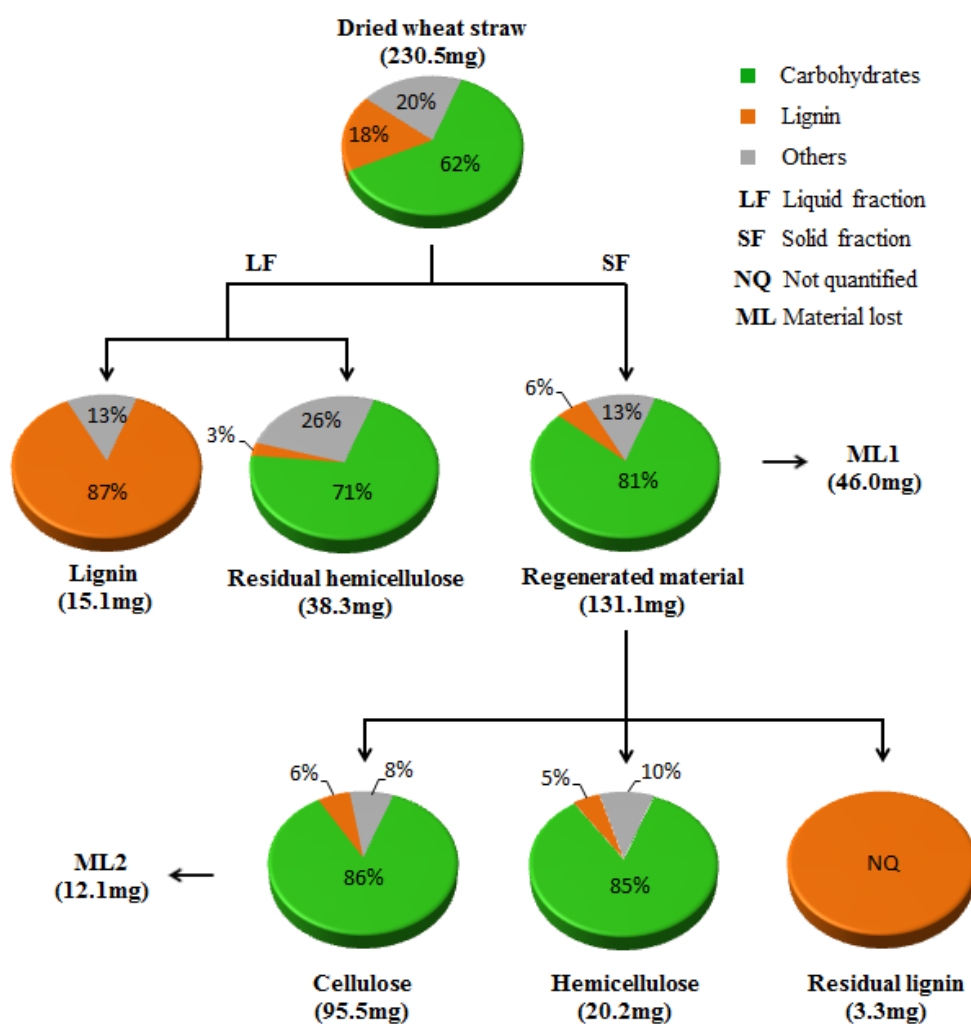


Figure 25. Fractionation of wheat straw by method C using [emim][CH<sub>3</sub>COO].

#### 4.4 IL effect on wheat straw pre-treatment

The versatility of method C was studied by examination of different ILs namely, [bmim][SCN], [bmim][N(CN)<sub>2</sub>] and [bmim][HSO<sub>4</sub>]. The selection of these ILs was based on previous dissolution experiments of carbohydrates, which demonstrated a high solubility in such ILs.<sup>61, 84</sup>

The pre-treatment with selected ILs followed the method C. The 6h pre-treatment with [bmim][SCN] and [bmim][N(CN)<sub>2</sub>] did not allow for complete dissolution of wheat straw contrary to [bmim][HSO<sub>4</sub>] in which a macroscopic complete dissolution was attained as it was also observed when [emim][CH<sub>3</sub>COO] was used. Thus it can be stated that [emim][CH<sub>3</sub>COO] and [bmim][HSO<sub>4</sub>] demonstrated to be the most efficient ILs in dissolution of wheat straw in this study.

It should also be noticed that the best results in the dissolution process were performed by IL with a strong basic anion [CH<sub>3</sub>COO] and also by the acidic IL such as [bmim][HSO<sub>4</sub>]. This means that dissolution was certainly performed in different processes by [emim][CH<sub>3</sub>COO] and [bmim][HSO<sub>4</sub>]. In the regeneration process similar to [emim][CH<sub>3</sub>COO] a brown flocculated material was precipitated while in pre-treatment with [bmim][HSO<sub>4</sub>] a black viscous solid was formed after 0.1M NaOH addition.

Evaluating obtained regeneration yields, [bmim][SCN] and [bmim][N(CN)<sub>2</sub>] experiments demonstrated very high regeneration yields (79.5% and 77.7%). This could be correlated with the partial dissolution observed for these ILs where the regenerated biomass should be mainly composed of insoluble material during IL dissolution. In the case of [bmim][HSO<sub>4</sub>] the regeneration yield (59.6%) was similar to that obtained for [emim][CH<sub>3</sub>COO].

Comparing pre-treatments with [bmim][SCN] and [bmim][N(CN)<sub>2</sub>] it can be stated that from the liquid stream after regeneration process, a higher lignin-rich material was recovered for [bmim][SCN] than from [bmim][N(CN)<sub>2</sub>] experiment. Furthermore the fractionation of the regenerated materials showed that it contains 83% and 76% of cellulose for [bmim][SCN] and [bmim][N(CN)<sub>2</sub>], respectively. Additionally, similar analogy was observed for hemicellulose-rich material. Achieved results indicate that among these two ILs, [bmim][SCN] is better IL as it led to higher amount of materials recovered in each principal fractions (cellulose, hemicellulose and lignin). However analysing obtained results it can be highlighted that in case of [bmim][N(CN)<sub>2</sub>] IL, the principle stream of hemicellulose was found in the liquid fraction together with lignin. It

may indicate that these two polymers are strongly linked by ester bonds and dicyanamide anion is not efficient in the deconstruction of this bond.

FT-IR qualitative analysis of the obtained samples from pre-treatments with [bmim][SCN] and [bmim][N(CN)<sub>2</sub>] demonstrated very similar results to [emim][CH<sub>3</sub>COO] samples. Basically, for all carbohydrate spectra (regenerated material, cellulose and hemicellulose spectra) slight differences were observed in the carbohydrate absorption characteristic region indicating that hemicellulose and cellulose content is varied in those samples.

Other interesting fact is that ester bonds between hemicellulose and lignin in the regenerated material from [bmim][SCN] experiment are still present. This proves that partial biomass dissolution was observed for this IL during pre-treatment.

Moreover, [bmim][N(CN)<sub>2</sub>] seemed to contaminate the regenerated material as the presence of the C-N stretching vibration in N(CN)<sub>2</sub><sup>-</sup> was observed at 2146cm<sup>-1</sup>. The analogous problem did not occur in SCN<sup>-</sup> as this band was not visible. In respect to both cellulose rich-materials spectra bands at 998 and 1235cm<sup>-1</sup> almost disappeared in comparison with that observed in [emim][CH<sub>3</sub>COO] cellulose-rich sample. This indicates that cellulose obtained by pre-treatments with [bmim][SCN] and [bmim][N(CN)<sub>2</sub>] are almost free of arabinan (998cm<sup>-1</sup>) and syringyl lignin type (1235cm<sup>-1</sup>). The hemicellulose-rich samples did not present significant differences.

The lignin samples (including residual lignin) obtained from the [bmim][SCN] experiment did not show significant differences in comparison with the corresponding [emim][CH<sub>3</sub>COO] lignin materials. However, the lignin sample (residual lignin) of [bmim][N(CN)<sub>2</sub>] demonstrated a high contamination of carbohydrates namely hemicelluloses (897, 1041 and 1079cm<sup>-1</sup>). Furthermore, presence of the band at 1734cm<sup>-1</sup> can be responsible for the existence of ester linkages of hemicellulose and lignin. Therefore, it confirms that [bmim][N(CN)<sub>2</sub>] was inefficient to separate hemicellulose from lignin as stated above. Unfortunately, the lignin-rich material from [bmim][N(CN)<sub>2</sub>] experiment was contaminated with nylon filter being impossible to analyse because it caused significant changes in the FT-IR spectrum.

The pre-treatment with [bmim][HSO<sub>4</sub>] demonstrated a different behaviour than other previously discussed ILs. After regeneration of the carbohydrate-rich fraction, only small quantities of lignin-rich and residual hemicellulose-rich materials were recovered from the liquid stream, in spite of the macroscopic complete dissolution achieved by

[bmim][HSO<sub>4</sub>]. The pH of the liquid stream containing the IL was determined to be pH=1.3, even with the addition of basic solution 0.1M NaOH that usually should rise pH to 12 as determined for other IL solutions. Therefore, these results suggest that acidic property of HSO<sub>4</sub><sup>-</sup> could perform acid hydrolysis of hemicellulose fraction. In acid hydrolysis the liquid stream was enriched in hydrolysed hemicelluloses (monosaccharides and oligosaccharides) and the solid material contained mostly cellulose and lignin.<sup>126</sup> As already referred, in the liquid stream a small quantity of lignin-rich fraction was recovered, possibly extracted during the washing of the regenerated material by water (neutral pH). A small quantity of hemicellulose-rich material was also recovered and it is expected to be non-hydrolysed hemicellulose.

The fractionation of the regenerated material into cellulose, hemicellulose and residual lignin-rich materials was also different regarding obtained quantities of each sample as presented in Table 10. Obtained results for [bmim][HSO<sub>4</sub>] confirmed the acid hydrolysis phenomenon as an insignificant quantity of hemicellulose was extracted from the regenerated material (1.5mg). The cellulose-rich sample was obtained with a high purity and its spectrum was compared with spectra of the regenerated material and standard cellulose as illustrated in Figure 26.

The regenerated material spectrum (blue) confirmed the presence of cellulose and lignin in this sample. In the carbohydrate characteristic region, sharp bands of cellulose with exactly the same chemical absorption vibrations as that for cellulose standard spectrum (black) were observed. The lignin content in the regenerated material was relatively high, where absorption bands at 1458, 1508, 1702, and 1718cm<sup>-1</sup> were present with high intensities. In case of the cellulose-rich sample (red spectrum below) these bands were almost absent, thus the fractionation process allowed to obtain a high purity sample. In comparison with cellulose standard (black spectrum) bands at 1260 and 1235cm<sup>-1</sup> attributed to lignin were observed in the sample of cellulose obtained in this work. It can be expected that these bands are of hemicellulose that is generally noticeable at 1251cm<sup>-1</sup> and in addition the hemicellulose was detected by the absorption band at 1734cm<sup>-1</sup>.

The pre-treatment with [bmim][HSO<sub>4</sub>] provided an impressive quantity of “residual” lignin-rich material (30.8mg). The spectrum of this sample showed that lignin was the major component but extraordinary amount of contamination was also present as shown in Figure 20. In fact, the major lignin content in wheat straw was not extracted in the liquid

stream after regeneration process as occurred in pre-treatments with other ILs, but it was extracted from the regenerated material as it happened in acid hydrolysis process. Therefore, [bmim][HSO<sub>4</sub>] did not only dissolve lignocellulosic biomass but also was able to hydrolyse. In fact, the potential of [bmim][HSO<sub>4</sub>] in biomass hydrolysis is for the first time demonstrated here as in the literature no special attention is given to this IL<sup>87</sup> or only the dissolution and fractionation abilities are attributed.<sup>127</sup>

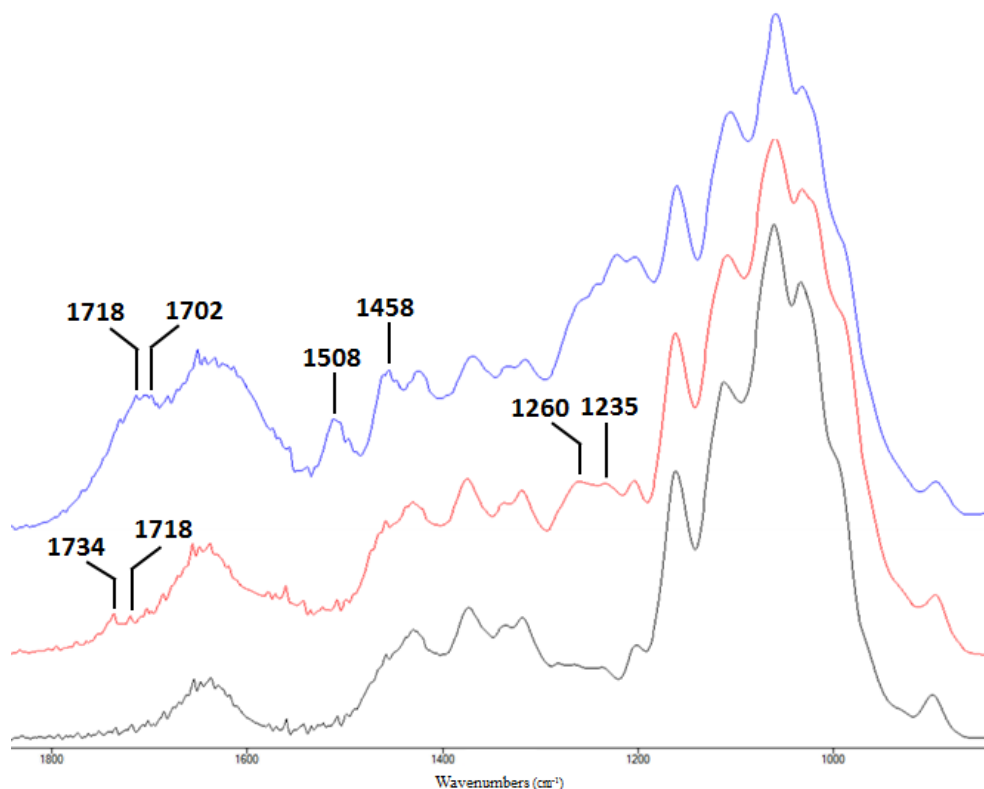


Figure 26. FT-IR spectrum of standard cellulose (black) comparing with spectra of regenerated material (blue) and cellulose-rich material (red) obtained in the pre-treatment with [bmim][HSO<sub>4</sub>].

Evaluating the IL recovery of tested ILs it can be concluded that the recovery process needed fine-tuning for [bmim][SCN], [bmim][N(CN)<sub>2</sub>] and [bmim][HSO<sub>4</sub>]. The obtained IL recovery yields were high, exceeding 90% of the initial mass used, with a special attention for [bmim][N(CN)<sub>2</sub>] experiment that achieved a 97% IL recovery.

#### 4.5 Quantification of pre-treatment samples using different ILs

The FT-IR quantitative analysis was used to determine the composition of produced fractions obtained by the pre-treatment with [bmim][SCN], [bmim][N(CN)<sub>2</sub>] and [bmim][HSO<sub>4</sub>].

The purity of fractions obtained from the pre-treatment with [bmim][SCN] is presented in Figure 27. As it is shown both cellulose and hemicellulose fractions contain more carbohydrates than raw biomass. The lignin obtained from the liquid fraction exhibited an elevated purity as high as 89%. Concluding it can be stated that the pre-treatment with [bmim][SCN] IL can be rather used to produce a high purity lignin than to obtain enriched carbohydrate fractions.

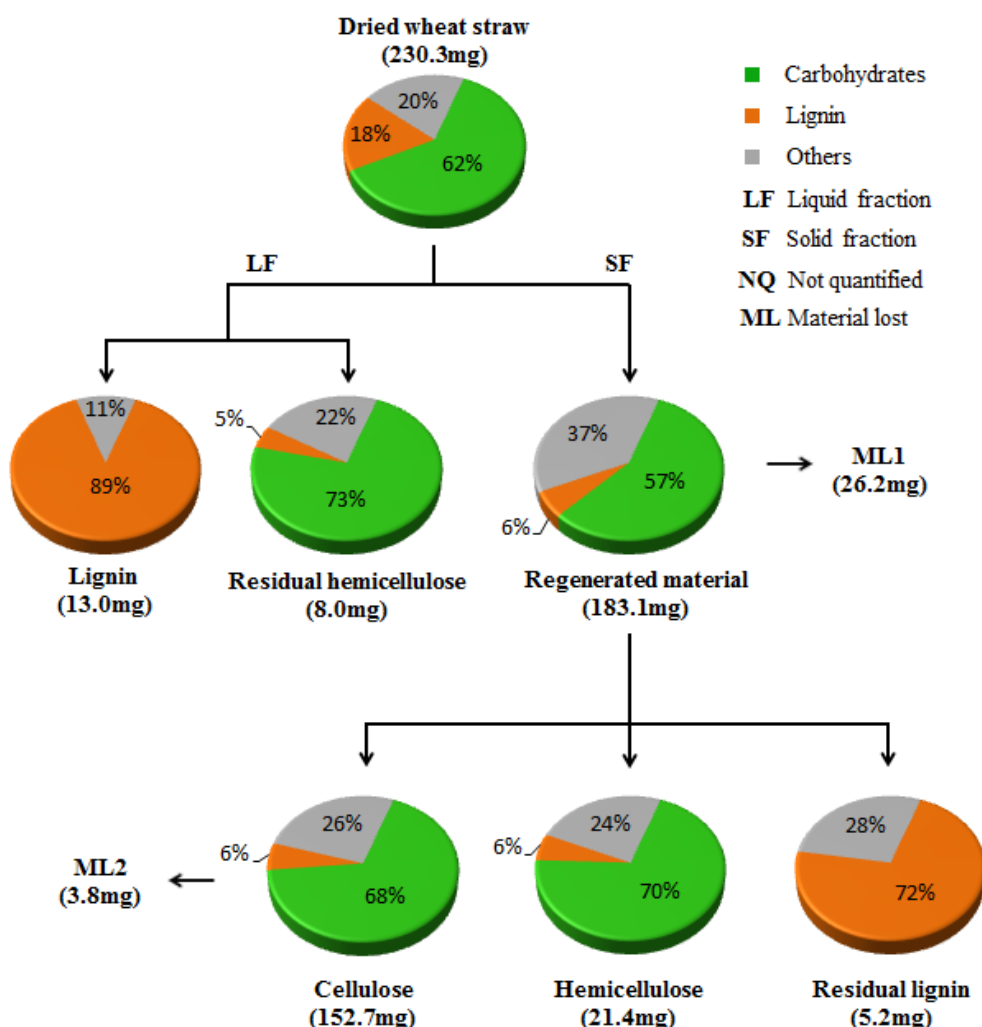


Figure 27. Fractionation of wheat straw using [bmim][SCN].

In case of the pre-treatment with [bmim][N(CN)<sub>2</sub>] cellulose-rich and hemicellulose-rich materials showed a high purity comparing to the previous IL investigated (87% and 85% respectively). Furthermore, as presented in Figure 28 the residual lignin was contaminated by hemicellulose and the composition of the residual lignin contained 1:1 lignin:carbohydrate composition. This result can be explained by only partial dissolution of biomass by this IL during the pre-treatment. The lignin-rich material was not quantified due to a filter nylon contamination as it was referred above. However, from the negligible amount of lignin detected in the residual hemicellulose it can be assumed that certainly lignin was a dominant component of this fraction. At a global evaluation, the pre-treatment with [bmim][N(CN)<sub>2</sub>] could be more selective for recovery of carbohydrate materials such as cellulose and hemicellulose fractions.

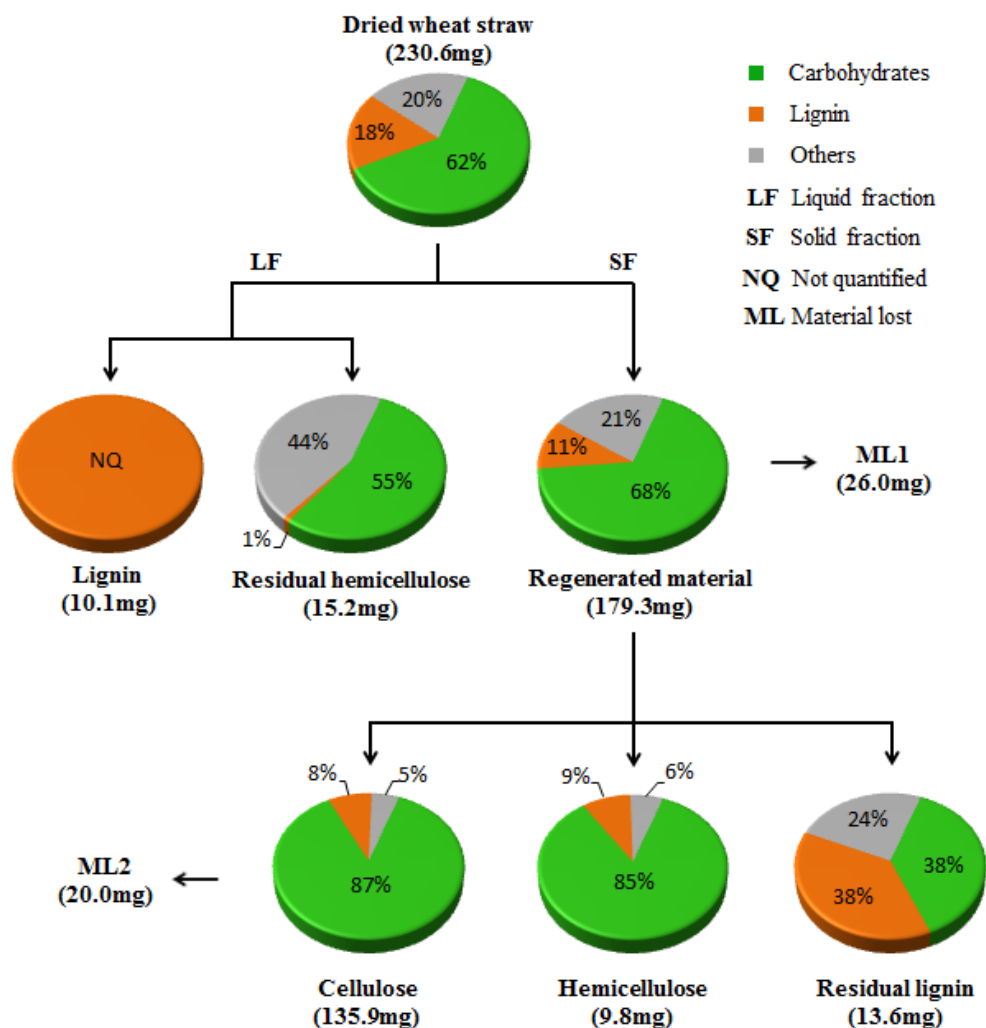


Figure 28. Fractionation of wheat straw by method C using [bmim][N(CN)<sub>2</sub>].

The data obtained from [bmim][HSO<sub>4</sub>] experiment resulted in a different approach of pre-treatment and fractionation of biomass as illustrated in Figure 29.

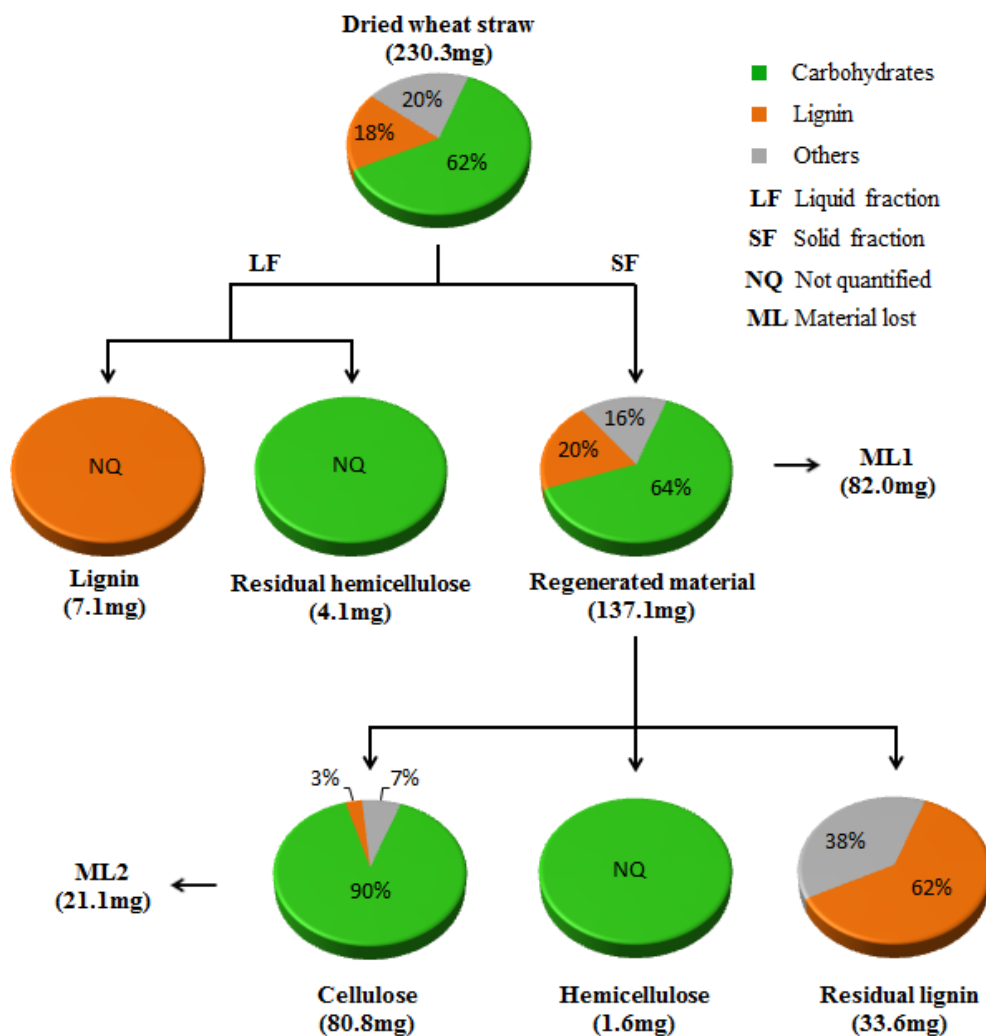


Figure 29. Fractionation of wheat straw by method C using [bmim][HSO<sub>4</sub>].

In the liquid stream small quantities of lignin-rich and residual hemicellulose-rich materials were attained which impeded to perform FT-IR quantitative analysis. The cellulose-rich material showed a carbohydrate content of 90%, the most enriched carbohydrate sample achieved in all performed pre-treatments in this work. The major lignin fraction was obtained as “residual” lignin-rich material, once small quantity was extracted in the liquid phase after regeneration process. However, only 62% lignin content was determined for this sample even with any trace of carbohydrates. For the hemicellulose-rich material, an insignificant quantity was recovered, thus it was not

quantified for the same reasons as presented above. As it was suggested, [bmim][HSO<sub>4</sub>] may perform acid hydrolysis, which major content of hemicellulose present in the original biomass was hydrolysed to reduced sugars dissolved in the liquid stream of the pre-treatment process.

#### 4.6 IL ability to biomass pre-treatment

The pre-treatment of biomass with different ILs showed that each IL can be dedicated to process leading to produce different high purity fractions. However it is important to point out that after the dissolution, antisolvent is used to form regenerated material rich in carbohydrates being a crucial step for further fractionation (Figure 25, 27, 28 and 29). FT-IR quantification of obtained regenerated materials from method C pre-treatments using four ILs are compiled in Table 19.

Table 19. The FT-IR quantification of regenerated materials obtained from wheat straw pre-treatment by [emim][CH<sub>3</sub>COO], [bmim][SCN], [bmim][N(CN)<sub>2</sub>] and [bmim][HSO<sub>4</sub>].

Entry	RY /%w/w	Composition		
		Carbohydrate /wt%	Lignin /wt%	Others /wt%
Dried wheat straw	-	62	18	20
[emim][CH <sub>3</sub> COO] <sup>a</sup>	57	81	6	13
[bmim][SCN]	80	57	6	37
[bmim][N(CN) <sub>2</sub> ]	78	68	11	21
[bmim][HSO <sub>4</sub> ]	60	64	20	16

RY - Regeneration yield; <sup>a</sup> Experiment C3

Obtained results showed that [emim][CH<sub>3</sub>COO] was the best IL, however it is important to point out that only 57% of the original biomass was recovered while in case of other ILs such values varied from 60% to 80%, but were associated with a lower purity of the carbohydrate fraction.

Obtained results also showed that each regenerated material had similar or higher amount of carbohydrates than raw wheat straw. In the optimal case, the carbohydrate-rich fraction contained even 81wt% and it was also accompanied by the decreased concentration of lignin. This result indicated that major lignin concentration was driven to the liquid stream.

#### 4.7 Wheat straw pre-treatment reusing [emim][CH<sub>3</sub>COO]

The feasibility of IL for the reuse and recycling was studied. For this purpose the pre-treatment process described by method A was used.

As the recovery of IL is not 100% the material loss was observed. The principal source of IL losses can be detected at the final step when solid NaCl enclosing IL. Although acetonitrile was used to wash out all IL from NaCl; it can be stated that further refining of this part of the process is needed. Nevertheless it is important to point out that the same [emim][CH<sub>3</sub>COO] was used in seven consecutive reactions and IL still demonstrated ability to fractionate biomass with a high efficiency as it is presented in Table 17. Other studies also confirmed the successful reuse of ILs achieving similar results.<sup>90, 97, 128</sup>

#### 4.8 Enzymatic hydrolysis

The pre-treatment efficiency of developed methods using [emim][CH<sub>3</sub>COO] were evaluated by performing enzymatic hydrolysis on the carbohydrate rich-material obtained in method A and cellulose-rich samples from methods B and C. As expected, the regenerated material from the method A presented a low glucose yield (49.3% w/w<sub>biomass</sub>) after enzymatic hydrolysis, because was enriched not only in cellulose but also in hemicellulose content. This result demonstrated the importance to fractionate the regenerated material into enriched cellulose samples to achieve better glucose yields after cellulose hydrolysis. As optimized pre-treatment, method C demonstrated to perform more selective fractionation for cellulose than method B giving a cellulose-rich sample with the highest glucose yield (76.5% w/w<sub>biomass</sub>) after hydrolysis. The worst result was observed for hydrolysis of native wheat straw (19.7% w/w<sub>biomass</sub>) caused by the lack of the pre-treatment of this material. The native intricate structure of wheat straw as well as the presence of other compounds hindered cellulase accessibility and activity to perform cellulose hydrolysis.<sup>82, 99, 100</sup> To validate these results the enzymatic hydrolysis of a high purity standard cellulose was performed where complete hydrolysis (98.3% w/w<sub>biomass</sub>) was confirmed. Therefore, the enzymatic hydrolysis at 50°C for 72h was appropriate to achieve complete cellulose hydrolysis, adding an equal amount of enzyme for each tested sample regarding to the total biomass loaded.

Not only glucose was released after enzymatic hydrolysis but also xylose was detected in hydrolysate. This could indicate that cellulase mixture Celluclast 1.5L and  $\beta$ -glucosidase Novozyme 188 showed activities towards cellulose, xylanase and  $\beta$ -xylosidase.<sup>129</sup>

The cellulose standard was verified to contain some amounts of xylose released after enzymatic hydrolysis and a complete carbohydrate hydrolysis was observed for cellulose-rich materials giving nearly 100% (w/w) of total sugar yield. In case of the native wheat straw hydrolysis less than a half of carbohydrate was converted to sugars, a very low conversion as expected.

The incomplete hydrolysis was also verified for regenerated material due to a high hemicellulose content in sample that could hinder the enzyme activity.<sup>130</sup> This could be overcome by the supplementary addition of xylanase and  $\beta$ -xylosidase enzymes with a higher activity to perform complete carbohydrate hydrolysis of these type of samples.<sup>131</sup>

The complete enzymatic hydrolysis allowed to estimate carbohydrate ratio (cellulose/hemicellulose) content in cellulose-rich samples. Therefore, from total carbohydrates, 84% and 89% corresponds to cellulose content present in cellulose-rich materials obtained by methods B and C, respectively. The remaining content (16% and 11%) was hemicellulose determined by xylan measurement. The presence of arabinose was considered insignificant in these samples as no detection in HPLC analysis was observed. However, other quantitative analysis of carbohydrate content should be performed as quantitative acid hydrolysis to produce more reliable composition. Furthermore obtained data showed that the method C was more adequate to process biomass as it produced sample richer in cellulose compared with method B.

In the literature, for a limited set of ILs tested, [emim][CH<sub>3</sub>COO] was found to be highly selective in extraction of lignin from lignocellulosic biomass and it simultaneously reduced the crystallinity of cellulose.<sup>73</sup> Thus, the accessibility of cellulases enhanced the enzymatic hydrolysis to release a total reduced sugar.<sup>99, 132, 133</sup> It is known that lignin hindered the enzymatic activity and generally maximal delignification should be attained to improve hydrolysis.<sup>134, 135</sup> However, Lee et al. demonstrated that removal of 40% of lignin from wood flour in pre-treatment with [emim][CH<sub>3</sub>COO] decreased the cellulose crystallinity index, resulting in >90% of the cellulose to be hydrolysed by cellulase.<sup>73</sup> This was confirmed by the total sugar released for all tested samples achieving >90%. As referred above lignin content was decreased drastically in pre-treated samples. The regenerated

material from method A contained 50% less lignin than the origin feedstock and in method B and C 44% and 67% of lignin removal was obtained, correspondingly. Therefore, considering the partial delignification, simultaneous reduction of cellulose crystallinity should be enough for appropriate enzymatic hydrolysis.

## 5 Conclusions

The pre-treatment of wheat straw using [emim][CH<sub>3</sub>COO] was successfully performed by three methods. The method A allowed to fractionate wheat straw into carbohydrate and lignin materials. The maximal exploitation of the wheat straw feedstock was achieved by method B that allowed the fractionation into cellulose-rich, hemicellulose-rich and lignin-rich materials. The method C optimised pre-treatment was based on the two previous methods tuned to obtain high purity samples. The better performance of this method was demonstrated by the high carbohydrate content in cellulose and hemicellulose samples determined to be 86% and 85%, respectively. Additionally, lignin was extracted by 0.1M NaOH aqueous solution and recovered with 87% purity.

The versatility of the optimised pre-treatment was examined using [bmim][SCN], [bmim][N(CN)<sub>2</sub>] and [bmim][HSO<sub>4</sub>]. [Bmim][SCN] and [bmim][N(CN)<sub>2</sub>] demonstrated to dissolve partially a wheat straw sample. By using these ILs in wheat straw pre-treatment, the biomass recovery and the purity of each fractionated sample can be tuned demonstrating a great flexibility of the process. The complete macroscopic dissolution was achieved by both [bmim][HSO<sub>4</sub>] and [emim][CH<sub>3</sub>COO]. A different behaviour was observed for [bmim][HSO<sub>4</sub>] that was capable to hydrolyse hemicellulose. The cellulose-rich material obtained by the pre-treatment with [bmim][HSO<sub>4</sub>] presented a 90% carbohydrate content.

After pre-treatment, ILs were recovered up to 97% (w/w) of the initial mass. Therefore, pre-treatment with ILs could be advantageous to the feasibility of the process. IL can be reused even six times without losses in biomass pre-treatment efficiency.

The enzymatic hydrolysis of carbohydrate-rich materials including cellulose pre-treatment samples resulted in a high total sugar release. The pre-treatment with [emim][CH<sub>3</sub>COO] was capable to perform a partial although sufficient delignification of wheat straw that enables cellulase enzymes to access carbohydrates and achieves complete hydrolysis into reducing sugars. Thus, hydrolysed reducing sugars from cellulose-rich samples could be further applied in fermentation systems to produce bioethanol and value added products.

## 6 Future Prospects

The use of ionic liquids in the pre-treatment of lignocellulosic biomass is very recent and has a great potential for the development of new fractionation processes to obtain high purity samples of cellulose, hemicellulose and lignin.

This thesis presented a green fractionation approach, where a diversity of ionic liquids can be used to process lignocellulosic biomass in different routes. Other ionic liquids that were not examined in this thesis should be used to verify their potential in the process here demonstrated. The hydrolysis ability of certain ionic liquids, such as [bmim][HSO<sub>4</sub>], should be investigated in order to determine the optimised conditions for hydrolysis. This is of great interest to achieve the fractionation and hydrolysis processes in one-step methodology.

The scale up of the optimised pre-treatment should be attained to verify the feasibility for a future application in industry. The major costs involved in the overall process could be associated to ionic liquid losses, thus ionic liquid recovery should have a focused investigation.

The fermentation of the reducing sugars released after enzymatic hydrolysis should also be studied to evaluate the ionic liquid effect on the production of bioethanol and value added products after pre-treatment and enzymatic hydrolysis.

## 7 Bibliography

1. SIADEB - Sociedade Ibero-Americana para o Desenvolvimento das Biorrefinarias, <http://www.siadeb.org/>, Accessed 13th June, 2012.
2. *Technology Roadmap - Biofuels for Transport*, International Energy Agency, 2011.
3. B. Kamm, P. R. Gruber and M. Kamm, *Biorefineries—industrial processes and products*, Wiley Online Library, 2007.
4. D. King, *The Future of Industrial Biorefineries*, World Economic Forum, 2010.
5. E. Commission, *Official Journal of the European Union*, 2009, 16-61.
6. J. Pickett, *Sustainable biofuels: prospects and challenges*, Report 0854036628, The Royal Society, 2008.
7. P. Kumar, D. M. Barrett, M. J. Delwiche and P. Stroeve, *Ind. Eng. Chem. Res.*, 2009, **48**, 3713-3729.
8. M. Galbe and G. Zacchi, *Biofuels*, 2007, **108**, 41-65.
9. O. J. Sanchez and C. A. Cardona, *Bioresource Technol.*, 2008, **99**, 5270-5295.
10. A. J. Ragauskas, C. K. Williams, B. H. Davison, G. Britovsek, J. Cairney, C. A. Eckert, W. J. Frederick, J. P. Hallett, D. J. Leak and C. L. Liotta, *Science*, 2006, **311**, 484-489.
11. N. Carels, in *Biofuels's Engineering Process Technology*, 2011, pp. 23-64.
12. M. Stöcker, *Angew. Chem. Int. Ed.*, 2008, **47**, 9200-9211.
13. G. Y. S. Mtui, *Afr. J. Biotechnol.*, 2010, **8**, 1398-1415.
14. F. Girio, C. Fonseca, F. Carvalheiro, L. Duarte, S. Marques and R. Bogel-Lukasik, *Bioresource Technol.*, 2010, **101**, 4775-4800.
15. R. D. Perlack, *Biomass as feedstock for a bioenergy and bioproducts industry: the technical feasibility of a billion-ton annual supply*, DTIC Document, 2005.
16. P. Harmsen, W. Huijgen, L. Bermudez and R. Bakker, *Literature review of physical and chemical pretreatment processes for lignocellulosic biomass*, Report 9789085857570, Wageningen UR, Food & Biobased Research, Wageningen, 2010.
17. J. Murphy and K. McCarthy, *Appl. Energ.*, 2005, **82**, 148-166.
18. L. P. Ramos, *Quim. Nova*, 2003, **26**, 863-871.
19. Y. Sun and J. Cheng, *Bioresource Technol.*, 2002, **83**, 1-11.
20. J. L. Faulon, G. A. Carlson and P. G. Hatcher, *Org. Geochem.*, 1994, **21**, 1169-1179.
21. Laghi, I. Cellulose strands, [http://en.wikipedia.org/wiki/File:Cellulose\\_strand.jpg#file](http://en.wikipedia.org/wiki/File:Cellulose_strand.jpg#file).
22. Kirk-Othmer, *Encyclopedia of chemical technology*, Wiley-Interscience, 2007.
23. T. Heinze and T. Liebert, *Prog. Polym. Sci.*, 2001, **26**, 1689-1762.
24. S. Richardson and L. Gorton, *Anal. Chim. Acta.*, 2003, **497**, 27-65.
25. S. Y. Oh, D. I. Yoo, Y. Shin and G. Seo, *Carbohydr. Res.*, 2005, **340**, 417-428.
26. C. Laine, *Structures of hemicelluloses and pectins in wood and pulp*, Helsinki University of Technology, Department of Chemical Technology, 2005.
27. G. Brodeur, E. Yau, K. Badal, J. Collier, K. B. Ramachandran and S. Ramakrishnan, *Enzyme Res.*, 2011, **2011**, 17.
28. D. Fengel, G. Wegener and A. Greune, *Wood Sci. Technol.*, 1989, **23**, 123-130.
29. K. Shimizu, *Wood and cellulosic chemistry*, 1991, 177-214.
30. E. Sjöström, *Wood chemistry: fundamentals and applications*, Academic Press, 1993.
31. Z. S. Cai and L. Paszner, *Holzforschung*, 1988, **42**, 11-20.

32. J. L. Ren, F. Peng and R. C. Sun, *Carbohydr. Res.*, 2008, **343**, 2776-2782.
33. F. T. Association, *ThermoWood handbook*, Finnish Thermowood Association, 2003.
34. F. Halverson, J. Lancaster and M. O'Connor, *Macromol.*, 1985, **18**, 1139-1144.
35. A. B. Blakeney, P. J. Harris, R. J. Henry and B. A. Stone, *Carbohydr. Res.*, 1983, **113**, 291-299.
36. N. Blumenkrantz and G. Asboe-Hansen, *Anal. Biochem.*, 1973, **54**, 484-489.
37. J. M. Lawther, R. Sun and W. Banks, *J. Agric. Food Chem.*, 1995, **43**, 667-675.
38. K. Freudenberg and A. C. Neish, *Constitution and biosynthesis of lignin*, Springer, 1968.
39. A. J. Ragauskas, Lignin Overview, [http://www.ipst.gatech.edu/faculty/ragauskas\\_art/technical\\_reviews/Lignin%20Overview.pdf](http://www.ipst.gatech.edu/faculty/ragauskas_art/technical_reviews/Lignin%20Overview.pdf), Accessed December, 2011.
40. F. S. Chakar and A. J. Ragauskas, *Ind. Crop. Prod.*, 2004, **20**, 131-141.
41. J. L. McCarthy and A. Islam, in *Lignin: Historical, Biological, and Materials Perspectives*, American Chemical Society, Washington, DC, 2000, vol. 742, pp. 2-99.
42. C. Bonini, M. D'Auria, L. Emanuele, R. Ferri, R. Pucciariello and A. R. Sabia, *J. Appl. Polym. Sci.*, 2005, **98**, 1451-1456.
43. Y. Li and S. Sarkanen, *Macromol.*, 2005, **38**, 2296-2306.
44. W. Thielemans, E. Can, S. Morye and R. Wool, *J. Appl. Polym. Sci.*, 2002, **83**, 323-331.
45. Y. Li and S. Sarkanen, *Macromol.*, 2002, **35**, 9707-9715.
46. Y. Pu, N. Jiang and A. J. Ragauskas, *J. Wood Chem. Technol.*, 2007, **27**, 23-33.
47. A. N. Glazer and H. Nikaidō, *Microbial biotechnology: fundamentals of applied microbiology*, Cambridge Univ Pr, 2007.
48. R. Rogers and K. R. Seddon, *Ionic Liquids: Industrial Applications for Green Chemistry*, American Chemical Society, Washington, DC, 2002.
49. C. Reichardt, *Green Chem.*, 2005, **7**, 339-351.
50. U. Domanska and R. Bogel-Lukasik, *J. Phys. Chem. B*, 2005, **109**, 12124-12132.
51. J. A. Widegren, E. M. Saurer, K. N. Marsh and J. W. Magee, *J. Chem. Thermodyn.*, 2005, **37**, 569-575.
52. U. Domanska, E. Bogel-Lukasik and R. Bogel-Lukasik, *J. Phys. Chem. B*, 2003, **107**, 1858-1863.
53. U. Domanska and R. Bogel-Lukasik, *Fluid Phase Equilib.*, 2005, **233**, 220-227.
54. R. Bogel-Lukasik, D. Matkowska, M. E. Zakrzewska, E. Bogel-Lukasik and T. Hofman, *Fluid Phase Equilib.*, 2010, **295**, 177-185.
55. M. E. Zakrzewska, E. Bogel-Lukasik and R. Bogel-Lukasik, *Energy Fuels*, 2010, **24**, 737-745.
56. P. J. Carvalho, V. H. Álvarez, I. M. Marrucho, M. Aznar and J. A. P. Coutinho, *J. Supercrit. Fluids*, 2010, **52**, 258-265.
57. F. S. Oliveira, M. G. Freire, M. J. Pratas, J. Pauly, J. L. Daridon, I. M. Marrucho and J. A. P. Coutinho, *J. Chem. Eng. Data*, 2009, **55**, 662-665.
58. C. M. S. S. Neves, P. J. Carvalho, M. G. Freire and J. A. P. Coutinho, *J. Chem. Thermodyn.*, 2011, **43**, 948-957.
59. A. V. Blokhin, Y. U. Paulechka, A. A. Strechan and G. J. Kabo, *J. Phys. Chem. B*, 2008, **112**, 4357-4364.

60. Y. U. Paulechka, G. J. Kabo, A. V. Blokhin, O. A. Vydrov, J. W. Magee and M. Frenkel, *J. Chem. Eng. Data*, 2003, **48**, 457-462.
61. M. E. Zakrzewska, E. Bogel-Lukasik and R. Bogel-Lukasik, *Chem. Rev.*, 2011, **111**, 397-417.
62. K. Marsh, J. Boxall and R. Lichtenthaler, *Fluid Phase Equilib.*, 2004, **219**, 93-98.
63. N. A. Lange and G. M. Forker, *Handbook of chemistry*, Handbook Publishers, 1952.
64. R. P. Swatloski, S. K. Spear, J. D. Holbrey and R. D. Rogers, *J. Am. Chem. Soc.*, 2002, **124**, 4974-4975.
65. R. Bogel-Lukasik, *Synthesis, Physico-Chemical Properties and Applications of Alternative Solvents*, Universidade Nova de Lisboa - Faculdade de Ciencias e Tecnologia, 2007.
66. D. Coleman and N. Gathergood, *Chem. Soc. Rev.*, 2010, **39**, 600-637.
67. M. J. Earle and K. R. Seddon, *Pure Appl. Chem.*, 2000, **72**, 1391-1398.
68. J. D. McMillan, in *Enzymatic Conversion of Biomass for Fuels Production*, ACS Publications, 1994, vol. 566, pp. 292-324.
69. M. J. Taherzadeh and K. Karimi, *Int. J. Mol. Sci.*, 2008, **9**, 1621-1651.
70. R. C. Remsing, R. P. Swatloski, R. D. Rogers and G. Moyna, *Chem. Commun.*, 2006, 1271-1273.
71. J. Wang, Y. Zheng and S. Zhang, in *Clean Energy Systems and Experiences*, 2010, pp. 71-84.
72. X. Wang, H. Li, Y. Cao and Q. Tang, *Bioresource Technol.*, 2011, **102**, 7959-7965.
73. S. H. Lee, T. V. Doherty, R. J. Linhardt and J. S. Dordick, *Biotechnol. BioEng.*, 2009, **102**, 1368-1376.
74. D. A. Fort, R. C. Remsing, R. P. Swatloski, P. Moyna, G. Moyna and R. D. Rogers, *Green Chem.*, 2007, **9**, 63-69.
75. I. Kilpeläinen, H. Xie, A. King, M. Granstrom, S. Heikkinen and D. S. Argyropoulos, *J. Agric. Food Chem.*, 2007, **55**, 9142-9148.
76. A. Brandt, J. P. Hallett, D. J. Leak, R. J. Murphy and T. Welton, *Green Chem.*, 2010, **12**, 672-679.
77. N. Sun, M. Rahman, Y. Qin, M. L. Maxim, H. Rodríguez and R. D. Rogers, *Green Chem.*, 2009, **11**, 646-655.
78. T. Leskinen, A. W. T. King, I. Kilpeläinen and D. S. Argyropoulos, *Ind. Eng. Chem. Res.*, 2011, **50**, 12349.
79. A. W. T. King, L. Zoia, I. Filpponen, A. Olszewska, H. Xie, I. Kilpeläinen and D. S. Argyropoulos, *J. Agric. Food Chem.*, 2009, **57**, 8236-8243.
80. M. Zavrel, D. Bross, M. Funke, J. Büchs and A. C. Spiess, *Bioresource Technol.*, 2009, **100**, 2580-2587.
81. J. Van Spronsen, M. A. T. Cardoso, G. J. Witkamp, W. De Jong and M. C. Kroon, *Chem. Eng. Process.*, 2010, **50**, 196-199.
82. S. Singh, B. A. Simmons and K. P. Vogel, *Biotechnol. BioEng.*, 2009, **104**, 68-75.
83. H. T. Vo, C. S. Kim, B. S. Ahn, H. S. Kim and H. Lee, *J. Wood Chem. Technol.*, 2011, **31**, 89-102.
84. L. J. A. Conceição, E. Bogel-Lukasik and R. Bogel-Lukasik, *RSC Adv.*, 2012, **2**, 1846-1855.
85. M. Abe, Y. Fukaya and H. Ohno, *Green Chem.*, 2010, **12**, 1274-1280.

86. N. Muhammad, Z. Man, M. A. Bustam, M. I. A. Mutalib, C. D. Wilfred and S. Rafiq, *Appl. Biochem. Biotechnol.*, 2011, **165**, 1-12.
87. C. Li, B. Knierim, C. Manisseri, R. Arora, H. V. Scheller, M. Auer, K. P. Vogel, B. A. Simmons and S. Singh, *Bioresource Technol.*, 2010, **101**, 4900-4906.
88. J. M. Crosthwaite, S. N. V. K. Aki, E. J. Maginn and J. F. Brennecke, *Fluid Phase Equilib.*, 2005, **228**, 303-309.
89. B. Li, J. Asikkala, I. Filpponen and D. S. Argyropoulos, *Ind. Eng. Chem. Res.*, 2010, **49**, 2477-2484.
90. T. A. D. Nguyen, K. R. Kim, S. J. Han, H. Y. Cho, J. W. Kim, S. M. Park, J. C. Park and S. J. Sim, *Bioresource Technol.*, 2010, **101**, 7432-7438.
91. T. V. Doherty, M. Mora-Pale, S. E. Foley, R. J. Linhardt and J. S. Dordick, *Green Chem.*, 2010, **12**, 1967-1975.
92. R. Arora, C. Manisseri, C. Li, M. D. Ong, H. V. Scheller, K. Vogel, B. A. Simmons and S. Singh, *BioEnerg. Res.*, 2010, **3**, 134-145.
93. D. Fu, G. Mazza and Y. Tamaki, *J. Agric. Food Chem.*, 2010, **58**, 2915-2922.
94. S. S. Y. Tan, D. R. MacFarlane, J. Upfal, L. A. Edey, W. O. S. Doherty, A. F. Patti, J. M. Pringle and J. L. Scott, *Green Chem.*, 2009, **11**, 339-345.
95. A. A. Shamsuri and D. K. Abdullah, *Mod. Appl. Sci.*, 2010, **4**, 19-27.
96. R. Pezoa, V. Cortinez, S. Hyvärinen, M. Reunanen, J. Hemming, M. Lienqueo, O. Salazar, R. Carmona, A. Garcia and D. Murzin, *Cellul. Chem. Technol.*, 2010, **44**, 165-172.
97. W. Lan, C. F. Liu and R. C. Sun, *J. Agric. Food Chem.*, 2011, **59**, 8691-8701.
98. Q. Li, Y. C. He, M. Xian, G. Jun, X. Xu, J. M. Yang and L. Z. Li, *Bioresource Technol.*, 2009, **100**, 3570-3575.
99. A. S. A. Silva, S. H. Lee, T. Endo and E. P. S. Bon, *Bioresource Technol.*, 2011, **102**, 10505-10509.
100. H. Zhao, G. A. Baker and J. V. Cowins, *Biotechnol. Prog.*, 2010, **26**, 127-133.
101. M. Selig, N. Weiss and Y. Ji, *Enzymatic saccharification of lignocellulosic biomass*, 2008.
102. L. Zhu, J. P. O'Dwyer, V. S. Chang, C. B. Granda and M. T. Holtzapple, *Bioresource Technol.*, 2008, **99**, 3817-3828.
103. F. Carvalheiro, T. Silva-Fernandes, L. C. Duarte and F. M. Gírio, *Appl. Biochem. Biotechnol.*, 2009, **153**, 84-93.
104. D. Fu and G. Mazza, *Bioresource Technol.*, 2011, **102**, 8003-8010.
105. B. Montaña-Leyva, F. Rodriguez-Felix, P. Torres-Chávez, B. Ramirez-Wong, J. López-Cervantes and D. Sanchez-Machado, *J. Agric. Food Chem.*, 2011, **59**, 870-875.
106. M. Sain and S. Panthapulakkal, *Ind. Crop. Prod.*, 2006, **23**, 1-8.
107. P. K. Adapa, C. Karunakaran, L. G. Tabil and G. J. Schoenau, *Qualitative and Quantitative Analysis of Lignocellulosic Biomass using Infrared Spectroscopy*, The Canadian Society for Bioengineering, 2009.
108. Y. Cai, G. Li, J. Nie, Y. Lin, F. Nie, J. Zhang and Y. Xu, *Sci. Hortic.*, 2010, **125**, 374-379.
109. R. C. Sun, J. Fang, J. Tomkinson and G. Jones, *Ind. Crop. Prod.*, 1999, **10**, 209-218.
110. B. Wang, H. Feng, X. Wang, B. Zhou, J. A. De Frias, *Deconstructing lignocellulosic biomass with a two-step method*, United States Pat., US8173406, 2012.

111. J. L. Ren, F. Xu, R. C. Sun, B. Peng and J. X. Sun, *J. Agric. Food Chem.*, 2008, **56**, 1251-1258.
112. F. Peng, J. L. Ren, F. Xu, J. Bian, P. Peng and R. C. Sun, *J. Agric. Food Chem.*, 2009, **57**, 6305-6317.
113. I. Pastorova, R. E. Botto, P. W. Arisz and J. J. Boon, *Carbohydr. Res.*, 1994, **262**, 27-47.
114. R. C. Sun and J. Tomkinson, *Carbohydr. Polym.*, 2002, **50**, 263-271.
115. M. Kacurakova, P. Capek, V. Sasinkova, N. Wellner and A. Ebringerova, *Carbohydr. Polym.*, 2000, **43**, 195-203.
116. F. Xu, J. Sun, Z. Geng, C. Liu, J. Ren, R. Sun, P. Fowler and M. Baird, *Carbohydr. Polym.*, 2007, **67**, 56-65.
117. S. Kubo and J. F. Kadla, *Biomacromolecules*, 2005, **6**, 2815-2821.
118. K. Pandey and A. Pitman, *J. Polym. Sci., Part A: Polym. Chem.*, 2004, **42**, 2340-2346.
119. Q. Yang, J. Shi, L. Lin, J. Zhuang, C. Pang, T. Xie and Y. Liu, *J. Agric. Food Chem.*, 2012, **60**, 4656-4661.
120. R. C. Sun and J. Tomkinson, *Ultrason. Sonochem.*, 2002, **9**, 85-93.
121. L. W. Yoon, T. N. Ang, G. C. Ngoh and A. S. M. Chua, *Biomass Bioenerg.*, 2012, **36**, 160-169.
122. S. P. Pinho and E. A. Macedo, *J. Chem. Eng. Data*, 2005, **50**, 29-32.
123. D. C. Dibble, C. Li, L. Sun, A. George, A. Cheng, Ö. P. Çetinkol, P. Benke, B. M. Holmes, S. Singh and B. A. Simmons, *Green Chem.*, 2011, **13**, 3255-3264.
124. F. Xu, Q. A. Zhou, J. X. Sun, C. F. Liu, J. L. Ren, R. C. Sun, S. Curling, P. Fowler and M. S. Baird, *Process Biochem.*, 2007, **42**, 913-918.
125. M. Funaoka, T. Kako and I. Abe, *Wood Sci. Technol.*, 1990, **24**, 277-288.
126. G. González, J. López-Santín, G. Caminal and C. Solà, *Biotechnol. BioEng.*, 1986, **28**, 288-293.
127. A. Brandt, M. J. Ray, T. Q. To, D. J. Leak, R. J. Murphy and T. Welton, *Green Chem.*, 2011, **13**, 2489-2499.
128. H. Wu, M. Mora-Pale, J. Miao, T. V. Doherty, R. J. Linhardt and J. S. Dordick, *Biotechnol. BioEng.*, 2011, **108**, 2865-2875.
129. K. Kovacs, S. Macrelli, G. Szakacs and G. Zacchi, *Biotechnol. Biofuels*, 2009, **2**, 14.
130. Q. Qing, B. Yang and C. E. Wyman, *Bioresource Technol.*, 2010, **101**, 9624-9630.
131. Q. Qing and C. Wyman, *Biotechnol. Biofuels*, 2011, **4**, 18.
132. K. Shill, S. Padmanabhan, Q. Xin, J. M. Prausnitz, D. S. Clark and H. W. Blanch, *Biotechnol. BioEng.*, 2011, **108**, 511-520.
133. K. Ninomiya, K. Kamide, K. Takahashi and N. Shimizu, *Bioresource Technol.*, 2011, **103**, 259-265.
134. S. Zhu, Y. Wu, Q. Chen, Z. Yu, C. Wang, S. Jin, Y. Ding and G. Wu, *Green Chem.*, 2006, **8**, 325-327.
135. H. Ooshima, M. Sakata and Y. Harano, *Biotechnol. BioEng.*, 1986, **28**, 1727-1734.

# APPENDIX

## **Appendix A – FT-IR calibration curves (examples)**

Carbohydrate and lignin calibration curves 1 (Tables)

Carbohydrate and lignin calibration curves 1 (Graphics)

Carbohydrate and lignin calibration curves 2 (Tables)

Carbohydrate and lignin calibration curves 2 (Graphics)

## **Appendix B – FT-IR spectra**

Pre-treatments with [emim][CH<sub>3</sub>COO]:

Regenerated material method A

Lignin-rich method A

Regenerated material method B

Cellulose-rich method B

Hemicellulose-rich method B

Lignin-rich method B

Residual lignin-rich method B

Regenerated material method C

Cellulose-rich method C

Hemicellulose-rich method C

Hemicellulose-rich method C

Lignin-rich method C

Residual lignin-rich method C

Pre-treatment with [bmim][SCN]:

Regenerated material method

Cellulose-rich method

Hemicellulose-rich method

Hemicellulose-rich method

Lignin-rich method

Residual lignin-rich method

Pre-treatment with [bmim][N(CN)<sub>2</sub>]:

Regenerated material method

Cellulose-rich method

Hemicellulose-rich method

Hemicellulose-rich method

Lignin-rich method

Residual lignin-rich method

Pre-treatment with [bmim][HSO<sub>4</sub>]:

Regenerated material method

Cellulose-rich method

Lignin-rich method

Residual lignin-rich method

Standards:

Wheat straw

Cellulose

Acid hydrolysed wheat straw

**Appendix C – NMR spectra**

<sup>1</sup>H NMR [emim][CH<sub>3</sub>COO] – method B

<sup>13</sup>C NMR [emim][CH<sub>3</sub>COO] – method B

<sup>1</sup>H NMR [emim][CH<sub>3</sub>COO] – method C

<sup>13</sup>C NMR [emim][CH<sub>3</sub>COO] – method C

<sup>1</sup>H NMR [bmim][SCN]

<sup>13</sup>C NMR [bmim][SCN]

<sup>1</sup>H NMR [bmim][N(CN)<sub>2</sub>]

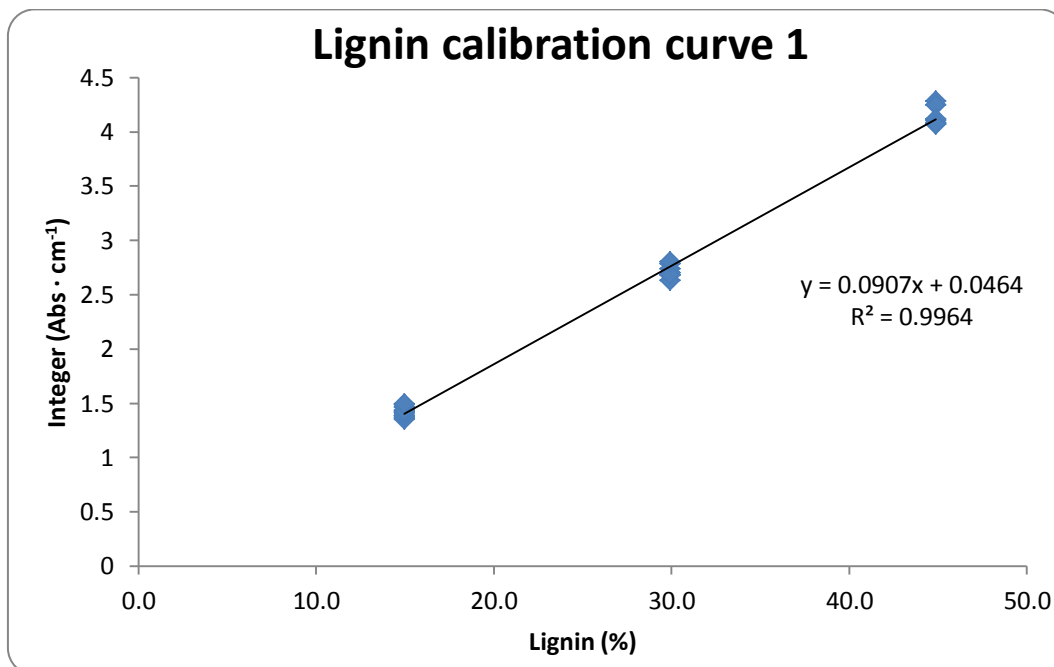
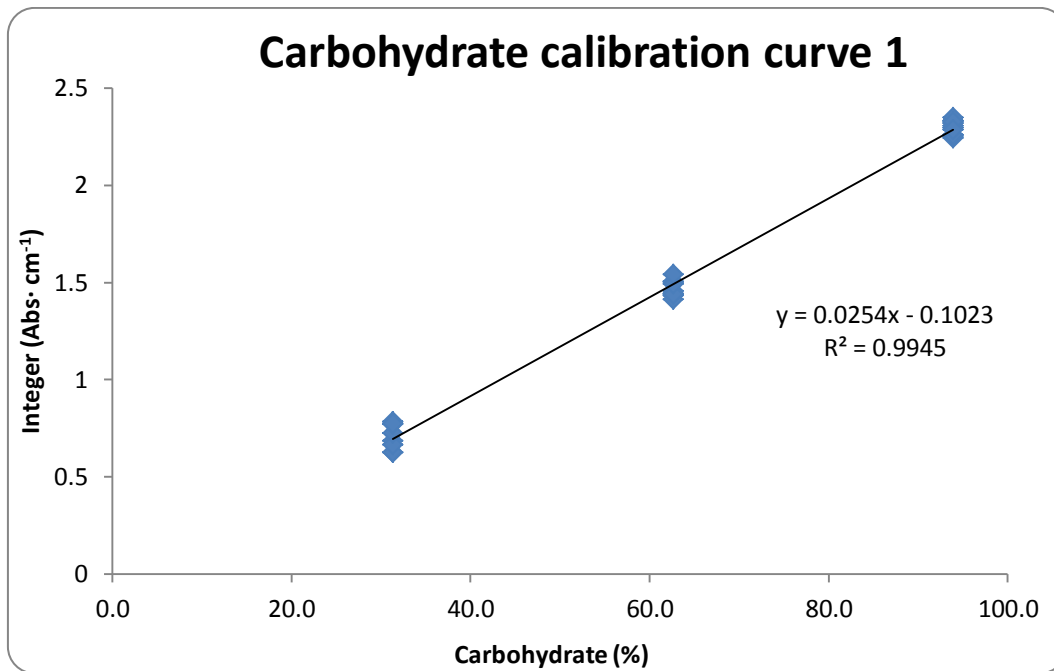
<sup>13</sup>C NMR [bmim][N(CN)<sub>2</sub>]

## Appendix A – FT-IR calibration curves (examples)

Carbohydrate and lignin calibration curves 1 (Tables)

Carbohydrate calibration curve 1			Lignin calibration curve 1		
Spectrum (n. <sup>o</sup> )	Carbohydrate (%)	Integer (Abs·cm <sup>-1</sup> )	Spectrum (n. <sup>o</sup> )	Lignin (%)	Integer (Abs·cm <sup>-1</sup> )
189	31.3	0.6265	189	15.0	1.3814
190	31.3	0.6262	190	15.0	1.4609
191	31.3	0.6842	191	15.0	1.3504
192	31.3	0.6638	192	15.0	1.3618
252	31.3	0.7829	193	15.0	1.3834
253	31.3	0.7249	194	15.0	1.4078
254	31.3	0.7705	252	15.0	1.4331
255	31.3	0.7729	253	15.0	1.4192
-----			254	15.0	1.4839
180	62.6	1.5054	255	15.0	1.4949
181	62.6	1.4339	-----		
182	62.6	1.4570	180	29.9	2.7829
187	62.6	1.4126	181	29.9	2.6766
188	62.6	1.5017	182	29.9	2.7034
261	62.6	1.4416	185	29.9	2.7390
262	62.6	1.4377	186	29.9	2.6282
263	62.6	1.4931	187	29.9	2.6851
264	62.6	1.5413	188	29.9	2.7983
-----			-----		
197	93.9	2.3182	203	44.9	4.2829
198	93.9	2.3320	205	44.9	4.2449
203	93.9	2.2424	258	44.9	4.0783
204	93.9	2.3481	259	44.9	4.1014
205	93.9	2.2537	260	44.9	4.1136
258	93.9	2.2968	339	44.9	4.0684
259	93.9	2.3073	340	44.9	4.0670
260	93.9	2.3271	-----		
341	93.9	2.2612			
342	93.9	2.2870			

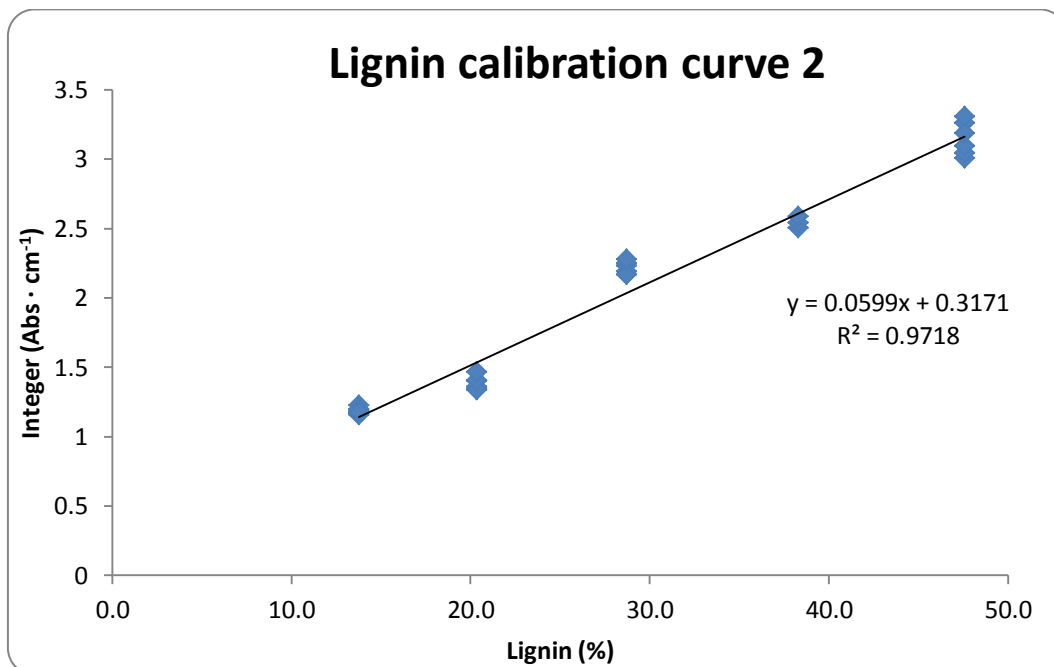
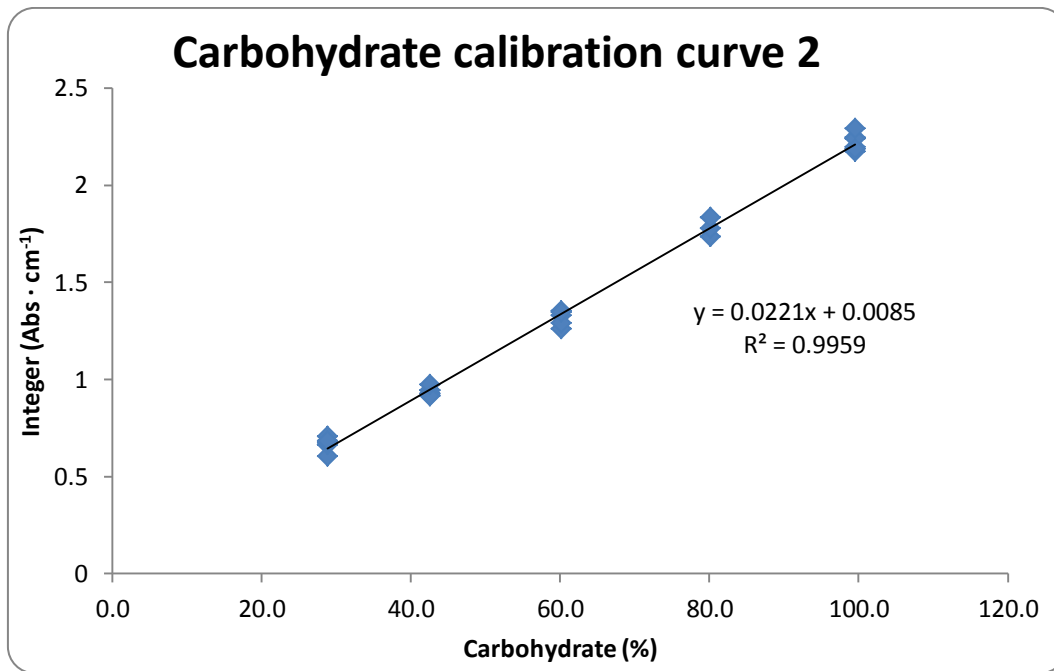
Carbohydrate and lignin calibration curves 1 (Graphics)



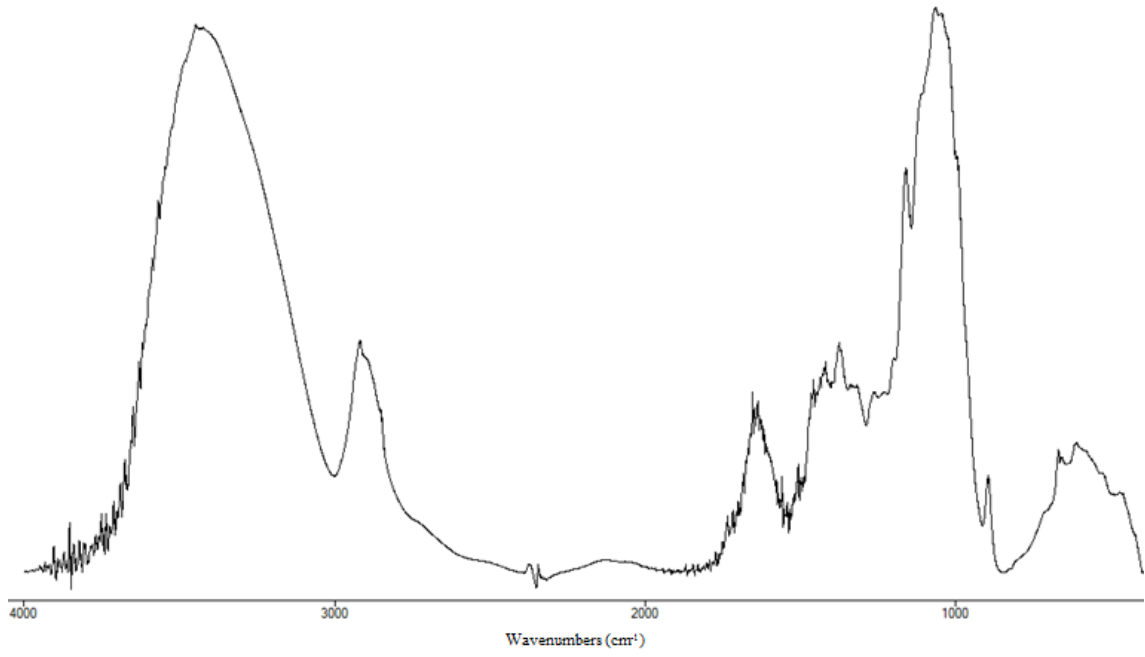
Carbohydrate and lignin calibration curves 2 (Tables)

Carbohydrate Calibration Curve 2			Lignin Calibration Curve 2		
Spectrum (n.º)	Carbohydrate (%)	Integer (Abs·cm <sup>-1</sup> )	Spectra (n.º)	Lignin (%)	Integer (Abs·cm <sup>-1</sup> )
110	28.8	0.6658	110	13.8	1.2272
111	28.8	0.6044	111	13.8	1.1668
112	28.8	0.6638	112	13.8	1.1981
116	28.8	0.7070	116	13.8	1.1566
117	28.8	0.6783	117	13.8	1.1833
118	28.8	0.6855	118	13.8	1.1746
113	42.6	0.9455	113	20.4	1.3575
114	42.6	0.9433	114	20.4	1.3437
115	42.6	0.9293	115	20.4	1.3379
119	42.6	0.9181	119	20.4	1.4005
120	42.6	0.9150	120	20.4	1.4046
121	42.6	0.9727	121	20.4	1.4642
122	60.1	1.2624	122	28.7	2.1901
123	60.1	1.3291	123	28.7	2.2296
124	60.1	1.3520	124	28.7	2.2504
128	60.1	1.2901	128	28.7	2.1682
129	60.1	1.3455	129	28.7	2.2777
125	80.1	1.7346	125	38.3	2.5025
126	80.1	1.7783	126	38.3	2.5405
127	80.1	1.8333	127	38.3	2.5856
135	99.5	2.1731	135	47.6	3.0063
136	99.5	2.1971	136	47.6	3.0456
137	99.5	2.2479	137	47.6	3.0945
139	99.5	2.2396	139	47.6	3.2606
140	99.5	2.1874	140	47.6	3.1846
141	99.5	2.2922	141	47.6	3.3052

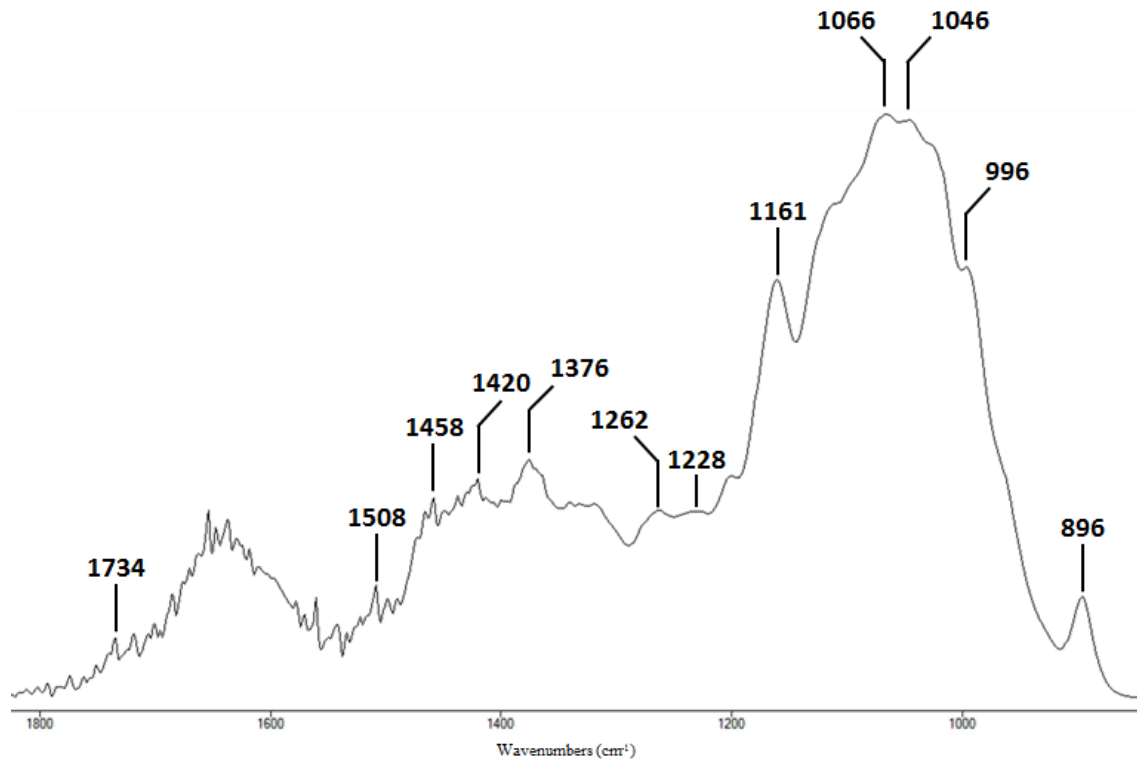
Carbohydrate and lignin calibration curves 2 (Graphics)



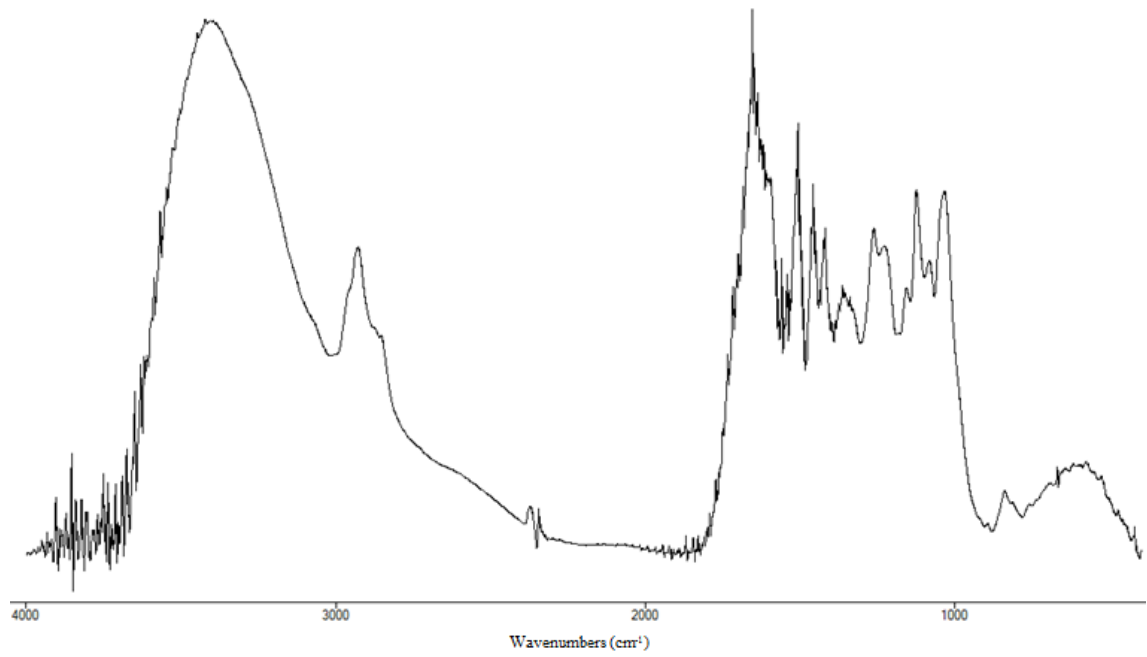
Regenerated material method A (4000-400  $\text{cm}^{-1}$ )



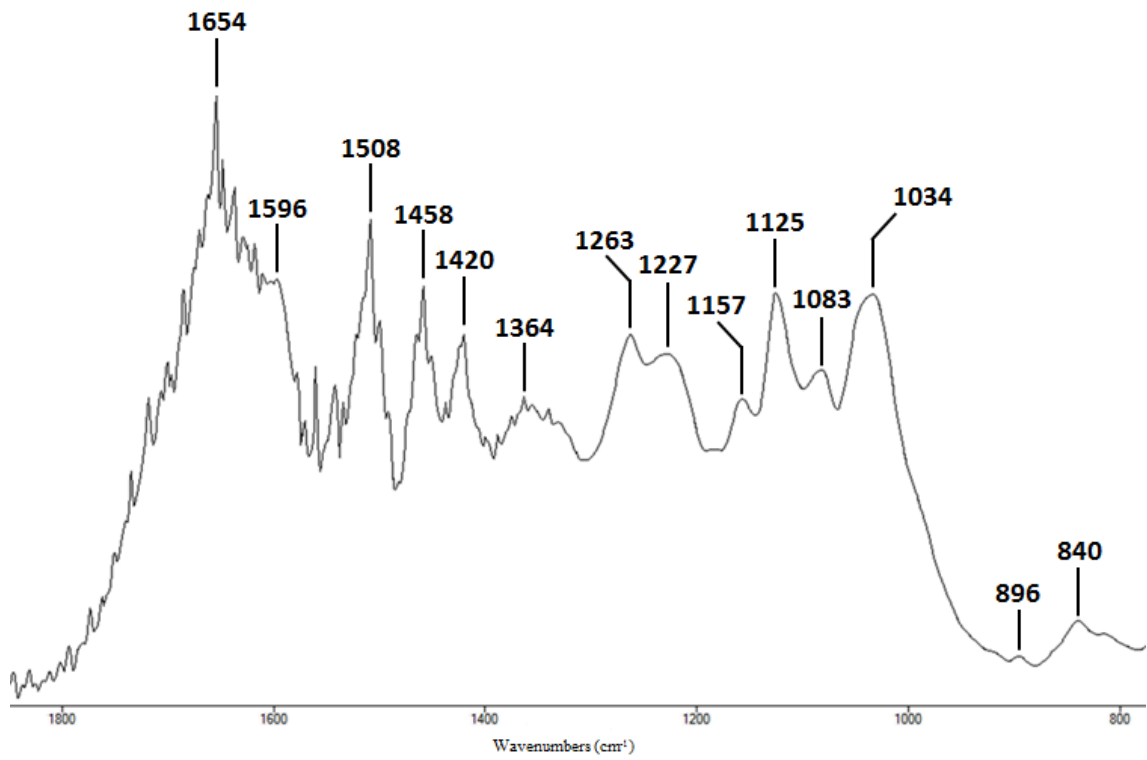
Regenerated material method A (1800-800  $\text{cm}^{-1}$ )



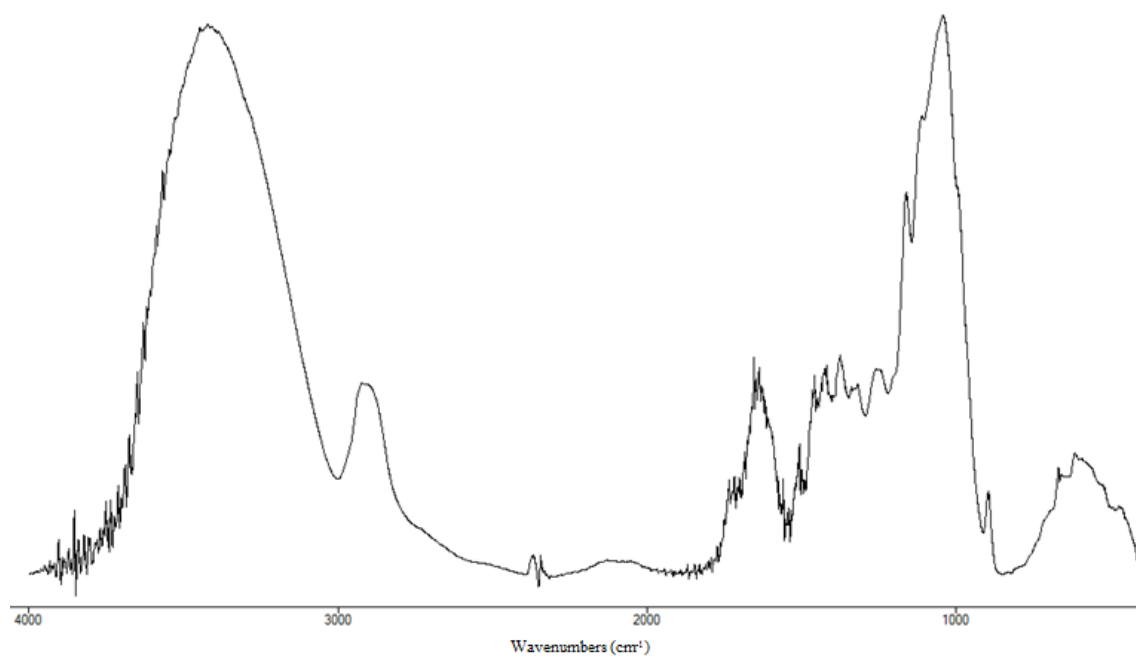
Lignin-rich method A (4000-400  $\text{cm}^{-1}$ )



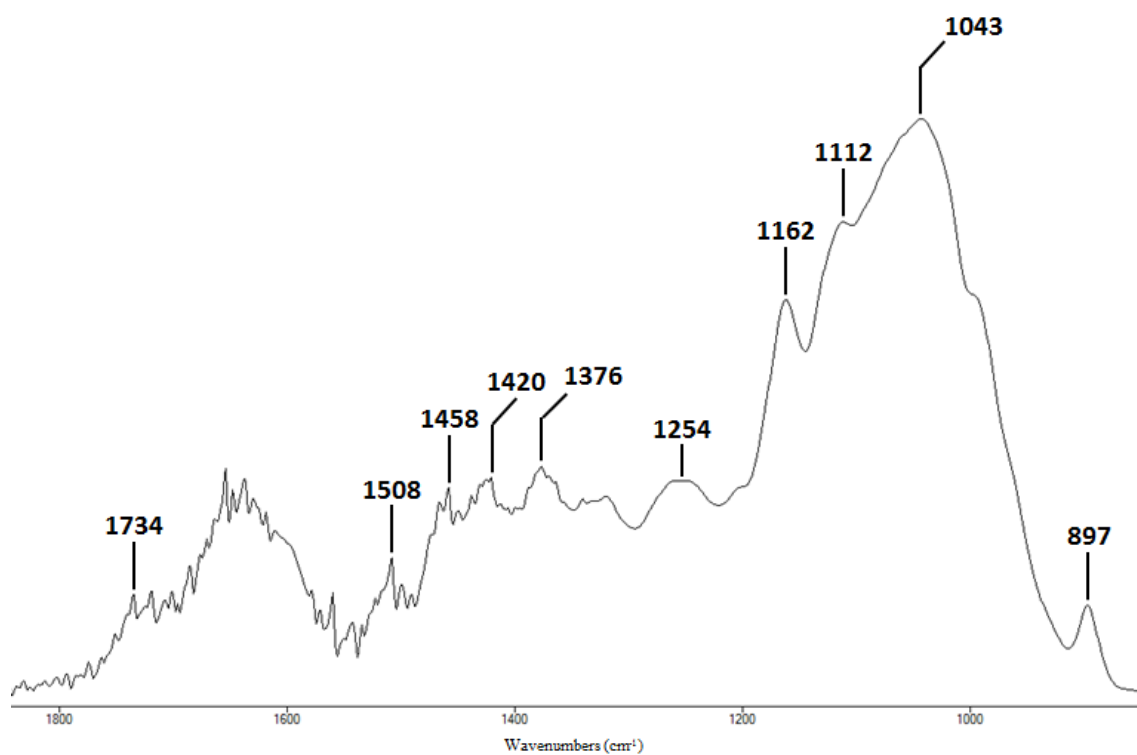
Lignin-rich method A (1800-800  $\text{cm}^{-1}$ )



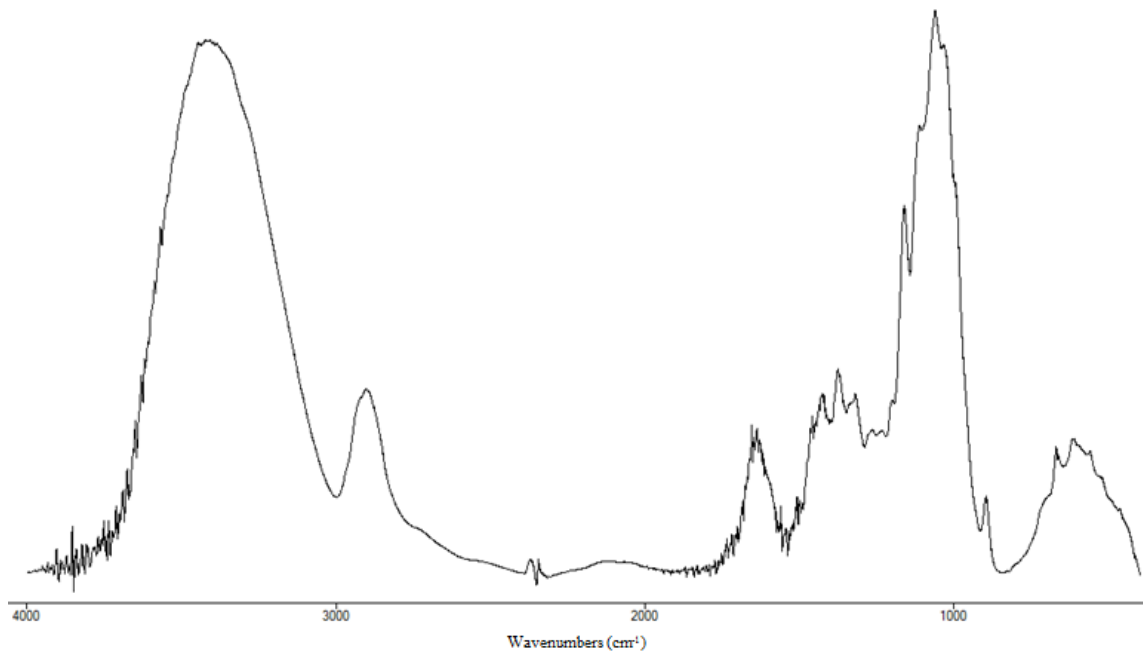
Regenerated material method B (4000-400  $\text{cm}^{-1}$ )



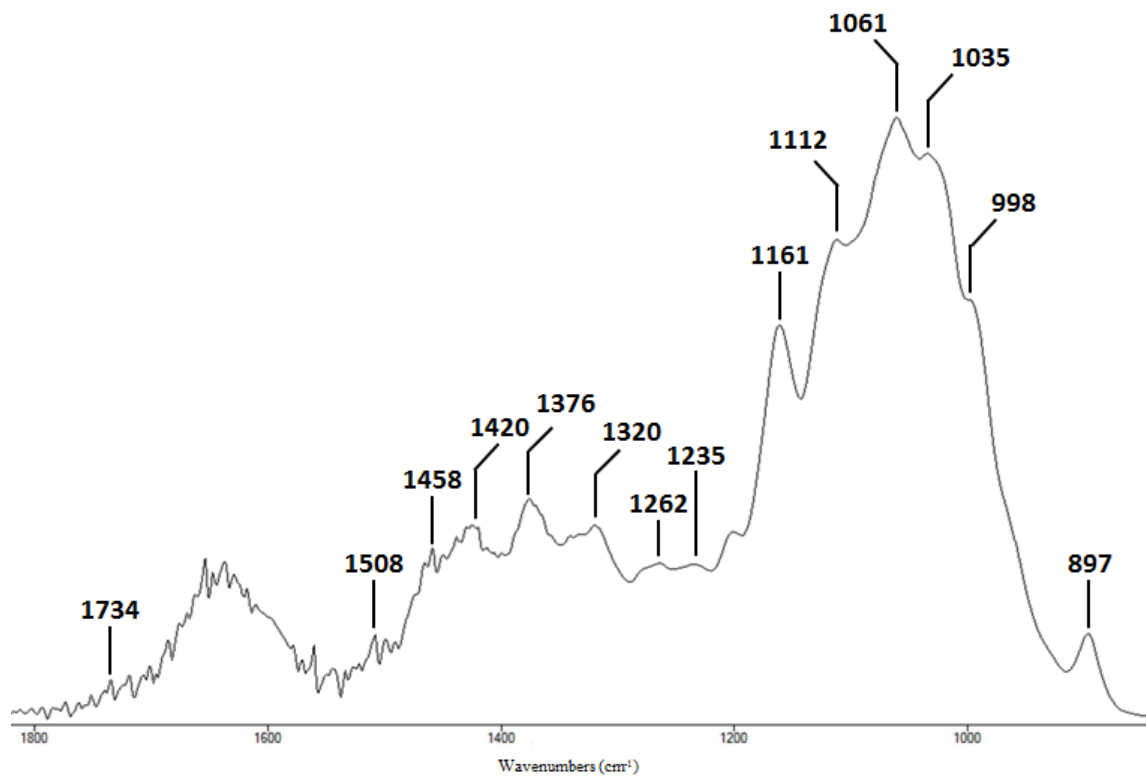
Regenerated material method B (1800-800  $\text{cm}^{-1}$ )



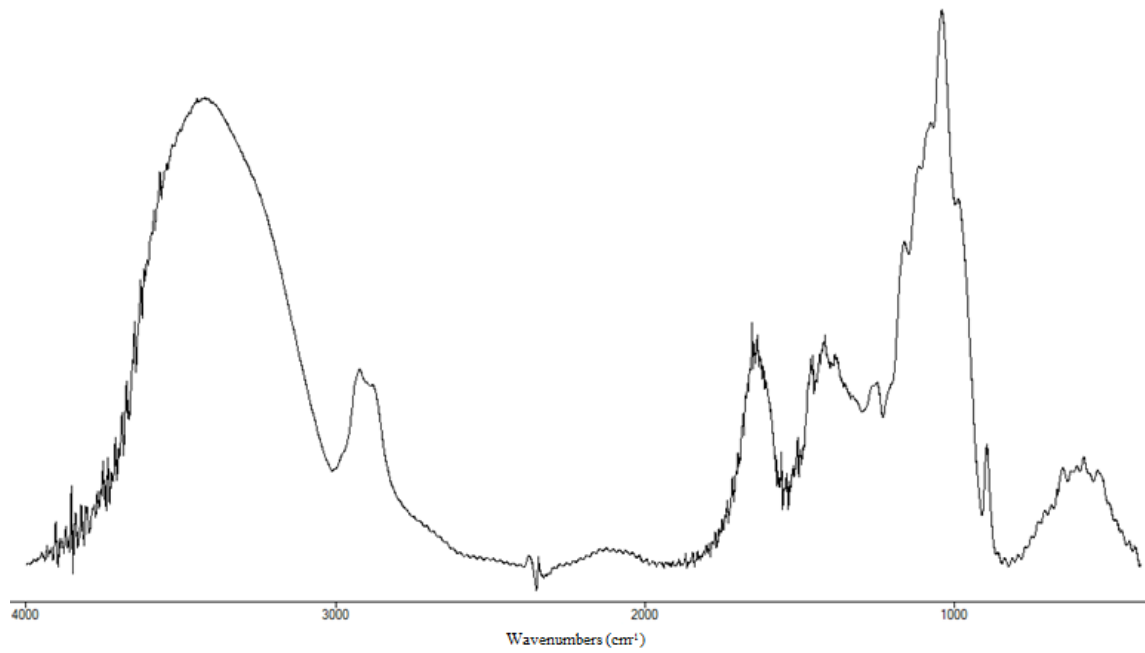
Cellulose-rich method B (4000-400  $\text{cm}^{-1}$ )



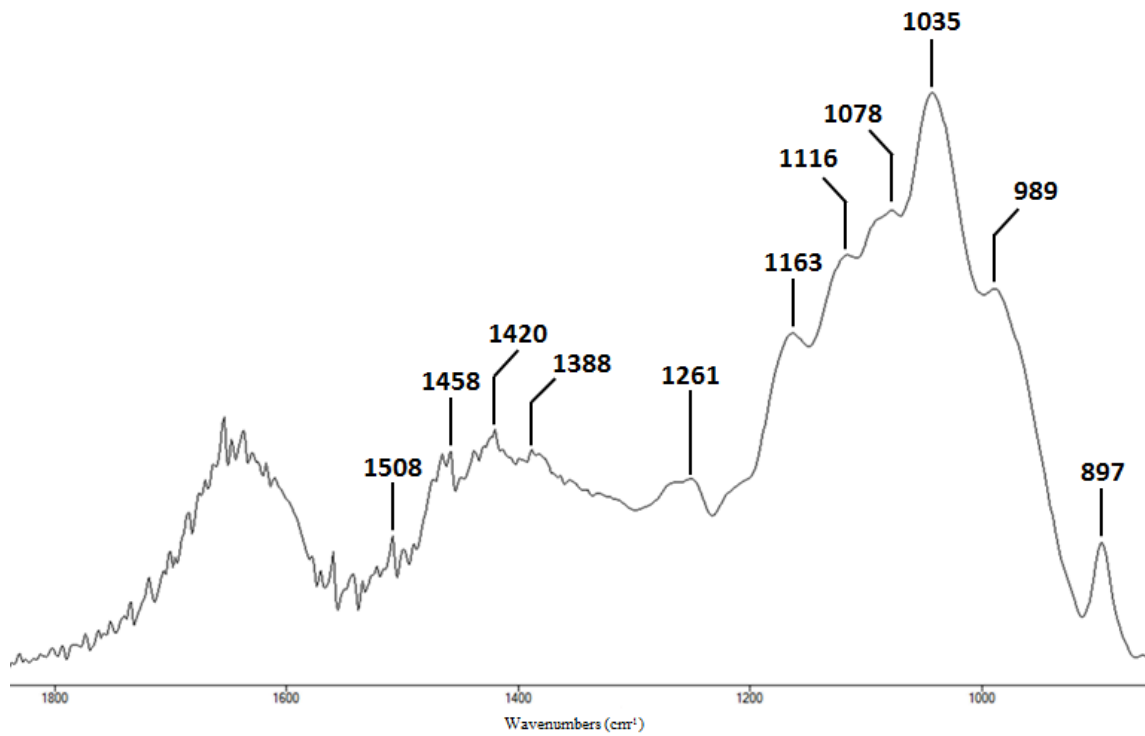
Cellulose-rich method B (1800-800  $\text{cm}^{-1}$ )



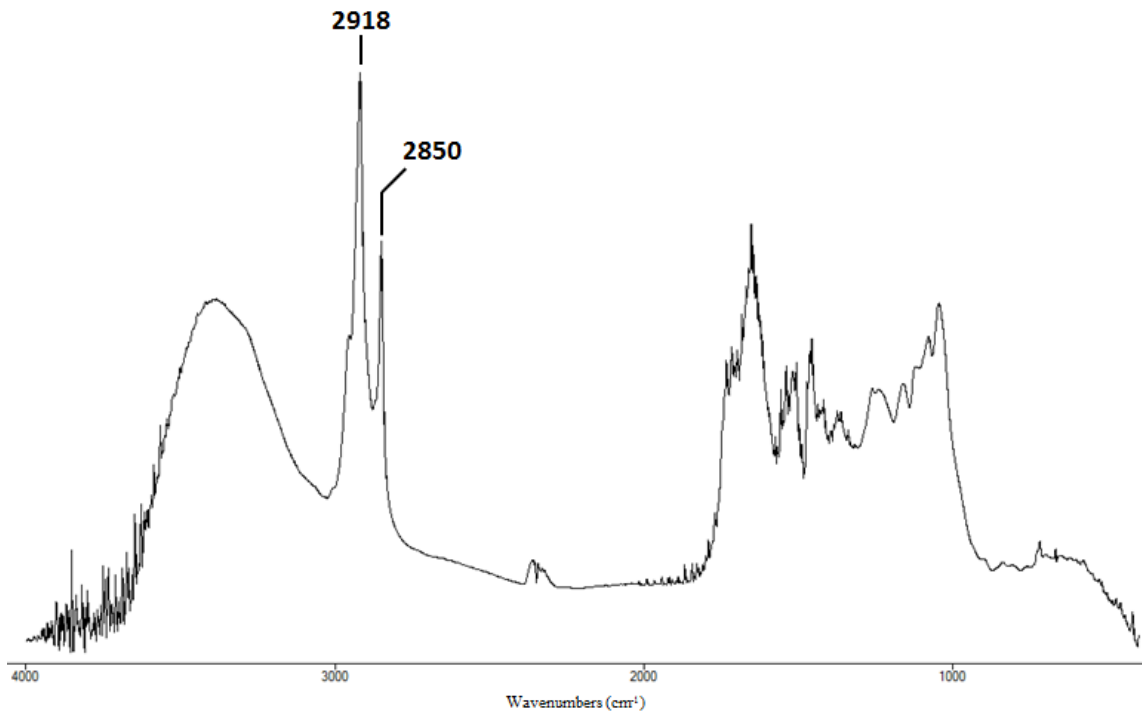
Hemicellulose-rich method B (4000-400  $\text{cm}^{-1}$ )



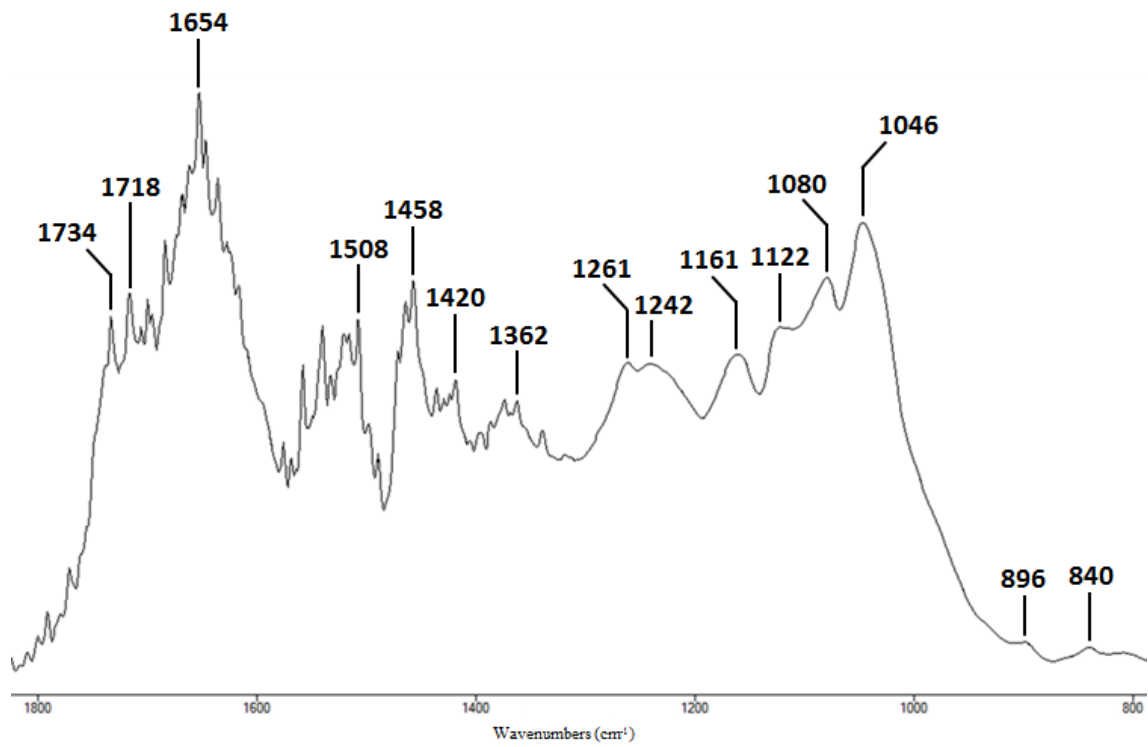
Hemicellulose-rich method B (1800-800  $\text{cm}^{-1}$ )



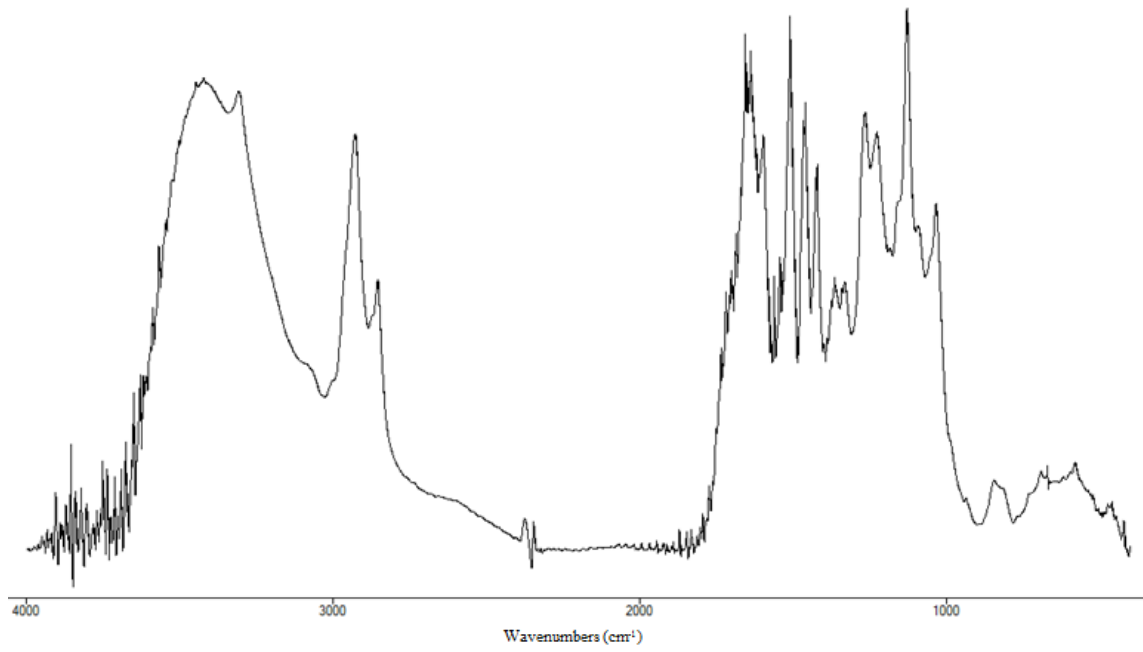
Acetone soluble lignin-rich method B (4000-400  $\text{cm}^{-1}$ )



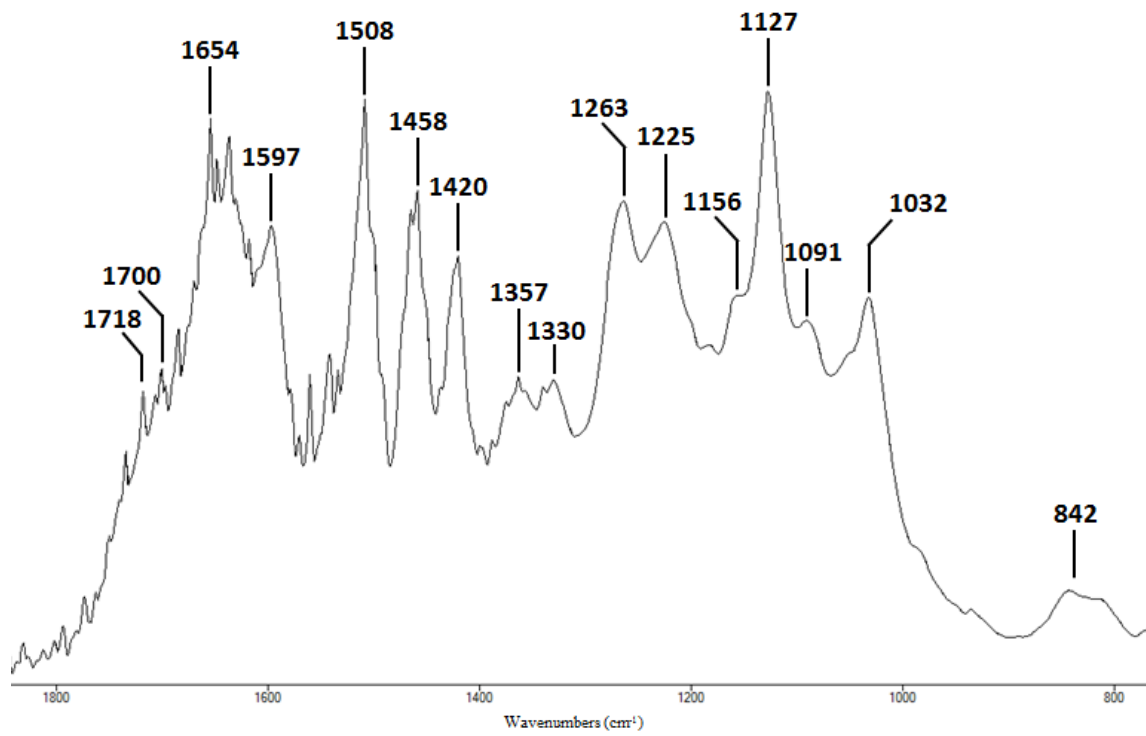
Acetone soluble lignin-rich method B (1800-800  $\text{cm}^{-1}$ )



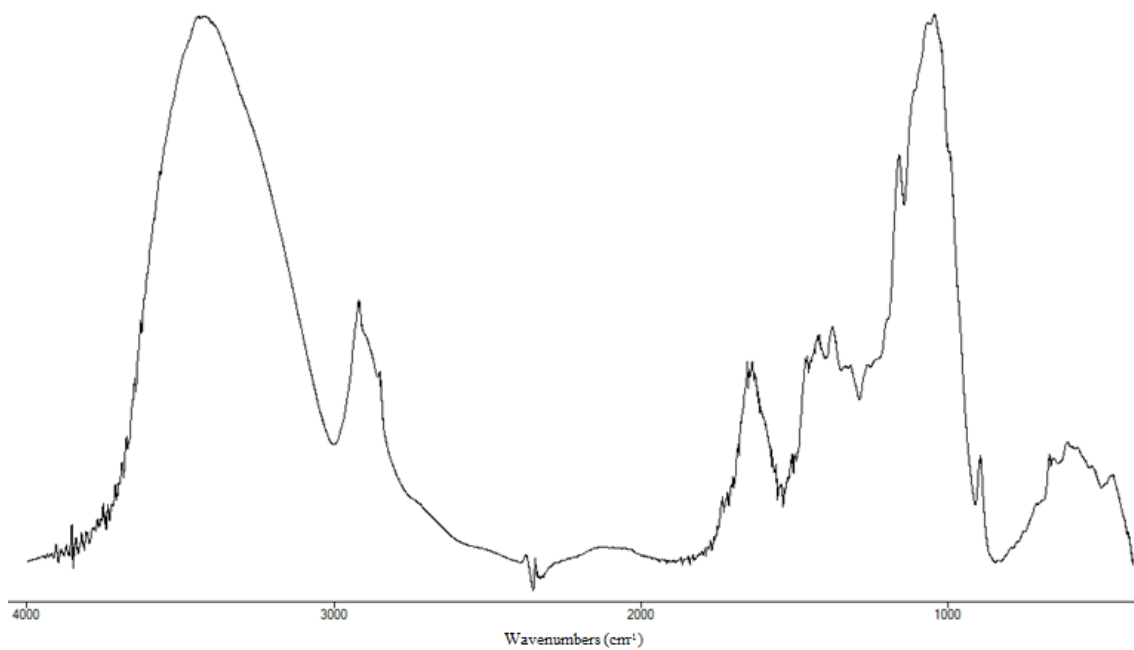
Residual lignin-rich method B (4000-400  $\text{cm}^{-1}$ )



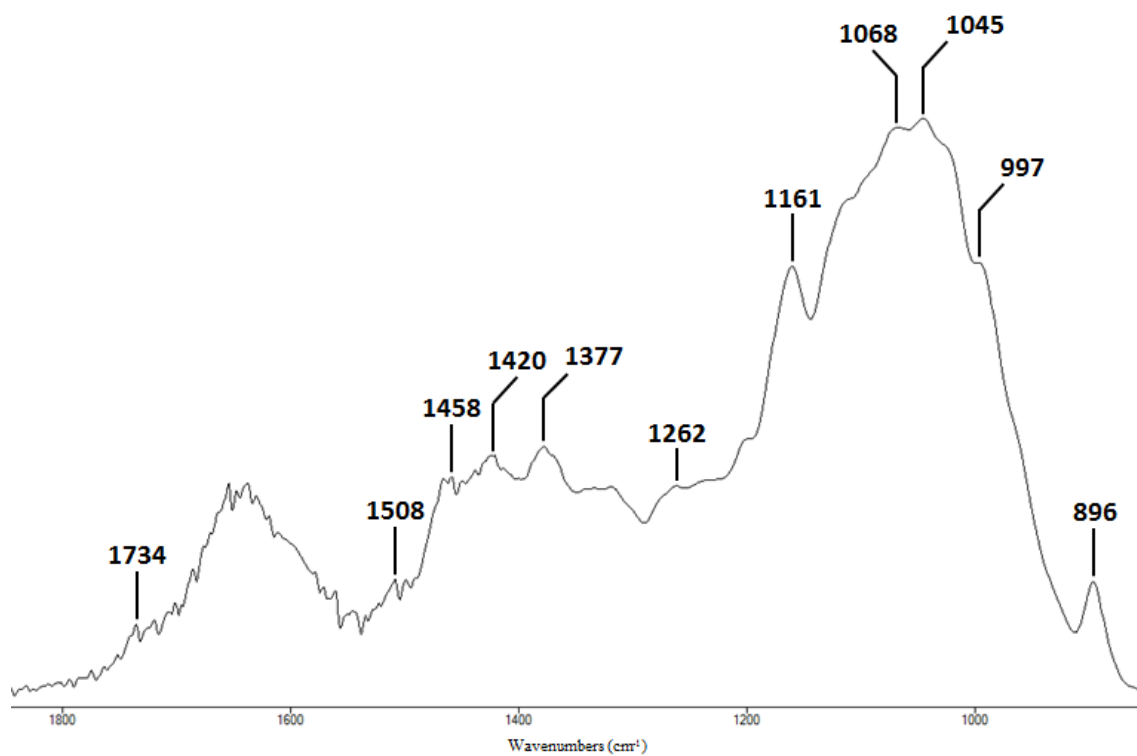
Residual lignin-rich method B (1800-800  $\text{cm}^{-1}$ )



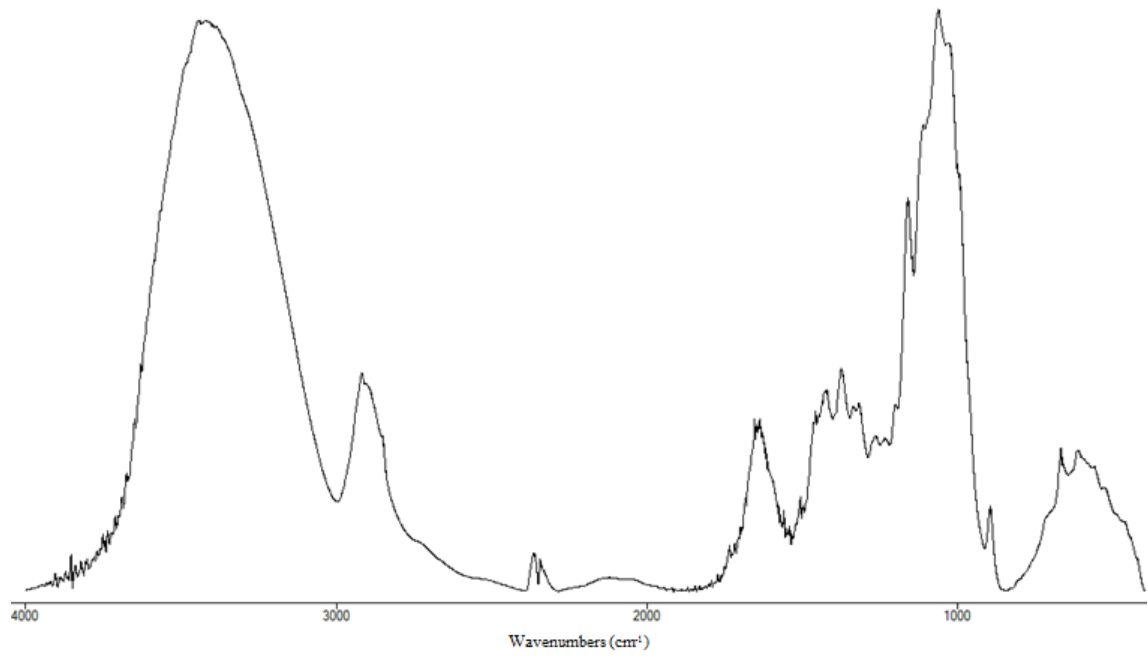
Regenerated material method C (4000-400  $\text{cm}^{-1}$ )



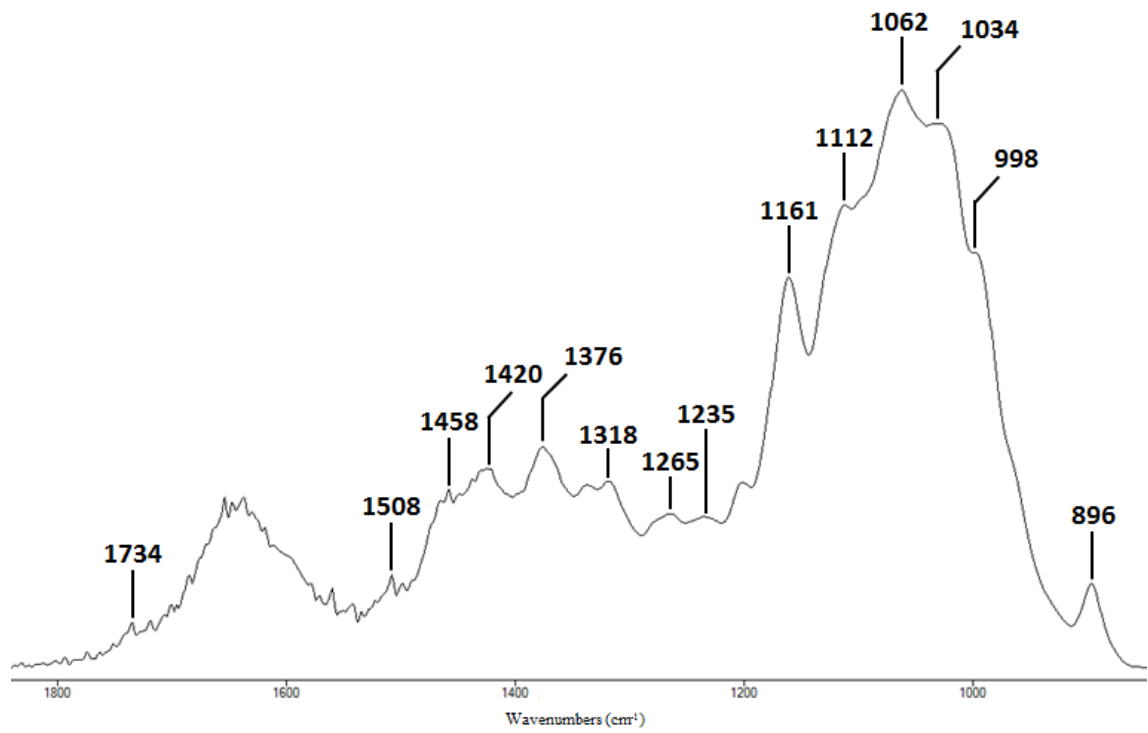
Regenerated material method C (1800-800  $\text{cm}^{-1}$ )



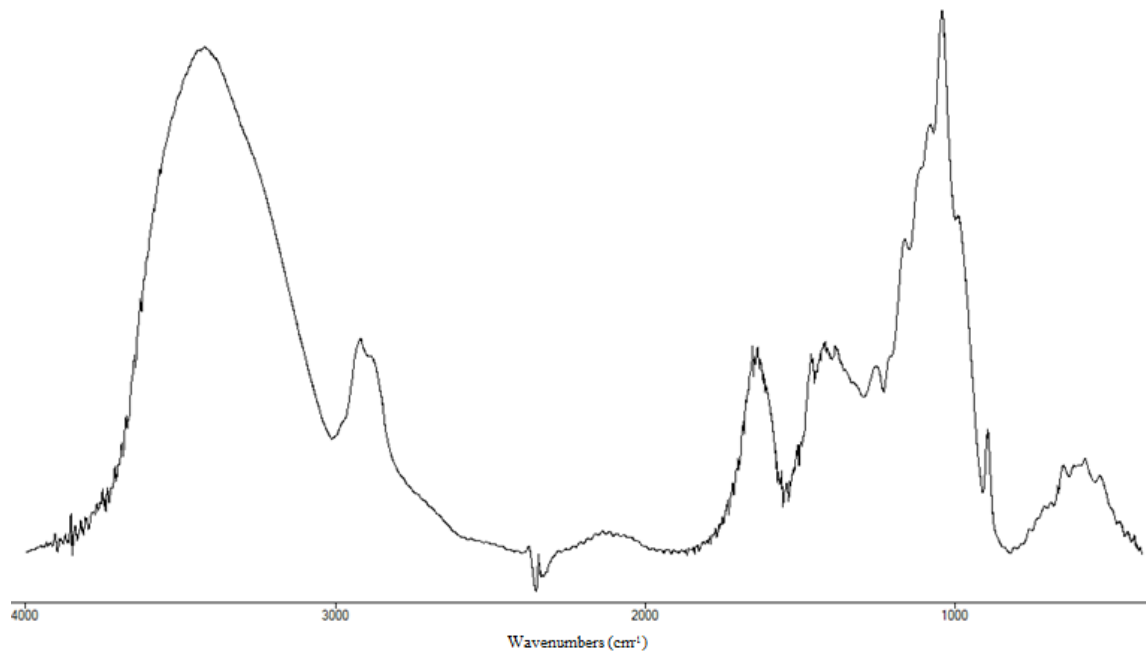
Cellulose-rich method C (4000-400  $\text{cm}^{-1}$ )



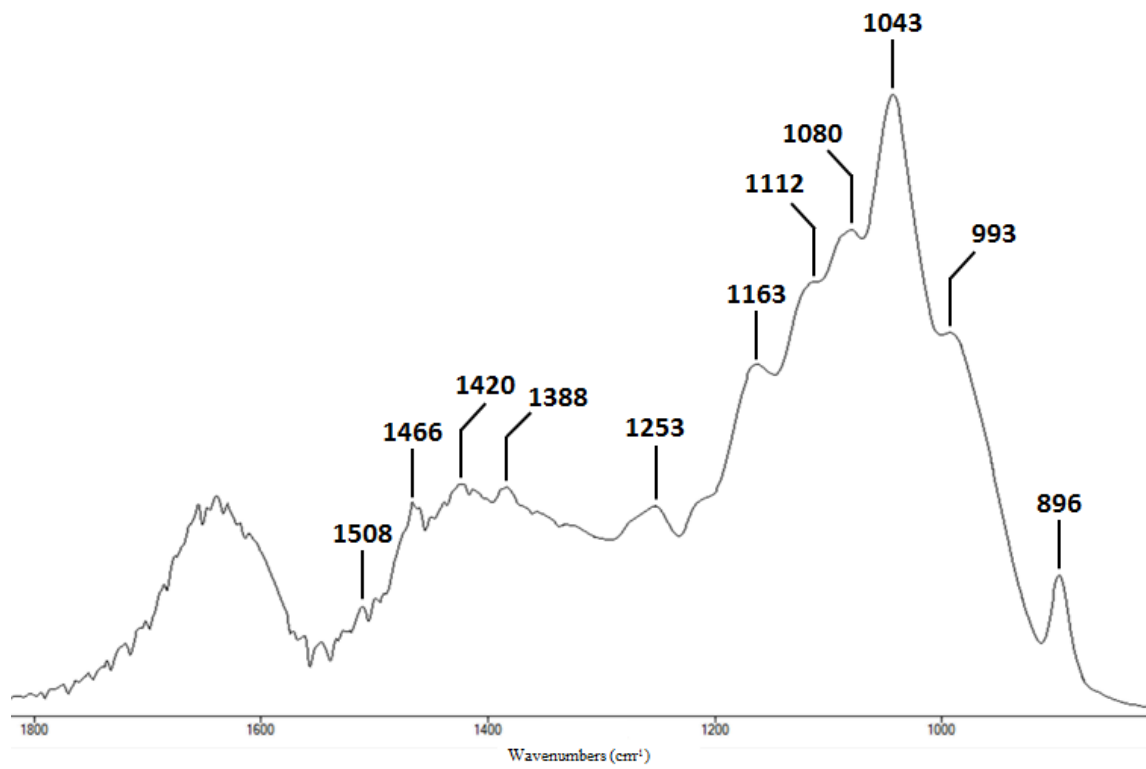
Cellulose-rich method C (1800-800  $\text{cm}^{-1}$ )



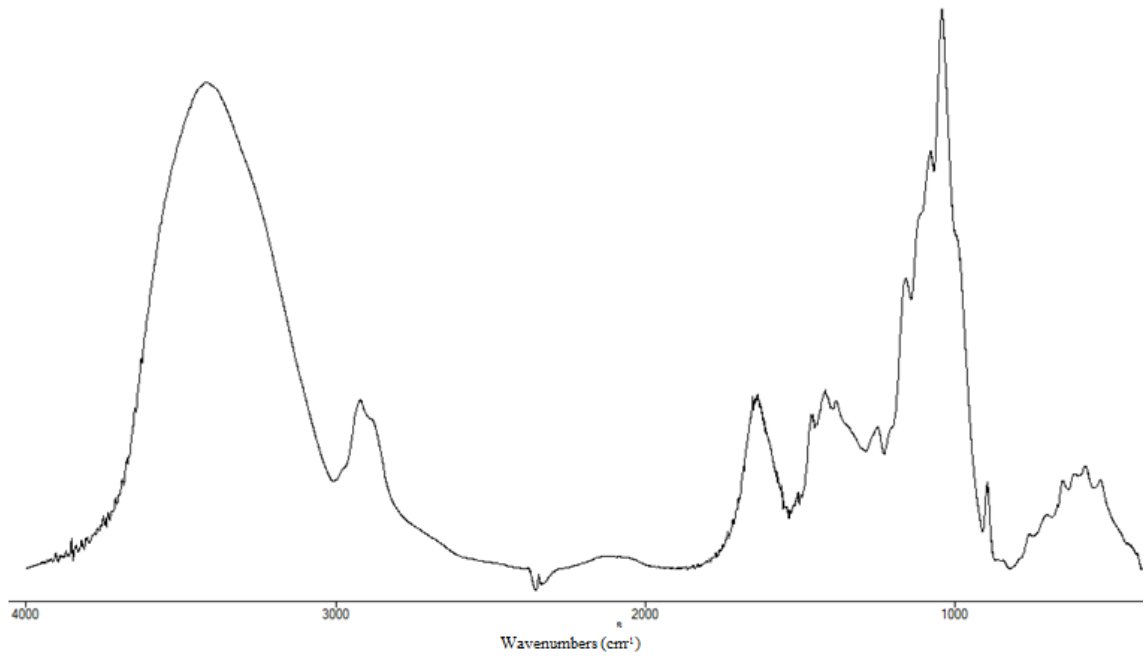
Hemicellulose-rich method C (4000-400  $\text{cm}^{-1}$ )



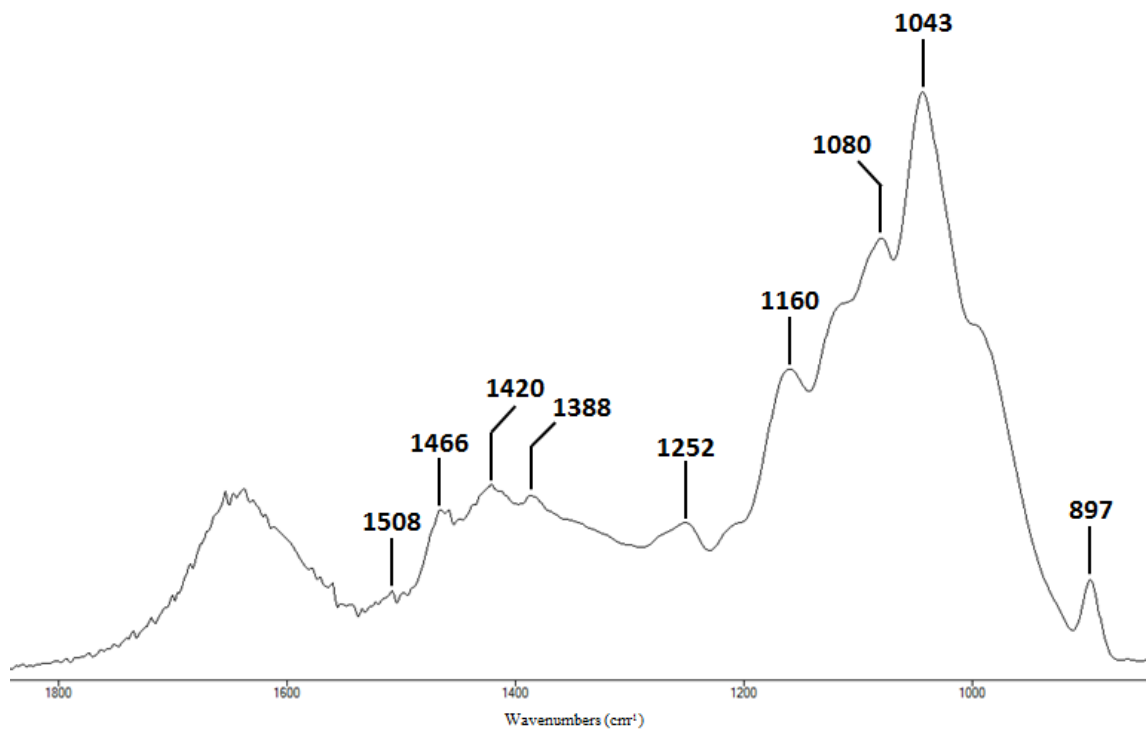
Hemicellulose-rich method C (1800-800  $\text{cm}^{-1}$ )



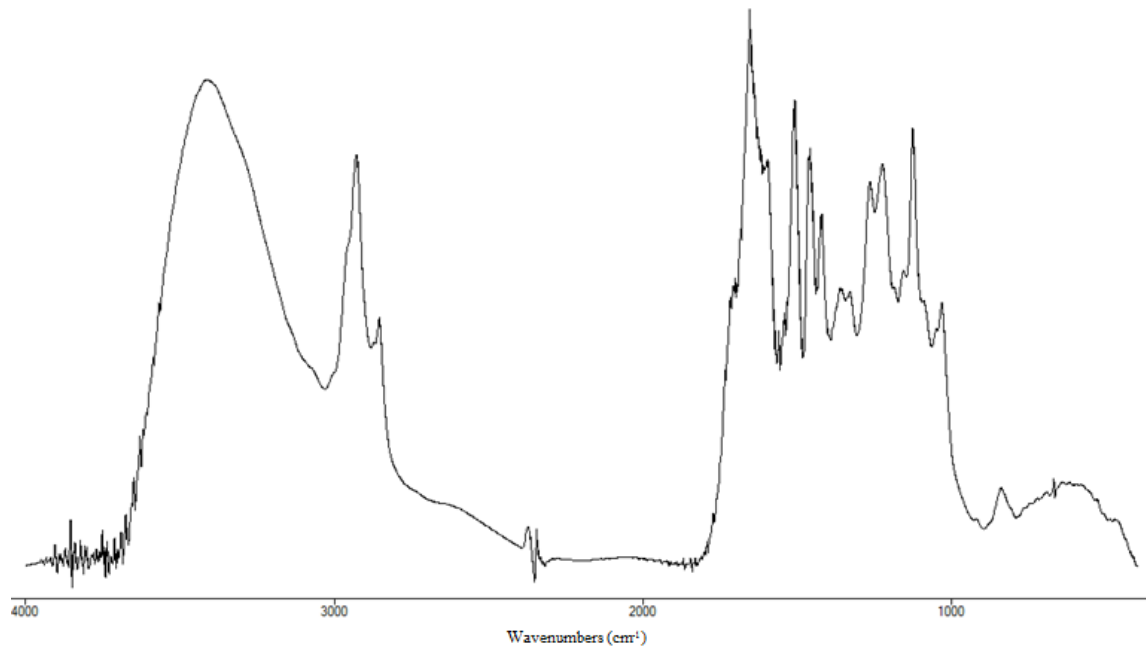
Residual hemicellulose-rich method C (4000-400  $\text{cm}^{-1}$ )



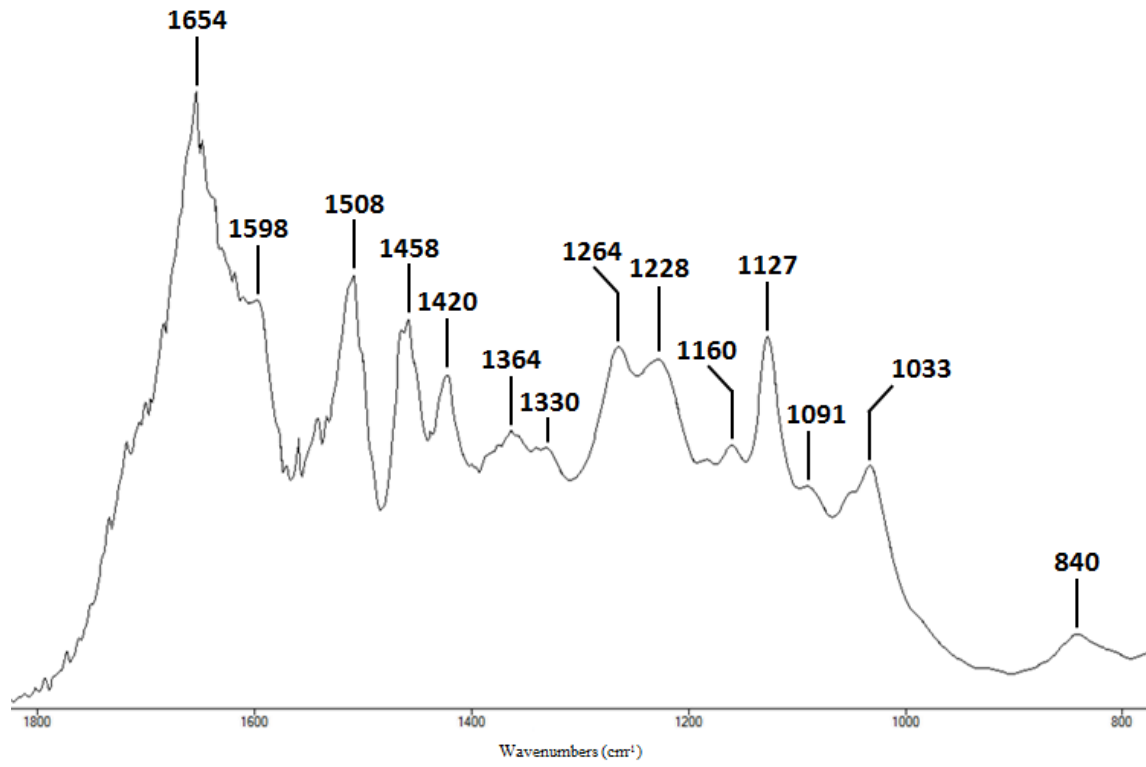
Residual Hemicellulose-rich method C (1800-800  $\text{cm}^{-1}$ )



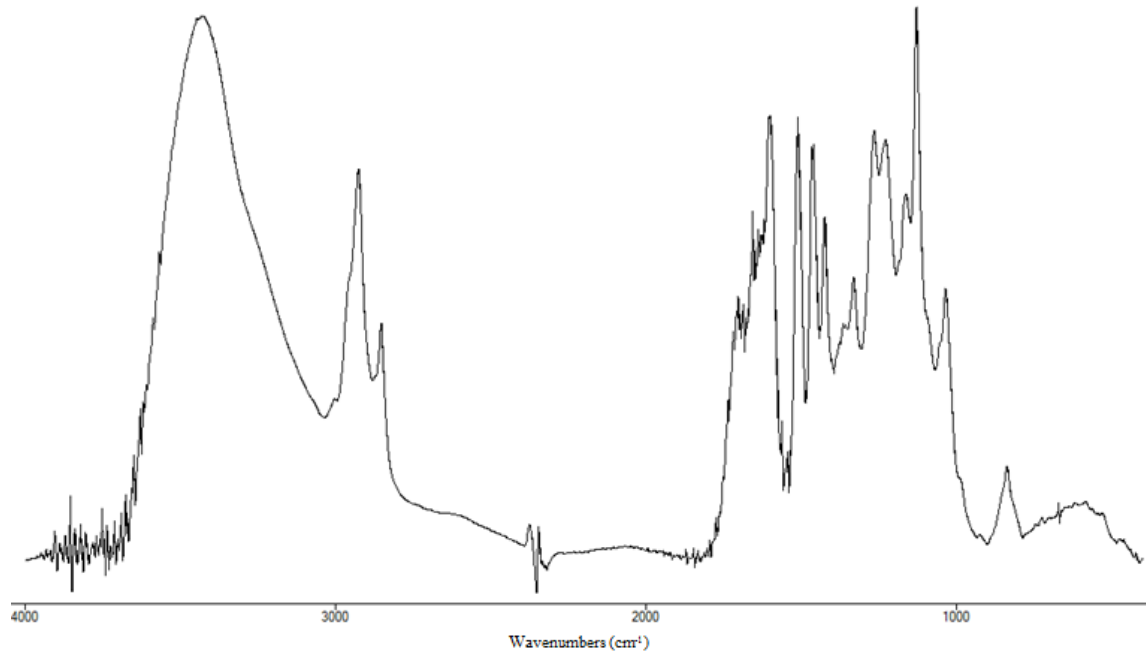
Lignin-rich method C (4000-400  $\text{cm}^{-1}$ )



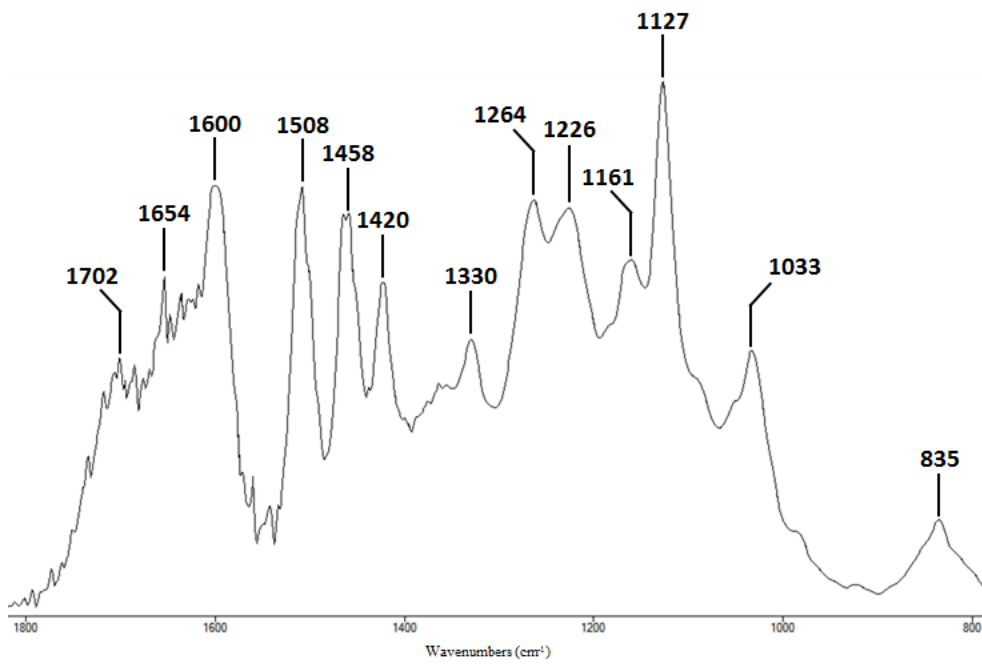
Lignin-rich method C (1800-800  $\text{cm}^{-1}$ )



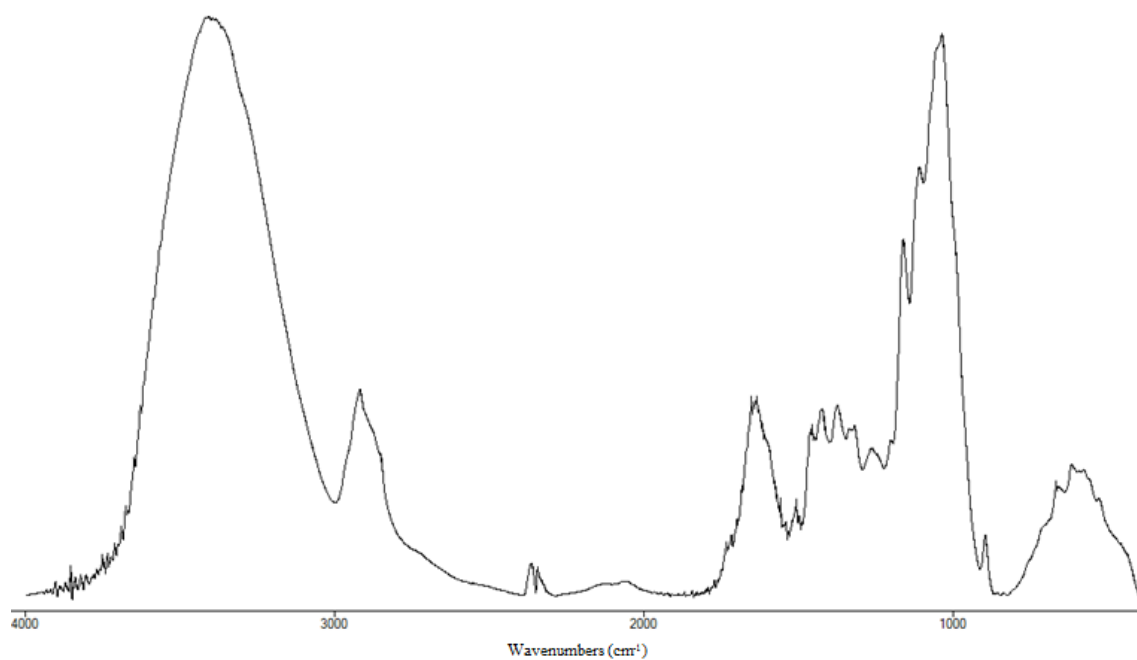
Residual lignin-rich method C (4000-400  $\text{cm}^{-1}$ )



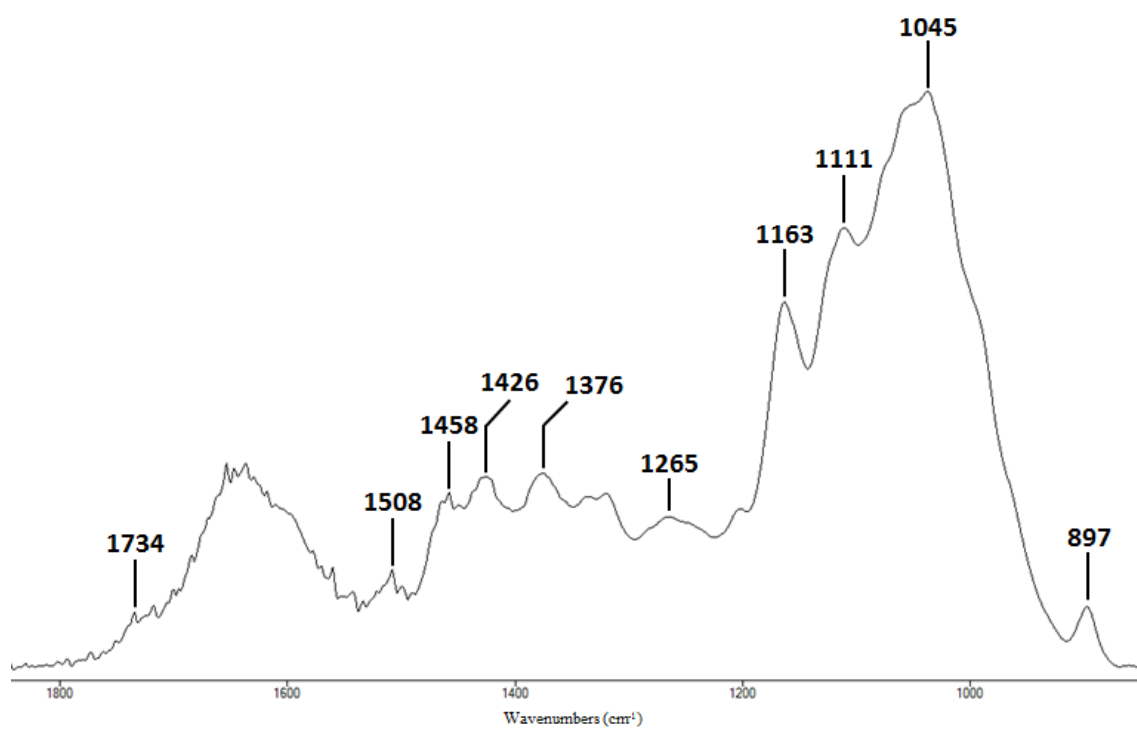
Residual lignin-rich method C (1800-800  $\text{cm}^{-1}$ )



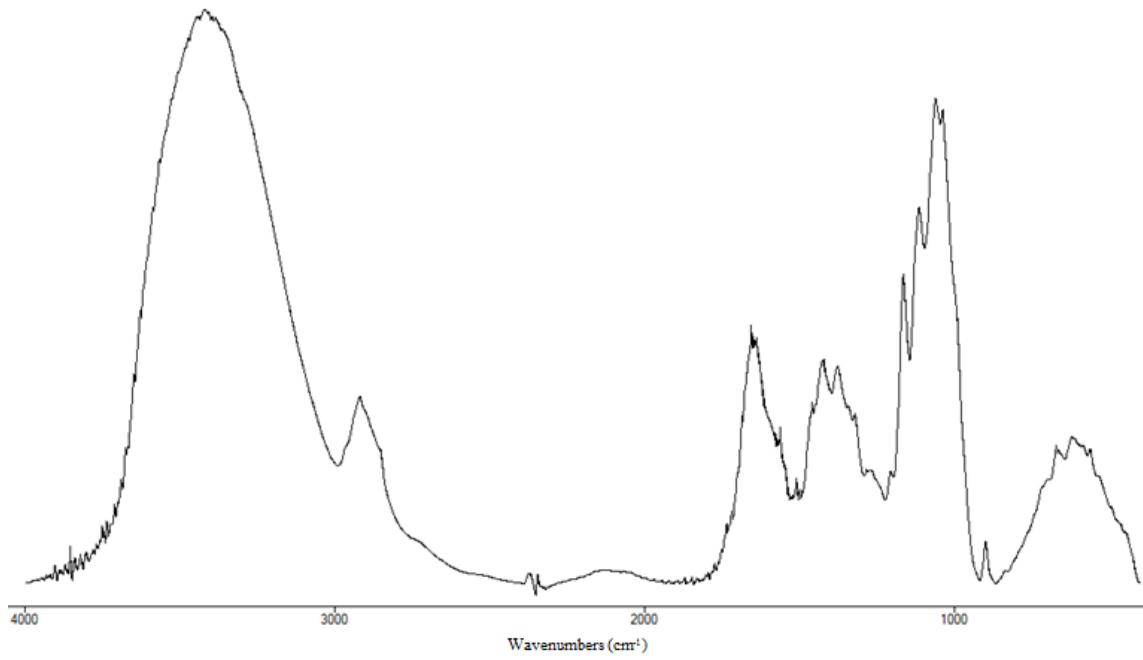
Regenerated material method C – [bmim][SCN] (4000-400  $\text{cm}^{-1}$ )



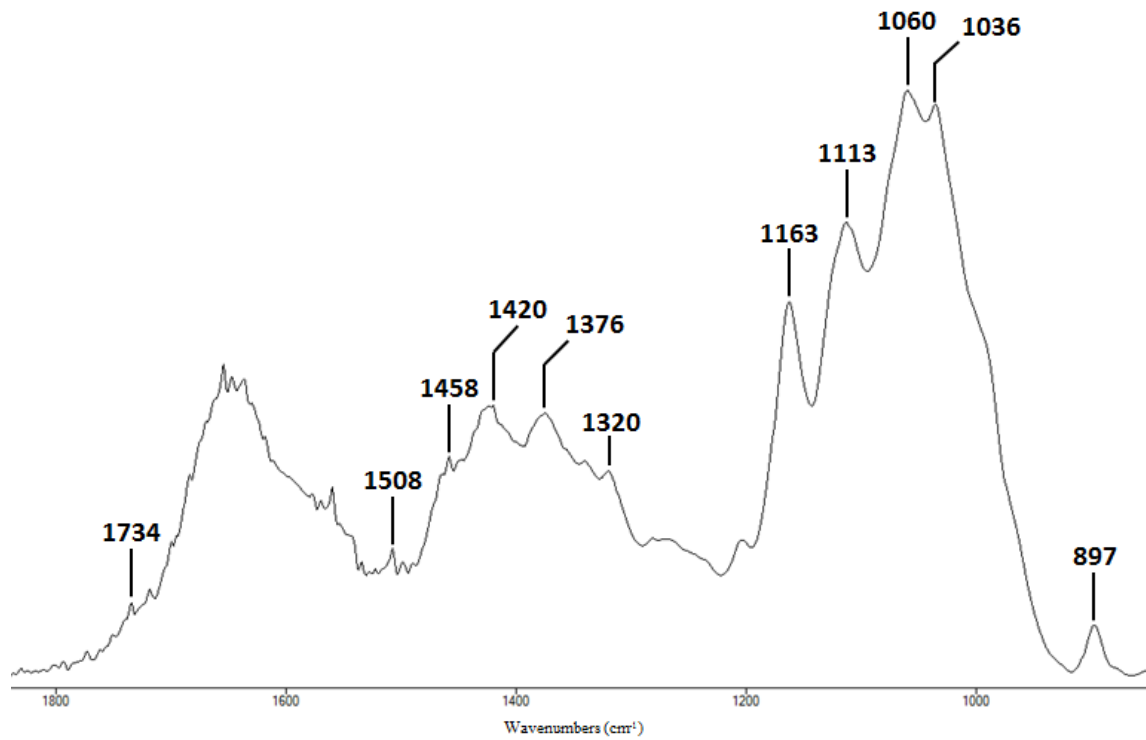
Regenerated material method C – [bmim][SCN] (1800-800  $\text{cm}^{-1}$ )



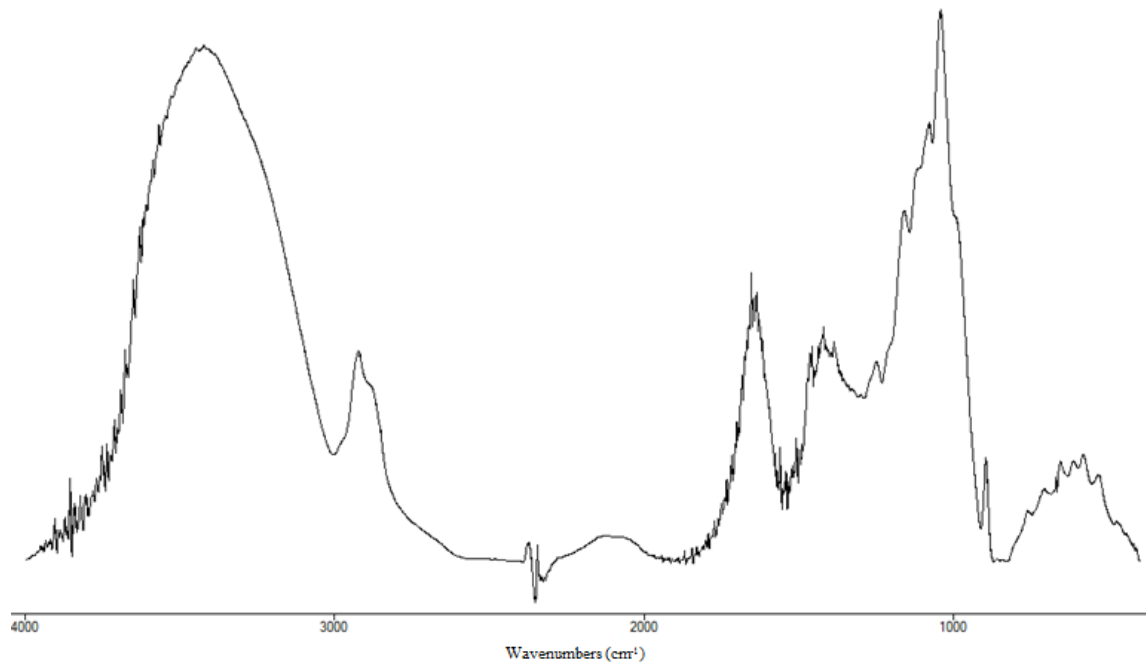
Cellulose-rich method C – [bmim][SCN] (4000-400  $\text{cm}^{-1}$ )



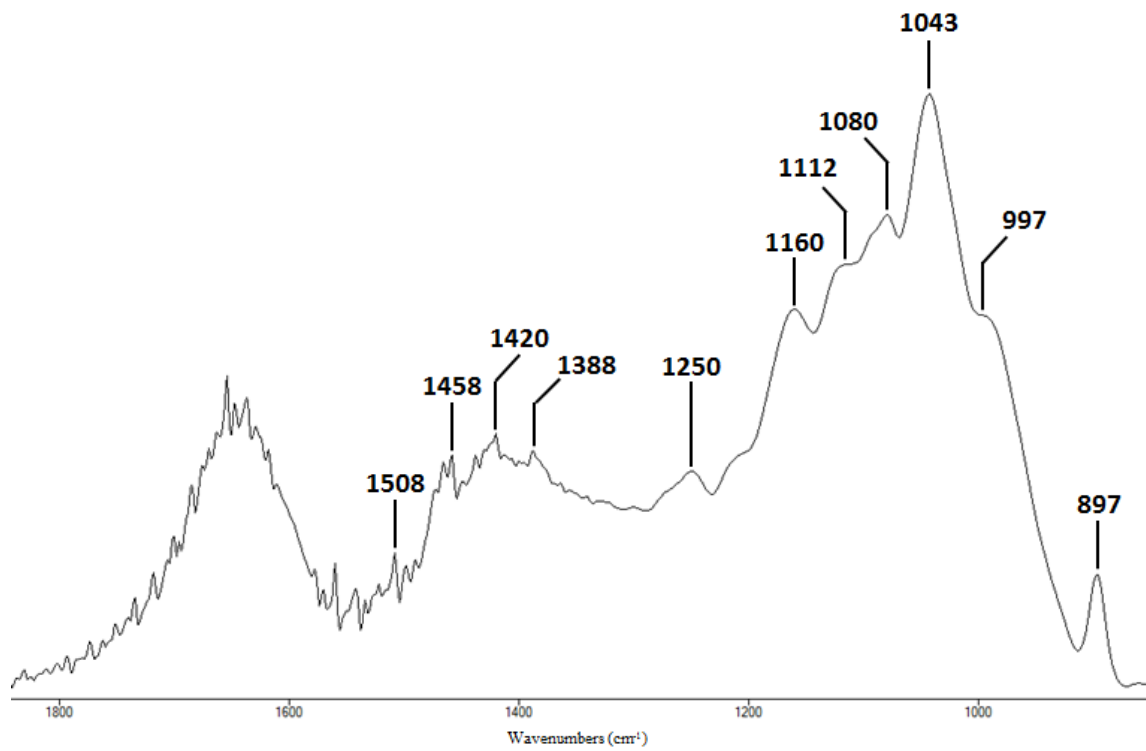
Cellulose-rich method C – [bmim][SCN] (1800-800  $\text{cm}^{-1}$ )



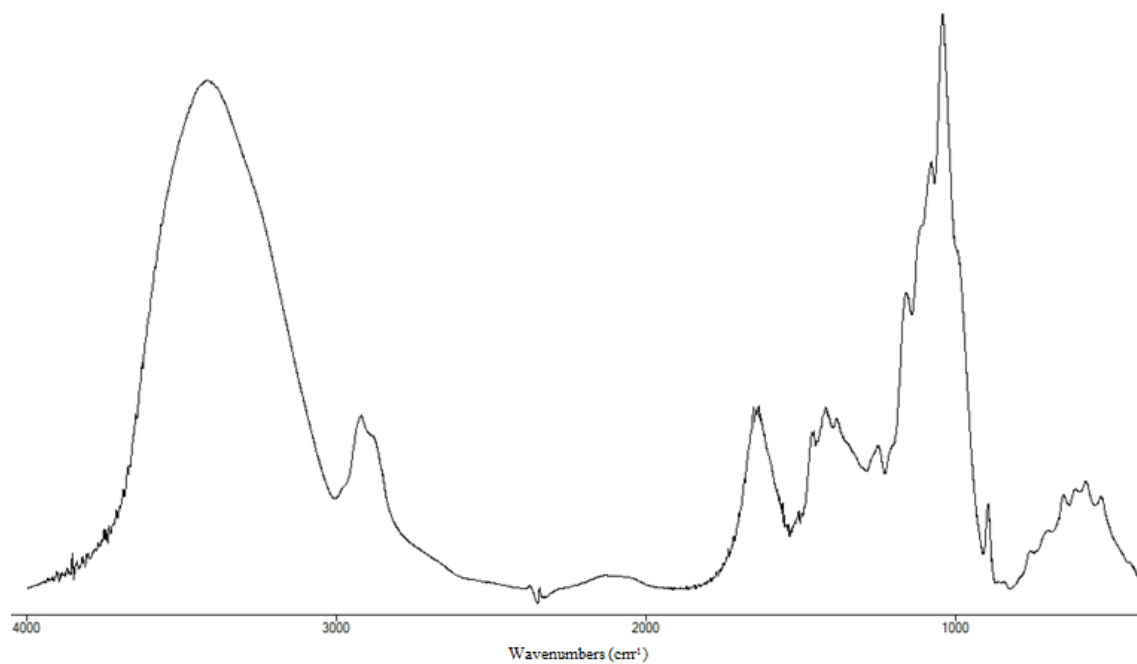
Hemicellulose-rich method C – [bmim][SCN] (4000-400  $\text{cm}^{-1}$ )



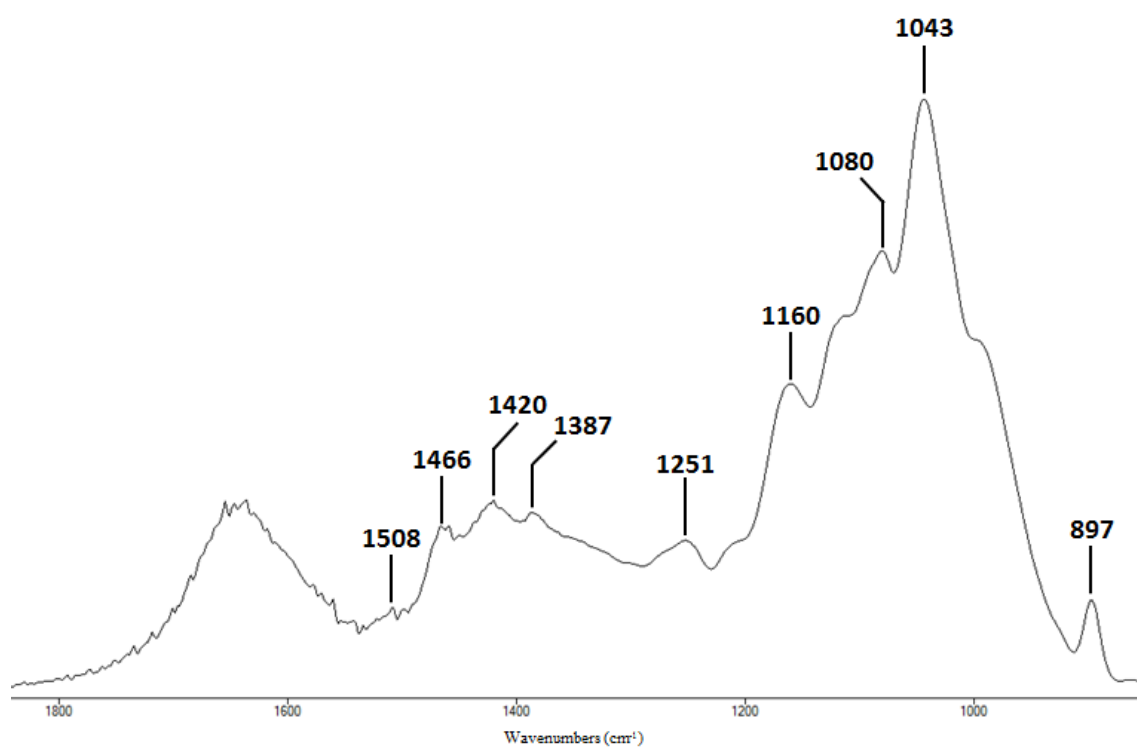
Hemicellulose-rich method C – [bmim][SCN] (1800-800  $\text{cm}^{-1}$ )



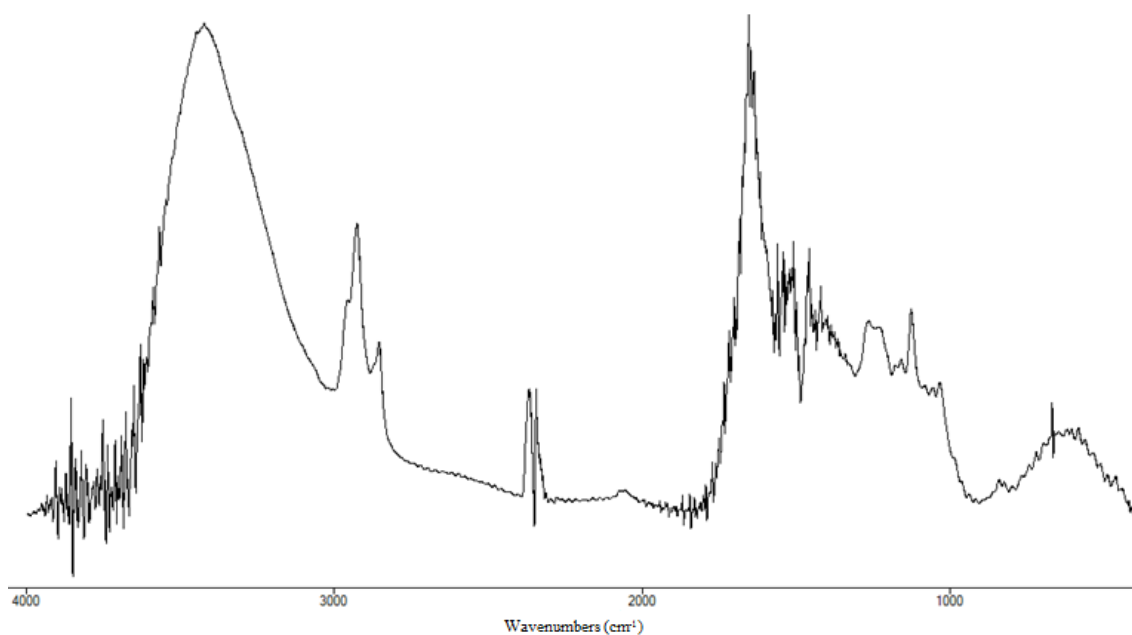
Residual hemicellulose-rich method C – [bmim][SCN] (4000-400  $\text{cm}^{-1}$ )



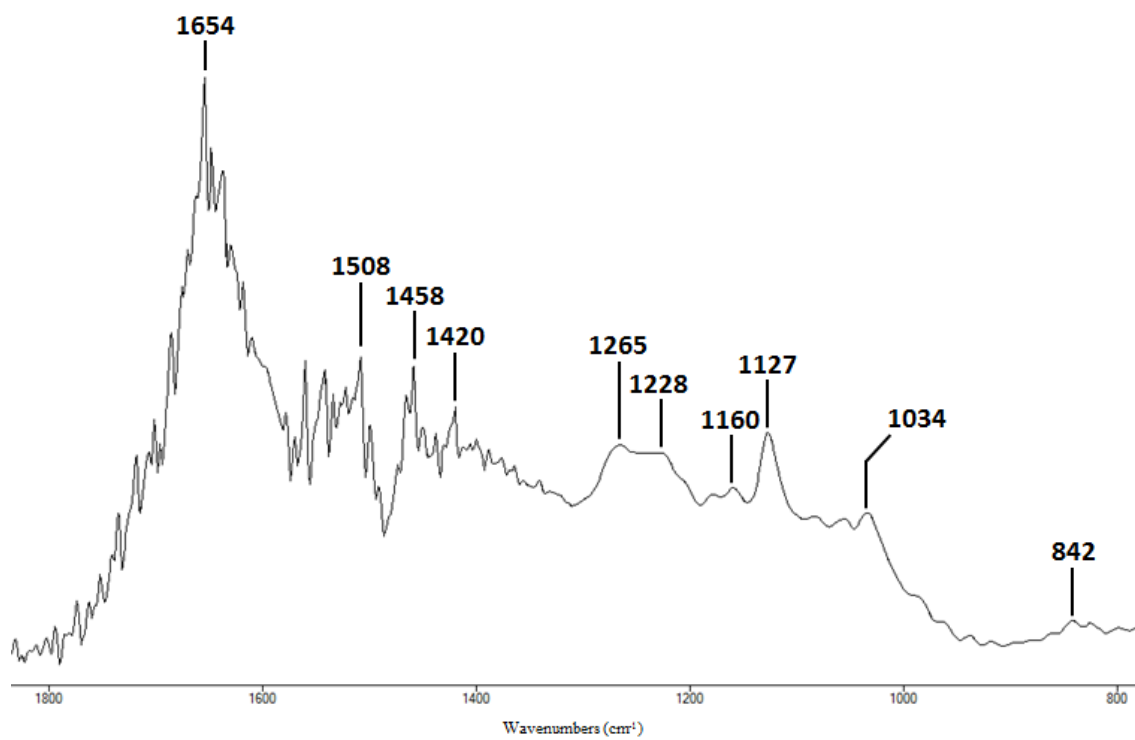
Residual hemicellulose-rich method C – [bmim][SCN] (1800-800  $\text{cm}^{-1}$ )



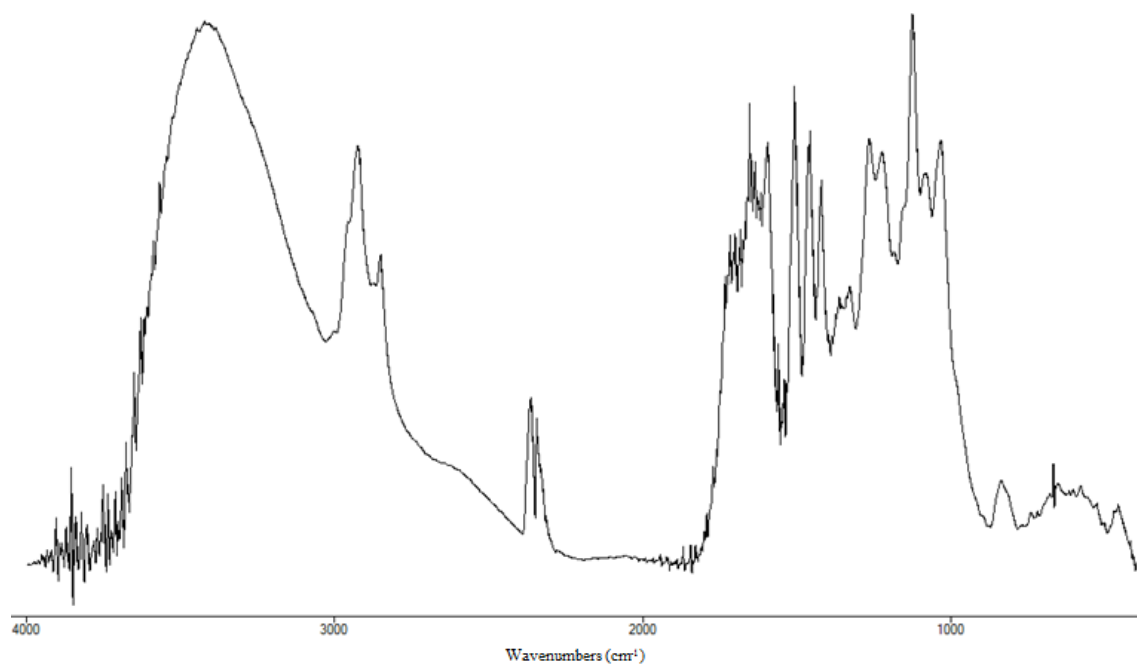
Lignin-rich method C – [bmim][SCN] (4000-400  $\text{cm}^{-1}$ )



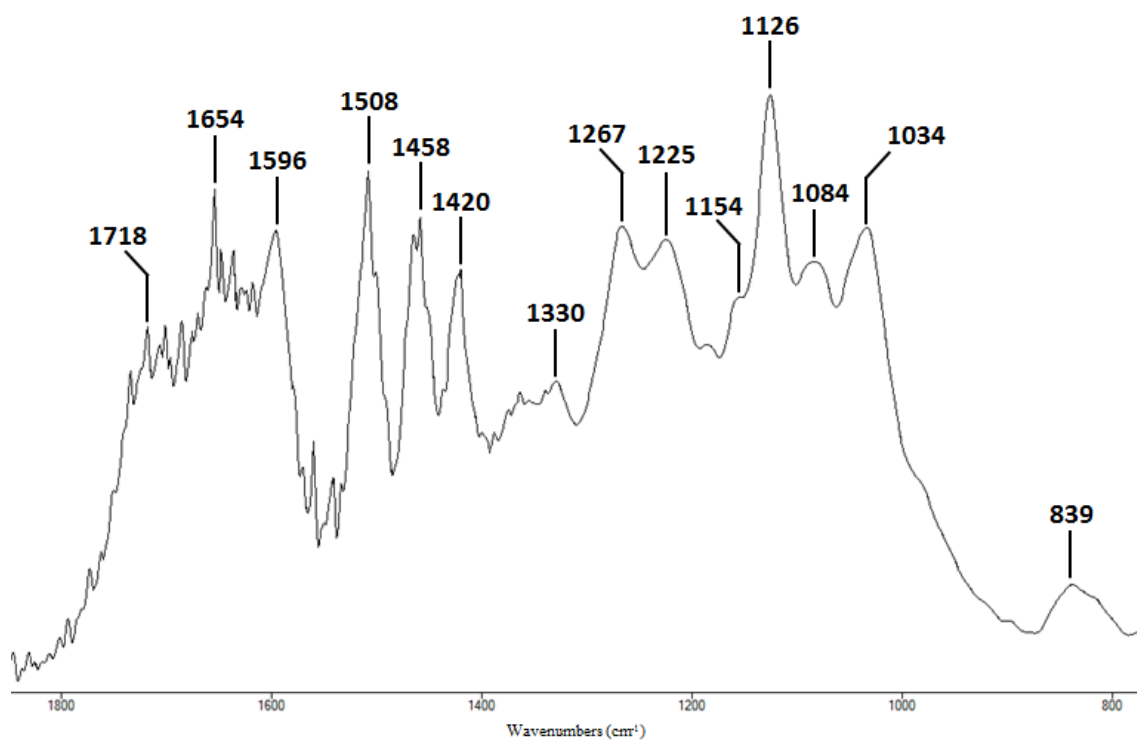
Lignin-rich method C – [bmim][SCN] (1800-800  $\text{cm}^{-1}$ )



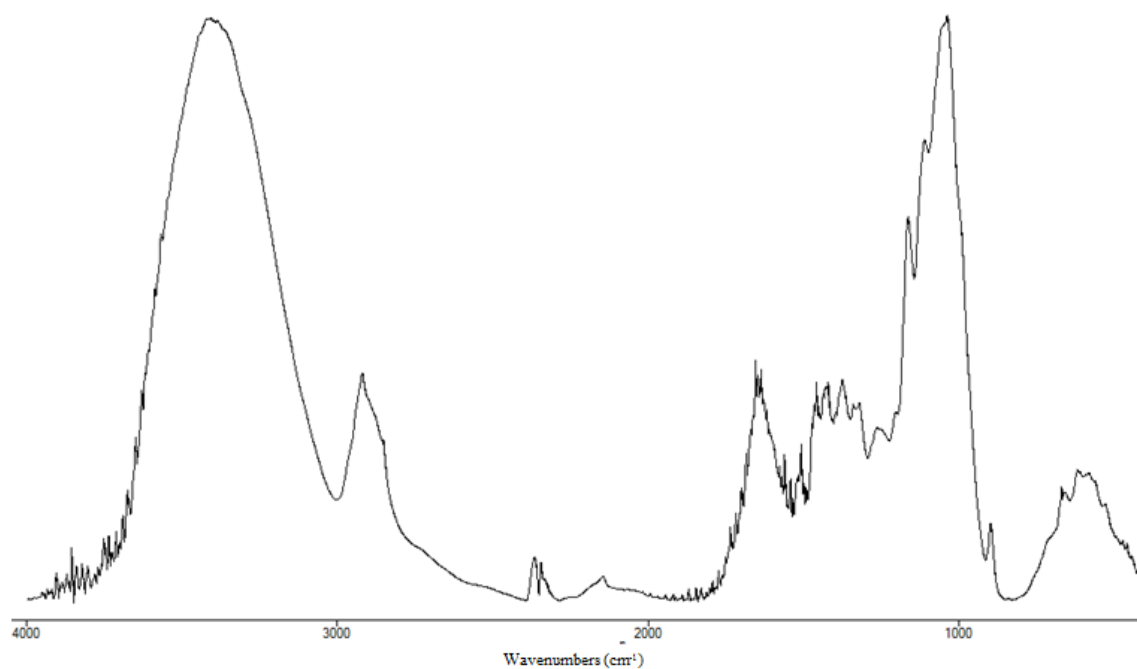
Residual lignin-rich method C – [bmim][SCN] (4000-400  $\text{cm}^{-1}$ )



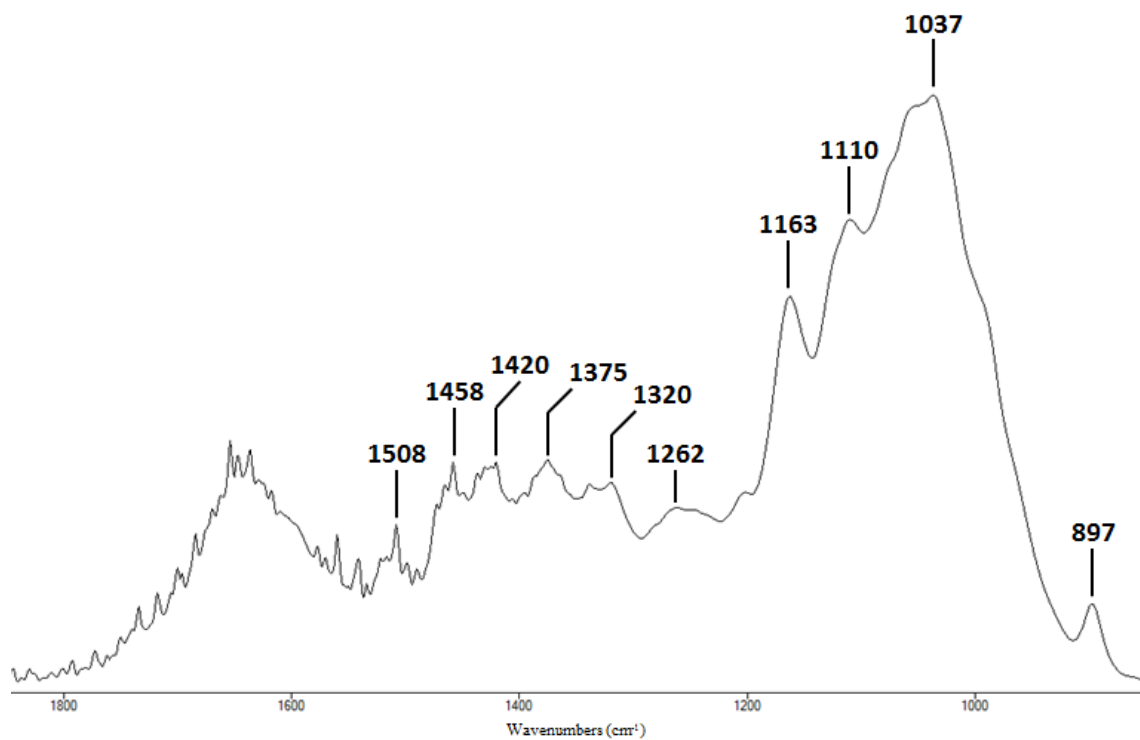
Residual lignin-rich method C – [bmim][SCN] (1800-800  $\text{cm}^{-1}$ )



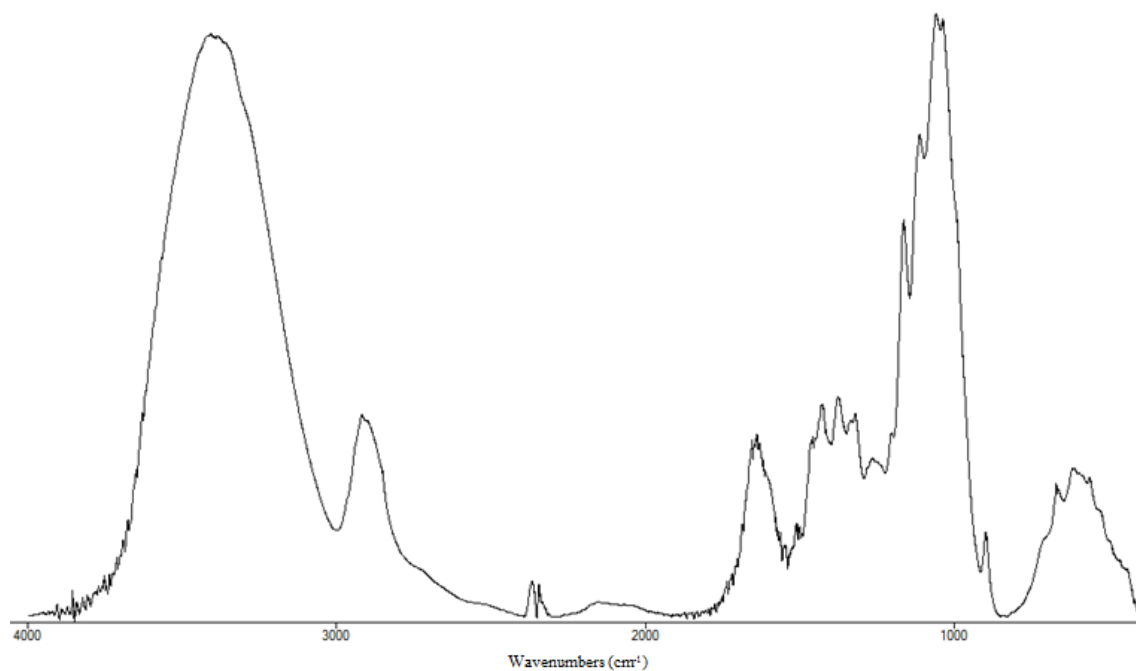
Regenerated material method C – [bmim][N(CN)<sub>2</sub>] (4000-400 cm<sup>-1</sup>)



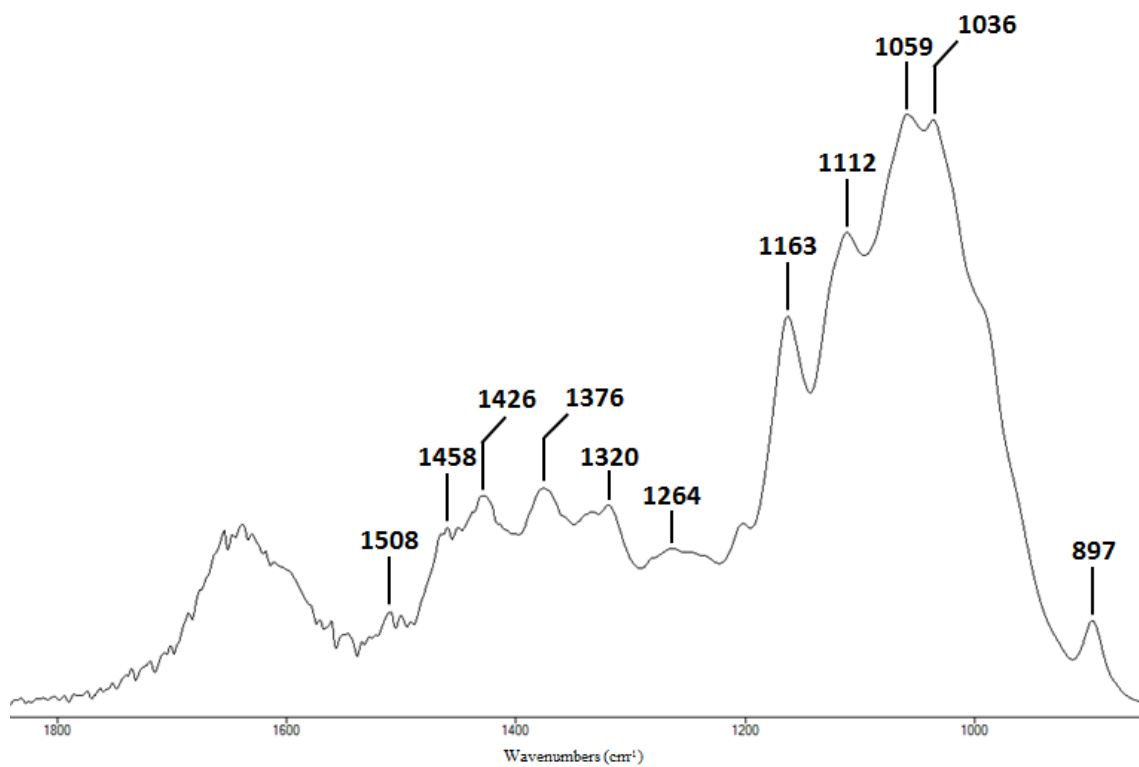
Regenerated material method C – [bmim][N(CN)<sub>2</sub>] (1800-800 cm<sup>-1</sup>)



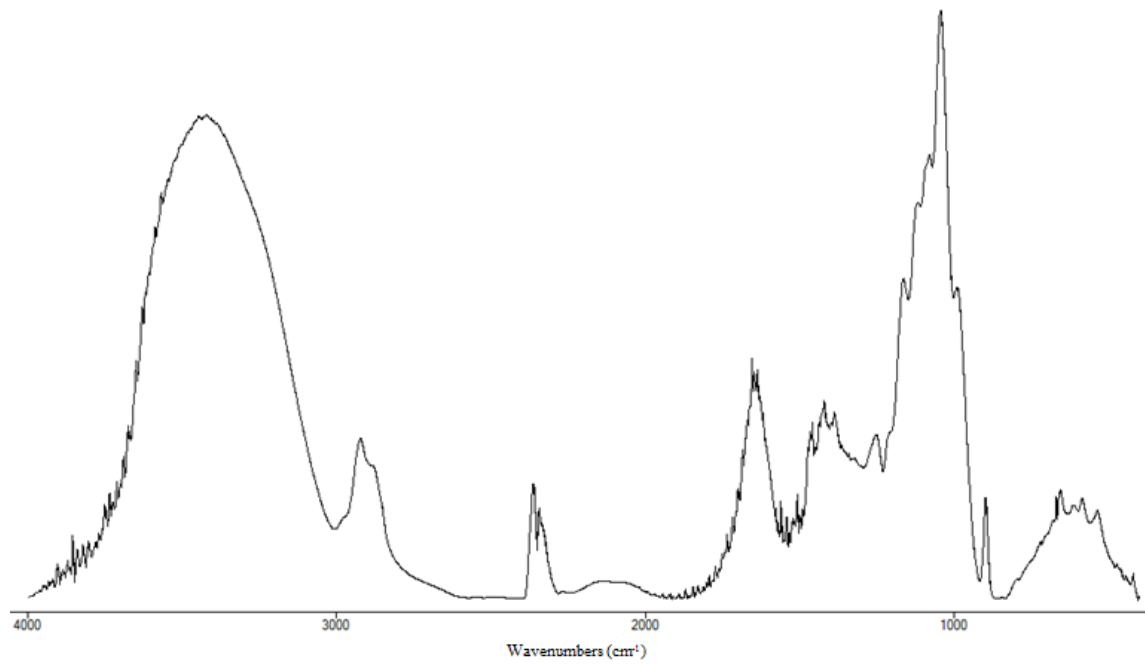
Cellulose-rich method C – [bmim][N(CN)<sub>2</sub>] (4000-400 cm<sup>-1</sup>)



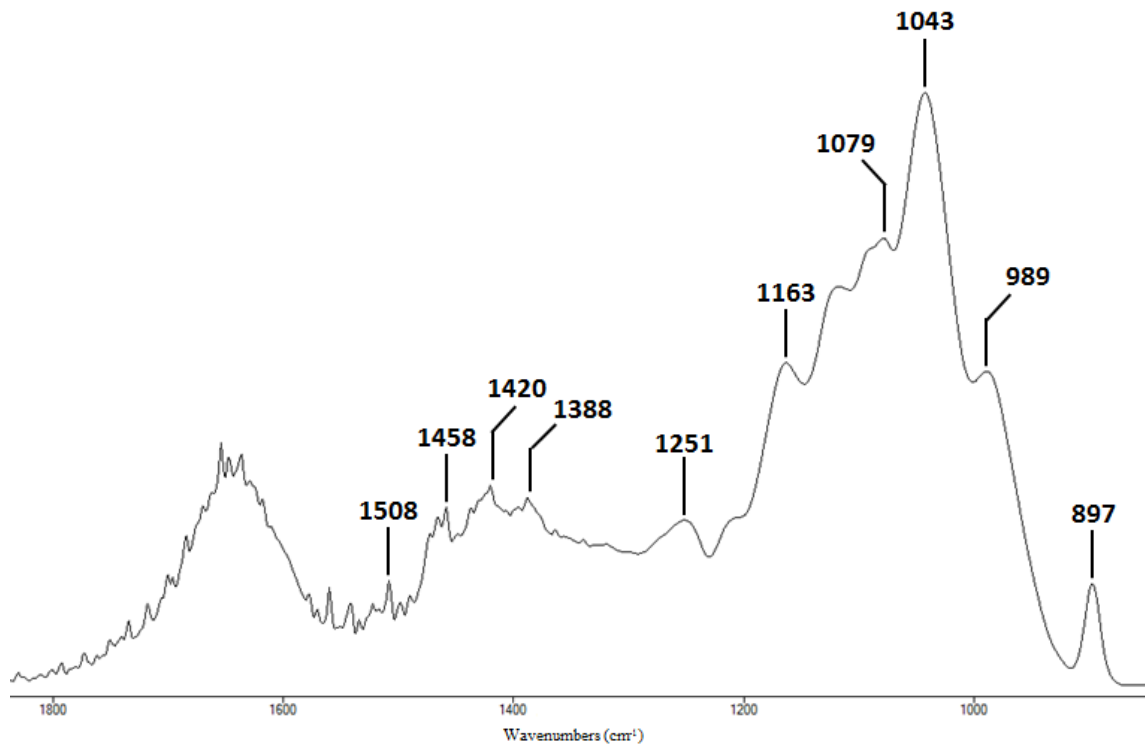
Cellulose-rich method C – [bmim][N(CN)<sub>2</sub>] (1800-800 cm<sup>-1</sup>)



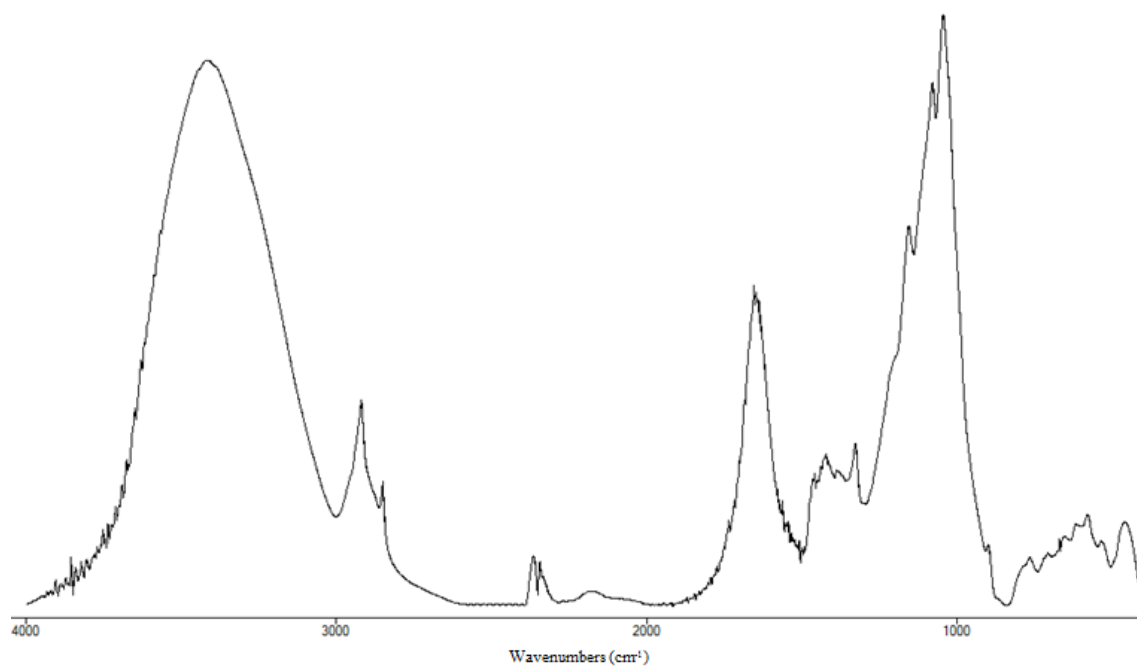
Hemicellulose-rich method C – [bmim][N(CN)<sub>2</sub>] (4000-400 cm<sup>-1</sup>)



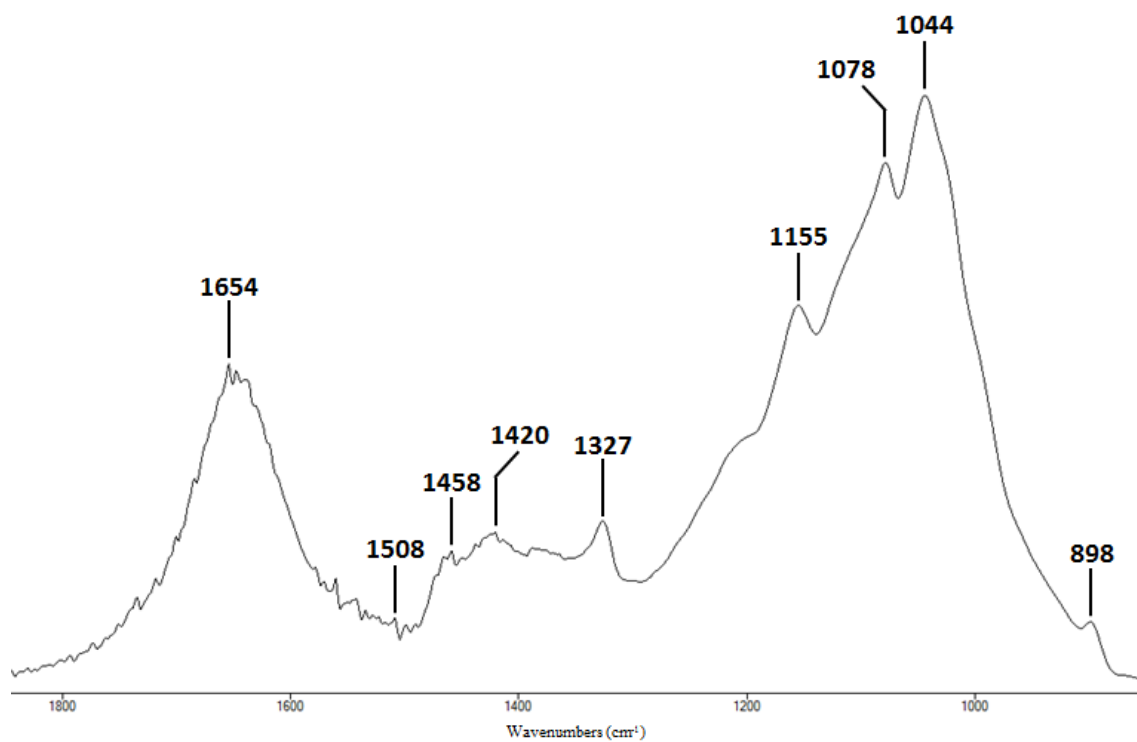
Hemicellulose-rich method C – [bmim][N(CN)<sub>2</sub>] (1800-800 cm<sup>-1</sup>)



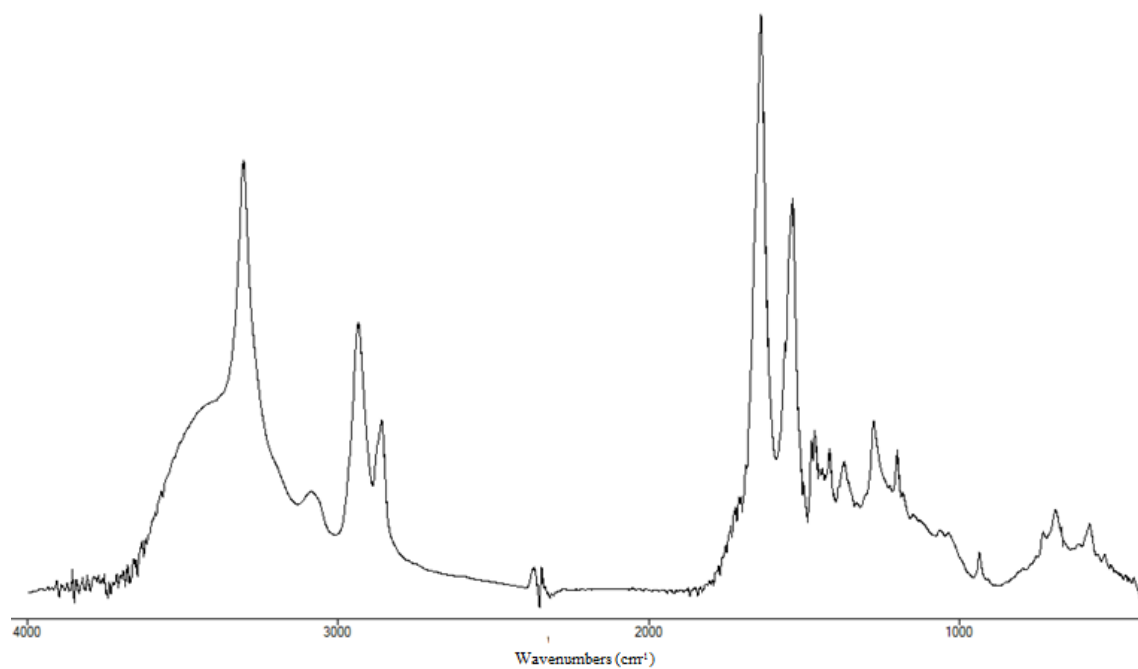
Residual hemicellulose-rich method C – [bmim][N(CN)<sub>2</sub>] (4000-400 cm<sup>-1</sup>)



Residual hemicellulose-rich method C – [bmim][N(CN)<sub>2</sub>] (1800-800 cm<sup>-1</sup>)

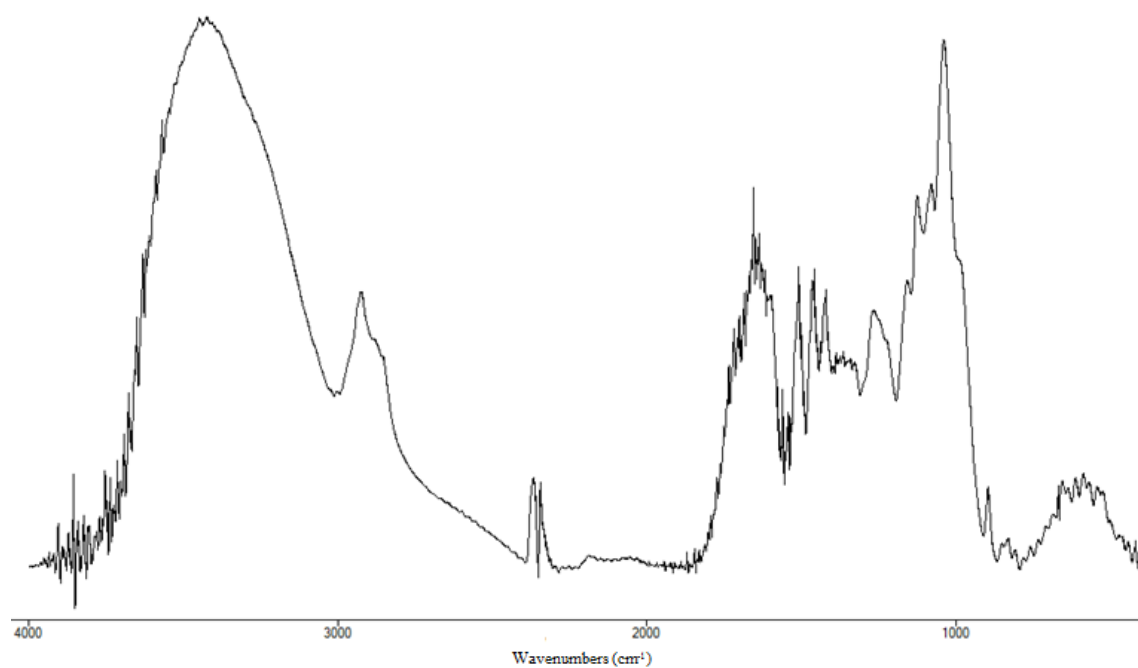


Lignin-rich method C – [bmim][N(CN)<sub>2</sub>] (4000-400 cm<sup>-1</sup>)

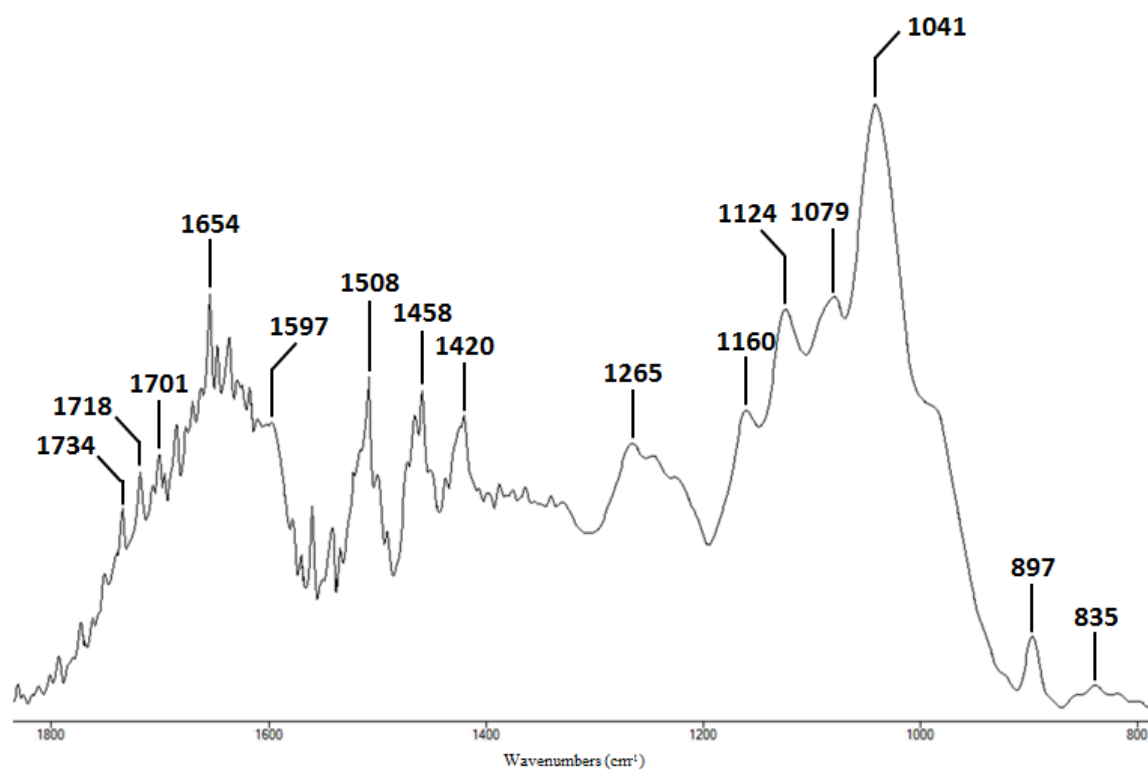


(nylon contamination)

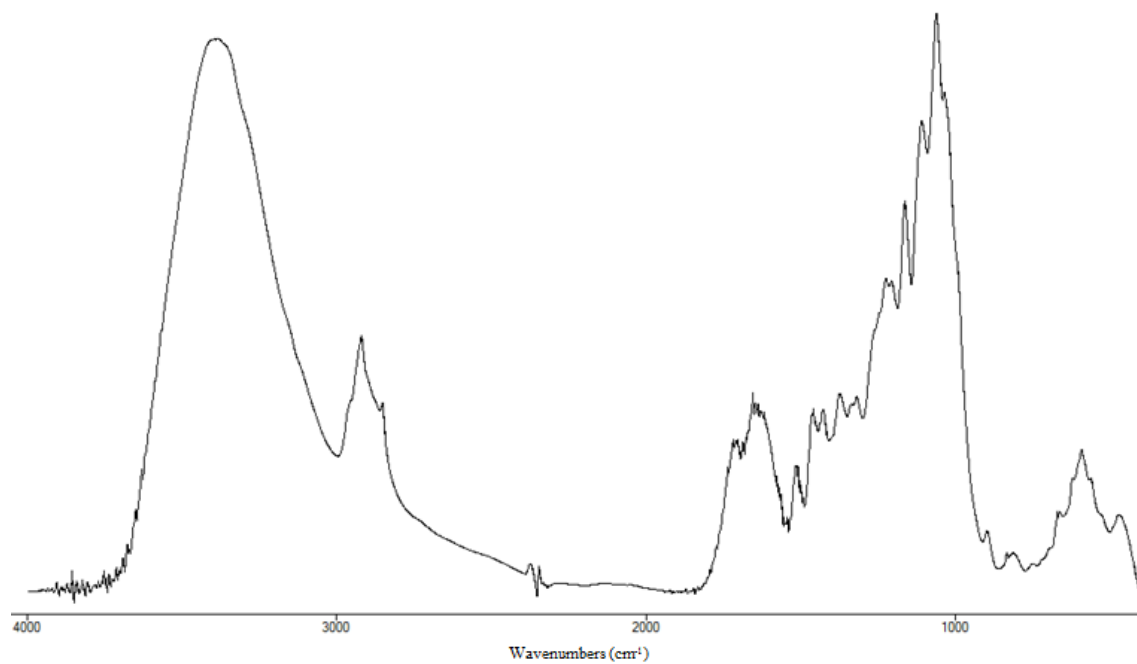
Residual lignin-rich method C – [bmim][N(CN)<sub>2</sub>] (4000-400 cm<sup>-1</sup>)



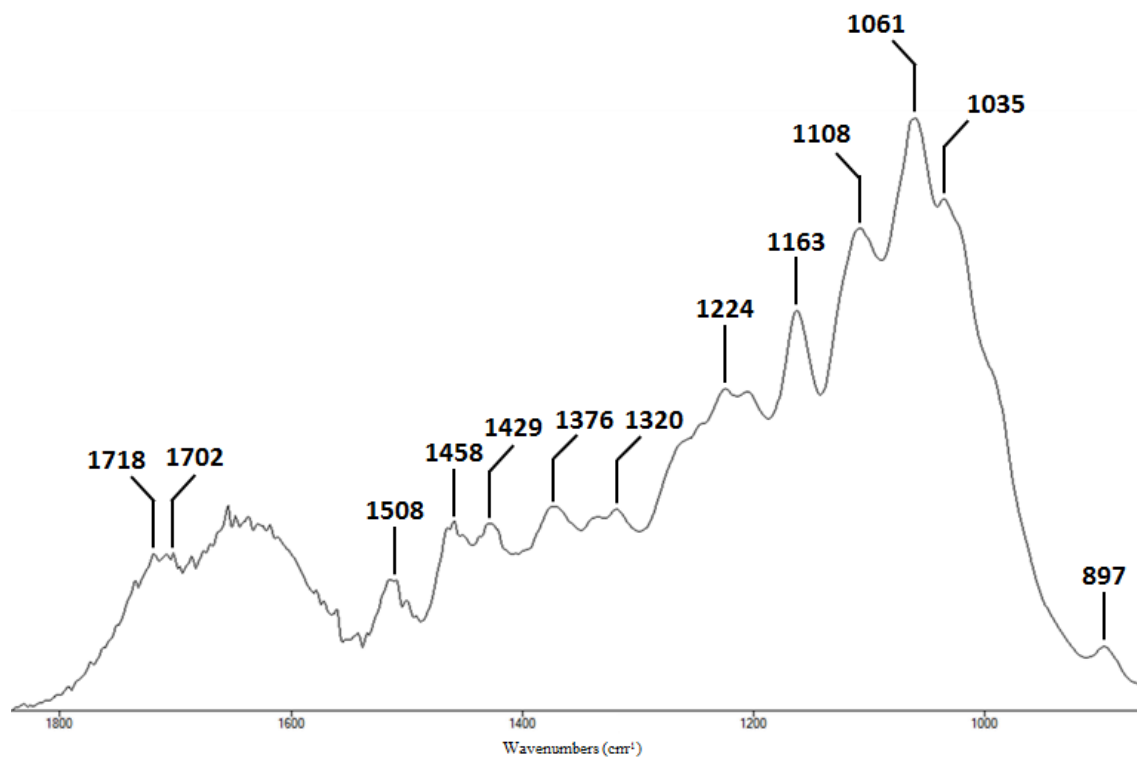
Residual lignin-rich method C – [bmim][N(CN)<sub>2</sub>] (1800-800 cm<sup>-1</sup>)



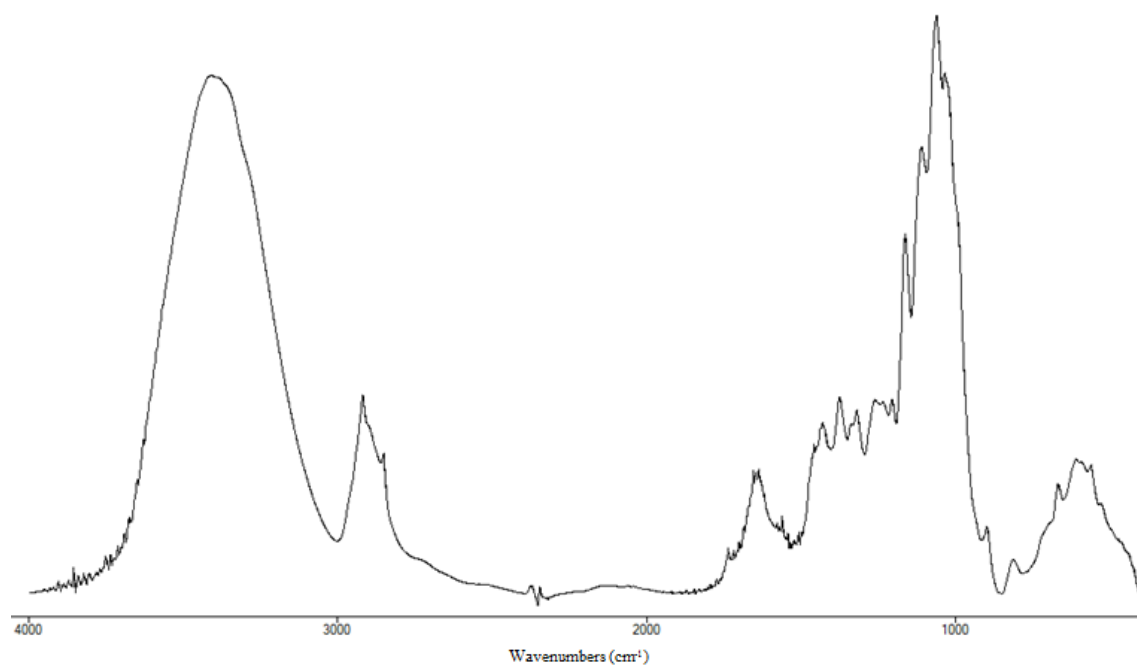
Regenerated material method C – [bmim][HSO<sub>4</sub>] (4000-400 cm<sup>-1</sup>)



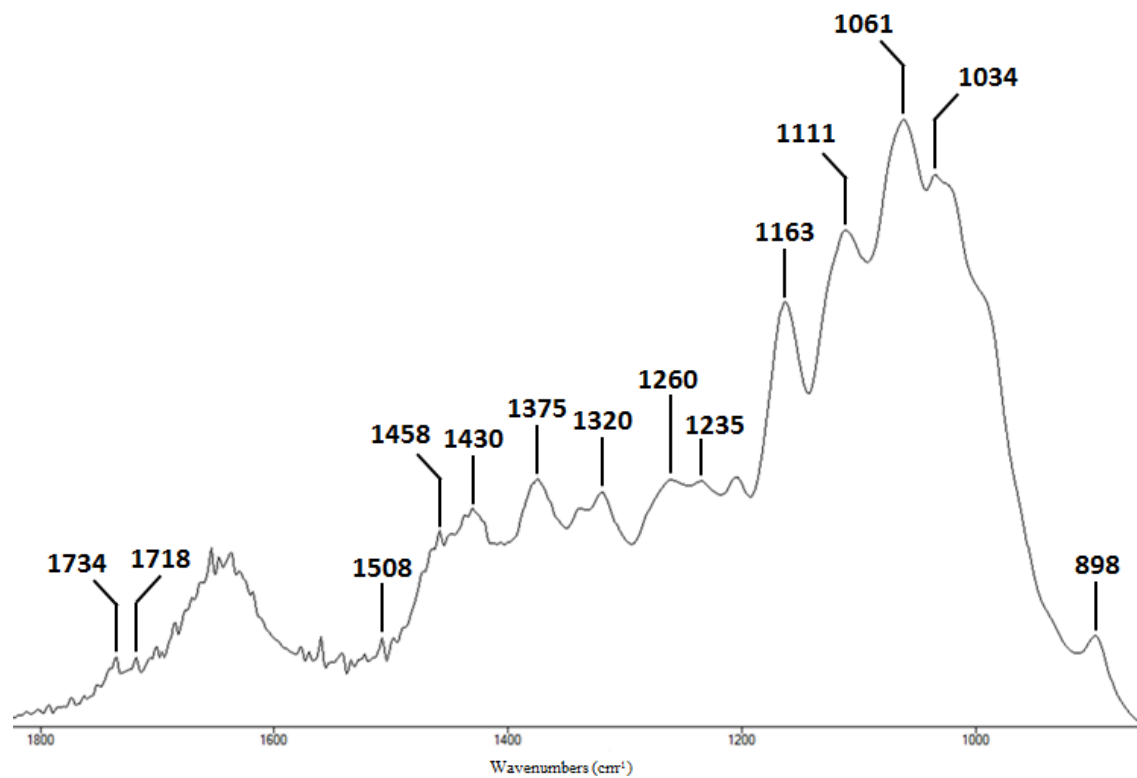
Regenerated material method C – [bmim][HSO<sub>4</sub>] (1800-800 cm<sup>-1</sup>)



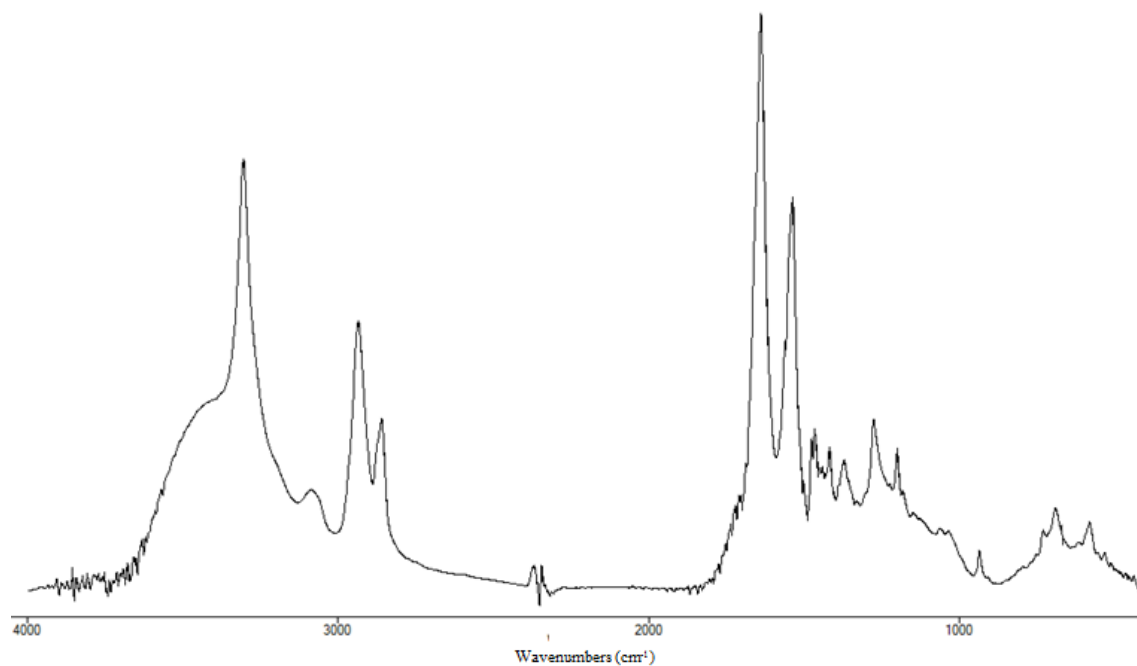
Cellulose-rich method C – [bmim][HSO<sub>4</sub>] (4000-400 cm<sup>-1</sup>)



Cellulose-rich method C – [bmim][HSO<sub>4</sub>] (1800-800 cm<sup>-1</sup>)

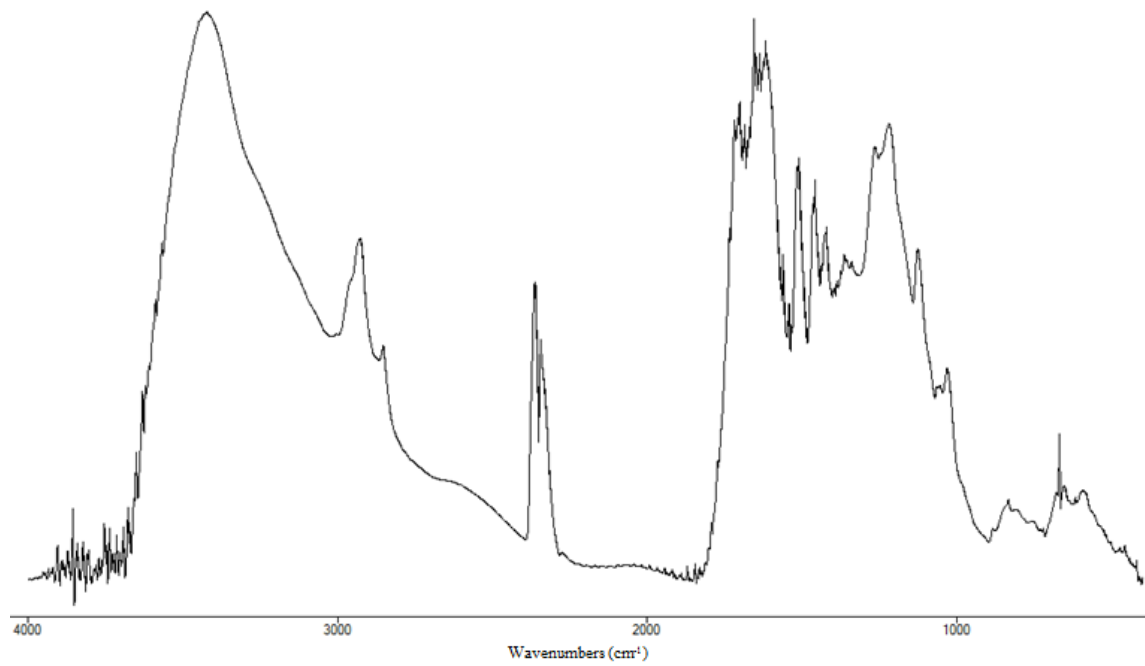


Lignin-rich method C – [bmim][HSO<sub>4</sub>] (4000-400 cm<sup>-1</sup>)

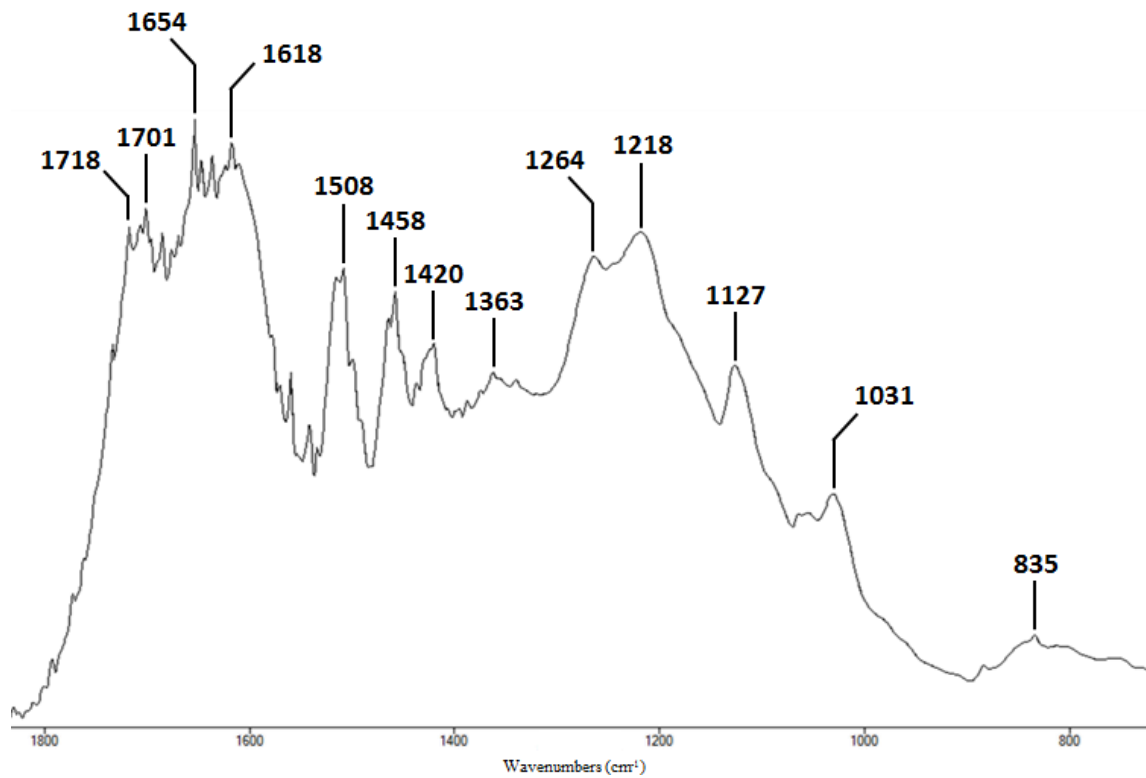


(nylon contamination)

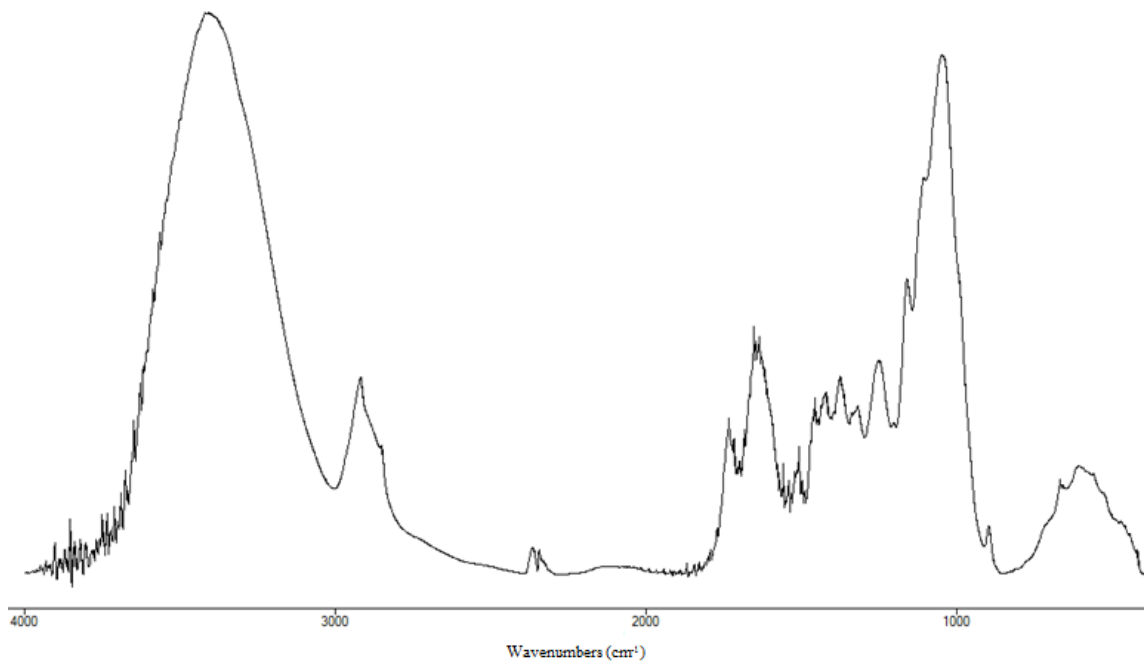
Residual lignin-rich method C – [bmim][HSO<sub>4</sub>] (4000-400 cm<sup>-1</sup>)



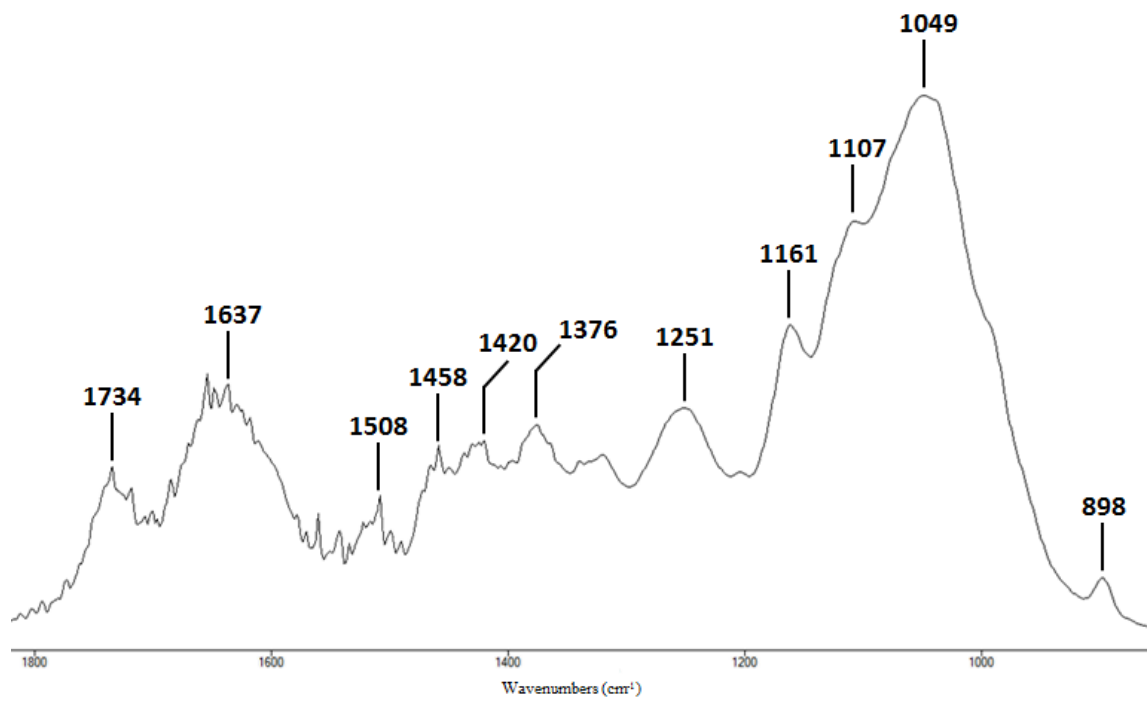
Residual lignin-rich method C – [bmim][HSO<sub>4</sub>] (1800-800 cm<sup>-1</sup>)



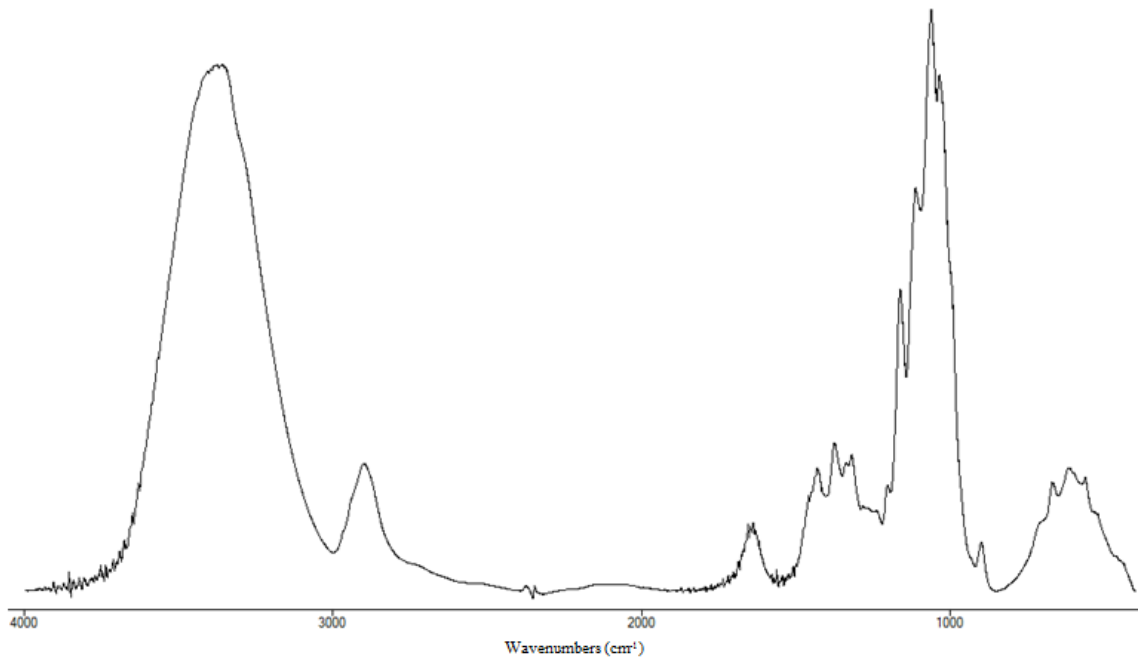
Wheat Straw (4000-400  $\text{cm}^{-1}$ )



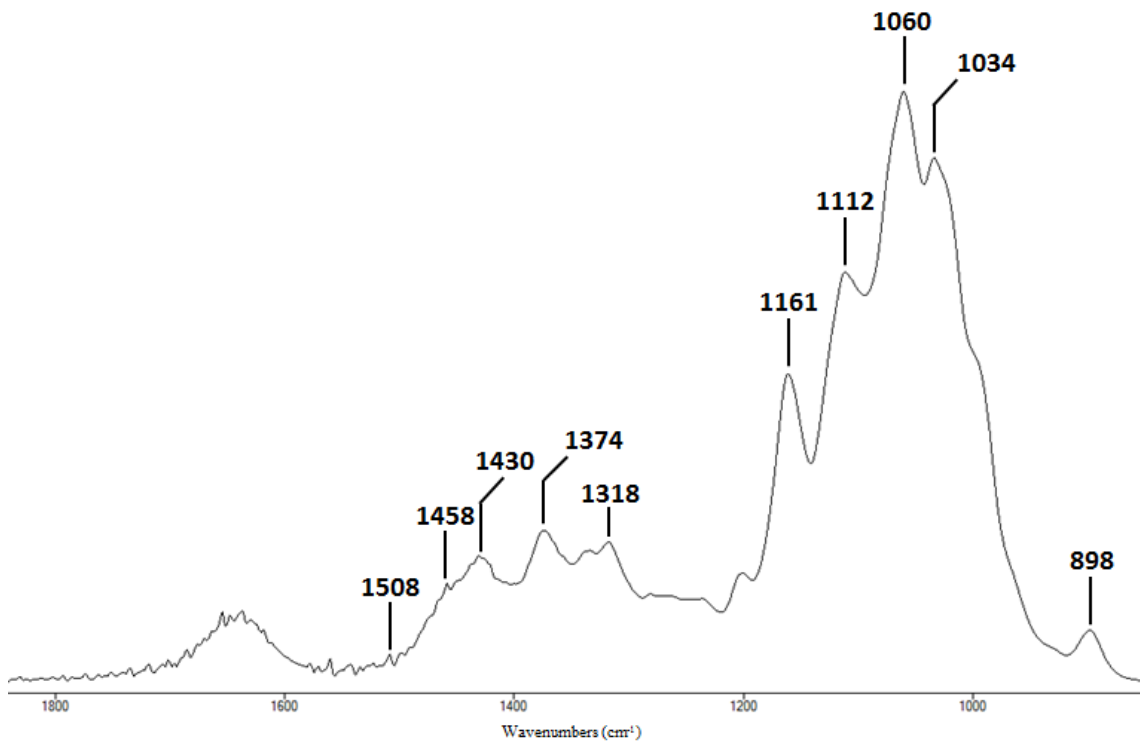
Wheat Straw (1800-800  $\text{cm}^{-1}$ )



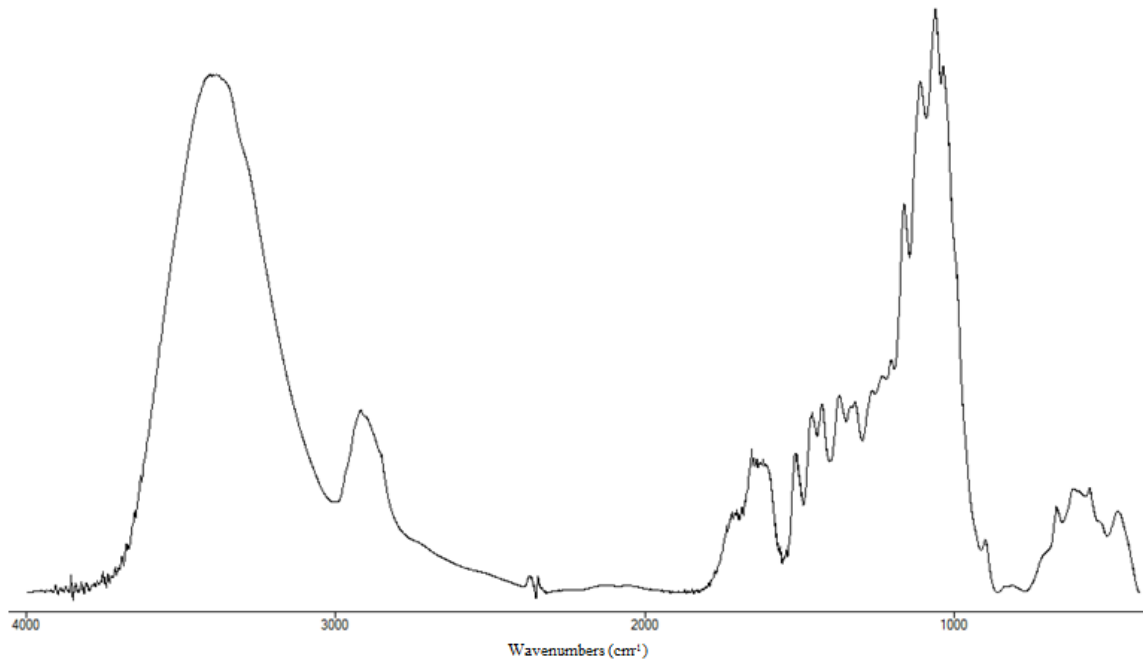
Cellulose standard (4000-400  $\text{cm}^{-1}$ )



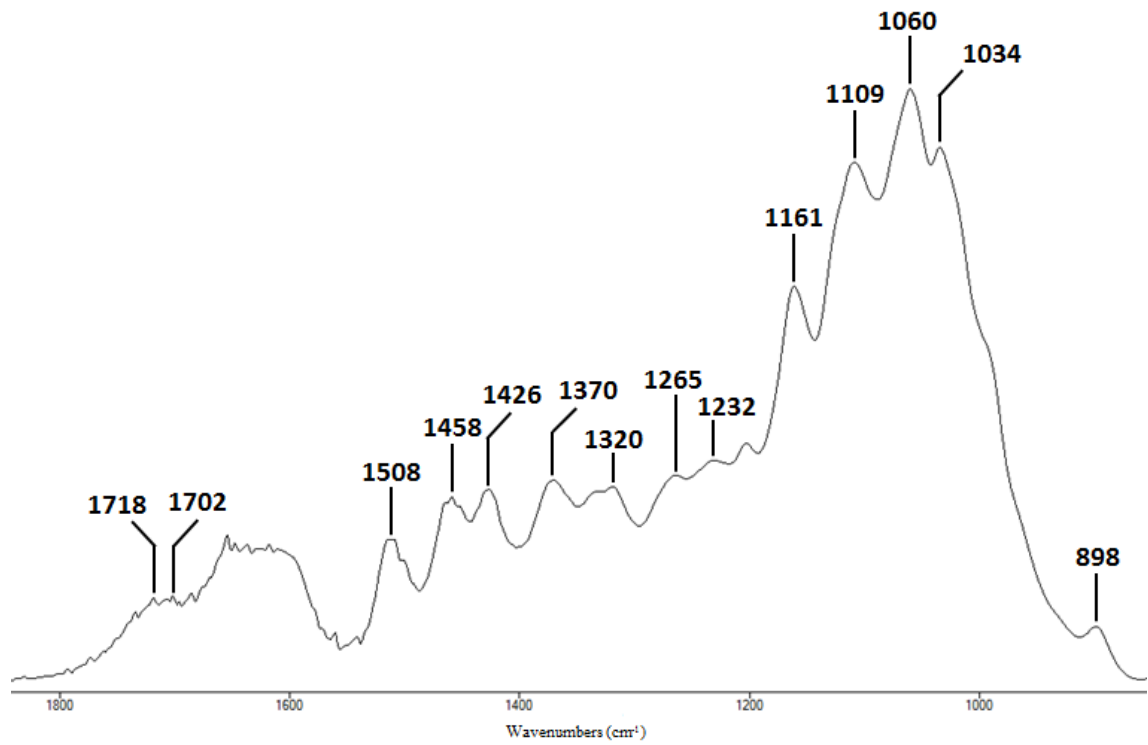
Cellulose standard (1800-800  $\text{cm}^{-1}$ )



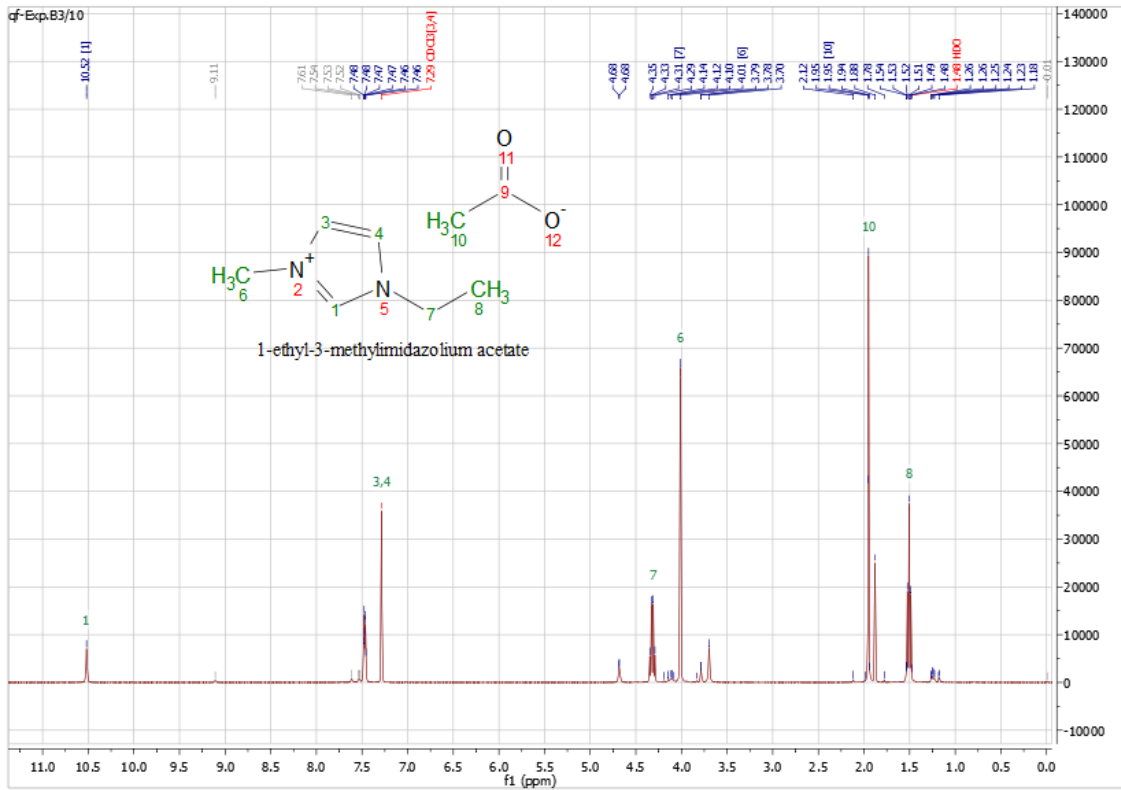
Acid hydrolysed wheat straw standard (4000-400  $\text{cm}^{-1}$ )



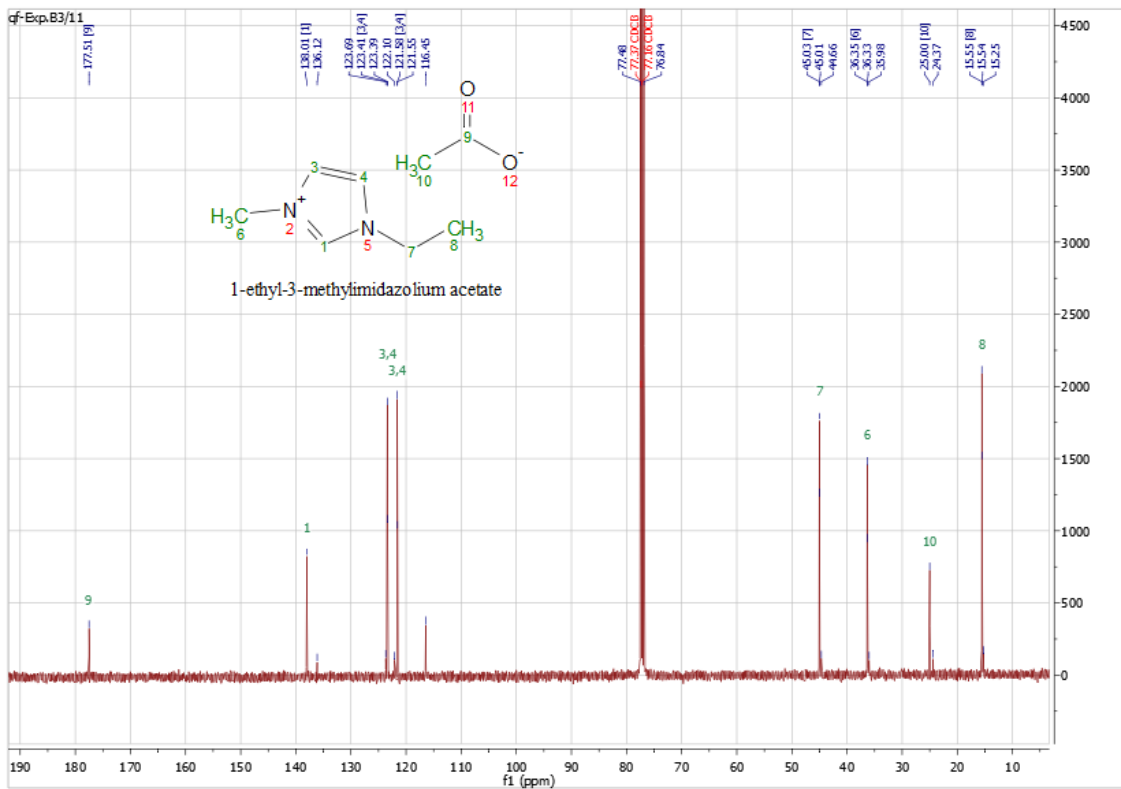
Acid hydrolysed wheat straw standard (1800-800  $\text{cm}^{-1}$ )



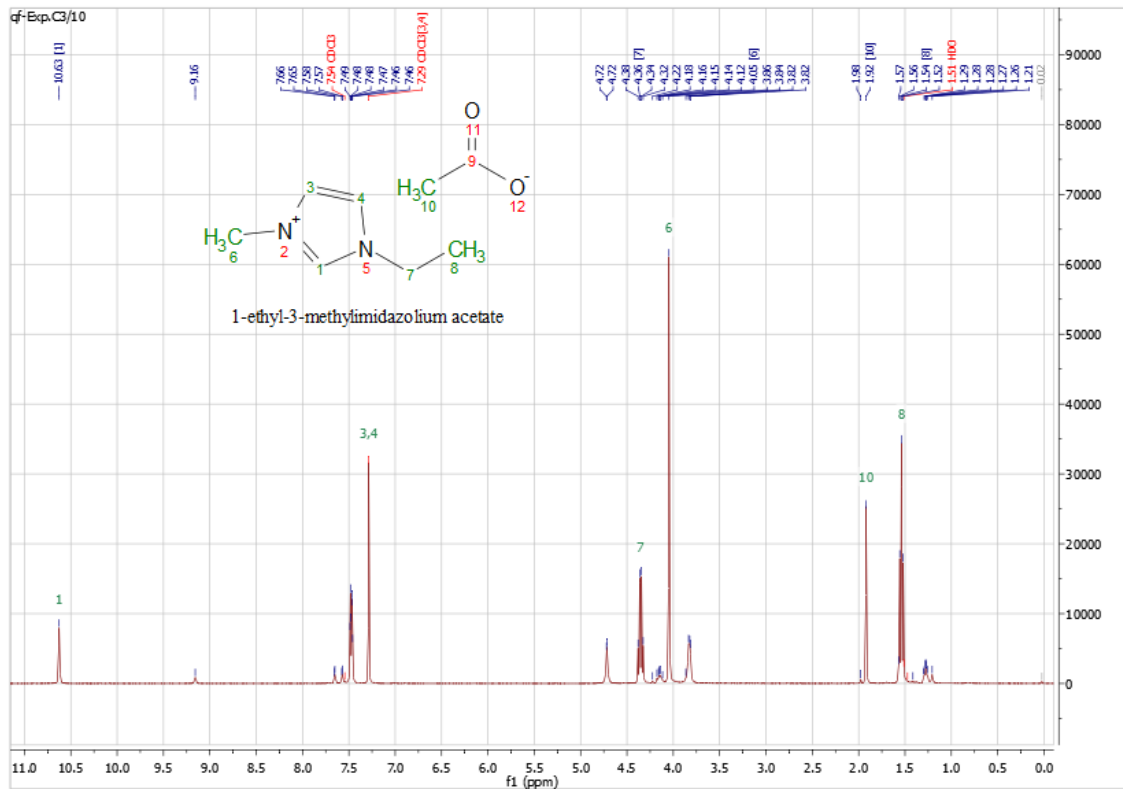
### $^1\text{H}$ NMR [emim][CH<sub>3</sub>COO] – method B



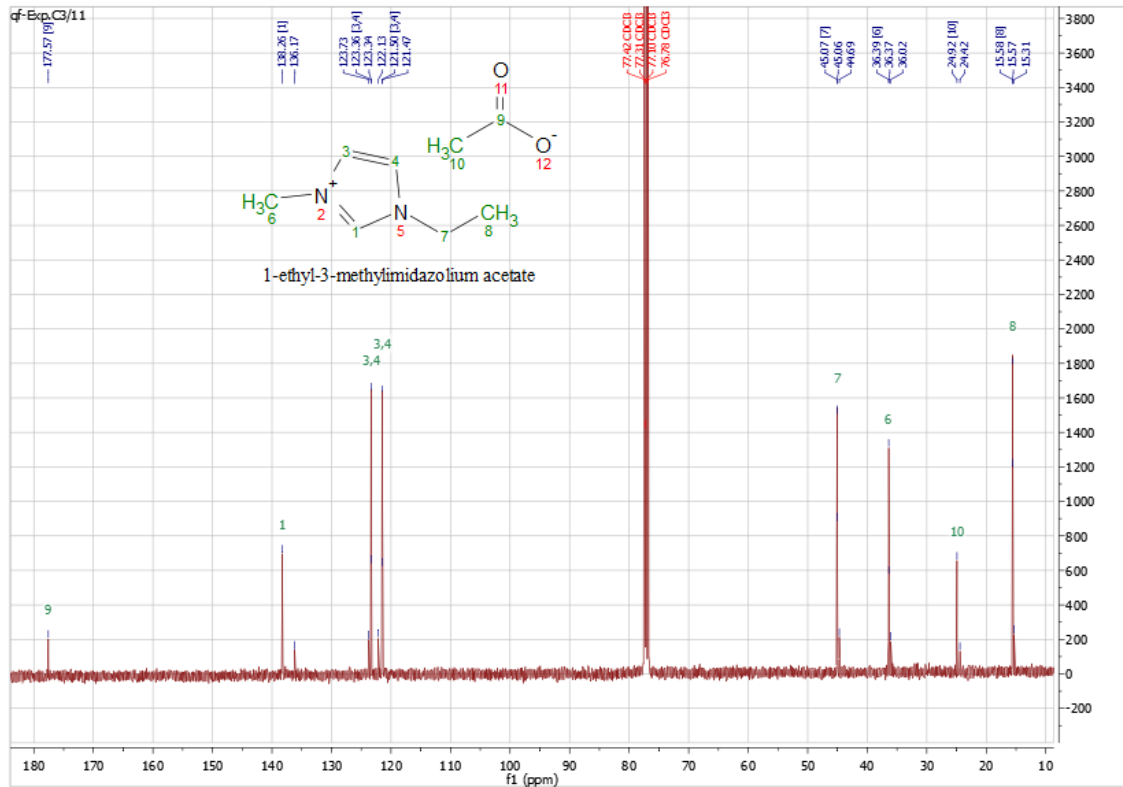
### $^{13}\text{C}$ NMR [emim][CH<sub>3</sub>COO] – method B



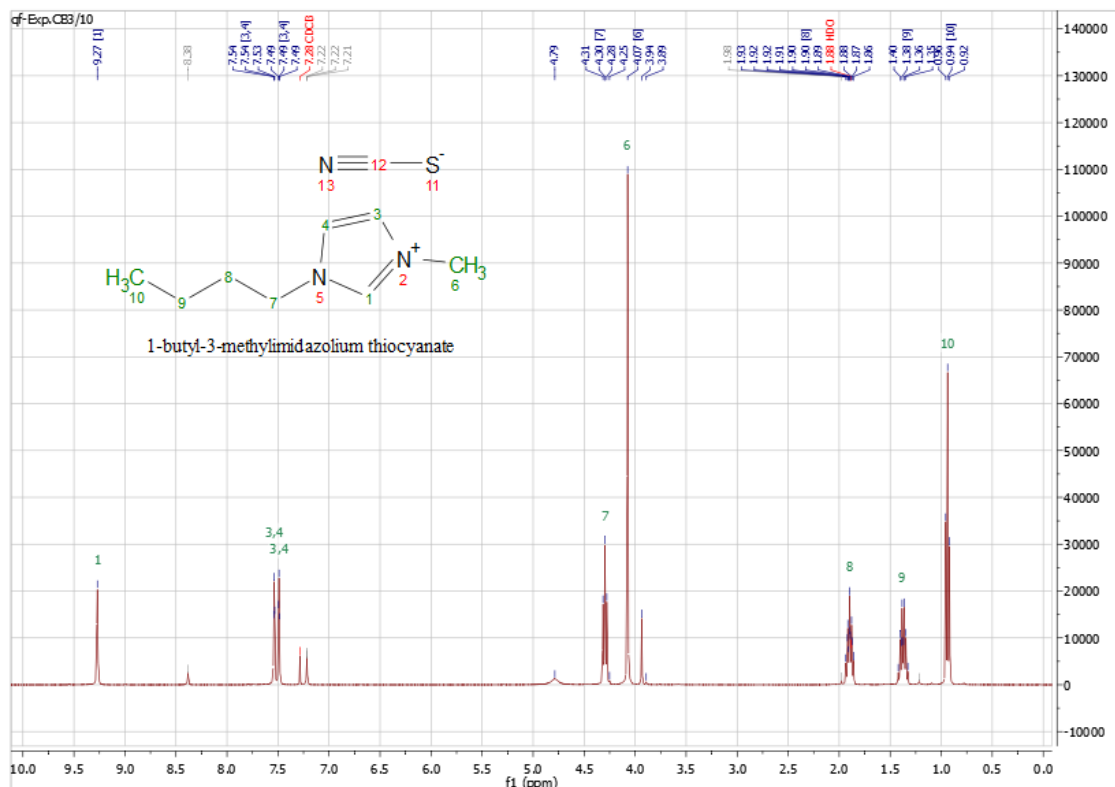
# <sup>1</sup>H NMR [emim][CH<sub>3</sub>COO] – method C



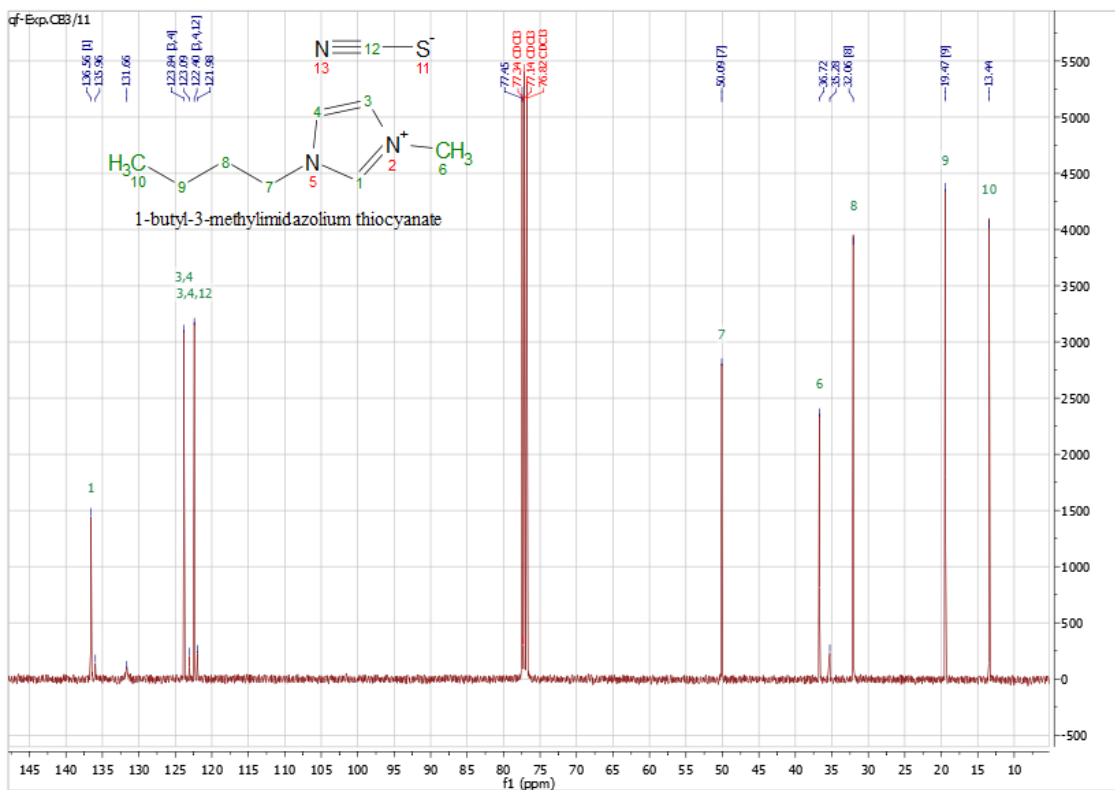
# <sup>13</sup>C NMR [emim][CH<sub>3</sub>COO] – method C



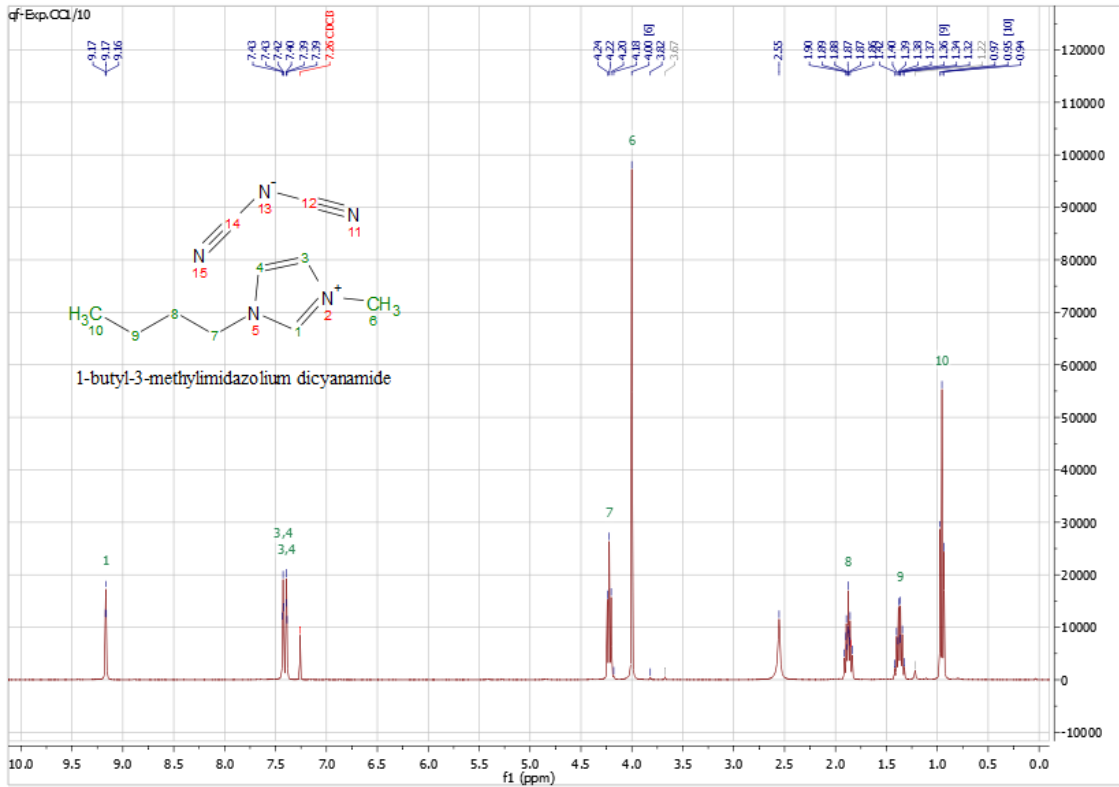
# $^1\text{H}$ NMR [bmim][SCN]



# $^{13}\text{C}$ NMR [bmim][SCN]



# $^1\text{H}$ NMR [bmim][N(CN)<sub>2</sub>]



# $^{13}\text{C}$ NMR [bmim][N(CN)<sub>2</sub>]

